ANTI-AGING AND ANTI-OXIDANT PHYTOCHEMICAL COMPOUNDS

ZIYUN WU

NATIONAL UNIVERSITY OF SINGAPORE

2013

ANTI-AGING AND ANTI-OXIDANT PHYTOCHEMICAL COMPOUNDS

ZIYUN WU

(M. Agr. & B.Sc., Hainan University, China)

A THESIS SUBMITTED FOR THE DEGREE OF

DOCTOR OF PHILOSOPHY

DEPARTMENT OF CHEMISTRY

FACULTY OF SCIENCE

NATIONAL UNIVERSITY OF SINGAPORE

2013

DECLARATION

I hereby declare that this thesis is my original work and it has been written by me in its entirety, under the supervision of associate professor Dejian Huang and the co-supervision of assistant professor Shao Quan Liu, (in the laboratory S13-05-02 and S9-02-01), Chemistry Department, National University of Singapore, between August, 2009 and July, 2013.

I have duly acknowledged all the sources of information which have been used in the thesis.

This thesis has also not been submitted for any degree in any university previously.

The content of the thesis has been partly published in:

1. Wu Z, Song L, Liu S and Huang D. Independent and additive effects of glutamic acid and methionine on yeast longevity. ***PLoS One***. 2013, 8(11): e79319.doi:10.1371/journal.pone.0079319.
2. Wu Z, Liu S and Huang D. Dietary restriction depends on nutrient composition to extend chronological lifespan in budding yeast *Saccharomyces cerevisiae*. ***PLoS One***. 2013, 8(5): e64448. doi:10.1371/journal.pone.0064448.
3. Wu Z, Song L, Feng S, Liu Y, He G, Yioe Y, Liu S and Huang D. Germination dramatically increases isoflavonoid content and diversity in chickpea (*Cicer arietinum* L.) seeds. ***Journal of Agricultural and Food Chemistry***. 2012, 60, 8606−8615.
4. Wu Z, Song L, Liu S and Huang D. A high throughput screening assay for determination of chronological lifespan of yeast. ***Experimental Gerontology***. 2011, 46, 915-922.
5. Wu Z, Song L and Huang D. Food grade fungal stress on germinating peanut seeds induced phytoalexins and enhanced polyphenolic antipxidants. ***Journal of Agricultural and Food Chemistry***. 2011, 59, 5993−6003.

Name	Signature	Date

ACKNOWLEDGEMENTS

It is difficult to overstate my gratitude to my PhD supervisor, Professor Dejian Huang. With passion, he has helped me to develop scientific instincts. Through my years in his lab, he has provided sound advice, innovative ideas and rigorous training. My research would have been at a loss without his continuous guidance. I thanks for all his guidance, support and encouragement throughout my PhD research work.

My special thanks go to my co-supervisor, Professor Shao Quan Liu for his guidance during my PhD study.

I would like to show my greatest gratitude to my wife for helping me through the difficult times with her emotional support and love. I also wish to thank my father. I appreciate his unconditional love and support, without which my life would not go on. To them I dedicate this thesis.

I would like to express my deepest appreciation to Dr Wei Yao for help in doing the NMR, and for his knowledge and expertise in the isolation of glyceollins. Next, I would like to express my heartfelt appreciation to Miss Seu Lan Lee, Mr Yitohiya Yoichi, Miss Yi Ling Quek, Miss Wei Chen, Miss Pei Chun Yip, Mr Caili Fu, Miss Hongyu Wang, Miss TingTing Liu, Miss Yan Yan, Miss Ik Chian Wong, Mr Restituto T. Tocmo and Mr Zhongwei Liu for their help, technical support, advice and assistance rendered throughout the project.

I am grateful for the learning opportunity at National University of Singapore. I thank Ms Chooi Lan Lee, Ms Huey Lee Lew, Miss Xiaohui Jiang and FST staff for their excellent technical support, advice and help throughout the project. Special thanks also go to Professor Weibiao Zhou, Dr. Hyun-Gyun Yuk, Dr. Lai Peng Leong, and NUS staff for their teaching and support.

I wish to thank my NUS friends Liangliang Wang, Jie Han, Lihua Ding, Dan Zhang and FST friends for their help, support and camaraderie.

Last but not least, the financial support from National University of Singapore is greatly appreciated.

TABLE OF CONTENTS

DECLARATION ..... **I**

ACKNOWLEDGEMENTS ..... **II**

TABLE OF CONTENTS ..... **III**

SUMMARY ..... **IX**

LIST OF TABLES ..... **XI**

LIST OF FIGURES ..... **XIII**

LIST OF ABBREVIATIONS ..... **XVII**

LIST OF PUBLICATIONS ..... **XIX**

LIST OF PRESENTATIONS ..... **XX**

Part I SCREENING OF ANTI-AGING FACTORS USING A HIGH THROUGHPUT ASSAY . **1**

Chapter 1 INTRODUCTION **2**

1.1 Background 2

1.2 Objectives 5

Chapter 2 LITERATURE REVIEW **7**

2.1 Aging models in budding yeast 7

2.2 Methods for measuring yeast CLS 8

2.2.1 Traditional colony count plating method 8

2.2.2 Flow cytometry method 10

2.2.3 High throughput method based on outgrowth of aging cells 11

2.3 Nutrients and longevity 12

2.3.1 Carbohydrates 12

2.3.2 Amino acids 13

2.3.3 Other nutrients 15

2.4 Natural products for lifespan extension 15

2.4.1 Resveratrol 19

2.4.2 Rapamycin 22

2.5 The evolutionarily conserved signaling pathways 25

2.5.1 TOR/Sch9 pathway 25

2.5.2 Ras/AC/PKA pathway 27

2.5.3 Sirtuins 29

Chapter 3 DEVELOPMENT OF HTS ASSAY FOR DETERMINATION OF CHRONOLOGICAL LIFESPAN OF YEAST 31

3.1 Introduction 31

3.2 Materials and methods 32

3.2.1. Materials 32

3.2.2 Modification of a shaker incubator for aging culture 34

3.2.3 High-throughput assay procedure 34

3.2.4 Data analysis 35

3.3 Results 38

3.3.1 Evaluation of reproducibility, precision and accuracy of HTS assay 38

3.3.2 Initial population size modulates CLS independent of CR 39

3.3.3 Effect of cellular state in YPD medium on Yeast CLS 41

3.3.4 Calorie level optimizes yeast CLS but not biomass production 42

3.3.5 Identification of calorie restriction mimetic gene 42

3.4 Discussion 45

Chapter 4 DIETARY RESTRICTION DEPENDS ON NUTRIENT COMPOSITION TO EXTEND CHRONOLOGICAL LIFESPAN IN BUDDING YEAST 50

4.1 Introduction 50

4.2 Materials and methods 52

4.2.1 Materials 52

4.2.2 Experimental design and statistical analysis 52

4.2.3 Lifespan, biomass and yeast cell growth assay 53

4.2.4 Data analysis 53

4.3 Results 58

4.3.1 DR regime is dependent on nutrients in media 58

4.3.2 Development of statistical design of experiments for evaluation of nutrition, biomass and lifespan 61

4.3.3 Nutrient composition is a key factor for longevity of yeast 62

4.3.4 Biomass production of the four strains has similar changes in response to nutrient composition 67

4.3.5 *sch9*Δ is more sensitive to nutrients than the other three strains 69

4.3.6 Aging media pH is dependent on glucose concentration and has no correlation with lifespan 71

4.3.7 The optimal SD medium for yeast 72

4.4 Discussion 74

4.5 Conclusion 80

Chapter 5 INDEPENDENT AND ADDITIVE EFFECTS OF GLUTAMIC ACID AND METHIONINE ON YEAST LONGEVITY 81

5.1 Introduction 81

5.2 Materials and methods 83

5.2.1 Materials 83

5.2.2 Lifespan, biomass and yeast cell growth assay 83

5.2.3 Acetic acid analysis 83

5.2.4 Data analysis 84

5.3 Results 84

5.3.1 Amino acids regulate lifespan and biomass changes in yeast 84

5.3.2 Methionine and glutamic acid cause lifespan and biomass alterations in yeast 89

5.3.3 Independent and additive effects of glutamic acid, methionine and glucose on lifespan extension 94

5.3.4 Conserved protein kinase Gcn2 mediates amino acids induced lifespan extension 99

5.4 Discussion 105

5.5 Conclusion 110

Chapter 6 CRYPTOTANSHINONE EXTENDS CHRONOLOGICAL LIFESPAN IN THE BUDDING YEAST 111

6.1 Introduction 111

6.2 Experimental Procedures 113

6.2.1 Materials 113

6.2.2 Lifespan and yeast cell growth assay 113

6.2.3 HPLC chromatogram analysis of compounds from Danshen 113

6.2.4 Intracellular ROS quantification and fluorescence images of yeast cells 114

6.2.5 Data analysis 115

6.3 Results 115

6.3.1 A high throughput assay identifies cryptotanshinone as the key compound from Danshen to extend yeast lifespan in a concentration and the time of addition dependent manner 115

6.3.2 Cryptotanshinone induced CLS extension is prevented by amino acid restriction 120

6.3.3 Essential amino acid sufficiency is required for cryptotanshinone induced longevity 122

6.3.4 Cryptotanshinone requires Tor1 and Sch9 for CLS extension 125

6.3.5 Tanshinones extend yeast lifespan via similar mechanisms 129

6.3.6 Gcn2 regulates essential amino acids and cryptotanshinone induced CLS extension 130

6.3.7 Cryptotanshinone extend lifespan without reduce in ROS level in *sod2*Δ..... 132

6.4 Discussion..... 133

6.5 Conclusion..... 139

Chapter 7 HORMESIS OF GLYCEOLLIN I, AN INDUCED PHYTOALEXIN FROM SOYBEAN, ON BUDDING YEAST CHRONOLOGICAL LIFESPAN EXTENSION 140

7.1 Introduction 140

7.2 Experimental Procedures..... 141

7.2.1 Materials 141

7.2.2 Isolation of glyceollins..... 141

7.2.3 Lifespan and yeast cell growth assay 142

7.2.4 Data analysis 142

7.3 Results and Discussion 142

7.3.1 Antiproliferation activity of glyceollins..... 142

7.3.2 Glyceollin I extends yeast CLS by CR-dependent regime..... 145

7.3.3 Hormetic effect of glyceollin I on yeast lifespan 147

7.4 Conclusion..... 148

Chapter 8 CONCLUSIONS AND FUTURE OUTLOOK 150

Part II ANTIOXIDANTS FROM GERMINATED LEGUME SEEDS 154

Chapter 9 INTRODUCTION..... 155

9.1 Introduction 155

9.1.1 Grain legume is important for human diet 155

9.1.2 Phytochemical profiling is significant for quality and safety control 156

9.1.3 Antioxidant capacity is a popular criterion of functional food..... 156

9.2 Objectives..... 158

Chapter 10 POLYPHENOLIC ANTIOXIDANTS AND PHYTOALEXINS CHANGES IN GERMINATING LEGUME SEEDS WITH FOOD GRADE FUNGAL *RHIZOPUS OLIGOPORUS* STRESS 160

10.1 Introduction 160

10.2 Materials and Methods 161

10.2.1 Materials 161

10.2.2 Germination and fungal inoculations..... 162

10.2.3 Quantification of antioxidant capacity and total phenolics 162
10.2.4 Phytochemicals and phytoalexins identification 163
10.2.5 Data analysis 163
10.3 Results and Discussion 164
10.3.1 Comprehensive evaluation of antioxidant contents of fungal-stressed sprouts 164
10.3.2 Phytochemical and phytoalexin changes in germinating legume seeds 167
10.4 Conclusion 173
Chapter 11 GERMINATION DRAMATICALLY INCREASES ISOFLAVONOID CONTENT AND DIVERSITY IN CHICKPEA (*CICER ARIETINUM* L.) SEEDS 174
11.1 Introduction 174
11.2 Materials and Methods 176
11.2.1 Materials 176
11.2.2 Instruments 176
11.2.3 Seed germination 176
11.2.4 Sample preparation procedures 177
11.2.5 Quantification of antioxidant capacity and TPC 177
11.2.6 Detection of isoflavonoids by PDA and MS 178
11.2.7 Isolation and identification of biochanin A and formononetin 179
11.2.8 Identification and quantification of isoflavonoids from chickpea and soybean 179
11.2.9 Statistical analysis 180
11.3 Results and Discussion 180
11.3.1 Antioxidant capacity and TPC 180
11.3.2 Profiles of isoflavonoids in germinated chickpea seeds 182
11.3.3 Quantification of isoflavonoids in chickpea and soybean 188
11.4 Conclusion 193
Chapter 12 FOOD GRADE FUNGAL STRESS ON GERMINATING PEANUT SEEDS INDUCED PHYTOALEXINS AND ENHANCED POLYPHENOLIC ANTIOXIDANTS 195
12.1 Introduction 195
12.2 Materials and Methods 196
12.2.1 Reagents 196
12.2.2 Instruments 196
12.2.3 Peanut germination and fungal inoculations 196
12.2.4 Sample preparation procedures 197

12.2.5 Quantification of antioxidant capacity and total phenolics 197
12.2.6 Detection of phytochemical by PDA and MS 198
12.2.7 Phytoalexin extraction and detection by HPLC and LC-MS 199
12.3 Results and Discussion 199
12.3.1 Profiles of phenolic acids in peanut seeds 200
12.3.2 Polyphenolic profiles in germinated peanuts 207
12.3.3 Phytoalexins in germinated peanuts 211
12.4 Conclusion 214
Chapter 13 CONCLUSIONS AND FUTURE OUTLOOK 216
BIBLIOGRAPHY 218

SUMMARY

This thesis consists of two parts. In the Part I, I focus on discovery of novel anti-aging factors from nutrients and natural products by using a high throughput assay based on yeast chronological aging model. Ageing population is one of the greatest challenges in the 21th century, and causes great economical burdens to individuals, family, and a country. Thus, looking for the elixir of youth is an emergency task for scientists. Taking advantage of the yeast chronological aging model, I developed a high throughput screening assay for determination of yeast chronological lifespan with a rapid and simple protocol, uncomplicated data analysis, and high sensitivity (**Chapter 3**).

I next studied the relationship between nutrients and yeast lifespan. I found that lifespan extension by a typical glucose restriction regime was dependent on the nutrients in media. My findings support the notion that nutrient composition might be a more effective way than simple dietary restriction to optimize lifespan and biomass production of yeast (**Chapter 4**). Furthermore, restriction of methionine and/or increase of glutamic acid caused longevity that was not the cause of low acetic acid production and acidification in aging medium. Remarkably, low methionine, high glutamic acid and glucose restriction extended lifespan additively. Preliminary findings demonstrate that glutamic acid, methionine and glucose restriction prompt yeast longevity through distinct mechanisms (**Chapter 5**).

In the discovery of anti-aging natural products, I found that cryptotanshinone can greatly extend yeast lifespan in a dose and the-time-of-addition dependent manner at nanomolar concentrations without disruption of cell growth. Cryptotanshinone prolongs lifespan via a nutrient-dependent regime, especially essential in amino acid sensing, and might be involved in the regulation of Tor1, Sch9, Gcn2 and Sod2. These

are highly conserved nutrient dependent longevity proteins found from yeast to humans (**Chapter 6**). In addition, glyceollin I has hormesis effect to extend yeast lifespan at low dose in a CR-dependent manner, while reduce lifespan and inhibit yeast cell proliferation at higher doses. The result indicates that glyceollin I might be a unique candidate of CRM (**Chapter 7**).

In the Part II, I focus on discovery of enriching anti-oxidant compounds from legume seeds by germination or fungus-stressed germination. I firstly investigated the phytochemical changes in food legume seeds under germination with or without fungal (*Rhizopus oligoporus*) stress. The results indicated that legume seeds can be divided into four groups: rich phytoalexins and enhanced phytochemicals; low phytoalexins but enhanced phytochemicals; less phytochemicals under germination with fungus-stress; less phytochemicals under germination (**Chapter 10**). Germination increased TPC and antioxidant capacity of most seeds. Particularly in chickpea seeds, germination could significantly increase isoflavonoids diversity. Twenty-five isoflavonoids were detected and identified tentatively. Total isoflavonoid content of germinated chickpea was approximately 5-fold of that of germinated soybean (**Chapter 11**).

Remarkably, the small peanuts synthesized the most number of phytoalexins when the sprouts are stressed by the fungus. From the LC-MS^n spectral data, 45 compounds were identified tentatively in the peanut sprouts, including 19 stilbenoids phytoalexins derivatives (**Chapter 12**).

LIST OF TABLES

Table 2.1 Comparison of traditional CFU plating method and high throughput method for measuring yeast CLS (Fabrizio & Longo 2003; Murakami et al. 2008) 12

Table 2.2 Comparison of the effect of other natural products on lifespan extension in different organisms 17

Table 2.3 Comparison of the effect of resveratrol on lifespan in different organisms investigated by different laboratories 20

Table 2.4 Comparison of effect of rapamycin on lifespan in different organisms investigated by different laboratories 24

Table 3.1 Final composition of synthetic defined (SD) medium used for yeast CLS analysis 33

Table 3. 2 Comparison of high throughput methods for measuring yeast CLS developed by Kaeberlein group and our group 45

Table 4.1 The three-factor/three-level response surface methodology of Box–Behnken design and pH, biomass and lifespan values of different cultures in the WT and *sch9*Δ strains 54

Table 4.2 Correlation among lifespan, biomass and viability at day 2 for the 15 media in the four *S. cerevisiae* strains 55

Table 4.3 Correlations among amino acid, YNB, glucose, pH, lifespan and biomass for the 15 media in the WT and *sch9*Δ strains 56

Table 4.4 The linear and the quadratic parameter estimates for lifespan and biomass production 57

Table 4.5 Membership function value f(x) and ranking for the 15 media according the two criteria of lifespan and biomass in the four yeast strains 73

Table 10.1 Comparative evaluation of total phenolic content (TPC), total flavonoid content (TFC) and oxygen radical absorbing capacity (ORAC) of 13 legume seeds 165

Table 10.2 Ranking of antioxidant capacity based on three criteria of TPC, TFC and ORAC under GS 166

Table 10.3 Comparison of the number of peaks in HPLC chromatograms for the thirteen legume seeds under non-germination (UG), germination (G) and germination and fungal stress (GS) 167

Table 11. 1 Peak assignments of isoflavonoids in germinated chickpea and soybean presented according to retention time, maximum UV absorption, and molecular Ions 184

Table 12.1 Peak assignment of compounds in GS peanut sprouts presented according to retention time, maximum UV absorption and molecular ions 202

Table 12.2 TPC, TFC, ORAC, HORAC, SORAC and DPPH values of ungerminated seed (UG), germinated seed (G) and germinated seed with fungal-stress (GS)..... 206

Table 12.3 Peak assignment of proposed phytoalexins in GS peanut sprouts presented according to retention time, maximum UV absorption and molecular ions 212

LIST OF FIGURES

Figure 3.1 A roadmap of a high-throughput assay for determination of yeast CLS 36

Figure 3.2 Outgrowth curves of budding yeast with several inoculum concentrations 39

Figure 3.3 Effects of initial population size on CLS 40

Figure 3.4 The effects of calorie level on yeast CLS 41

Figure 3.5 Effect of single gene deletion on CLS 44

Figure 4.1 DR regime is dependent on nutrients in medium 59

Figure 4.2 Comparison of relative lifespan, biomass and viability in the four yeast strains (WT, *sch9*Δ, *tor1*Δ, and *sir2*Δ) 64

Figure 4.3 Response surfaces for lifespan of the four yeast strains (WT, *sch9*Δ, *tor1*Δ, and *sir2*Δ) cultured at various concentrations of amino acids (AAs), glucose (Glu), and yeast nitrogen base (YNB) 65

Figure 4.4 Response surfaces for biomass production of yeast cultured at various concentrations of amino acids (AAs), glucose (Glu), and yeast nitrogen base (YNB) 66

Figure 4.5 Survival curves of four yeast strains 67

Figure 4.6 Effect of medium nutrient composition on yeast biomass production 68

Figure 4.7 Different media have little effect on cell growth during lag phase in most yeast strains 70

Figure 4.8 Representative cell images of the four yeast strains in different media at day 22 .. 71

Figure 5.1 Ratio of essential and non-essential amino acids regulates lifespan and biomass changes 85

Figure 5.2 Growth curves of WT yeast were cultured in media with diverse amino acids compositions 87

Figure 5.3 EAA and NEAA change pH value and acetic acid production of aging media 88

Figure 5.4 Effect of individual amino acids on yeast lifespan and biomass production 90

Figure 5.5 Methionine and glutamic acid cause lifespan and biomass alterations in yeast 92

Figure 5.6 Glutamic acid addition, methionine and glucose restriction not inhibit yeast growth 93

Figure 5.7 Comparison of pH and acetic acid in media containing various levels of methionine and glutamic acid 94

Figure 5.8 Independent and additive effects of glutamic acid, methionine and glucose on lifespan extension 95

Figure 5.9 Lifespan extending capacity of the combination of glutamic acid and methionine was impaired by the medium supplying with 5-fold NEAA..... 96

Figure 5.10 The combination is sufficient to extend lifespan in glucose restriction, 1E1N (standard), 1E5N and pH buffered conditions 97

Figure 5.11 Acetic acid may be not the cause of lifespan shortening in buffered media (pH 6.0) 98

Figure 5.12 Comparative evaluation of the pH of aging media in WT, *sch9*Δ and *gcn2*Δ..... 99

Figure 5.13 Conserved protein kinase Gcn2 mediates amino acids induced lifespan extension 101

Figure 5.14 Comparative evaluation of the amino acids induced longevity in different single gene deletion strains..... 102

Figure 5.15 The acetic acid production of aging media in *sch9*Δ and *gcn2*Δ..... 105

Figure 6.1 A high throughput assay identifies cryptotanshinone as the key compound from Danshen to extend yeast lifespan in a concentration and the time of addition dependant manner 116

Figure 6.2 HPLC chromatogram analysis compounds from Danshen..... 119

Figure 6.3 Cryptotanshinone (CPT) induced CLS extension is prevented by amino acids restriction 121

Figure 6.4 EAA sufficiency was required for cryptotanshinone induced CLS extension 123

Figure 6.5 Survival curves (mean, n = 6) of the WT, *sch9*Δ and *gcn2*Δ yeast cultured in 7 SD based media with different amount of EAA and NEAA with or without cryptotanshinone (78 nM)..... 124

Figure 6.6 Effect of individual amino acid restriction on cryptotanshinone induced CLS extension 125

Figure 6.7 Cryptotanshinone induced lifespan extension depends on Sch9 and Tor1 activity 127

Figure 6. 8 Survival curves of WT yeast (A) and *tor1*Δ (B) cultured in SD medium containing 0.1%, 0.5%, 2% and 5% glucose with (red line) or without (blue line) cryptotanshinone (78 nM; mean ± SEM, n = 6) 128

Figure 6.9 Tanshinones have no synergetic effect on yeast longevity via similar mechanisms 130

Figure 6.10 Gcn2 regulated amino acids homeostasis to extend lifespan and impaired cryptotanshinone induced longevity in different media 132

Figure 6.11 Cryptotanshinone mediates reactive oxygen species (ROS) production 134

Figure 6.12 A proposed pathways induced by cryptotanshinone for longevity in yeast 137

Figure 7.1 Structure (A), and HPLC chromatogram at 285 nm (B) of glyceollin isomers I, II, and III obtained from black soybean sprouts with food grade fungus *R. oligosporus* stress. 143

Figure 7.2 Influence of glyceollin I, II, and III on proliferation of yeast..... 144

Figure 7.3 Glyceollin I as a CRM extends the budding yeast CLS 146

Figure 7.4 Glyceollin II (A) and III (B) do not extend yeast CLS..... 147

Figure 7.5 Dose-response curve of glyceollin I on yeast CLS with a hormetic effect..... 148

Figure 10.1 HPLC chromatogram (300 nm) of small peanut after 3 days germination without *R. oligosporous* stress (G3d) and 3 days with the fungal stress (GS3d) 169

Figure 10.2 HPLC chromatogram (300 nm) of kidney bean (UG) after 4 days germination without *R. oligosporous* stress (G 4 day)..... 170

Figure 10.3 HPLC chromatogram (300 nm) of yardlong bean after 4 days germination without *R. oligosporous* stress (G 4 day) and 4 days with the fungal stress (GS 4 day) 171

Figure 10.4 HPLC chromatogram (300 nm) of yellow soybean bean (UG) after 4 days germination without *R. oligosporous* stress (G 4 day)..... 172

Figure 11.1 Structures, maximum UV absorptions and molecular weights of major isoflavonoids aglycones and a few representatives of their glycoside conjugates identified from germinated chickpea and soybean in this study 175

Figure 11.2 TPC and ORAC values of ungerminated seed (0 day), germinated seed (1–4 days) in nine legumes (also see Table 10.1)..... 181

Figure 11.3 Effect of germination time on phytochemicals production in chickpea 183

Figure 11.4 HPLC chromatogram (260 nm) and UV absorption spectra of isoflavonoids in germinated chickpea 186

Figure 11.5 Comparative HPLC chromatogram (260 nm) of isoflavonoids between black soybean, chickpea, and their germinated seeds at day 4 in acetone/methanol/water (2:2:1) extracts 189

Figure 11.6 Quantitative analysis of isoflavonoids in chickpea and black soybean 190

Figure 11.7 Proposed isoflavonoids biosynthesis pathway in legumes 193

Figure 12.1 HPLC chromatograms (310 nm) of three types of peanut seeds in acetone/ethanol/water (2:2:1) extracts 201

Figure 12.2 UV spectra of major phytochemcials in peanut sprouts under food grade fungus *R. oligosporus* stress..... 203

Figure 12.3 ESI (negative ion) mass spectra of major phytochemicals in peanut sprouts under food grade fungus *R. oligosporus* stress 204

Figure 12.4 Proposed phenylpropanoid biosynthetic pathway in peanut sprouts under food grade fungus *R. oligosporus* stress..... 205

Figure 12.5 Comparative HPLC chromatograms (310 nm) between red and black peanuts after 3 days germination with or without fungal inoculation (G or GS)..... 208

Figure 12.6 HPLC chromatogram (310 nm) of germinated reddish peanut after 12 hours (G0.5d) and 3 days (G3d) without *R. oligosporus* stress, 3 days with the fungal stress (GS3d), and thermal-deactivated seeds inoculated without (D) or with (DS) fungal stress for 3 da... 209

Figure 12.7 HPLC chromatogram (310 nm) of peanut phytoalexins in peanut sprouts under food grade fungus *R. oligosporus* stress 211

LIST OF ABBREVIATIONS

1E5N	1-fold eaa and 5-fold neaa
4EBP1	4e binding protein 1
AA	amino acid
AC	adenylate cyclase
AEW	acetone/ethanol/water
AMPK	amp activated protein kinase
ANOVA	analysis of variance
BCAA	branched side chain amino acids
cAMP	cyclic adenosine monophosphate
CBS	citrate phosphate buffer solution
CDK	cyclin-dependent kinase
CFU	colony forming unit
CLS	chronological lifespan
CPT	cryptotanshinone
CR	calorie restriction
CRM	calorie restriction mimetics
DHE	dihydroergotamine
DMSO	dimethyl sulfoxide
DR	dietary restriction
DS/D	deactivated seed with/without fungal stress
DPPH	2,2-diphenyl-1-picrylhydrazyl
EAA	essential amino acids
eIF2	eukaryotic initiation factor-2
ER	endoplasmic reticulum
ERC	extrachromosomal rdna circles
ESI	electrospray ionization
FCM	flow cytometry
FDA	the Food and Drug Administration of the USA
FKBP12	FK506 binding protein 12
FRAP	FKBP-rapamycin associated protein
FW	fresh weight
GAAC	general amino acid control
GAE	gallic acid equivalents
GI50	50% growth inhibition
GLU	glucose
GS/G	germinated with/without fungal stress
GTP/GDP	guanosine triphosphate/guanosine diphosphate
H2DCFDA	2',7'-dichlorodihydrofluorescein diacetate
HDACs	histone deacetylases
HORAC	hydroxyl radical absorbance capacity
HPLC	high-performance liquid chromatography
HT	high throughput
HTS	high throughput screening
IGF	insulin-like growth factor
ITP	interventions testing program
LC-MS	liquid chromatography–mass spectrometry
MS	mass spectrometry
mTOR	mechanistic target of rapamycin

mTORC1	mTOR complex 1
NAD	nicotinamide adenine dinucleotide
NEAA	non-essential amino acids
NIA	national institute on aging
NMR	nuclear magnetic resonance
OD	optical density
ORAC	oxygen radical absorbance capacity
PBS	phosphate buffer solution
PDA	photodiode array
PDGF	platelet-derived growth factor
PI	propidium iodide
PI3K	phosphatidylinositol 3-kinase
PKA	protein kinase a
pRB	phosphorylated retinoblastoma protein
PTFE	polytetrafluoroethylene
RAFT	rapamycin and fkbp target
Ras	rat sarcoma
rDNA	ribosomal DNA
RLS	replicative lifespan
ROS	reactive oxygen species
RP-HPLC	reversed-phase high-performance liquid chromatography
RSD	relative standard deviation
RSM	response surface methodology
S6K1	s6 kinase 1
SD	synthetic defined
SD2D	synthetic defined medium with 2% dextrose
SDS	sodium dodecyl sulfate
Sir	silent information regulator
sirtuin	silent information regulator two (sir2) protein
SOD	superoxide dismutase
SORAC	superoxide radical absorbance capacity
STACs	sirtuin-activating compounds
TCM	traditional Chinese medicine
TFC	total flavonoids content
TOF-MS	time-of-flight mass spectrometry
TOR	target of rapamycin
TPC	total phenolic content
UG	non-germinated
USDA	united states department of agriculture
WT	wild type
YNB	yeast nitrogen base
YODA	yeast outgrowth data analyzer
YPD	1% yeast extract, 2% peptone and 2% glucose

LIST OF PUBLICATIONS

1. Wu Z, Song L, Liu S and Huang D. Cryptotanshinone extends yeast life span via conserved nutrient signaling pathways. In preparation.

2. Liu Y, Wu Z, Feng S, Yang X, Huang D. Hormesis of glyceollin I, an induced phytoalexin from soybean, on budding yeast chronological lifespan extension. In preparation.

3. Wu Z, Song L, Liu S and Huang D. Independent and additive effects of glutamic acid and methionine on yeast longevity. *PLoS One.* 2013, *8(11)*: e79319.doi:10.1371/journal.pone.0079319.

4. Wu Z, Song L, Liu S and Huang D. Dietary restriction depends on nutrient composition to extend chronological lifespan in budding yeast *Saccharomyces cerevisiae*. *PLoS One.* 2013, *8(5)*: e64448. doi:10.1371/journal.pone.0064448.

5. Wu Z, Song L, Feng S, Liu Y, He G, Yioe Y, Liu S and Huang D. Germination dramatically increases isoflavonoid content and diversity in chickpea (*Cicer arietinum* L.) seeds. *Journal of Agricultural and Food Chemistry*. 2012, *60*, 8606−8615.

6. Wu Z, Song L, Liu S and Huang D. A high throughput screening assay for determination of chronological lifespan of yeast. *Experimental Gerontology*. 2011, *46*, 915-922.

7. Wu Z, Song L and Huang, D. Food grade fungal stress on germinating peanut seeds induced phytoalexins and enhanced polyphenolic antioxidants. *Journal of Agricultural and Food Chemistry*. 2011, *59*, 5993−6003.

LIST OF PRESENTATIONS

1. Poster presentation. Independent and additive effects of glutamic acid and methionine on yeast longevity, *CSH-Asia Conference: Molecular Basis of Aging & Disease*, Suzhou, China, 2013.

2. Oral presentation. Amino acids extend yeast chronological lifespan, The 20th IAGG World Congress of Gerontology and Geriatrics, Seoul, South Korea 2013.

3. Oral presentation. A powerful high throughput assay based on yeast chronological aging model, *FST lunch time seminar*, Singapore 2012.

4. Poster presentation. Germination dramatically increases isoflavonoid content and diversity in chickpea (*Cicer arietinum* L.) seeds, *NUS-WUR Postgraduate Symposium*, Singapore, 2012.

5. Oral presentation. Polyphenolic antioxidants and phytoalexins changes in germinating legume seeds with food grade fungal *Rhizopus oligoporus* stress, *The 12th ASEAN Food conference*, Bangkok, Thailand 2011.

6. Oral presentation. Food grade fungal stress on germinating peanut seeds induced phytoalexins and enhanced antioxidants, *SIFST Student Symposium/Competition*, Singapore 2011.

7. Oral presentation. A high-throughput assay for screening caloric restriction mimetics by determination of chronological lifespan of yeast, *3rd NUS-TUMSAT symposium*, Singapore 2010.

8. Poster presentation. A high throughput assay for measuring antiageing activity of polyphenols, *IUFoST 15th World congress of food science and technology*, South Africa 2010.

Part I

SCREENING OF ANTI-AGING FACTORS USING A HIGH THROUGHPUT ASSAY

Chapter 1

INTRODUCTION

1.1 Background

Aging is a slow and very complex process, usually defined as the gradual, insidious, and progressive decline in structure and function of many different systems and tissues after the achievement of sexual maturity. Since ancient times, people have been interested in looking for the elixir of youth, and yet studies on genetic mechanisms of aging at molecular levels are relatively new and are far from being understood. Importantly, studies on yeast aging have had a significant impact on discovering the fountain of youth (Steinkraus *et al.* 2008; Kaeberlein 2010a; Longo *et al.* 2012). Some of the most promising longevity factors and potential anti-aging drugs (e.g. rapamycin and resveratrol) were first identified and characterized using yeast as a model organism (Howitz *et al.* 2003; Powers *et al.* 2006).

The major challenge for aging studies is extensive time consumption in measuring lifespans of organisms (Mair & Dillin 2008). By comparison with other organisms, the single-cell budding yeast *Saccharomyces cerevisiae* has a much shorter lifespan, well-established genetics and high throughput screening assays for measuring lifespan, which allows researchers to conveniently study genetic mechanisms of aging and to discover potential genetic and environmental factors that influence lifespan (Kaeberlein 2010a). However, it is important to understand which mechanisms of aging are conserved between yeast and mammals and which are specific to yeast (Bishop & Guarente 2007), because the evolutionarily conserved progress of aging in multispecies could be considered as intrinsic biological aging.

Advances in aging studies have shown that the yeast aging model can enable discovery of the evolutionarily conserved signaling pathways on regulation of longevity in various organisms and mammals (Fontana *et al.* 2010). In addition, recent work has shown that nutrients, small molecules, genetic modifications and other factors can substantially extend lifespan of multispecies, ranging from yeast to mammals.

Among these longevity factors, nutrient balance has been emerging as an important factor in extending lifespan. Yet, the effect of many nutrient factors on longevity is not well investigated. Most anti-aging studies focus on dietary restriction (DR) or calorie restriction (CR), the mere reduction of food intake without malnutrition, which has become a gold standard in aging studies. Dietary restriction was found to extend the average and maximum lifespan from yeast to rodents, and it also protects against age-related pathologies, such as diabetes, cancer, and cardiovascular disease in rhesus monkeys and humans (Mair & Dillin 2008; Fontana *et al.* 2010). However, studies have shown that changing the dietary components could eliminate lifespan extension by dietary restriction, suggesting that nutrient balance other than dietary restriction plays a pivotal role in regulation of longevity (Piper *et al.* 2011; Mattison *et al.* 2012).

Besides the nutrient factors, small molecule natural products also show their potential activity in prevention of age-related diseases and promotion of healthy aging in humans. So far the most extensively studied natural products are resveratrol and rapamycin (Kaeberlein 2010b). Resveratrol is an induced phytoalexin found in red wine and grapes. Rapamycin, isolated from a bacterium, is a prescription medicine as an immunosuppressant. Both compounds target conserved longevity pathways and

have been proposed to act as dietary restriction mimetics to delay aging in multiple model organisms.

Currently, it is commonly believed that a relatively effective and simple way to uncover the secrets of human longevity is focusing on studies of the genetic mechanism of longevity that is evolutionarily conserved in multiple organisms, from yeast to human, such as the sirtuin, the IGF (insulin-like growth factor)/insulin and the TOR (target of rapamycin) pathways. These pathways are considered as nutrient-sensing signaling pathways in modulating the beneficial effects of nutrients.

The biggest limitation for aging study is the large amount of time needed to measure lifespan of an organism. Using yeast chronological aging model could reduce experimental period significantly since yeast has a shorter chronological lifespan (CLS) relative to other model organisms. Herein, some **major gaps** for current aging studies are summarised:

- Several assays have been developed to measure yeast CLS. Most methods are based on the traditional CFU (colony forming unit) plating method that requires a relatively large investment of time and resources, and are not suitable for high throughput studies.
- Yeast is a preeminent model organism in studies of the fundamental biology of aging. However, nutrient composition as an important aging factor is little studied in yeast model, because recent studies suggested that dietary composition but not dietary restriction plays a key role for longevity in higher organisms.
- Resveratrol and rapamycin have been proposed as relatively promising anti-aging products. However, resveratrol cannot extend lifespan in mice and

rapamycin has strong side effects (see **Chapter 2.4**). Therefore, further exploration of better anti-aging candidates is needed.

1.2 Objectives

The **main aim of Part I of this thesis** is to explore the genetic mechanism of lifespan extension by nutrients and compounds using a high throughput assay in yeast chronological aging model. The **specific objectives of Part I research** were to:

- Develop a high throughput screening assay for determination of yeast CLS that could be convenient and easy to set up in a typical biology research lab (**Chapter 3**).
- Evaluate the role of pH, organic acids, and nutrients on influencing yeast CLS (**Chapter 4, 5**).
- Study the mechanism that a specific nutrient could extend lifespan (**Chapter 4, 5**).
- Carry out large-scale screening of botanical extracts and natural products for their anti-aging activity and explore the conserved longevity mechanism of a targeted compound (**Chapter 6, 7**).

The results of this study may have a significant impact on yeast chronological aging studies and aging related studies via two major contributions:

- ✓ Provide a comprehensive result for understanding the relationship between nutrients and lifespan, which suggest that yeast aging model could serve as an excellent model for studying nutrition and aging in future.
- ✓ Discover firstly a few novel longevity factors (nutrients and compounds) that could significantly extend yeast lifespan in addition to their potential longevity

mechanism, which may prompt further study on longevity effect in other higher organism models and develop anti-aging intervention based on these factors.

Although other factors could change yeast CLS, such as genes, proteins, and reactive oxygen species (ROS), this research concentrates on nutrients and compounds that can extend lifespan by using a high throughput assay. Furthermore, the studies on longevity mechanism focus only on those conserved pathways from different species, and other than the mechanism that is specific in budding yeast.

Chapter 2

LITERATURE REVIEW

2.1 Aging models in budding yeast

Studies of aging in mammals are time consuming due to their long lifespans. Mice and rats live 3–5 years and primates up to 40 years (Steinkraus *et al.* 2008). The use of invertebrate organisms as models is more rapid and straightforward for genetic and environmental manipulation. Although longevity has been studied in a number of organisms, most studies have employed fruit fly (*Drosophila melanogaster*), worm (*Caenorhabditis elegans*), or yeast (*S. cerevisiae*). Worms live approximately 2–3 weeks and flies 2–3 months (Steinkraus *et al.* 2008). Budding yeast has a much shorter lifespan (chronological mean lifespan is 6–15 days), well-established genetics, and is suitable for high-throughput screening (Mortimer & Johnston 1959; Kennedy *et al.* 1995; Sinclair *et al.* 1998; Steinkraus *et al.* 2008).

In the yeast model, two common aging assays have been established (Laun *et al.* 2006). Replicative lifespan (RLS) of yeast aging refers to the number of cell division occurring in a mother cell (Sinclair 2002). Yeast replicative aging may serve as a suitable model for the aging of mitotic cells in multicellular eukaryotes, such as human stem cell populations (Zimmermann & Martens 2008). Replicative aging is thought to occur through the asymmetric segregation of damage to mother cells during yeast budding (Kaeberlein 2010a).

CLS refers to the capability of cells to maintain viability in a growth-arrested state, such as stationary phase (Fabrizio & Longo 2003). Viability is calculated by the fraction of yeast able to re-enter the cell cycle after an extended state of quiescence

(Kaeberlein *et al.* 2007). Chronological aging has been used to model age-associated changes in post mitotic tissues (like neurons or skeletal muscle) of higher organisms.

Recent studies indicated that the two distinct aging models are regulated by partly overlapping mechanisms. For example, decreasing glucose of the media (CR), affecting Ras-cAMP-PKA or TOR/Sch9 signaling and reducing oxidative damage to mitochondrial and cytoplasmic proteins can increase both RLS and CLS. The two models thus provide a unique opportunity to study and compare cellular aging processes of dividing and non-dividing cells. However, it is important to focus on the common denominators that are responsible for regulation of aging in the both models. In this chapter, I focus on chronological aging and review the main methods for determination of CLS and their advantages and key remaining issues.

2.2 Methods for measuring yeast CLS

2.2.1 Traditional colony count plating method

The method for measuring CLS in budding yeast was first developed by Longo (Longo *et al.* 1996a, Longo 1999). In this protocol, the inoculation time point is day 0. Every 2-4 days, aliquots from aging culture are diluted and plated onto YPD plates. The cell survival is then calculated based on the number of colonies arising (CFU) on YPD plates within 3 days. The number of CFUs of aging culture at day 2 or 3 is usually considered to be the initial age-point or time point survival (defined as 100% survival) and CLS is based on measuring the estimated fraction of cells retaining viability as a function of time. CFUs are normally monitored until at least 99.9% of the population dies (Fabrizio & Longo 2003). There are at least three traditional methods to measure CLS according to the medium used.

Aging culture in synthetic defined medium. This is the most common method for monitoring survival of yeast grown and maintained in liquid synthetic defined (SD) medium during the entire chronological aging period (stationary phase) (Fabrizio *et al.* 2001). It is a widely accepted method for studies in yeast chronological aging. The method is relatively time-saving due to yeast has a short lifespan in SD medium, usually 4-15 days depending on their genetic background. The exhausted medium contains many highly stressing metabolites during the stationary phase, such as ethanol, acetic acid, and other organic acids (Burtner *et al.* 2009b). A study reported by the Kaeberlein lab showed that nutritional metabolites in the medium contribute to aging. In particular, acetic acid was proposed as a key toxic factor inducing cell death (Burtner *et al.* 2009b; Kaeberlein 2010a). However, a potential artefact that could be observed in this model is regrowth, which might confound the explanation of survival data (Fabrizio & Longo 2003). The regrowth is important for adaptation to starvation conditions, and many wild type (WT) laboratory microorganisms have adaptive regrowth when usually 90-99% of the population dies. A good way to prevent any occurrence of regrowth is transferring aging cultures to water during stationary phase.

Aging culture in water. The method which was firstly developed in the Longo lab is that yeast is first grown to the stationary phase in liquid SD medium at high metabolic rates for 1 to 5 days and then switched to water (Longo *et al.* 1996a). Chronological aging in water mimics the environment in the wild since yeast survive in a low-metabolising stationary phase under nutrient-depleted conditions, which have low nutritional metabolites interference and no regrowth phenomenon. However, yeast can survive much longer in water than yeast maintained in the SD medium, usually by more than 15 days, hence significantly prolonging the period of experiment needed for measuring the CLS (Fabrizio & Longo 2003). On the other hand, the water

condition is distinct to the cells of higher organisms grown in a nutrient-rich environment.

Aging culture in YPD medium. The nutrient-rich YPD (1% yeast extract, 2% peptone and 2% glucose) medium is also chosen for chronological aging studies. The shape of mortality curves for yeast grown in the YPD was similar to mortality patterns observed in multicellular eukaryotes (Minois *et al.* 2009). On the other hand, pH values of yeast cultures grown in YPD medium are much closer to that of body fluids (7.1 to 8.6), which are higher than the pH of yeast cultures maintained in the SD medium (2 to 4). The acidification of aging cultures was reported to accelerate chronological and replicative aging in yeast (Murakami *et al.* 2012). However, yeast cultivated in the YPD medium was similar to that cultivated in water, in terms of lifespan, which result in extensive time-consumption for the lifespan determining experiment. Moreover, individual components in the YPD medium are undefined and it thus is not suitable for studies on the roles of individual nutrients (i.e. amino acids, nitrogen sources, vitamins, minerals, and other nutrients) in yeast lifespan regulation.

2.2.2 Flow cytometry method

Recently, an alternative approach to the CFU counts, based on propidium iodide (PI) staining combined with flow cytometry (PI-FCM), was proposed for the assessment of yeast chronological aging (Ocampo & Barrientos 2011). The PI staining method is commonly used for assessment of microbial viability and is based on the fact that PI will not diffuse into viable cells due to its plasma membrane impermeability. Dead cells will lose the PI membrane impermeability and therefore become strained. Combined with FCM, this method provides a quick, less labor-intensive, reproducible and high-throughput quantification of yeast populations.

However, a later study showed that this method is highly influenced by the aging media. A correlation between CFU counts and PI-FCM measured cells is only achieved for yeast maintained in the exhausted media and not for yeast chronologically age in water (Pereira & Saraiva 2013).

2.2.3 High throughput method based on outgrowth of aging cells

A high throughput based method for measuring yeast CLS was firstly developed by the Kaeberlein group (Murakami *et al.* 2008). The assay applies a Bioscreen C MBR machine to monitor outgrowth of aging cells at each age-point, aging culture (5 µL) is inoculated into YPD medium (145 µL) in an individual well of 100-well Bioscreen Honeycomb plate. It shows that this assay is faster, less labor-intensive and less costly than the traditional CFU plating method. The Bioscreen instrument can incubate a maximum of 200 wells/samples per assay at 30 °C under constant agitation, and the optical density (OD) at approximately 420-580 nm of each well is recorded in intervals of 30 minutes for 24 hours. It means a maximum throughput of 1400 samples per week can be measured by the instrument. Outgrowth curves for each well/sample can be plotted from the OD measurements as a function of time, and the viability is then determined by outgrowth curve. This method provides reduced variance comparing to the CFU platting method. In addition, more information on the aging cells, such as doubling time, growth curve/rate, and cell optical density can be measured. Overall, this high throughput method offer several advantages as summarized in **Table 2.1**.

Table 2.1 Comparison of traditional CFU plating method and high throughput method for measuring yeast CLS (Fabrizio & Longo 2003; Murakami et al. 2008)

	CFU plating method (100 samples)	High throughput method (100 samples)	Advantages/disadvantages of HT method
Culture dishes used	>100 culture dishes	one 100-well plate	Cost saving
Medium amount	>2000 mL YPD medium	15 mL YPD medium	Cost saving
Time consumption for medium and sample plating	> 5 h	0.5 h	Time saving
Incubation time	> 48 h	24 h	Time saving
Recording way	manual count	plate reader	Reduced error
Quantitative data	CFU	lag-time, growth rate, doubling time, survival, OD	More information
Limitation of detection	Until all cell died	99.9%	Low LOD

2.3 Nutrients and longevity

2.3.1 Carbohydrates

Granot and coworkers were the first to report D-glucose, not L-glucose, as an important nutrient affecting yeast CLS (Granot & Snyder 1991). They demonstrated that stationary phase yeast cells lose viability more rapidly when cells were incubated in the presence of glucose than in the absence of glucose in a medium. Glucose restriction, typically referred to as CR or DR in yeast aging model, was found to extend both yeast RLS and CLS significantly. In yeast aging studies, the most common protocol for CR is based on the decrease of the glucose concentration in the medium from the standard 2% to 0.5. However, a number of studies reported that the further restriction (to 0.05% glucose) is considered as extreme CR to enhance the longevity of CR, as well as the one achieved by transferring cells grown in 2% glucose to water, even though the extreme CR is considered to cause malnutrition in

higher organisms. Currently, although the mechanism of CR induced longevity is still not fully understood, recent studies have revealed that the major nutrient-signaling pathways TOR, Sch9, and Ras/AC/PKA are all involved in longevity regulation by glucose.

In addition to glucose, glycerol as a non-fermentable carbon source was also reported to prolong both RLS and CLS (Kaeberlein *et al.* 2002; Burtner *et al.* 2009b; Wei *et al.* 2009). Burtner *et al.* suggested that glycerol induced longevity in chronological aging is due largely to the reduction in acetic acid accumulation (Burtner *et al.* 2009b). Acetic acid toxicity was proposed as the predominant cause of chronological aging under the standard conditions used in the majority of previous studies. On the other hand, another study showed that glycerol did not adversely affect CLS extension induced by CR, suggesting that glycerol affects chronological aging through the regulation of stress resistance systems, such as enhancing resistance to osmotic stress and modulating the redox balance of the cell (Wei *et al.* 2009). A recent study showed that WT cells accumulate ethanol and rapidly deplete glycerol, while long-lived mutants *tor1*Δ, *sch9*Δ and *ras2*Δ accumulate glycerol whereas ethanol was depleted first. These observations indicated that inhibition of Tor1/Sch9 mediated a metabolic switch from biosynthesis and release of ethanol to activation of glycerol biosynthesis and its consequent release (Wei *et al.* 2009).

2.3.2 Amino acids

Amino acids are important nutrients that can be recycled by autophagy in yeast. In nature, yeast are prototroph capable of synthesizing most of amino acids from simple carbon and nitrogen sources, while laboratory strains usually are auxotrophic to confer a nutrient-limiting growth phenotype useful for genetic manipulation. They

commonly defect a few genes involved in the biosynthesis of specific amino acids or nucleotides.

Limiting levels of auxotrophy-complementing amino acids (essential amino acids, EAA) in the growth medium caused a reduced final biomass, a decreased resistance to oxidative stress, an early arrest in G2/M phase together, and finally resulted in a shorter CLS (Gomes *et al.* 2007). In accordance, a reduction of total amino acid concentration, including essential ones, of the growth medium also decreases CLS (Murakami *et al.* 2008). Deprivation of leucine or uracil in nondividing leucine or uracil auxotrophic yeast cells induces an exponential loss of viability with a half-life of less than 2 days (Boer *et al.* 2008). Nevertheless, the survival rates of nongrowing auxotrophs deprived of leucine or uracil is partially dependent on the carbon source present in the starvation medium but not in that used in the growth medium. However, not all EAA have the same effect on CLS. In fact, methionine restriction of methionine auxotrophic yeast strain has no effect on viability (Unger & Hartwell 1976).

Nonessential amino acids (NEAA) were also reported to modulate yeast lifespan. Alvers *et al.* reported that the NEAA isoleucine and valine, and the essential amino acid leucine, extended CLS in autophagy-deficient (*atg1*Δ, *atg7*Δand *atg11*Δ) as well as autophagy-competent (WT strain *S. cerevisiae* BY4742 (MATα *his3*Δ1 *leu2*Δ0 *lys2*Δ0 *ura3*Δ0)) yeast in SD minimal media (Alvers *et al.* 2009a). The authors demonstrated that CLS was extended by the branched side chain amino acids (BCAA) leucine, isoleucine and valine, via the general amino acid control (GAAC) pathway. A reduced concentration of BCAA activates GAAC and shortens CLS, while an increased level of BCAA suppresses GAAC and lengthens CLS in minimal medium (Alvers *et al.* 2009a). In addition, lowering the total amino acids concentration of the

growth medium was reported to extend the mean and maximal RLS (Jiang *et al.* 2000). Removal of preferred amino acids asparagine (a high nitrogen quality amino acid) or glutamate (an intermediate nitrogen quality amino acid) conferred CLS extension in synthetic complete media (Powers *et al.* 2006).

2.3.3 Other nutrients

In yeast culture, NH_4^+ is commonly used as a major nitrogen source for growth and has a central role in nitrogen metabolism both in degradative and biosynthetic pathways (ter Schure *et al.* 2000). Inorganic nitrogen sources need to be converted into glutamate and glutamine before they are transferred to other biomolecules through transaminase. Yeast can select the nitrogen sources through nitrogen catabolite repression mechanism. Recently, a study reported that ammonium was toxic for aging cells and acted as an extrinsic factor affecting CLS (Santos *et al.* 2012). Decreasing the concentration of NH_4^+ increases yeast CLS in amino acid restricted media. In contrast, increasing $(NH_4)_2SO_4$ concentration (from 0.5% to 1%), either with or without restriction of amino acids, decreases cell survival. Moreover, after transferring aging cells to water, NH_4^+ addition decreases the CLS considerably, indicating that ammonium alone could also induce loss of cell viability (Santos *et al.* 2012). The cell death induced by ammonium was thought to be mediated via the regulation of the evolutionarily conserved pathways PKA, and TOR/Sch9 (Santos *et al.* 2012).

2.4 Natural products for lifespan extension

Perhaps the most effective anti-aging intervention is CR. Recent research suggested that the beneficial health effects of CR might be attained by a compound

that alters the activity of some evolutionarily conserved longevity proteins in response to nutrient availability (Kaeberlein 2010b). The compound could act as a "CR mimetic" by delaying age-associated diseases and extending lifespan without requiring reduced food intake (Ingram *et al.* 2006). There are a number of natural products that have been reported to have lifespan extending capacity or anti-aging benefit, including vitamin E, metformin, spermidine, curcumin, royal jelly, astragalan et al (Lebel *et al.* 2012; Pan *et al.* 2012; Spindler 2012; Lucanic *et al.* 2013) (**Table 2.2**). However, most of these compounds were found to suffer from serious confounding variables and only a few compounds could have potential effects of CR in mammals, such as resveratrol and rapamycin (Spindler 2012). The low reproducibility of these anti-aging compounds in different studies might be due to variation in animal model and food components involved (Spindler 2012).

Table 2.2 Comparison of the effect of other natural products on lifespan extension in different organisms

Compound	Strain/animal model	Culture condition	Dose / treatment time	Lifespan extension effect	Reference
Caffeine	*S. cerevisiae* BY4741	SD medium	0.4, 0.8, 1 mM, exponential growth phase	CLS: significant increase	Wanke *et al.* 2008
Spermidine	*S. cerevisiae* BY4741	SC medium	4 mM, stationary cultures (day 1)	CLS: significant increase	Eisenberg *et al.* 2009
Spermidine	*S. cerevisiae* BY4741	SC medium	1 mM, added at day 0	RLS (old cell): significant increase	Eisenberg *et al.* 2009
Spermidine	*C. elegans* N2	NGM with *E. coli* OP50	A range of concentrations, L4 larval stage	15% increase at 0.2 mM	Eisenberg *et al.* 2009
Spermidine	*D. melanogaster* isogenized w^{1118}	Liquid food medium	10 μM to 10 mM, newly eclosed flies	30% increase at 1 mM	Eisenberg *et al.* 2009
Curcumin	*C. elegans* N2	NGM with *E. coli* OP50	20 or 200 μM, L1 larvae	39% increase at 20 μM	Liao *et al.* 2011
Curcumin	*D. melanogaster* Canton-S and Ives	CSY medium	10 to 1000 μM, Newly eclosed adult	19% Canton-S female at 100 μM, 16% Ives male at 250 μM	Lee *et al.* 2010
Curcumin	*D. melanogaster* Ra	AL food	100 mM, different life stages	stage-specific extension	Soh *et al.* 2013
Metformin	*C. elegans* N2	NGM with *E. coli* OP50	1, 10, 50, or 100 mM, L4 stage	40% increase at 50 mM	Onken & Driscoll 2010
Metformin	*C. elegans* N2	NGM with *E. coli* OP50	25, 50, or 100 mM, L4 stage	36% increase at 50 mM	Cabreiro *et al.* 2013
Metformin	*M. musculus* Female transgenic HER-2/neu	standard laboratory chow	100 mg/kg, age of 2 months	8% increase	Anisimov *et al.* 2005; Anisimov *et al.* 2010a
Metformin	*M. musculus* Outbred Swiss-derived female SHR mice	standard laboratory chow	100 mg/kg, age of 3 months	37.8% increase	Anisimov *et al.* 2008
Metformin	*M. musculus* inbred 129/Sv	standard laboratory chow	100 mg/kg, age of 2 months	13.4% decrease in male, 4.4% increase in female	Anisimov *et al.* 2010b
Metformin	*Rattus norvegicus* Male F344, rats	standard chow diet	300 mg/kg, age of 6 months	no significant increase	Smith *et al.* 2010

Table 2.2 Continued

Metformin	*M. musculus* Outbred Swiss-derived female SHR mice	standard laboratory chow	100 mg/kg, 3, 9, 15 months old	14% (3), 6% (9), no increase (15)	Anisimov *et al.* 2011a
Tyrosol	*C. elegans* N2	NGM with *E. coli* OP50	250 μM, the egg stage	21% increase	Canuelo *et al.* 2012
Quercetin	*C. elegans* N2	NGM with *E. coli* OP50-1	100 μM, days after hatching	15% increase	Kampkotter *et al.* 2008
Quercetin	*C. elegans* N2	NGM with *E. coli* OP50	100, 200 μM, days after hatching	15% increase	Pietsch *et al.* 2009
Lithocholic acid	*S. cerevisiae* BY4742	YPD medium	5 μM to 100 μM, added at day 0	CLS: significant increase	Goldberg *et al.* 2010; Burstein *et al.* 2012
Baicalein	*C. elegans* N2	NGM with *E. coli* OP50	100 μM, day 3 after egg laying	45% increase	Havermann *et al.* 2013
D-chiro-inositol	*D. melanogaster* Canton-S	CSY medium	20 to 200 μM, Newly eclosed adult	16.7% male and 13% female increase at 20 μM	Hada *et al.* 2013
Pinitol	*D. melanogaster* Canton-S	CSY medium	20 to 200 μM, Newly eclosed adult	13% male and 12.5% female increase at 20 μM	Hada *et al.* 2013

2.4.1 Resveratrol

Resveratrol and its analogues are polyphenolic phytoalexins that occur naturally in many plant species, including Japanese knotweed, grapes, berries and peanuts. A number of reports highlighted resveratrol benefits *in vitro* and *in vivo* in many physiological models of human diseases, such as cancer, heart disease, inflammation, diabetes, ischaemic, and especially aging. Resveratrol extends RLS in the yeast *S. cerevisiae* (Howitz *et al.* 2003) and prolongs the lifespan in different organisms (**Table 2.3**). However, resveratrol extends only yeast RLS by up to 100% (>10 μM) (Jarolim *et al.* 2004), and does not extend CLS even at 100 μM in the short lived PSY316AT strain (Howitz *et al.* 2003). Although many studies reported the longevity extending activity of resveratrol, there is still no strong evidence to show that resveratrol prolongs lifespan in mammals.

Resveratrol is still a promising anti-aging compound because it was proposed to be the activator of histone deacetylase or sirtuins. Sirtuins (silent mating type information regulation 2 homolog) belong to a family of nicotinamide adenine dinucleotide (NAD)-dependent histone deacetylases (HDACs). In mammals, seven SIRTs are found with different biochemical activities, and are differentially located within the cellular compartments: the nucleus (SIRT1, SIRT2, SIRT6,) and nucleolus (SIRT7), the cytoplasm (SIRT1 and SIRT2), and the mitochondria (SIRT3, SIRT4, and SIRT5). SIRT1 plays important roles in various metabolic pathways, cell survival, DNA repair and apoptosis (Haigis & Sinclair 2010; Chalkiadaki & Guarente 2012).

Table 2.3 Comparison of the effect of resveratrol on lifespan in different organisms investigated by different laboratories

Strain/animal model	Culture condition	Dose / treatment time	Lifespan effect	Reference
S. cerevisiae PSY316AT	YPD medium	10 to 100 µM, added at day 0	RLS: 70% increase at 10µM CLS: no increase	Howitz *et al.* 2003
S. cerevisiae K6001	SC medium	10 to 100 µM, added at day 0	RLS: significant increase at 10µM	Jarolim *et al.* 2004
S. cerevisiae W303R, BY4742, PSY316	YPD medium	10 to 100 µM, added at day 0	RLS: no significant increase	Kaeberlein *et al.* 2005a
S. cerevisiae PSY316AT	YPD medium	10 µM, added at day 0	RLS: 68% increase for derivative 5	Yang *et al.* 2007
S. cerevisiae EMY74.7	SC medium	10 to 200 mM, added at day 0	CLS: no significant increase	Yu *et al.* 2013
C. elegans N2	NGM media with *E. coli* OP50	10 to 100 µM, 2 days after hatching	10% increase at 100µM	Wood *et al.* 2004
C. elegans N2	NGM media with *E. coli* OP50	100 to 1000 µM, L4 to young adult	18% increase at 1000µM	Viswanathan *et al.* 2005
C. elegans N2	NGM media with *E. coli* OP50	100 µM, 2 days after hatching	Slight increase in some trials but not others	Bass *et al.* 2007
C. elegans N2	NGM media with *E. coli* OP50	50 µM, 2 days after hatching	mean LS 64%, maximum LS 30%	Gruber *et al.* 2007
C. elegans N2	NGM with *E. coli* OP50–1	100 µM, the days after hatching	a modest, but statistically significant increase	Greer & Brunet 2009
C. elegans N2	NGM with *E. coli* OP50	0.5, 5 µM, the days after hatching	mean LS3.6 %, maximum LS3.4 % at 5 µM	Zarse *et al.* 2010
C. elegans N2	NGM with *E. coli* OP50	65 µg/mL, 3 days after hatching	significant increase	Sunagawa *et al.* 2011
D. melanogaster Canton-S	CSY media	10 to 100 µM, newly eclosed adults	20% in females and 16% in males at 100µM	Wood *et al.* 2004
D. melanogaster Canton-S	CSY media without yeast	200 µM, newly eclosed adults	16% in females and 10% in males at 200µM	Bauer *et al.* 2004

Table 2.3 Continued

Strain/animal model	Culture condition	Dose / treatment time	Lifespan effect	Reference
D. melanogaster Dahomey and Canton S	SY or MSY medium	1 to 1000 µM, Once-mated	Females and males: no significant increase	Bass *et al.* 2007
Anastrepha ludens, Fly	Sugar:yeast medium	100 µM, newly eclosed adults	no or little significant increase	Zou *et al.* 2009
D. melanogaster Oregon	Standard corn meal	0.43 mM, 15 days after emerging from the pupa	maximum LS: 34% increase	Bonilla *et al.* 2012
D. melanogaster Canton-S	CSY media	100, 200, 400 µM, 2 days after eclosion	Increase depends on gender and diet	Wang *et al.* 2013
Apis mellifera, Honey bees	1.5 g pollen in 30 mL of 30% sucrose solution	30, or 130 µM, four-day-old honey bees	38% increase at 30µM , 33% increase at 130µM	Rascon *et al.* 2012
Nothobranchius furzeri, Gonarezhou, Fish	Bloodworm larvae (*Chironomus sp*.)	24 to 600 µg/g(food), after sexual maturity	Median LS 56%, maximum LS 59% at 600 µg/g(food)	Valenzano *et al.* 2006
Nothobranchius furzeri TZ 97-2, Fish	brine shrimp and bloodworm larvae	200 µg/g food, 16 weeks of age	median LS 19%, maximum LS 28%	Yu & Li 2012
Nothobranchius furzeri, Fish	not stated	12 µg resveratrol/fish/day, 12 weeks of age	median LS 42.9%, maximum LS 17%	Genade & Lang 2013
M. musculus C57BL/6NIA	Standard or high-calorie (hydrogenated coconut oil) AIN-93G diet	0.01%, or 0.04%(food), 1 year male	High-calorie diet: 26% for 0.01%, 25% for 0.04%; Standard diet: No significant increase	Pearson *et al.* 2008
M. musculus UM-HET3	TestDiet, free water	300 or 1200 ppm, age of 10 or 12 months male and female	no significant increase	Miller *et al.* 2011; Strong *et al.* 2013
Rattus norvegicus Wistar, Rats	Standard food	0.0015, 4 mg/kg, 12 months old male	no significant increase	da Luz *et al.* 2012
M. musculus SAMP8 and SAMR1	Standard diet	1g/kg, 2 months of age male	mean LS: 33% SAMP8, 22% SAMR1	Porquet *et al.* 2012

Naturally occurring (resveratrol, butein, fisetin, quercetin) and chemically synthetic (SRT1460, SRT1720, SRT2183) sirtuin-activating compounds (STACs) activate SIRT1 *in vitro* by lowering its peptide Michaelis constant for both the acetylated substrate and NAD^+, and increase cell survival by stimulating SIRT1-dependent deacetylation of p53 (Howitz *et al.* 2003). In yeast, resveratrol mimics CR by stimulating Sir2 (the yeast homologue of human SIRT1), increasing DNA stability and extending lifespan. Although the legitimacy of STACs as direct SIRT1 activators has been widely debated (Kaeberlein *et al.* 2005a; Couzin-Frankel 2011), Sinclair group reported recently that SIRT1 can be directly activated through an allosteric mechanism common to resveratrol and other STACs *in vitro*, but only under certain conditions (Hubbard *et al.* 2013).

2.4.2 Rapamycin

Rapamycin, also known as sirolimus, was first discovered by Brazilian researchers as a new antibiotic with strong antifungal activity, secreted by the bacterium *Streptomyces hygroscopicus* that was isolated from a soil sample in Easter Island, an island also known as Rapa Nui (Sehgal *et al.* 1975; Vezina *et al.* 1975). Since then, rapamycin was widely studied as an immunosuppressant before its mechanism of action was known, and in 1999 it was approved by US Food and Drug Administration (FDA) for use in post-transplantation therapy (Johnson *et al.* 2013).

The mode of action of rapamycin is to bind the cytosolic protein FK-binding protein 12 (FKBP12), and then the rapamycin-FKBP12 complex inhibits the mechanistic (previously referred to as mammalian) target of rapamycin (mTOR) pathway by directly binding the mTOR Complex1 (mTORC1). mTOR has also been called FRAP (FKBP-rapamycin associated protein), RAFT (rapamycin and FKBP

target), RAPT1, or SEP. However, mTOR is now the widely accepted name, since a study in the yeast *S. cerevisiae* first identified the target of rapamycin genes *TOR1* and *TOR2* as genetic mediators of rapamycin's growth inhibitory effects (Powers *et al.* 2006). The mTOR signaling pathway senses and integrates a variety of environmental cues to regulate organismal growth and metabolism (Wullschleger *et al.* 2006). The pathway regulates many major cellular processes, including protein synthesis, lipogenesis, energy metabolism, autophagy, lysosome biogenesis and cytoskeletal organization. Thus, mTOR is implicated in an increasing number of pathological conditions, including cancer, obesity, type 2 diabetes, neurodegeneration and aging (Laplante & Sabatini 2012).

The role of rapamycin in longevity extension has been clearly demonstrated in both simple model organisms and mammals. Rapamycin at relatively low concentration is sufficient to increase lifespan in yeast, nematode, flies and mice (**Table 2.4**). To date, rapamycin is proposed as the only molecule that appears to influence the intrinsic rate of aging in mammals, as evidenced by a robust extension of maximum lifespan. The multicentric aging Interventions Testing Program (ITP) from the National Institute on Aging reported that inhibition of mTOR by rapamycin expands median and maximal lifespan of genetically heterogeneous mice (Miller *et al.* 2007; Harrison *et al.* 2009; Miller *et al.* 2011). Remarkably, the lifespan extension was observed even in male and female mice when fed beginning at 600 days old, at a stage roughly equivalent to 60-year-old human. Although these results cannot be directly extrapolated to humans, they suggest that these findings have implications for further development of interventions targeting mTOR for the treatment and prevention age-related diseases even when the treatment is initiated at mid-age (Harrison *et al.* 2009).

Table 2.4 Comparison of effect of rapamycin on lifespan in different organisms investigated by different laboratories

Strain/animal model	Culture condition	Dose / treatment time	Lifespan effect	Reference
S. cerevisiae BY4743 diploid	YPD medium	100 to 1000 pg/mL, added at day 0	CLS: significant increase at 1ng/mL	Powers *et al.* 2006
S. cerevisiae W303AR	YPD medium	1 nM, added at day 0	RLS: 15% increase	Medvedik *et al.* 2007
S. cerevisiae BY4742	SC minimal medium	0.1 to 40 nM, added at day 0	CLS: significant increase at 20 and 40 nM	Alvers *et al.* 2009b
S. cerevisiae DBY2006	SD medium	200 nM, added at day 0	CLS: significant increase	Pan *et al.* 2011
C. elegans N2	NGM with *E. coli* OP50–1	100 μM, late L4 stage	19% increase	Robida-Stubbs *et al.* 2012
D. melanogaster white Dahomey (w^{Dah})	Standard SYA media	1 to 400 μM, newly eclosed adults	17% for females at 200 μM	Bjedov *et al.* 2010
M. musculus CB6F1 females × C3D2F1 males	Test Diet	14mg/kg food, at 600 days of age	14% for females, 9% for males	Harrison *et al.* 2009
M. musculus FVB/N HER-2/neu	not stated	1.5 mg/kg food, age of 2 months	maximal LS 12.4%; transgenic cancer-prone female	Anisimov *et al.* 2010c
M. musculus UM-HET3	Test Diet, free water	14 mg/kg food, age of 9 months	10% increase in males, 18% increase in females	Miller *et al.* 2011
M. musculus 129/Sv	not stated	1.5 mg/kg food, age of 2 months	7.8% increase for females	Anisimov *et al.* 2011b
M. musculus C57B1/6	not stated	1.5 mg/kg food, the age < 5 months	28% increase, p53+/- male	Komarova *et al.* 2012
M. musculus C57B1/6	not stated	0.5 mg (nanoformulated micelles of rapamycin)/kg food, age of 2 months	30% increase, p53-/- male	Comas *et al.* 2012

Earlier human trials have shown that rapamycin can have serious side effects, including hyperlipidaemia and hyperglycaemia, anaemia and stomatitis (Johnson *et al.* 2013). Because it is an immunosuppressant, it can make users susceptible to opportunistic infections (Shiffman *et al.* 2004). Recent evidence suggests that chronic treatment with rapamycin impairs glucose homeostasis and induce diabetes-like symptoms such as decreased glucose tolerance and insensitivity to insulin (Lamming *et al.* 2012). However, optimal dosage and duration of treatment are still not established, the lower bioavailability and the different pharmacokinetic of rapamycin have probably limited the exposure of the tissues to the drug, thus reducing its adverse effects.

2.5 The evolutionarily conserved signaling pathways

Change in both nutrient compositions and nutrient-sensing pathway activity can extend lifespan, protect against age-related diseases or lower the incidence of age-related loss of functions and diseases from yeast to human. Thus, evolutionarily conserved nutrient-sensing signaling pathways are highlighted as the primary targets for development of anti-aging interventions (Fontana *et al.* 2010). Herein, I focus on the main nutrient-sensing pathways in yeast and discuss their functions in regulation of lifespan.

2.5.1 TOR/Sch9 pathway

TOR kinases and the ribosomal S6 kinase Sch9 are highly conserved in organisms ranging from yeast to humans and function to control growth, metabolism, stress resistance, and aging in response to nutrient and growth factor cues (Fontana *et al.* 2010).

Yeast possesses two TOR genes (*TOR1* and *TOR2*), while higher eukaryotes have only a single TOR gene (Crespo & Hall 2002). TOR exists in two complexes with different functions in all eukaryotes. The budding yeast TORC1, which is sensitive to rapamycin, contains Tor1 or Tor2, Kog1, Lst8 and Tco89, and controls cell size, proliferation and lifespan via a variety of downstream pathways (Wullschleger *et al.* 2006; Kapahi *et al.* 2010; McCormick *et al.* 2011). On the other hand, TORC2 (which is insensitive to rapamycin) contains Tor2, Lst8, Avo1, Avo2, Avo3 and Bit61. Its function is involved in regulation of actin organization, cell wall integrity, and sphingolipid metabolism (Wullschleger *et al.* 2006; Kapahi *et al.* 2010; McCormick *et al.* 2011). Rapamycin binds peptidylprolyl isomerase FKBP12, the formed complex then binds to the amino-terminal of Tor1 or Tor2, and consequently inhibits TORC1 activity, but fails to bind TORC2 from yeast to mammal (Loewith *et al.* 2002). In budding yeast, Tor1 is not essential for cell viability, since it can be substituted by Tor2 in TORC1 when the cell is short of Tor1. In contrast, Tor2 is essential for viability, because Tor2 processes an essential function as core component of TORC2, and Tor1 cannot replace Tor2 in TORC2 (Kunz *et al.* 1993; Helliwell *et al.* 1994; Stan *et al.* 1994; Schmidt *et al.* 1996). Overall, the two TOR complexes as well as their rapamycin sensitivity are all conserved from yeast to man.

The AGC kinase Sch9 is a substrate of TORC1, and its function may be similar to the mammalian TORC1 substrate S6K1 (S6 kinase 1) rather than the mTORC2 substrate PKB/Akt. In yeast, *sch9*Δ mutant cells show a small-sized phenotype (60% of WT in volume) and slow growth rate, while possessing strong stress resistance and prolonged lifespan (Wei *et al.* 2008). Deletion or inhibition of either *SCH9* or *TOR1* causes substantial lifespan extension in both chronological and replicative aging model. However, the effects on both CLS and RLS caused by deficiency in Sch9

activity are more robust than those observed in the strain lacking Tor1, and the mean CLS of *tor1*Δ*sch9*Δ and *sch9*Δ have no significant difference (Kaeberlein *et al.* 2005b; Wei *et al.* 2009). These observations suggest that the lack of *TOR1* contributes to the further reduction of the Sch9 activity and also supports the notion that Sch9 is a major substrate of yeast TORC1 (Urban *et al.* 2007; Wei *et al.* 2009).

It was reported that reduced Tor1 or Sch9 activity acts downstream of dietary restriction to increase CLS and RLS. During chronological aging, the TOR/Sch9 and Ras/AC/PKA pathways appear to be mediated by the down regulation of the protein kinase Rim15 and consequent control of Gis1 and Msn2/4 stress-responsive transcription factors. Inhibition of TOR/Sch9 pathway also decreases ROS production and enhances cellular stress responses, culminating in lifespan extension (Fontana *et al.* 2010).

2.5.2 Ras/AC/PKA pathway

In the presence of glucose, the budding yeast Ras/AC/PKA pathway is activated. The major components of this pathway include guanosine triphosphate/guanosine diphosphate (GTP/GDP)-binding proteins (Ras1 and Ras2), a GTP-GDP exchange factor (Cdc25), GTP hydrolysis factors (Iral and Ira2), the adenylate cyclase (AC, Cdc35/Cyr1), phosphodiesterases (Pde1 and Pde2) that catalyse the hydrolysis of cyclic adenosine monophosphate (cAMP), a protein kinase A (PKA) regulatory subunit (Bcy1), and a PKA catalytic subunit (Tpk1, Tpk2, and Tpk3) (Thevelein & de Winde 1999; Lin *et al.* 2000b).

Yeast *RAS1* and *RAS2* are highly homologous to mammalian RAS genes (Sun *et al.* 1994). The G proteins Ras1 and Ras2 function upstream of Cyr1 (AC) and play overlapping roles in functions including growth, pseudohyphal development, stress

resistance, and aging (Fabrizio *et al.* 2003). Ras proteins cycle between inactive GDP-bound (Ras-GDP) and active GTP-bound (Ras-GTP) states. In the presence of glucose, Ras proteins become activated, and the resulting Ras-GTP binds to Cyr1 and stimulates the production of cAMP. Ras proteins activity is regulated positively by the guanine nucleotide exchange factors (RasGEF) (Cdc25 and Sdc25 in yeast) and negatively by the GTPase-activating proteins (RasGAP) (Ira1 and Ira2 in yeast). Deletion of *RAS1* gene increases RLS and slightly decreases CLS, while deletion of *RAS2* gene decreases RLS and doubles CLS (Sun *et al.* 1994; Fabrizio *et al.* 2003). Deletion of *RAS2* promotes an increase of heat and oxidative stress resistance (Fabrizio *et al.* 2003).

Ras proteins directly activate AC and a mutation causing loss of AC activity was shown to extend CLS (Fabrizio *et al.* 2001). The *CYR1* gene encodes AC, which is a key enzyme that catalyses the synthesis of cAMP from ATP and plays important roles in pathways that are involved in glucose-dependent signaling and stress resistance. In fact, deletion of one of the mammalian adenylate cyclase isoforms *AC5*, increased mice's median lifespan by approximately 30%, protected against oxidative stress, apoptosis, and osteoporosis (Yan *et al.* 2007).

In the budding yeast, cAMP-PKA is composed of three catalytic subunits encoded by the genes *TPK1*, *TPK2* and *TPK3*, and one regulatory subunits encoded by the gene *BCY1* (Toda *et al.* 1987a; Toda *et al.* 1987b). The intracellular level of cAMP is controlled by two routes involving either the Ras proteins Ras1/Ras2, or the G_{α} protein Gpa2. The GTP-bound form of Ras proteins (active) directly interacts with the Cyr1, and stimulates the production of cAMP. An increased intracellular cAMP binds to the regulatory subunit of PKA (Bcy1), causing PKA (inhibitive) to dissociate from the catalytic subunits (Tpk1, 2 and 3). These catalytic subunits (active) are then

free to phosphorylate their respective targets and thereby exert their influence on cell physiology (Ramachandran & Herman 2011). Deletion of *CYR1*, *CDC25*, or the PKA catalytic subunits (Tpk1, Tpk2 and Tpk3) reduces the activity of PKA and lengthens yeast RLS, whereas deletion of gene (*PDE2*) dampens PKA signaling and shortens yeast RLS (Lin *et al.* 2000b). In the chronological aging, CR reduces Ras/AC/PKA signaling activity, and then inactivates stress-resistance transcription factors Msn2/Msn4 and Gis1 and consequently down-regulates the expression of many stress-resistance genes, including *SOD2* (Fabrizio *et al.* 2003).

2.5.3 Sirtuins

The sirtuins are a highly conserved family of NAD^+-dependent proteins that regulate aging in different organisms. In the budding yeast, four *SIR* (silent information regulator) genes (*SIR1*, *SIR2*, *SIR3*, and *SIR4*) were identified as important components for silencing at the mating type locus (*HML* and *HMR*) as well as telomeric DNA. Yeast RLS depended on the presence of *SIR2*, *SIR3*, and *SIR4*, but not on *SIR1*. Again, deletion or overexpression of *SIR2* was shown to have the largest effect on RLS reduction or extension, respectively, among the three genes (*SIR2*, *SIR3*, and *SIR4*) (Kaeberlein *et al.* 1999). Likewise, overexpression of Sir-2.1, the homolog of yeast Sir2, increases lifespan in *C. elegans* (Tissenbaum & Guarente 2001) and *D. melanogaster* (Rogina & Helfand 2004). In contrast, deletion of *SIR2* is reported to extend yeast CLS (Fabrizio *et al.* 2005; Smith *et al.* 2007; Murakami *et al.* 2008).

In yeast replicative aging, a proposed mechanism for Sir2 induced longevity is that Sir2 inhibits ribosomal DNA (rDNA) recombination and extrachromosomal rDNA circles (ERC) formation. Accumulation of ERCs in old cell cause fast aging (Sinclair & Guarente 1997). In the absence of *SIR2*, the rate of ERC formation is

enhanced and cells are short lived (Kaeberlein *et al.* 1999). Reduced rDNA recombination mediated by *SIR2* overexpression or deletion of the *FOB1* leads to lower ERC levels and results in extended RLS (Defossez *et al.* 1999).

In addition, asymmetric segregation and CR are closely interrelated with Sir2. Asymmetric segregation in the yeast replicative aging was observed in that oxidatively damaged proteins (carbonylated proteins) are retained in mother cells and are not inherited by daughter cells. However, *sir2*Δ mother cells fail to retain oxidatively damaged proteins during cytokinesis (Aguilaniu *et al.* 2003). The increased yeast RLS under CR conditions was proposed by activating Sir2, which was supported by the observation that deletion of *SIR2* prevents RLS extension under CR. Several studies found that CR might enhance Sir2 activity via elevated NAD^+ (a substrate of Sir2), decreased nicotinamide (an inhibitor of Sir2), or decreased NADH (an inhibitor of Sir2) (Lin *et al.* 2002; Anderson *et al.* 2003; Lin *et al.* 2004). However, the link between Sir2 and CR is still an open question (Kaeberlein 2010a).

Chapter 3

DEVELOPMENT OF HTS ASSAY FOR DETERMINATION OF CHRONOLOGICAL LIFESPAN OF YEAST

3.1 Introduction

The budding yeast *S. cerevisiae* serves as a leading model organism for studying evolutionarily conserved mechanism relevant to human aging and age-related diseases (Fontana *et al.* 2010; Kaeberlein 2010a; Longo *et al.* 2012). In the traditional CLS assay, viability is calculated based on the number of CFUs on the nutrient agar (Fabrizio & Longo 2003; Murakami *et al.* 2008). Recently, Kaeberlein and co-workers have developed a high-throughput method to measure CLS, which involves quantifying survival based on measuring outgrowth of aging cells in nutrient-rich liquid medium by monitoring optical density at 420-580 nm using a combined shaker/incubator/plate reader, called the Bioscreen C MBR instrument (Burtner *et al.* 2009a; Murakami & Kaeberlein 2009). Furthermore, yeast outgrowth data analyzer (YODA), a software specifically for quantification of CLS and growth rate of yeast cells, has been developed (Olsen *et al.* 2010).

Inspired by the success of these researchers, I focus on the establishment of experimental systems and assay conditions suitable for development of a rapid and simple assay for screening of CRMs by determination of yeast CLS. The high throughput method is based on previous reports with some modifications (Toussaint & Conconi 2006; Murakami & Kaeberlein 2009). The results indicate that the high

throughput screening (HTS) assay can quantitatively measure CLS for several hundred independently aging cultures with high sensitivity and uncomplicated data analysis. It also provides reliable and reproducible measures of yeast growth including lag-time, growth rate, doubling time, survival percentage, and death rates for future screening of CRM activity of natural products.

3.2 Materials and methods

3.2.1. Materials

The WT strain *S. cerevisiae* W303 (MATα *ura3-52 trp1*Δ2 *leu2-3_112 his3-11 ade2-1 can1-11*), BY4742 (MATα *his3*Δ1 *leu2*Δ0 *lys2*Δ0 *ura3*Δ0) and single gene deletion mutant strains in the BY4742 genetic background, were all obtained from Thermo Scientific Open Biosystems (Huntsville, AL, USA). *S. cerevisiae* Lalvin EC1118 and AH109 (MATa *trp1-901 leu2-3_112 ura3-52 his3-200 gal4*Δ *gal80*Δ *LYS2::GAL1*$_{UAS}$*-GAL1*$_{TATA}$*-HIS3 GAL2*$_{UAS}$*-GAL2*$_{TATA}$*-ADE2 URA3::MEL1*$_{UAS}$*-MEL1*$_{TATA}$*-lacZ MEL1*) were provided by Professor Hao Yu of the National University of Singapore, Singapore. The culture of each yeast reference strain was aliquoted into 10 μL and stored at –80°C. All L-amino acids were from GL Biochem (Shanghai, China), yeast nitrogen base w/o amino acids (YNB) and ammonium sulfate, peptone, agar, yeast extract were from Amresco (Solon, OH, USA). YPD Broth and other chemicals were from Sigma-Aldrich Chemical Company (St. Louis, MO, USA).

Table 3.1 Final composition of synthetic defined (SD) medium used for yeast CLS analysis

Component	Concentration (1×)
Glucose	20 g/L
Yeast Nitrogen Base (-AA/-AS)	1.7 g/L
Potassium phosphate	*1 g/L*
Magnesium sulfate	*500 mg/L*
Sodium chloride	*100 mg/L*
Calcium chloride	*100 mg/L*
Biotin	*0.002 mg/L*
Pantothenate	*0.4 mg/L*
Folate	*0.002 mg/L*
Inositol	*2 mg/L*
Niacin	*0.4 mg/L*
PABA	*0.2 mg/L*
Pyridoxine, HCl	*0.4 mg/L*
Riboflavin	*0.2 mg/L*
Thiamine, HCl	*0.4 mg/L*
Riboflavin	*0.2 mg/L*
Thiamine, HCl	*0.4 mg/L*
Boric acid	*0.5 mg/L*
Copper sulfate	*0.04 mg/L*
Potassium iodide	*0.1 mg/L*
Ferric chloride	*0.2 mg/L*
Manganese sulfate	*0.4 mg/L*
Sodium molybdate	*0.2 mg/L*
Zinc sulfate	*0.4 mg/L*
Ammonium sulfate	5 g/L
Amino acids (1×)	
Essential	
Uracil	*100 mg/L*
L-histidine	*100 mg/L*
L-leucine	*300 mg/L*
L-lysine-HC1	*150 mg/L*
Non-Essential	
Adenine	*80 mg/L*
L-arginine	*40 mg/L*
L-aspartic acid	*100 mg/L*
L-glutamic acid	*100 mg/L*
L-methionine	*80 mg/L*
L-phenylalanine	*50 mg/L*
L-serine	*400 mg/L*
L-threonine	*200 mg/L*
L-tryptophan	*200 mg/L*
L-tyrosine	*40 mg/L*
L-valine	*150 mg/L*
L-isoleucine	*60 mg/L*

3.2.2 Modification of a shaker incubator for aging culture

A flat shaker incubator was modified in order to increase the capacity of yeast aging culture for high throughput screening assay. Firstly, flask clamps, nuts and bolts on flat platform of a shaking incubator with precise temperature control were removed. Twenty five of 24-well polystyrene, bottom flat microplates (Nunc, Rochester, NY, USA) were then adhered to the flat platform of the incubator using double-faced adhesive tape. Thus, 5-mL glass sample vial with screw cap can be placed in the wells of 24-well microplates. This modified incubator can accommodate up to 600 sample tubes (5 mL) containing 1.0 mL culture media in each tube.

3.2.3 High-throughput assay procedure

The aging yeast culture is prepared by streaking a strain from frozen stocks onto YPD (1% yeast extract/2% peptone/2% dextrose) agar plates. After incubating the cells at 30˚C for 2 days or until colonies appear, a single colony is picked and inoculated into a 1.0 mL YPD liquid medium (Sigma YPD Broth, St. Louis, MO, USA) in a 5 mL tube and cultured at 30˚C for 2 days in the flat incubator with shake at 200 rpm. The 2-day culture ($\approx 2\times10^7$ cells/mL) was diluted with autoclaved 18 MΩ Milli-Q grade water (1:10) and stored in refrigerator at 4˚C for at least 24 h. This diluted culture could be stored at 4˚C for one week. After one day incubation at 4˚C, 5 μL ($\approx 1\times10^4$ cells) of the diluted culture was transferred to a 1.0 mL of synthetic defined (SD) medium (**Table 3.1**) and maintained at 30˚C with constant agitation (200 rpm) for the entire experiment (generally 2 or more weeks). After 2 days of culture ($\approx 1\times10^7$ cells/mL) in SD media, the cells reached stationary phase and the first age-point is ready to be taken. Subsequent age-points were taken every 2–4 days. For each age point, 5.0 μL of the mixed culture was pipetted into each well of 96-well

microplate. One hundred μL YPD medium was then added to each well. The cell population was monitored with a Synergy HT microplate reader (BioTek, Winooski, VT, USA) by recording the optical density (OD) every 5 or10 min during 12–24 h at the wavelength of 660 nm. The outline of this assay was shown in **Figure 3.1**.

3.2.4 Data analysis

The raw data was exported to Excel (Microsoft, San Leandro, CA, USA) and the OD curves were plotted as shown in **Figure 3.2A**. From the growth curve, the viability of the yeast can be obtained through the following doubling time:

$$D_t = \frac{\ln(2)}{\frac{\ln(OD_2) - \ln(OD_1)}{t_2 \quad t_1}}$$

where OD_1 and OD_2 represent successive OD measurements, and t_1 and t_2 are the time between measurements. The average doubling times ($\overline{Dt_n}$), defined as the average of the five lowest (except the first one) doubling times only between OD values of 0.2 to 0.5, is the doubling time for that well. The lag time was calculated as follows:

$$\lambda = \frac{\frac{\ln(2)}{\overline{Dt_n}} \times \frac{OD_{<0.3}}{OD_{>0.3}} \times t_{OD<0.3} - \frac{\ln(2)}{\overline{Dt_n}} \times t_{OD>0.3}}{1 - \frac{OD_{<0.3}}{OD_{>0.3}}}$$

where $OD_{>0.3}$ and $OD_{<0.3}$ represent the OD value first measured to be greater than 0.3001 or less than 0.3001 (0.3001 is to avoid the case that OD is 0.300), and $t_{OD>0.3}$ and $t_{OD<0.3}$ are the time corresponding to the intersection of the maximal slope of the ln curve with the x-axis (Toussaint & Conconi 2006). An easy way to determine $OD_{<0.3}$ and $OD_{>0.3}$ is to use the Excel function “SMALL” and “LARGER”. Next, the function “MATCH” was used to determine the relative position (order) of $OD_{<0.3}$ and $OD_{>0.3}$ in the running time range of the column.

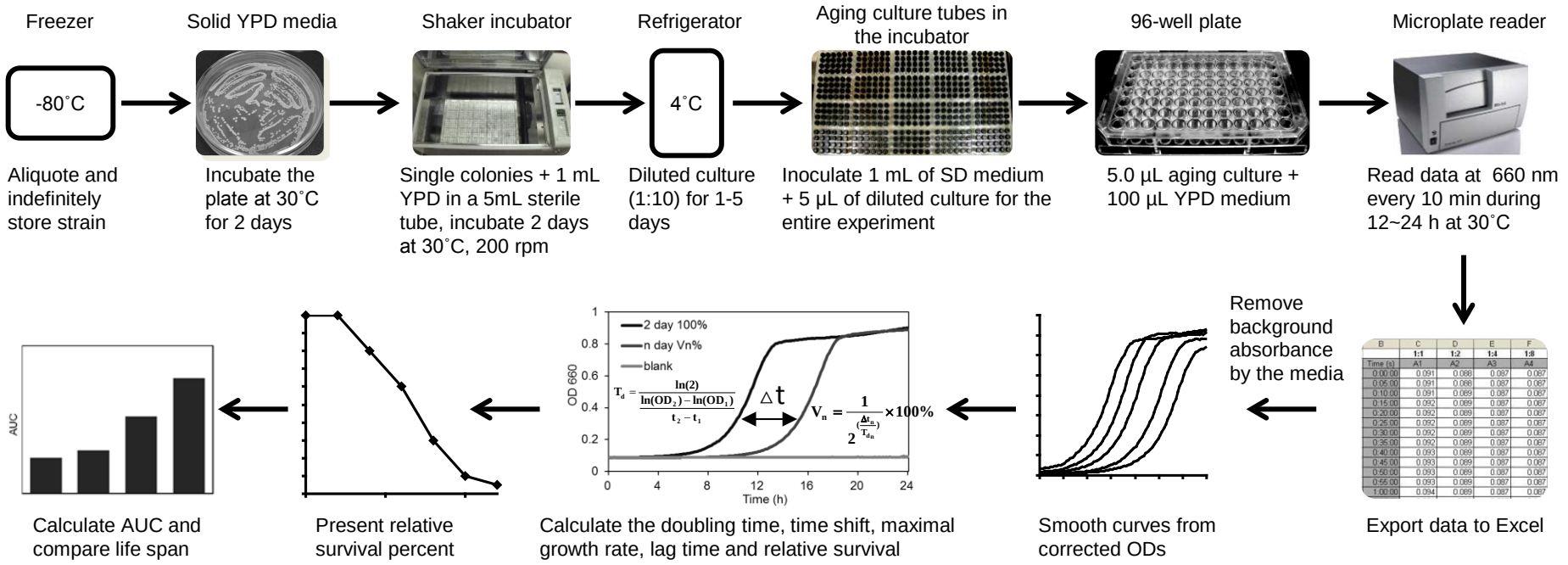

Figure 3.1 A roadmap of a high-throughput assay for determination of yeast CLS

The key components of the high throughput screening protocol include (a) a modified high capacity shaker incubator that can fit 600 culture tubes, (b) well-studied and commercially available WT strain *S. cerevisiae* BY4742, a relatively short outgrowth measuring time (12–24 h), (c) a commonly used 96-well microplate reader with shaking and temperature control, and (d) a comprehensive evaluation of yeast relative viability through analysis of doubling time, lag time, survival percentage and integral using uncomplicated software Excel.

Finally, the function “INDEX” was used to return $t_{OD>0.3}$ and $t_{OD<0.3}$ values of the cell at the intersection of the row of order and the column of time, in the running time range (0–24 h). It took different length of time for each well to reach an OD of 0.3 between the initial age-point and each subsequent age-point. For each age-point, the time shift was calculated as follows:

$$\Delta t = \left(\frac{t_{OD>0.3} - t_{OD<0.3}}{OD_{>0.3} - OD_{<0.3}} \times 0.3 + t_{OD>0.3} - \frac{t_{OD>0.3} - t_{OD<0.3}}{OD_{>0.3} - OD_{<0.3}} \times OD_{>0.3}\right) - t_{OD=0.3,2day}$$

where $t_{OD=0.3,2day}$ is the time that OD value of day 2 age-point reaches 0.3 in the outgrowth curves. The initial age-point (day 2) is defined to be 100% viability and the relative survival percent of each successive age-point can be calculated as follows:

$$V_n = \frac{1}{2^{\frac{\Delta t_n}{\overline{Dt_n}}}} \times 100$$ n = days, $\overline{Dt_n}$ represent the average doubling time

The survival integral (SI) for each well is defined as the area under the survival curve (AUC) and can be estimated by the formula:

$$SI = \sum_{2}^{n} \left(\frac{V_{n-1} + V_n}{2}\right)\left(day_n - day_{n-1}\right)$$

where day_n is the age point, such as day 2, 4, 6, 8, 10, 12, 14 (Murakami & Kaeberlein 2009). The analysis of variance for each set of biological replicates was carried out with the SAS statistical program (version 9.00, SAS Institute Inc, Cary, NC, USA), and differences between the means of SI for treatments were determined by Duncan’s multiple range test (more than two treatments) or TTEST procedure (two treatments) at $P < 0.05$ and 0.01.

3.3 Results

3.3.1 Evaluation of reproducibility, precision and accuracy of HTS assay

A comprehensive flow diagram of this HTS protocol for modifiers of CLS is shown in **Figure 3.1**. To validate this method, the CLS of different strains of *S. cerevisiae* was investigated. Based on prior studies, the cell viability (maximal cell density) is defined to be 100% after 2 days of culture in YPD medium (1% yeast extract, 2% peptone, 2% dextrose). At this time, 5 µL yeast culture (defined as 100% viability) with a range of dilution ratio (1 to 1024) were inoculated into individual wells of a 96-well plate along with 100 µL of fresh YPD medium in each well. The cell growth kinetics were monitored by recording the OD value every 10 min for 24 h at 660 nm. Based on the relative position of the outgrowth curves, I calculated the relative number of viable cells in each dilution. As shown in **Figure 3.2**, the correlation between the known dilution ratio of inoculum concentration and the relative viability determined by our HTS microplate reader assay was quite high in four different budding yeast strains: BY4742 ($r = 0.996$), W303 ($r = 0.999$), Lalvin EC1118 ($r = 0.989$) and AH109 ($r = 0.997$). From this, I can conclude that the HTS protocol provides accurate measures of relative viability over a 1000-fold range of cell viability for four different *S. cerevisiae* strains.

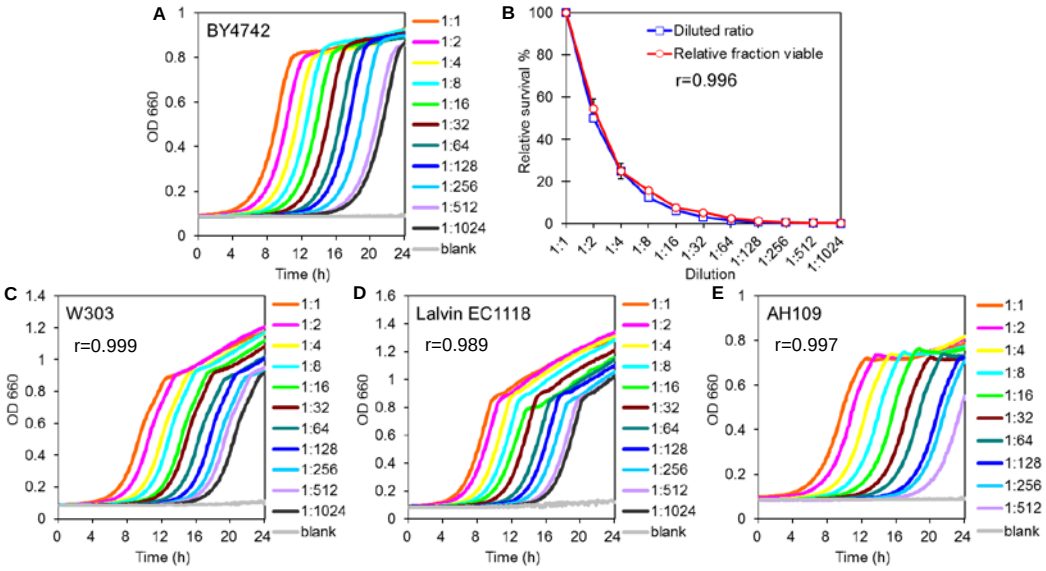

Figure 3.2 Outgrowth curves of budding yeast with several inoculum concentrations
(A) Strain *S. cerevisiae* BY4742, a commonly used strain in aging research or cellular and molecular biology study, derived from S288C. There is a distinct shift in the curves with different living cell number (different dilutions or inoculum concentrations). (B) Correlations exist between the measured value of relative viability (means ± SD, n = 4) and diluted ratio in strain BY4742 (correlation coefficient, r = 0.996). (C) *S. cerevisiae* W303, a common WT strain in aging research and molecular biology study (r = 0.999). (D) *S. cerevisiae* Lalvin EC1118 (r = 0.989), an excellent wine strain used in a wide range of applications (such as sparkling wines, fruit wines and ciders). (E) *S. cerevisiae* AH109 (r = 0.997), designed for detecting protein-protein interactions using the two-hybrid system for molecular biology study.

3.3.2 Initial population size modulates CLS independent of CR

An aspect of chronological aging that has not been previously explored is the effect, if any, that the size of the initial cell population might have on chronological aging of the stationary phase culture. I studied the influence of population size on CLS in BY4742 by inoculating three different cell concentrations into SD media for subsequent aging studies. The three inoculum concentrations were prepared through 20-fold dilution of an overnight YPD culture: 1 (52,000 ± 8600 cells/5 µL), 1:20 (2,800 ± 240 cells/5 µL) and 1:400 (130 ± 10 cells/5 µL) (**Figure 3.3**); the viable cell number was determined by colony forming units (CFU) on solid YPD plates. Five µL of cultures were individually inoculated into 1 mL SD medium with 2% glucose (SD2D, control) and 0.5% glucose (SD0.5D, CR) medium for aging culture. Since the aging cultures inoculated with fewer cells were still showing growth after day 2, I

defined day 3, 4, and 5 as the initial age point (100% viability) for dilution 1, 1:20 and 1:400 in the control condition, respectively. As shown in **Figure 3.3E**, the maximal cell density based on OD660 of the aging culture did not change significantly in response to the dilution of the initial inoculum. For cells aged in SD2D, reducing the size of the inoculum significantly ($P < 0.05$) extended the lifespan (**Figure 3.3A, C**). The survival integral (SI) of 3 inoculum sizes (1, 1:20, 1:400) were 275, 305, and 376 correspondingly. Similarly, under CR (SD0.5D), yeast CLS was increased when inoculation was decreased (dilution 1:20, 1:400) (**Figure 3.3B, D**), while CR greatly reduce the saturation density of the culture (**Figure 3.3F**). Overall, reducing inoculum concentration could increase CLS under both normal and CR conditions, which acts as a CR-independent regime.

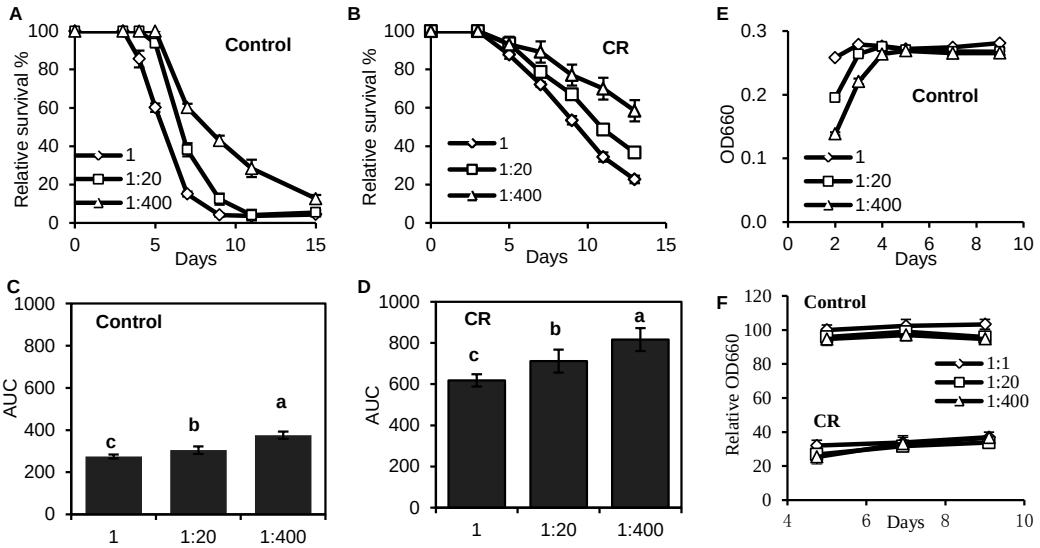

Figure 3.3 Effects of initial population size on CLS

(A) Survival curves of three inoculum concentrations cultured in SD2D (SD medium contains 2% dextrose, control) for 15 days. (B) Survival curves of three inoculum concentrations in SD0.5D medium (0.5% dextrose, CR). Error bars represent SEM within 12 replicates. (C) AUC of the three treatments under control and (D) CR condition; AUC represents the survival integral, the variance of AUC (mean + SEM, n = 12) between the three treatments is compared using the Duncan's multiple range test at $P < 0.01$, different letters (a–c) show significant differences. (E) The OD value has little change after yeast enter into stationary phase. 20 µL cultures and 80 µL water were added into each well of microplate, and OD value was measured at 660 nm. (F) CR reduces the saturation density of culture. The OD value of control culture at day 5 is defined to be 100 relative OD value. Error bars represent SEM within 12 replicates.

3.3.3 Effect of cellular state in YPD medium on Yeast CLS

In prior studies, CLS assays have been typically begun by culturing cells in YPD medium overnight prior to inoculation in SD2D (or other media compositions) for aging. During culturing in YPD, yeast cells begin with the logarithmic phase (day 1) and progress through diauxic (day 2–3), and post-diauxic (day 4–6) phases to the true stationary (after day 7) phase. During this process, cells entirely consume glucose during the logarithmic phase, and then establish a diet-specific pattern of metabolism and organelle dynamics during diauxic and post-diauxic phases (Goldberg *et al.* 2009; Goldberg *et al.* 2010). To determine how growth phase of yeast cells at the beginning of a chronological aging experiment might influence subsequent CLS, I initiated aging cultures in SD2D with cells obtained from YPD medium after 1 (log phase), 2 (diauxic), 4 (post-diauxic), or 8 (stationary phase) days. As can be seen in **Figure 3.4A**, length of time cultured in YPD medium had little effect on the CLS of yeast in SD2D medium.

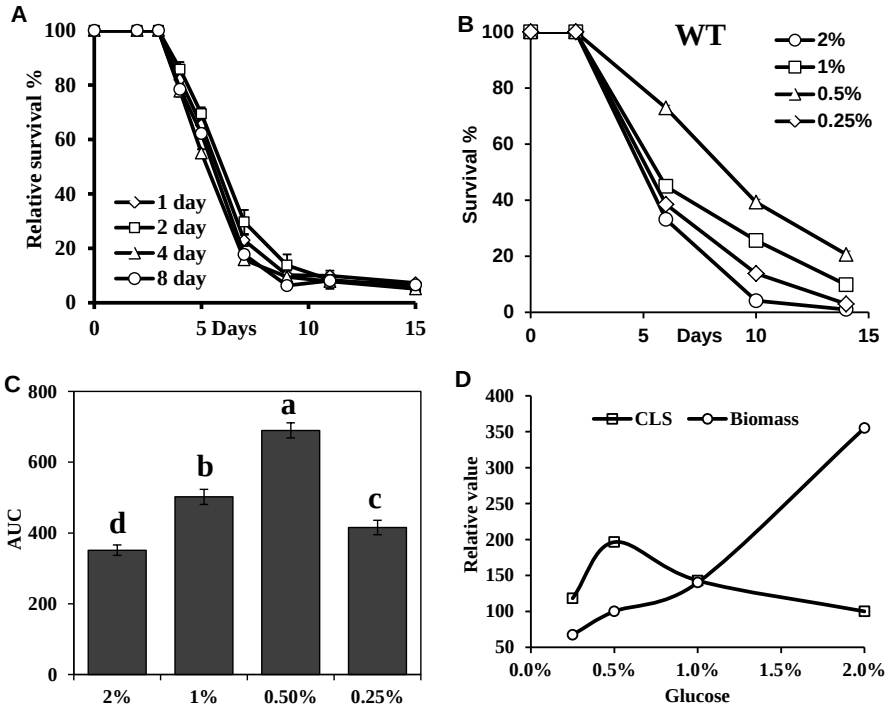

Figure 3.4 The effects of calorie level on yeast CLS

(A) Culture days of yeast have little effect on the CLS. Strain BY4742 cultured in YPD medium (2% glucose) for 1, 2, 4 and 8 days and then transferred into the SD medium (2% glucose) for 15 days. Error bars represent SEM within 12 replicates. (B) Calorie levels affect yeast lifespan. Strain BY4742 was incubated in YPD medium for 2 days and then inoculated in SD medium containing 2%, 1%, 0.5% and 0.25% glucose for 14 days (mean + SEM, n = 12). (C) AUC of the four glucose levels, AUC represents the survival integral, the variance of AUC (mean + SEM, n = 12) between the four treatments is compared using the Duncan's multiple range test at $P < 0.01$, different letters (a–d) show significant differences. (D) Effect of CR on CLS and biomass production. CLS increases as glucose concentration is reduced from 2% until 0.5% (CR) that the maximum CLS extension is reached, while further restriction results in reduced lifespan due to starvation (0.25%). Conversely, biomass production shows a constant decline.

3.3.4 Calorie level optimizes yeast CLS but not biomass production

Prior studies have shown that CR through reduction of the glucose concentration of the medium can increase both RLS and CLS. In this study, I re-examined the CLS of yeast cells in SD medium containing different levels of glucose. As shown in **Figure 3.4B**, I confirmed that CR at 0.5% glucose (SI = 690) could greatly extend CLS. CR at 0.25% glucose (SI = 415) or 1% glucose (SI = 502) also resulted in moderate lifespan extension, compared with the control conditions (2% glucose, SI 351). In addition, the effect of glucose level on yeast CLS and biomass production was shown in **Figure 3.4C**. CLS was calculated via SI value and biomass was based on OD660 value of aging culture at day 2. CLS increased as glucose level was reduced from 2% to 0.5% (CR) whereby optimization of longevity was reached, while further restriction reduced lifespan due to starvation (0.25%). However, biomass gradually decreased over five-fold from 2% to 0.25% glucose (**Figure 3.4D**).

3.3.5 Identification of calorie restriction mimetic gene

Several studies have indicated that TOR signaling may play a conserved role in mediating beneficial health and longevity effects associated with CR (Fontana *et al.* 2010; Kaeberlein 2010a). Inhibition of the TOR signaling pathway by genetic or pharmacological intervention extends lifespan in invertebrates, including yeast (Kaeberlein *et al.* 2005b; Powers *et al.* 2006), nematodes (Jia *et al.* 2004), fruit flies

(Kapahi *et al.* 2004) and mice (Harrison *et al.* 2009). *TOR1* deletion increases RLS but fails to further increase RLS under CR conditions, being consistent with the model that Tor1 mediates CR-dependent RLS extension (Kaeberlein *et al.* 2005b). Reduction of TOR complex 1 (TORC1) activity with rapamycin and deletion of *TOR1* increases lifespan significantly (Kaeberlein *et al.* 2005b; Powers *et al.* 2006). However, it is not clear if deletion of *TOR1* could further extend yeast CLS subjected to CR. Therefore, I studied effect of deletion of the gene *TOR1* on CLS. As illustrated in **Figure 3.5A**, deletion of *TOR1* increased CLS under the control conditions, but did not further extend CLS under CR conditions.

The AGC kinase Sch9 (homologous to protein kinases A, G, and C) was proposed as a substrate of yeast TORC1 (Urban *et al.* 2007). The observation that deletion of *SCH9* significantly increased CLS under normal condition and decreased CLS in CR (**Figure 3.5B**) is consistent with previous reports that Sch9 increases resistance to oxidants and extends CLS and RLS (Fabrizio *et al.* 2001; Longo 2003; Kaeberlein *et al.* 2005b). These results suggest that *TOR1* and *SCH9* act as CRM genes in the CLS model.

In yeast, the Ras-adenylate cyclase-protein kinase A (Ras-AC-PKA) pathway is also proposed to be an important nutrient-sensing pathway that can extend CLS and RLS (Fontana *et al.* 2010). Yeast *RAS1* and *RAS2* are highly homologous to mammalian RAS genes. Deletion of *RAS1* increases RLS and slightly decreases CLS, while deletion of *RAS2* decreases RLS and dramatically extends CLS (Sun *et al.* 1994; Fabrizio *et al.* 2003; Burtner *et al.* 2009b). As presented in **Figure 3.5D**, under normal condition, deletion of *RAS2* increases CLS, but not further extends CLS under CR conditions. The results imply that *RAS2* acts at downstream of CR.

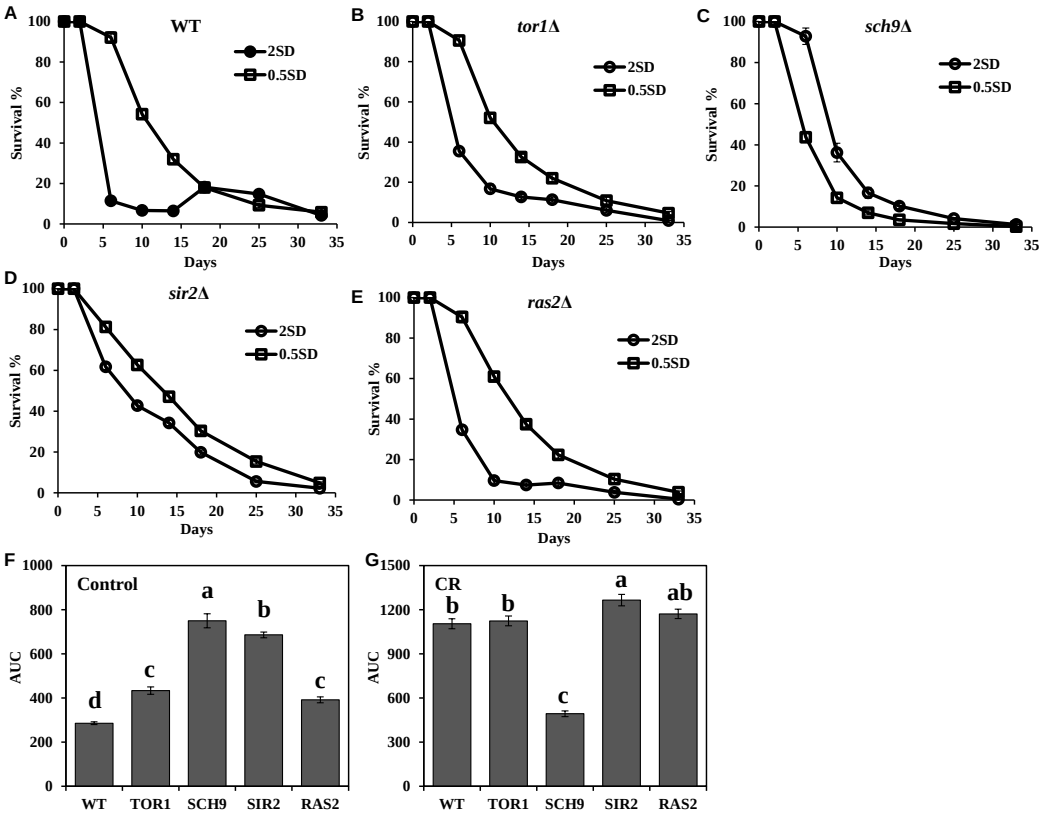

Figure 3.5 Effect of single gene deletion on CLS

WT strain BY4742 (A) and single gene knockout strain *tor1*Δ (B), *sch9*Δ (C), *sir2*Δ (D), and *ras2*Δ (E) were cultured in SD2D (2% glucose, control) and SD0.5D (0.5% glucose, CR). Error bars represent SEM within 16 replicates. AUC represents the survival integral, the variance of AUC (mean + SEM, n = 16) among the five strains under control (F) and CR (G) were compared using the Duncan's multiple range test at $P < 0.01$, different letters (a–d) show significant differences.

I also investigated the effect of *SIR2* deletion on CLS (**Figure 3.5C, D**). Sir2 has been proposed to mediate lifespan extension (Lin *et al.* 2000b; Lamming *et al.* 2005). Deletion of *SIR2* decreases RLS, whereas over-expression of *SIR2* increases RLS (Kaeberlein *et al.* 1999). Deletion of *SIR2* also prevents RLS extension by CR (Lin *et al.* 2000b); however, this is thought to be due to indirect effects caused by hyper-accumulation of ERCs (Kaeberlein *et al.* 2004). In contrast, deletion of *SIR2* is reported to have little effect on CLS under control conditions, but may enhance lifespan extension from deletion of *SCH9* (Fabrizio *et al.* 2005). Consistent with prior reports (Smith *et al.* 2007; Murakami *et al.* 2008), I found that deletion of *SIR2* mediated CLS extension and could not prevent lifespan extension through CR, but through CR-independent regime (**Figure 3.5C**).

3.4 Discussion

I have established a simple and rapid HTS assay to measure the CLS of budding yeast under normal and CR conditions. The advantages of this assay include a high capacity for simultaneous culture growth and quantification of CLS, well-studied and commercially available WT strain, short running time, common equipment, quantifiable data, and uncomplicated data processing. This method is modified from that developed by the Kaeberlein lab using a Bioscreen C MBR machine (Murakami *et al.* 2008), and provides the advantage that a standard plate reader can be used. This difference is important, as the Bioscreen C MBR machine uses non-standard 100-well plates, while a standard plate can accommodate chemical or genetic libraries that are contained in 96- or 384-well plates (**Table 3.2**).

Table 3. 2 Comparison of high throughput methods for measuring yeast CLS developed by Kaeberlein group and our group

	Kaeberlein group	Our group	Advantages/disadvantages of our method
Equipment of aging culture incubation	Roller incubator	Flat incubator	Commonly used
Quantity of incubator	180 samples	600 samples	High throughput
Culture tube	25 mL	4 mL	Reduce medium
Plate reader	Bioscreen C MBR machine	Synergy HT Microplate reader	Advanced
Multi-well plate	100-well	96-well	Commonly used
Monitoring time	24 h	10-20 h	Time saving
Sample and YPD medium in each well	5 µL sample + 145 µL medium	5 µL sample + 100 µL medium	Reduce medium
Absorption spectrum	420-580 nm	660 nm	Small OD value
Recording Interval	30 min	5 min	Accurate doubling time
Data analysis	A self-developed software YODA	Microsoft Office Excel	simpler data analysis

In this assay, initial inoculum size is regularly limited to approximately 1×10^4 cells in each aging culture tube, and yeast cells proliferate to about 1×10^7 cells after two days incubation in SD2D medium, which means this aging culture contains 0.1% original cells. For the CLS assay, the viability is usually followed until it has declined to 0.1–1% of its original value, which allows a simple comparison of yeast CLS results with other lifespan assays. Previous reports have identified that low viability could be a problem because cell lysis and regrowth may be observed in some CLS assays (as see in **Figure 3.5A**) (Fabrizio & Longo 2003; Fabrizio & Longo 2008). On the other hand, my unpublished data showed that this microplate reader assay could detect a very low cell number (< 10) in the 5 μL aging sample during 48 hours in YPD medium, which means I could measure the relative viability when the number of viable cells in 1.0 mL aging culture is less than 10^2–10^3.

Initial population size could affect cellular/microbial metabolism, growth, division, and communication with each other (Ding *et al.* 2009). Herein, I examined the effect of inoculum size on the yeast lifespan. Three inoculum sizes were used to determine its effect on yeast lifespan. The cells in the medium containing the lower inoculum size underwent a higher number of divisions. As shown in **Figure 3.3**, different initial inoculum concentrations had a similar number of cells when they reached the stationary phase (**Figure 3.3F**).The lower inoculum size groups took more time than the higher inoculum size groups before they entered the stationary phase (longer lag phase) (**Figure 3.3E**). Previous studies suggested that the ages of individual cells follow geometrical distribution and virgin daughter cells represent half of the population at each division, and the fraction of original mother cell could be negligible (< 1%) (Shcheprova *et al.* 2008; Steinkraus *et al.* 2008). During the

chronological aging, yeast cells usually undergo several divisions (< 10) before they enter the stationary phase. In this assay, the three inoculum sizes were approximately 140, 2,800 and 52,000 cells per tube, thus, they had undergone approximately 16, 12 and 8 divisions as they entered the stationary phase with 1×10^7 cells. Accordingly, there were different fractions of original mother cells, younger mothers and daughters in the stationary phase population among the three inoculums sizes. They had significantly different CLS (**Figure 3.3A, C**) and the smaller inoculum size can increase biomass production period and CLS of the three groups were shown by the 100% survival at day 3, 4, and 5, respectively. Cells of the higher inoculum size firstly entered stationary phase and age, which is possible to affect the results of measured CLS. However, the absolute survival also shows that the low inoculum concentration had much higher viability than the high inoculum size at day 7–15 (data not shown). Furthermore, the effect of inoculum size on CLS under CR also shows lower inoculum number can extend CLS. The detailed mechanism of this phenomenon requires further examination.

CR in mammals commonly defined as reduction in calorie intake without malnutrition by 10% to 50% of *ad libitum* (Mair & Dillin 2008; Fontana *et al.* 2010). However, CR in yeast is modeled by glucose reduction/restriction, reducing glucose level in the SD medium from 2% (normal condition) to 0.5% (moderate CR) and 0.05% (severe DR) could extend RSL and CLS in different stains (Bishop & Guarente 2007). In addition, strains and conditions that are involved during the experiments vary between laboratories and might lead to different lifespan (Minois *et al.* 2009). The variation of culture media, SD of limited amount of nutrients, YPD of rich nutrients and even the distilled water, also have profound impact on the lifespan of yeasts. The most widely used laboratory wild-type yeast strains are BY4742, PSY316,

W303AR5 and DBY746 (Fabrizio *et al.* 2001; Kaeberlein *et al.* 2002; Lamming *et al.* 2005; Shcheprova *et al.* 2008). I selected the well-studied and relatively short CLS strain BY4742 and cultured it in SD medium with 2% to 0.25% glucose to better compare these CLS results obtained with that in other labs. As shown in **Figure 3.4D**, CR (0.5%) optimizes median lifespan, and further restriction results in reduced lifespan due to starvation (0.25%), whereas CLS but not biomass is optimized by CR.

Those observations differ somewhat from prior studies, which indicated that 0.05% glucose can increase CLS to an extent even greater than 0.5% glucose (Murakami *et al.* 2008; Burtner *et al.* 2009b). These observations are likely attributable to differences in the culture conditions and medium composition. It has been demonstrated that medium components, including carbon source and amino acid composition, are critical to yeast lifespan. Recent evidences have demonstrated that diets of amino acids modulate lifespan of model organisms in the laboratory, including yeast (Alvers *et al.* 2009a), flies (Grandison *et al.* 2009), and mice (Miller *et al.* 2005). It is now generally accepted that amino acids can control autophagy through changes in the activity of signal transduction pathways. Therefore, I modified the composition of SD medium with ingredients listed in **Table 3.1**. Additionally, I applied a shaker incubator with a high capacity of 600 aging culture tubes with a relatively small volume of 1 mL. Growth kinetic curve is employed for data analysis in this assay. The most important advantage of the kinetic assay is that it is highly sensitive, provides quantifiable data and is flexible to variable assay conditions. Compared with the CFU on solid media, the growth curve assay was able to uncover the subtle phenotypes when cells were treated with low doses of compounds (Smith *et al.* 2007).

3.5 Conclusion

In this Chapter, I have reported a highly sensitive high throughput assay for evaluation of the CLS of yeasts. The assay is not labour-intensive and can be used to rapidly screen a large number of potential anti-aging compounds and yeast strains. The method provides quantifiable data including lag-time, growth rate, doubling time, percentage survival, and allows us to discover next generation anti-aging activity of CRMs from plant secondary metabolites.

Chapter 4

DIETARY RESTRICTION DEPENDS ON NUTRIENT COMPOSITION TO EXTEND CHRONOLOGICAL LIFESPAN IN BUDDING YEAST

4.1 Introduction

The traditional opinion on DR has been challenged in four model organisms, namely yeast (Jiang *et al.* 2000; Powers *et al.* 2006), worms (Greer & Brunet 2009), flies (Lee *et al.* 2008; Fanson *et al.* 2009; Grandison *et al.* 2009; Ja *et al.* 2009), and mice (Zimmerman *et al.* 2003; Miller *et al.* 2005), because studies in these organisms have shown that changing the dietary components can increase their lifespans. Moreover, different DR regimes extend lifespan via distinct genetic pathways (Greer & Brunet 2009), which suggests that nutrient balance, in addition to dietary reduction, also plays a pivotal role in regulation of longevity (Piper *et al.* 2011). Although studies of yeast aging have had a significant impact on aging-related research, the new findings that nutrient composition can alter lifespan have not been systematically explored in a yeast model.

In yeast aging studies, glucose plays an important role in yeast lifespan. DR can be accomplished by only reducing the glucose concentration of growth medium to extend CLS and RLS significantly, the glucose level in standard SD medium could be from 2% (normal condition) to 0.5% (moderate DR) or 0.05% (severe DR) (Bishop &

Guarente 2007). Recently, acidification of culture medium was proposed to accelerate chronological and replicative aging in yeast (Burtner *et al.* 2009b; Murakami *et al.* 2011; Murakami *et al.* 2012). Thus, it is suggested that lifespan extension by reducing the glucose level of the culture medium from 2% to 0.5% or 0.05% is likely due to decreased production of organic acids and reduced medium acidification (Burtner *et al.* 2009b) .

Recent evidences have demonstrated that dietary amino acid compositions modulate lifespan of laboratory model organisms such as yeast (Alvers *et al.* 2009a), flies (Grandison *et al.* 2009), and mice (Miller *et al.* 2005). A report showed that reducing the amino acid concentration in the medium could promote an increase in the mean and maximum RLS of yeast (Jiang *et al.* 2000). Another study showed that removing preferred amino acids such as asparagine or glutamate while keeping the total amino acid concentration constant could significantly increase CLS of yeast (Powers *et al.* 2006). It is postulated that amino acids and glucose balance extends yeast lifespan and that individually reducing amino acids or glucose is a major factor in regulation of yeast longevity. It is expected that other nutrients such as minerals and vitamins may also be important in regulating yeast CLS. It would be important to know how critical these nutrients are in extending or reducing lifespan. In most aging studies, single-factorial design was employed in experiments with nutrients as the variant, resulting in an exclusive elucidation of effects of other nutrients on lifespan. By using multifactorial design, a few studies on flies have found that the nutrient balance, not DR, extends lifespan (Lee *et al.* 2008; Skorupa *et al.* 2008; Fanson *et al.* 2009). Multifactorial design in relation to nutrient change has not been applied in yeast aging studies.

To uncover the relationship between nutrients and CLS, I chose a three-factor (glucose, yeast nitrogen base (YNB), amino acids)/three-level experimental design with 15 media using the SAS program (version 9.2) to arrange experiments on yeast CLS measurement (totally 240 treatments, 15 media × 16 repeats). The design was based on a classical response surface methodology (RSM) by Box–Behnken design to explore the relationships between nutrients and lifespan as well as biomass production in a WT yeast strain (Baş & Boyacı 2007). I applied this design in three single gene deletion mutants (*sch9*Δ, *tor1*Δ and *sir2*Δ) to determine their changes of lifespan and biomass in response to the different nutrient compositions. Reported herein is the discovery.

4.2 Materials and methods

4.2.1 Materials

The materials were as described in **Chapter 3** (**3.2.1**).

4.2.2 Experimental design and statistical analysis

The three experimental factors under study were glucose, amino acids, and YNB in SD medium (**Table 3.1**). Values for these parameters were chosen to test conditions known to produce significant effects on lifespan from previous study (Baş & Boyacı 2007). To test for the curvature of the responses, three levels of each nutritional parameter were required (**Table 4.1**). A Box-Behnken design based on response surface methodology (RSM) was chosen to estimate the responses of both the linear and the quadratic behavior over the design region to minimize the number of experiments (Baş & Boyacı 2007). This design was generated from the SAS

program (version 9.2, SAS Institute Inc, Cary, NC, USA), and required a total of 15 runs, including three center points (run 13, 14 and 15).

4.2.3 Lifespan, biomass and yeast cell growth assay

The lifespan, biomass and yeast cell growth assays have been described in the **Chapter 3** (**3.2.3**).

4.2.4 Data analysis

The data analysis on lifespan has been described in **Chapter 3** (**3.2.4**). For surface-response data analysis, the SAS program automatically provides tools that are appropriate for examining the linear and the quadratic effects, for estimating model parameters, for carrying out an analysis of variance (**Table 4.4**), for fitting models that can be used to find optimal factor settings, and for generating the surface-response plots (**Figure 4.3 and 4.4**). Correlations among lifespan, biomass production and viability of day 2 were computed by using the SAS CORR procedure, which can provide Pearson correlation coefficients and associated probabilities (**Table 4.2**).

Table 4.1 The three-factor/three-level response surface methodology of Box–Behnken design and pH, biomass and lifespan values of different cultures in the WT and *sch9*Δ strains

Run	Factors & levels (coded)						pH					Biomass (OD660 %)		Lifespan (AUC)	
	AAs (1×)		YNB (g/L)		Glucose (%)		Day 0	WT day 2	WT day 4	*sch9*Δ day 2	*sch9*Δ day 4	WT	*sch9*Δ	WT	*sch9*Δ
1	0.5	(-1)	0.85	(-1)	3.0	(0)	4.73	3.00	3.09	3.00	3.12	11.7	36.5	594.0	413.8
2	0.5	(-1)	9.35	(1)	3.0	(0)	4.60	3.21	3.27	3.26	3.34	52.1	59.7	559.7	303.9
3	3.5	(1)	0.85	(-1)	3.0	(0)	4.75	3.65	3.60	3.88	4.04	50.9	47.6	344.4	2455.8
4	3.5	(1)	9.35	(1)	3.0	(0)	4.72	4.80	4.42	4.67	4.24	226.8	263.1	762.0	678.1
5	2.0	(0)	0.85	(-1)	0.5	(-1)	4.77	5.46	6.61	4.90	6.55	29.2	48.6	408.6	285.6
6	2.0	(0)	0.85	(-1)	5.5	(1)	4.72	3.17	3.36	3.25	3.37	45.2	55.9	898.2	2701.4
7	2.0	(0)	9.35	(1)	0.5	(-1)	4.71	5.88	5.93	5.88	5.93	53.1	69.5	688.9	770.2
8	2.0	(0)	9.35	(1)	5.5	(1)	4.71	3.54	3.56	3.67	3.49	105.9	191.3	443.5	780.0
9	0.5	(-1)	5.10	(0)	0.5	(-1)	4.71	3.82	3.94	3.63	3.78	30.9	45.3	894.6	318.2
10	3.5	(1)	5.10	(0)	0.5	(-1)	4.76	6.67	6.83	6.25	6.66	40.8	65.7	426.4	319.9
11	0.5	(-1)	5.10	(0)	5.5	(1)	4.68	2.73	2.81	2.79	2.82	55.6	57.0	308.6	504.1
12	3.5	(1)	5.10	(0)	5.5	(1)	4.73	3.89	3.84	4.16	4.58	245.3	284.9	831.0	2397.2
13	2.0	(0)	5.10	(0)	3.0	(0)	4.73	4.11	3.55	4.11	3.33	112.2	171.0	760.1	497.4
14	2.0	(0)	5.10	(0)	3.0	(0)	4.73	4.10	3.57	4.13	3.35	126.5	185.0	778.0	496.3
15	2.0	(0)	5.10	(0)	3.0	(0)	4.73	4.11	3.53	4.14	3.36	121.8	176.8	775.1	502.3
SD	1.0		1.7		2.0		4.72	3.45	3.52			108.4		356.4	
CBS	1.0		1.7		2.0		6.00	5.92	5.89			225.1		1395.6	

The pH, biomass and lifespan data are presented as mean pH of several biological replicates.

Table 4.2 Correlation among lifespan, biomass and viability at day 2 for the 15 media in the four *S. cerevisiae* strains

			WT			*sch9*Δ			*tor1*Δ			*sir2*Δ	
		Lifespan	Biomass	Viability	Lifespan	Biomass	Viability	Lifespan	Biomass	Viability	Lifespan	Biomass	Viability
	Lifespan		0.40	0.38	0.18	0.40	0.37	0.30	0.39	0.37	0.52	0.37	0.37
WT	Biomass	0.14		0.94	0.13	0.97	0.79	0.31	0.99	0.95	0.31	0.99	0.96
	Viability	0.16	<.0001		-0.11	0.88	0.92	0.42	0.92	0.98	0.34	0.89	0.98
	Lifespan	0.52	0.64	0.71		0.24	-0.26	-0.12	0.20	0.00	0.20	0.28	-0.01
*sch9*Δ	Biomass	0.14	<.0001	<.0001	0.39		0.75	0.33	0.96	0.87	0.37	0.97	0.88
	Viability	0.17	0.00	<.0001	0.35	0.00		0.47	0.77	0.90	0.42	0.72	0.86
	Lifespan	0.28	0.26	0.12	0.67	0.23	0.08		0.23	0.37	0.87	0.27	0.37
*tor1*Δ	Biomass	0.15	<.0001	<.0001	0.47	<.0001	0.00	0.40		0.94	0.26	0.99	0.95
	Viability	0.18	<.0001	<.0001	0.99	<.0001	<.0001	0.18	<.0001		0.33	0.92	0.99
	Lifespan	0.04	0.27	0.22	0.48	0.17	0.12	<.0001	0.35	0.23		0.30	0.31
*sir2*Δ	Biomass	0.17	<.0001	<.0001	0.32	<.0001	0.00	0.32	<.0001	<.0001	0.28		0.93
	Viability	0.17	<.0001	<.0001	0.98	<.0001	<.0001	0.17	<.0001	<.0001	0.27	<.0001	

Pearson coefficient (r) is shown in top right of the table and corresponding *P*-value is shown in bottom left of the table.

Table 4.3 Correlations among amino acid, YNB, glucose, pH, lifespan and biomass for the 15 media in the WT and *sch9*Δ strains

		nutrient			WT				*sch9*Δ			
		AA	YNB	Glucose	pH day 2	pH day 4	Lifespan	Biomass	pH day 2	pH day 4	Lifespan	Biomass
	AA		0.00	0.00	0.53	0.42	0.00	0.54	0.60	0.50	0.48	0.57
nutrient	YNB	1.00		0.00	0.18	0.04	0.10	0.46	0.24	-0.01	-0.37	0.41
	Glucose	1.00	1.00		-0.72	-0.74	0.03	0.42	-0.65	-0.67	0.53	0.41
	pH day 2	0.06	0.55	0.01		0.96	-0.07	0.04	0.99	0.93	-0.27	0.03
WT	pH day 4	0.15	0.90	0.0056	<.0001		-0.16	-0.11	0.92	0.98	-0.28	-0.12
	Lifespan	0.99	0.74	0.92	0.83	0.60		0.35	-0.04	-0.17	0.25	0.36
	Biomass	0.06	0.12	0.16	0.90	0.73	0.25		0.12	-0.06	0.20	0.97
	pH day 2	0.03	0.44	0.02	<.0001	<.0001	0.90	0.70		0.91	-0.17	0.11
*sch9*Δ	pH day 4	0.08	0.98	0.01	<.0001	<.0001	0.59	0.85	<.0001		-0.14	-0.05
	Lifespan	0.09	0.21	0.06	0.37	0.35	0.41	0.51	0.57	0.64		0.29
	Biomass	0.04	0.16	0.16	0.93	0.70	0.22	<.0001	0.73	0.88	0.33	

Pearson coefficient (r) is shown in top right of the table and corresponding *P*-value is shown in bottom left of the table.

Table 4.4 The linear and the quadratic parameter estimates for lifespan and biomass production

Term		WT		*sch9*Δ		*tor1*Δ		*sir2*Δ	
		Lifespan	Biomass	Lifespan	Biomass	Lifespan	Biomass	Lifespan	Biomass
AA	Estimate a	0.63	57.85	538.88	51.69	262.63	61.98	294.50	67.28
	P > |t|	0.9880	0.0007	<.0001	0.0070	0.0233	0.0002	0.0276	0.0002
YNB	Estimate	26.13	49.38	-415.63	37.61	75.75	47.84	-18.75	44.61
	P > |t|	0.5394	0.0014	0.0001	0.0239	0.3947	0.0007	0.8525	0.0014
GLU	Estimate	7.75	45.00	586.00	37.25	-309.88	57.29	-207.00	54.21
	P > |t|	0.8529	0.0021	<.0001	0.0248	0.0125	0.0003	0.0830	0.0006
AA x AA	Estimate	-100.25	-26.99	107.58	0.00	-194.88	-30.65	-94.29	-23.00
	P > |t|	0.1468	0.0636	0.1241	0.9998	0.1647	0.0224	0.5332	0.0773
AA x YNB	Estimate	113.00	48.08	-417.00	33.88	119.00	44.13	142.25	36.33
	P > |t|	0.1002	0.0070	0.0007	0.0969	0.3486	0.0045	0.3416	0.0148
AA x GLU	Estimate	247.75	51.88	472.75	44.95	192.25	55.78	255.75	61.73
	P > |t|	0.0069	0.0051	0.0004	0.0424	0.1557	0.0016	0.1176	0.0016
YNB x YNB	Estimate	-105.75	-48.89	357.08	-34.80	-187.63	-45.33	-120.29	-39.63
	P > |t|	0.1300	0.0077	0.0017	0.1003	0.1781	0.0048	0.4324	0.0123
YNB x GLU	Estimate	-183.75	28.63	-601.25	9.20	10.50	29.40	-152.75	26.35
	P > |t|	0.0221	0.0471	0.0001	0.6035	0.9309	0.0225	0.3106	0.0457
GLU x GLU	Estimate	-55.50	-37.39	278.83	-27.02	162.13	-49.93	138.21	-36.23
	P > |t|	0.3857	0.0217	0.0049	0.1788	0.2339	0.0032	0.3719	0.0174

4.3 Results

4.3.1 DR regime is dependent on nutrients in media

Recent studies on flies suggested that the traditional observation on DR-induced longevity was mainly due to nutrient balance (Skorupa *et al.* 2008; Fanson *et al.* 2009; Piper *et al.* 2011). This indicates that the imbalance between nutrients resulted in lifespan reduction. To test this new insight in yeast CLS model, I chose four media with different glucose levels to examine CLS in a commonly used WT yeast strain BY4742. As shown in **Figure 4.1**, the four media are standard SD, YPD (1% yeast extract/2% peptone/2% dextrose), SD with four-fold excess of amino acids and SD with four-fold excess of YNB. Consistent with results in **Chapter 3**, I found that DR (0.5% glucose) increased CLS and severe DR (0.05% glucose) reduced CLS possibly due to glucose deficiency (**Figure 4.1A, B**). Moreover, DR optimized CLS but not biomass as shown in **Figure 4.1C**. The biomass production in the medium containing 2% glucose was higher than that with 0.5% glucose. These results are similar to those observed in most higher eukaryotes, in which starvation does not extend lifespan, and high food intake results in high reproduction but shorter lifespan (Fontana *et al.* 2010). The difference between my results and those observations that severe DR (0.05%) extended lifespan could arise from different culture conditions (Kaeberlein *et al.* 2006; Lamming *et al.* 2006; Smith *et al.* 2007).

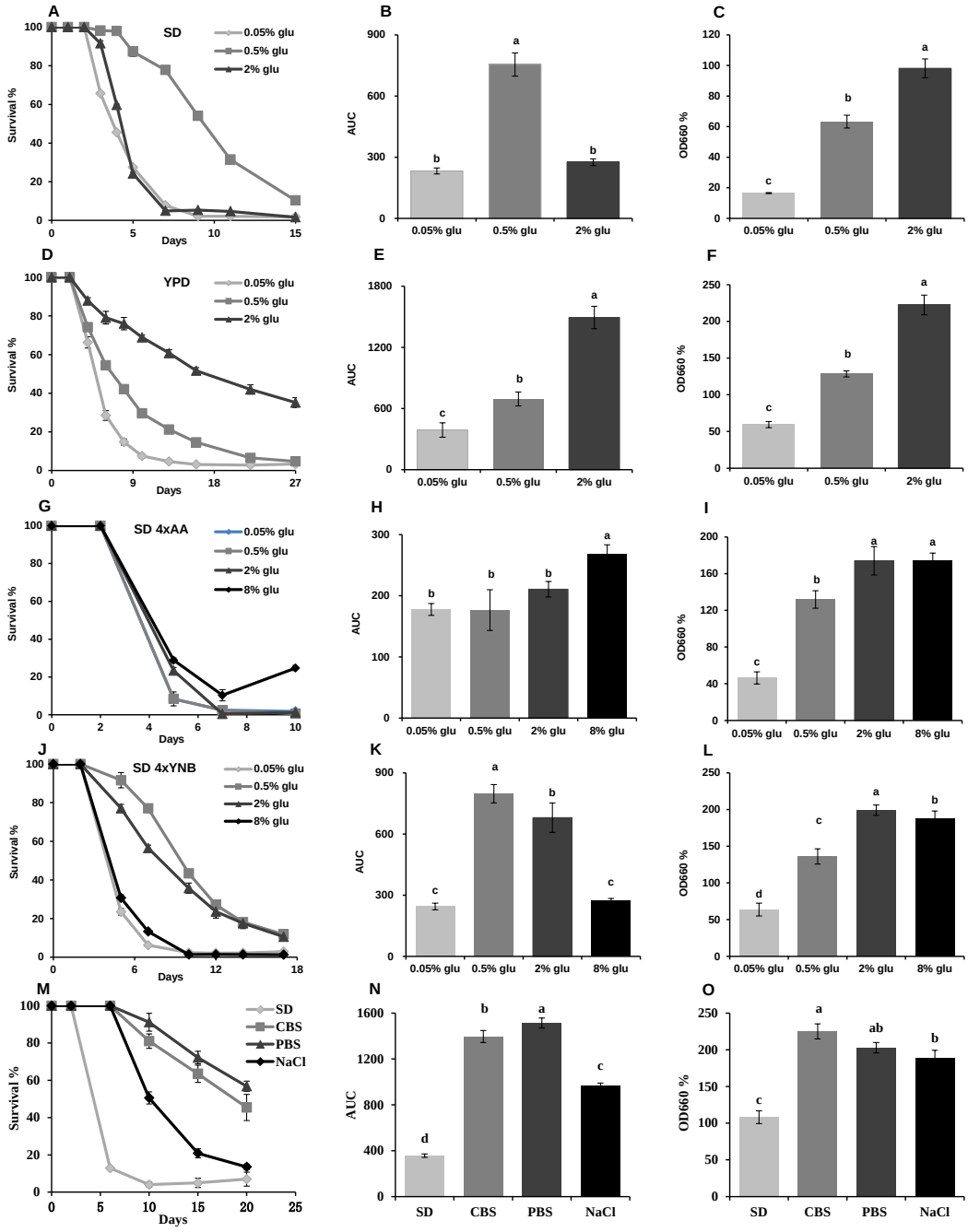

Figure 4.1 DR regime is dependent on nutrients in medium

(A, B and C) Influence of glucose levels in SD medium on yeast CLS. Survival curve (A) of WT strain BY4742 was inoculated in SD medium containing 2%, 0.5% and 0.05% glucose for 15 days (mean + SEM, n = 8). (B) AUC represents the survival integral. DR (0.5% glu) greatly extended yeast lifespan, but further DR (0.05%) did not extend lifespan due to glucose deficiency. (C) Effect of glucose concentration in SD medium on yeast biomass production. Yeast grown in higher glucose medium produced higher biomass, and DR optimized CLS but not biomass.

(D, E and F) Influence of glucose levels in YPD medium on yeast CLS. (D) Survival curve of yeast was cultured in YPD (1% yeast extract and 2% peptone) medium with different glucose levels (mean + SEM, n = 8). (E) Moderate DR (0.5%) and severe DR (0.05%) did not extend lifespan compared to normal condition (2% glu). (F) DR did not optimize CLS and biomass.

(G, H and I) Influence of glucose concentrations in SD medium containing four fold amino acids on yeast CLS. (G) Survival curve (mean + SEM, n = 8) and AUC comparison (H) shown that different glucose levels had little effect on lifespan. (I) Yeast cultured in normal condition produced higher biomass than DR condition, but further addition of glucose did not increase biomass.

(J, K and L) Influence of glucose levels in SD medium with 4-fold YNB (6.8 g/L) on yeast CLS. (J and K) DR extend lifespan, but the difference was less than that in SD medium as show in A and B, which, due to addition of YNB, increased lifespan in 2% glucose (mean + SEM, n = 8). (L) The biomass results were similar with the observation in SD medium with four fold amino acids. Yeast grown in 8% glucose medium did not produce higher biomass than that in 2% glucose medium.

(M, N and O) High osmolarity and buffered media extend CLS. Yeast were inoculated into SD, SD medium supplemented with 0.3 M NaCl (high osmolarity), and SD medium prepared with phosphate buffer solution at (PBS, Na_2HPO_4 and NaH_2PO_4, pH 6.0) or citrate phosphate buffer solution (CBS, Na_2HPO_4 and citric acid, pH 6.0). (M) Survival curve (mean + SEM, n = 6) and AUC comparison (N) shown that the three media significantly prolonged CLS, as well produced higher biomass than SD medium (O).

Biomass of each aging vial at one age-point was measured as the average reading of OD values at 660 nm from 10 to 30 min in outgrowth curve. The OD value of SD medium at day 2 was defined to be 100 relative OD value. The variance of AUC (mean + SEM, n = 8) and relative OD600 values (mean + SD, n = 8) between the treatments was compared using the Duncan's multiple range test at $P < 0.05$, different letters (a–d) showing significant differences.

YPD medium was also chosen for DR studies in yeast chronological aging model (Aragon *et al.* 2008; Goldberg *et al.* 2009). To my surprise, the yeast cultured in YPD medium containing 0.5% glucose had a shorter lifespan than that grown in YPD with 2% glucose, and those grown in YPD with 0.05% glucose had lifespan further reduced, similar to the results in SD medium (**Figure 4.1A, D, E**). For biomass, the observation was also similar to the results in SD medium that higher glucose concentrations produced higher biomass; however, the biomass at the same glucose level was significantly higher than that of SD medium (**Figure 4.1C, F**). YPD medium is rich in nutrients; I propose that 2% glucose in YPD medium could mimic DR condition of the 0.5% glucose in SD medium and hence induce longevity of yeast. The lifespan reduction in 0.5% and 0.05% glucose YPD would be due to glucose deficiency.

For preliminary study of effect of amino acids and YNB in yeast CLS, four-fold of total amino acids were added into the SD medium containing different glucose levels. As shown in **Figure 4.1G-I**, the addition of total amino acids did not extend CLS, but increased biomass production, and the DR condition (0.5% glucose) did not produce longer lifespan than the normal condition (2% glucose). Interestingly, the results showed that the addition of four-fold YNB (6.8 g/L) significantly extended

CLS and increased biomass production more than that of the SD medium with 2% glucose (**Figure 4.1J-L**). Yeasts in the high YNB medium with 0.5% glucose had longer CLS than that in the high YNB medium with 2% glucose. Therefore, the results from high amino acids and YNB media suggested that the concentrations of both components played important roles in regulation of yeast CLS. Furthermore, it was observed that yeast grown in glucose levels from 0.05% to 2% produced more biomass but not longer CLS. In contrast, 8% glucose could not further increase biomass in either high amino acids or YNB media. This may be due to shortages of YNB and amino acids relative to high glucose content (**Figure 4.1I, L**).

Previous studies proposed that acetic acid induced cell death was the key mechanism of chronological aging in yeast in standard medium and that environmental and genetic interventions via increasing cellular resistance to acetic acid could extend CLS (Fabrizio *et al.* 2004; Burtner *et al.* 2009b; Murakami *et al.* 2011). In this study, the results are consistent with these reports. I have showed that high osmolarity medium (0.3 M NaCl) and buffered media (pH 6.0) can significantly extend CLS of yeast (**Figure 4.1M, N**). Interestingly, the high osmolarity and buffered media produced more biomass than the standard SD medium even though they had the same amounts of glucose and other nutrients (**Figure 4.1O**). In accordance to this study, buffered media induced biomass increase was also observed in a previous study (Burtner *et al.* 2009b).

4.3.2 Development of statistical design of experiments for evaluation of nutrition, biomass and lifespan

To determine the relationships between nutrients and lifespan as well as biomass production of yeast, a 15-media experimental protocol with three-factors (glucose,

YNB, amino acids)/three-levels (-1, 0, 1) was selected according to the classical RSM Box–Behnken design. This design can generate the relationships between several explanatory variables (nutrients) and response variables (lifespan, biomass) with the minimal number of experimental runs. Concentrations of three factors, i.e. glucose (0.5 to 5.5 %), amino acids (0.5 to 3.5 ×) and YNB (0.85 to 9.35 g/L), were chosen to test conditions known to alter lifespan in a typical SD medium. The WT strain BY4742 and three single gene deletion strains (*sch9*Δ, *tor1*Δ, and *sir2*Δ) were chosen because the three genes are highly conserved and play critical functions in regulating aging from yeast to mammals (Fontana *et al.* 2010; Haigis & Sinclair 2010; Kaeberlein 2010a; Guarente 2011). Thus, this experimental design contains a total of 1024 runs that include the standard SD medium (4 strains × 16 media × 16 repetitions). Relative lifespan of the four strains (WT, *sch9*Δ, *tor1*Δ, and *sir2*Δ) are shown in **Figure 4.2**, and response surfaces for lifespan and biomass of the four strains cultured at various concentrations of amino acids, glucose, and YNB are plotted in **Figure 4.3** and **Figure 4.3**, respectively.

4.3.3 Nutrient composition is a key factor for longevity of yeast

To elucidate whether nutrient balance is a core factor for longevity in different yeast strains, I did an analysis based on the strains of yeast respectively.

WT Strain. Under three fixed GLU concentrations of 0.5, 3, and 5%, the trends of response surface were greatly different in regards to YNB and AA concentrations (**Figure 4.3 top row**). It is clearly that the typical DR (0.5% GLU) does not always produce longer CLS than normal (3%) or high (5.5%) GLU level when yeast cultured in media containing diverse concentrations of YNB and AA. The higher YNB and lower AA caused longer lifespan under 0.5% GLU. The response surface of 3% GLU

showed an optimal lifespan within the testing concentration ranges of amino acids and YNB. The trends in lifespan changes at 5.5% GLU were almost opposite as that of 0.5% GLU. Lower YNB and higher AA induced longer lifespan under 5.5% GLU. Analysis in linear and quadratic effects of AA, GLU and YNB on lifespan (**Table 4.4**) suggested that changes in AA × GLU ($P = 0.0069$) and YNB × GLU ($P = 0.0221$) had significant effect on WT yeast CLS. AA × GLU positively altered CLS while YNB × GLU negatively affect CLS. However, changes in other terms (AA, GLU, YNB, AA × AA, YNB × YNB, GLU × GLU, YNB × AA) had less influence on yeast CLS. Altogether, these data indicate that nutrients in medium greatly impact CLS in WT yeast.

***sch9*Δ Strain.** The response surface plots of *sch9*Δ also showed that nutrients changed lifespan significantly, and the trends were greatly different from those of the WT at the three GLU levels (**Figure 4.3 second row**). Only the term of AA × AA had no significant effect on yeast CLS (**Table 4.4**). The *sch9*Δ had longer CLS when grown in media with higher AA and lower YNB under 3% and 5.5% GLU, but had longer CLS in either media containing lower AA and higher YNB or higher AA and lower YNB under 0.5%.

***tor1*Δ and *sir2*Δ Strains**. The trends of response surfaces bore some similarities (**Figure 4.3 3rd and 4th row**), and this was consistent with the result that *tor1*Δ and *sir2*Δ had a good correlation ($P < 0.0001$) in lifespan change (**Table 4.2**). However, the trends of the two strains differed to that of WT and *sch9*Δ. Under 0.5% GLU, longer lifespan was observed than that 3% and 5.5% GLU. Both AA and GLU had more significant effect than other terms on lifespan change in *tor1*Δ and *sir2*Δ (**Table 4.4**).

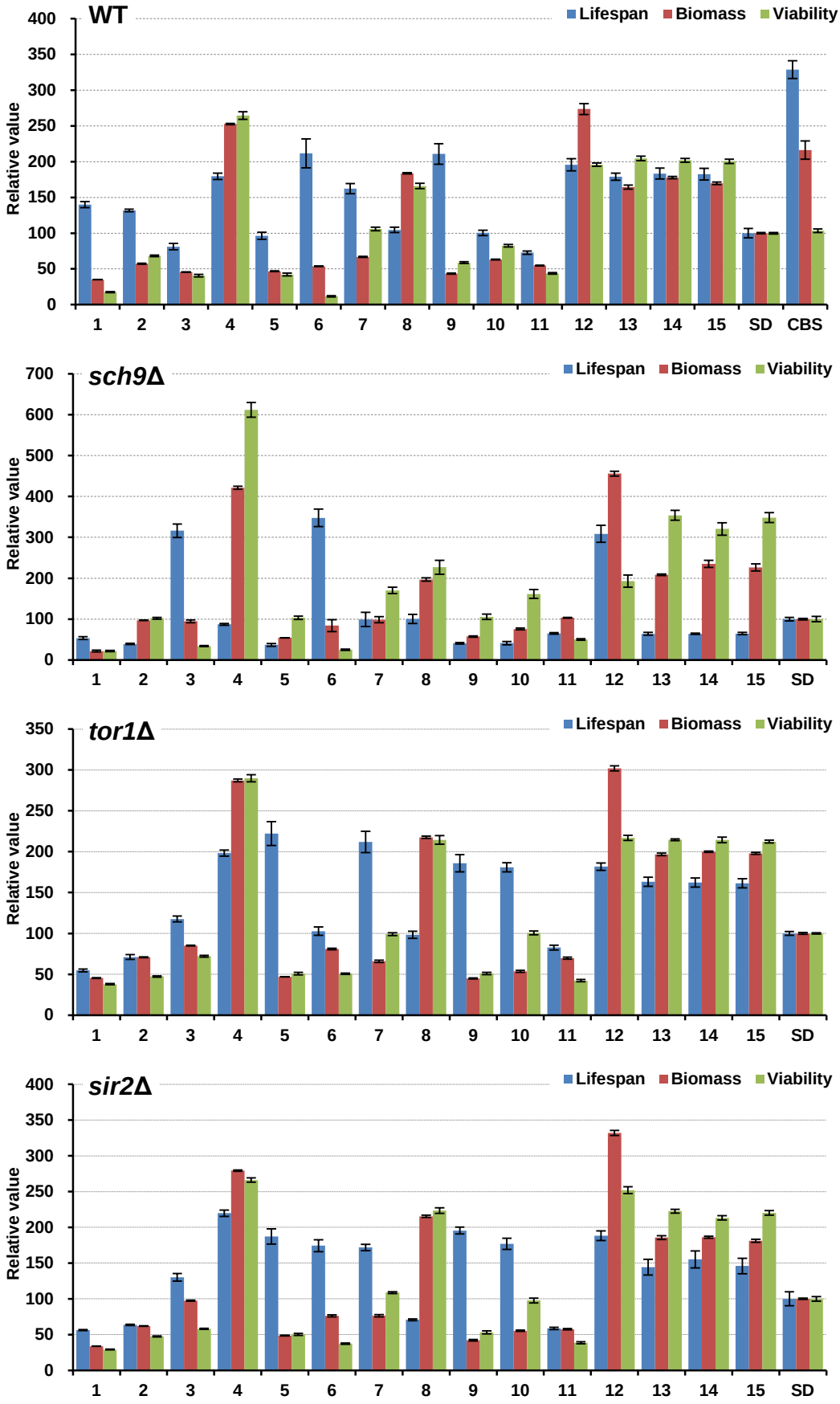

Figure 4.2 Comparison of relative lifespan, biomass and viability in the four yeast strains (WT, *sch9*Δ, *tor1*Δ, and *sir2*Δ)

AUC represents the survival integral for lifespan comparison, the AUC of yeast aging in SD medium is defined as 100%, and error bars represent SEM within 12 replicates. Biomass production was measured as the average values at OD660 of each medium from day 10 to day 22 (see **Figure 4.6**), the biomass of SD medium was defined as 100%, (mean + SEM, n = 12). Viability was the survival at day 2, and the survival of SD at day 2 was defined as 100%, (mean + SEM, n = 12).

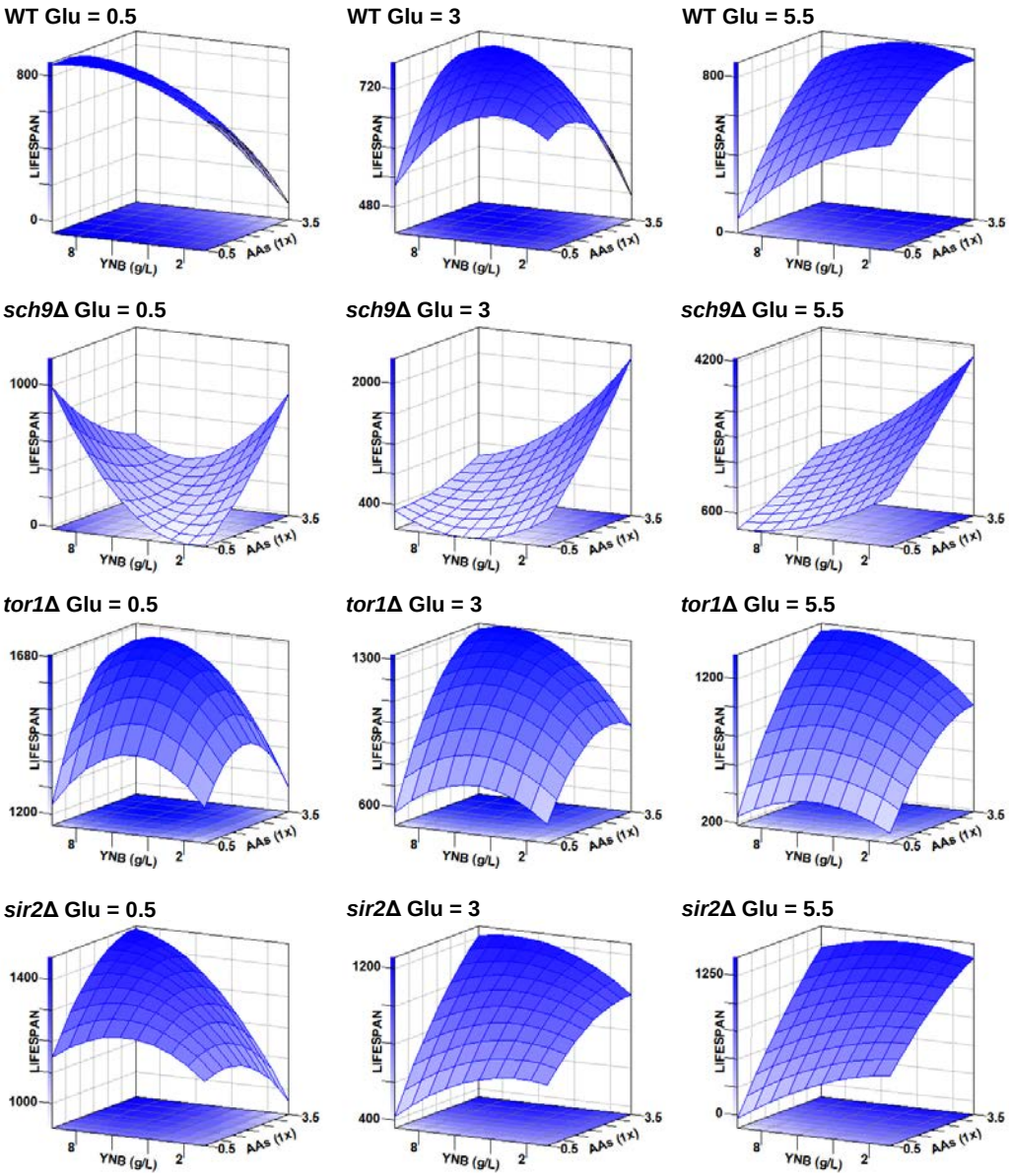

Figure 4.3 Response surfaces for lifespan of the four yeast strains (WT, *sch9*Δ, *tor1*Δ, and *sir2*Δ) cultured at various concentrations of amino acids (AAs), glucose (Glu), and yeast nitrogen base (YNB)

For each strain, three AA/YNB-lifespan plots are shown at specific GLU levels 0.5% (low), 3% (medium) and 5.5 % (high) respectively. The AAs concentration ranged from 0.5× to 3.5× and YNB from 0.85 to 9.35 g/L. The surface-response in *sch9*Δ was clearly different from that in WT, *tor1*Δ and *sir2*Δ, while these plots displayed similar trends in *sir2*Δ and *tor1*Δ. All these surface-response plots were generated automatically by SAS program, and those surface plots for biomass production are seen in **Figure 4.4**.

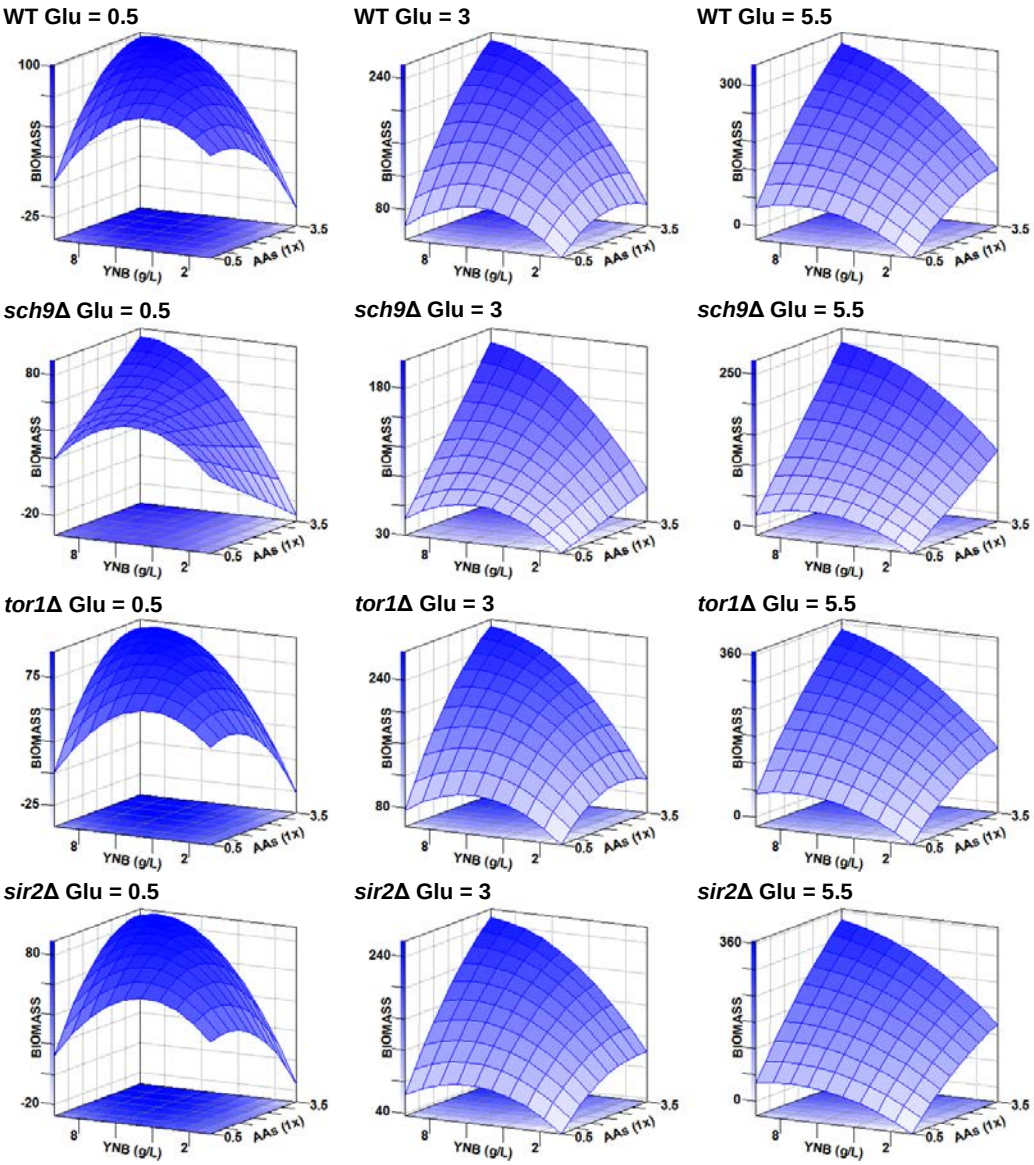

Figure 4.4 Response surfaces for biomass production of yeast cultured at various concentrations of amino acids (AAs), glucose (Glu), and yeast nitrogen base (YNB).
For each strain, three AA/YNB-lifespan plots are shown at specific GLU levels 0.5% (low), 3% (medium) and 5.5 % (high) respectively. The AAs concentration ranged from 0.5× to 3.5× and YNB from 0.85 to 9.35 g/L. These surface-response plots displayed similar trends in the four strains. All these surface-response plots were generated automatically by SAS program, and those surface plots for lifespan are seen in **Figure 4.3**.

Estimation of lifespan from linear and quadratic parameters showed that the same term had marked differences among the four strains (**Table 4.4**), which was totally different from the biomass results (*vide infra*). It also suggests that nutrient composition is an important factor for longevity of budding yeast and the three nutrients and their interactions play different roles in lifespan of different strains.

Overall, the diverse change of lifespan of the four strains in these media suggested that nutrient composition, instead of glucose alone, played a more important role in regulation of lifespan.

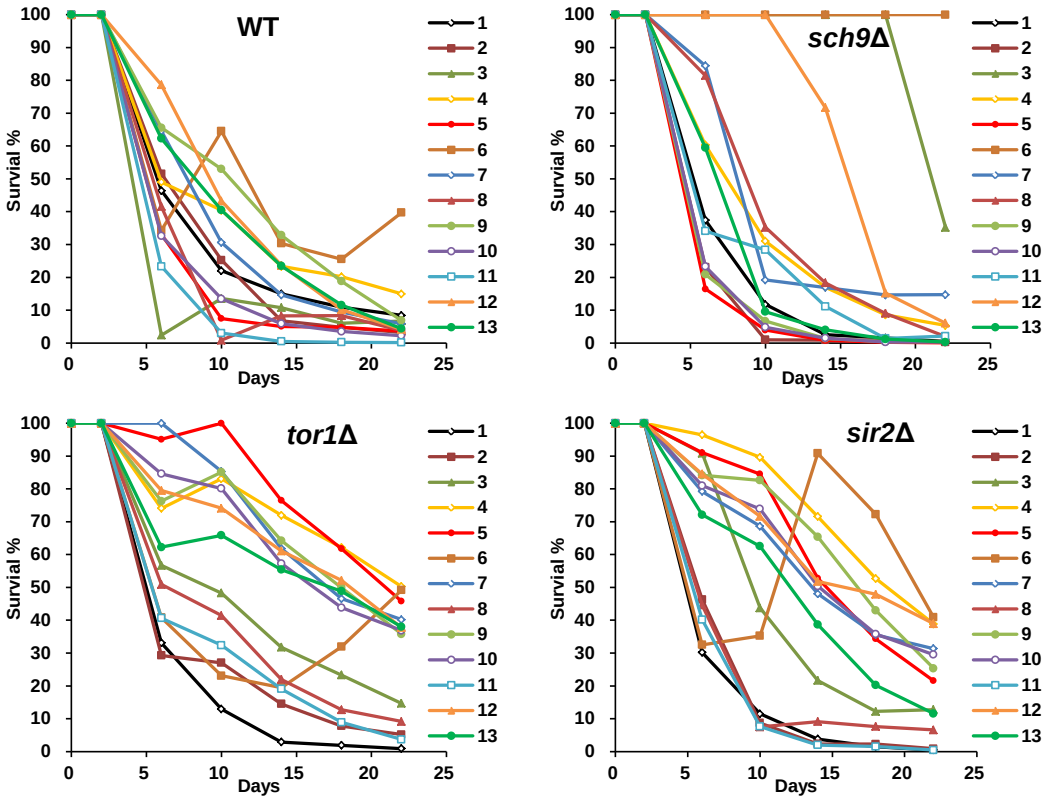

Figure 4.5 Survival curves of four yeast strains
Four yeast strains (WT, *sch9*Δ, *tor1*Δ, and *sir2*Δ) were cultured in 13 media for 22 days. The relative survival of each age-point was shown as the mean within 12 replicates.

4.3.4 Biomass production of the four strains has similar changes in response to nutrient composition

During chronological aging, the total cell number in the medium (defined as biomass production) had little change (**Figure 4.6**), but the number of living cells (survival %) had been reducing stage by stage. As listed in **Table 4.2**, the biomass and viability had a good positive correlation among the four strains, which indicates that viability at day 2 represent the biomass production of the medium. This suggests that

there might be no need to measure the OD660 values of medium at each age-point as the biomass.

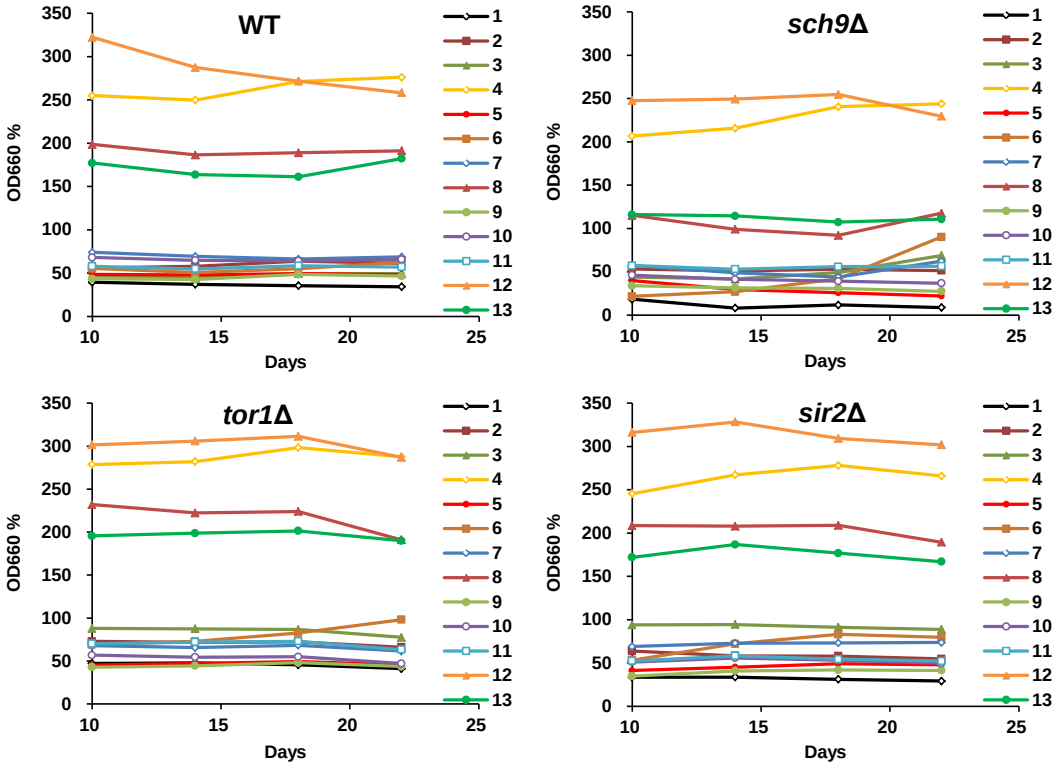

Figure 4.6 Effect of medium nutrient composition on yeast biomass production
Biomass of each aging vial at one age-point was measured as the average reading of OD values at 660 nm from 10 to 30 min in outgrowth curves. The OD value of SD medium at day 2 was defined as 100%. Data is shown as the mean within 12 replicates (RSD < 10%).

It is known that the four strains had significant lifespan changes in various media (**Figure 4.3**); however, these results were not observed in biomass production. On the contrary, the biomass production of the four strains had similar change trends among the 15 media (**Figure 4.4**). Firstly, the Pearson coefficient (r) of WT with *sch9*Δ, *tor1*Δ and *sir2*Δ were very high at 0.97 ($P < 0.0001$), 0.99 ($P < 0.0001$), and 0.99 ($P < 0.0001$) (**Table 4.2**) respectively. However, for lifespan, the corresponding r values were poor at 0.18 ($P = 0.52$), 0.30 ($P = 0.28$) and 0.52 ($P = 0.04$). Secondly, all linear terms (AA, YNB and GLU) and all cross terms (AA × YNB, AA × GLU and YNB × GLU) had positive effects, and all quadratic terms (AA × AA, YNB × YNB, GLU ×

GLU) had negative effects on biomass production in the four strains. However, these results were different from the data on lifespan (**Table 4.4**).

For the optimal medium for biomass production, as can be seen in, the response surface plots indicated that only the low level of GLU (0.5%) medium had a maximal biomass from the coded concentration range of amino acids (0.5–3.5 ×) and YNB (0.85–9.35 g/L), while the media with middle or high levels of GLU had not (**Figure 4.4**). This means that higher nutrient amounts in media produced higher biomass for all stains.

4.3.5 Strain *sch9*Δ is more sensitive to nutrients than the other three strains

For the changes in lifespan of *sch9*Δ strain in response to various nutrient compositions, the response surface plots showed that nutrients changed lifespan significantly, as the trends were greatly different from those of the other strains (**Figure 4.3**) and almost all term had significant effect on yeast CLS (**Table 4.4**). These data suggest that the lifespan of *sch9*Δ is more sensitive to nutrients than the other three strains.

For cell growth in the different media, the yeast cells of WT, *tor1*Δ, and *sir2*Δ grew well as indicated by the biomass production that was dependent on the available nutrients in the media (**Figure 4.7**). In contrast, growth of *sch9*Δ cell was greatly disturbed in some media, the cells cultured in medium 1, 3, 5, 6, and SD did not grow better than the yeast in other media. Nevertheless, *sch9*Δ strain grew well in a few media such as 7, 11 and YPD and the growth curves were similar to those of the other strains. Thus, this result could indicate that the growth of *sch9*Δ is more sensitive to nutrients.

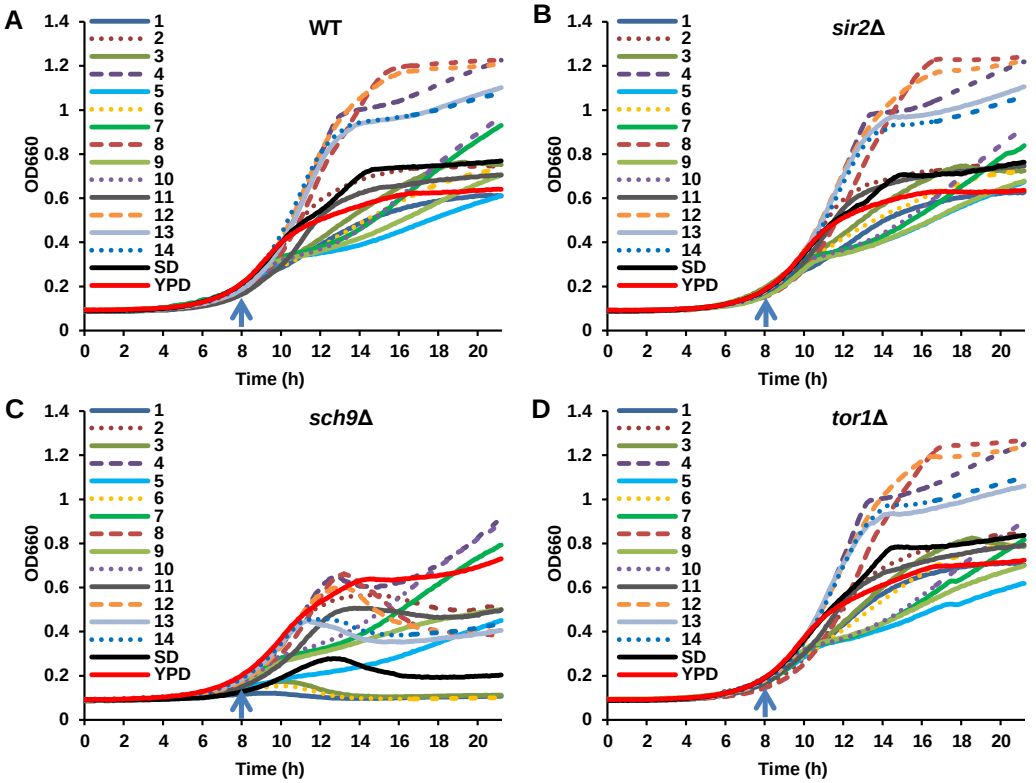

Figure 4.7 Different media have little effect on cell growth during lag phase in most yeast strains
The growth curves show that yeast cells of WT (A), *sir2*Δ (B) and *tor1*Δ (D) proliferated well with nutrients available in different media since the lag time (≈ 8 h) of each curve had no significant changes. Yeast cultured in media containing high and balanced AAs, GLU and YNB content produced a higher number of cells. However, *sch9*Δ did not grow well in several media, even in the SD (C). Five µL of diluted and nutrient free yeast culture (≈ 1×10^4 cells) was pipetted into each well of 96-well microplate. One hundred µL of different media was then added to each well. The cell population was monitored with a microplate reader by recording the OD every 5 min at 660 nm.

I also observed that *sch9*Δ cells would cluster together in several media (**Figure 4.8**). Moreover, these aggregative cells formed macroscopic agglomerates and settled to the bottom of sample vials. In addition, this aggregation phenomenon can be seen from the growth curve (**Figure 4.7**), which had a clear descending trend after the maximal OD660 value, such as 1, 2, 3, 6, 8, 12, 13, 14, 15 and SD. However, this phenomenon was not found in other strains (**Figure 4.7, 4.8**), and the aggregation did not relate to biomass production and lifespan (**Figure 4.2**). Overall, these results suggest that Sch9 regulates cell aging, growth and size and that *sch9*Δ strain is highly sensitive to nutrients change.

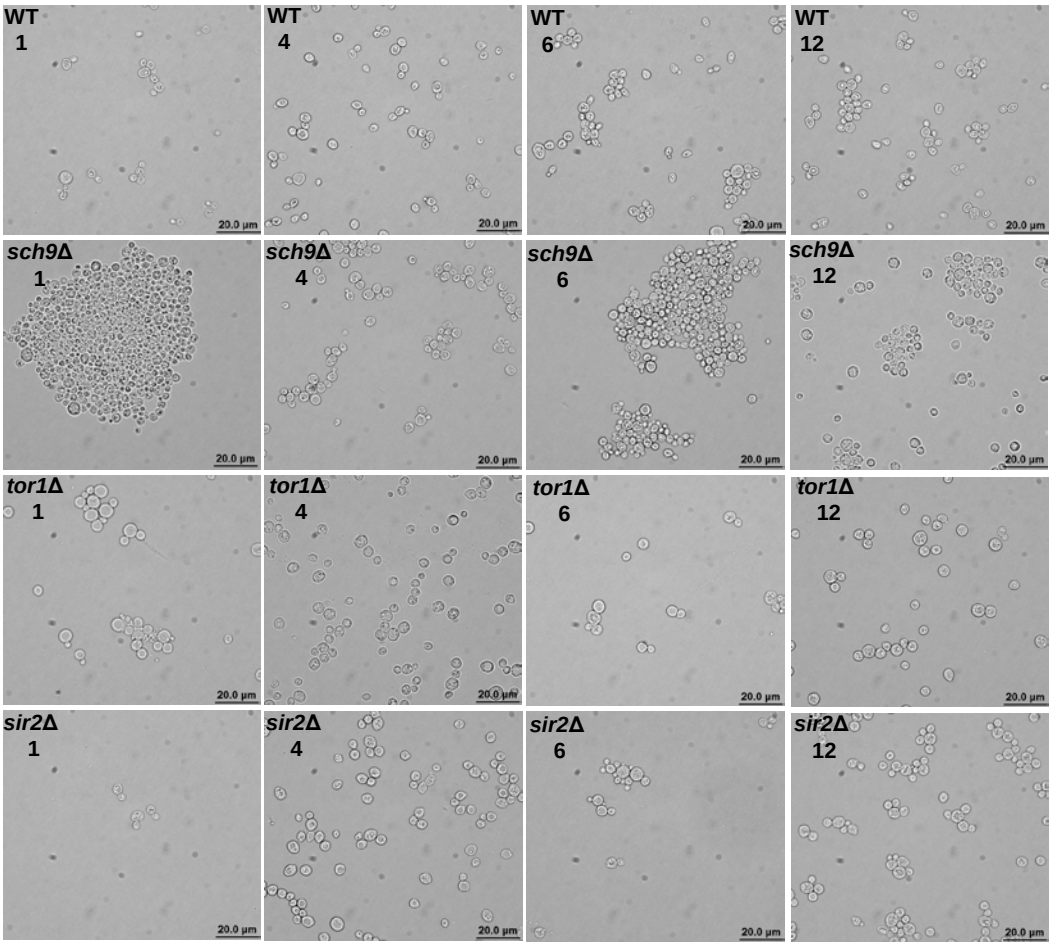

Figure 4.8 Representative cell images of the four yeast strains in different media at day 22
Yeast cells at different aging-points were collected and observed using an optical microscope (Olympus CX31, Tokyo, Japan) with 1000× magnification. *sch9*Δ cells gathered together in response to nutrient imbalance in the medium.

4.3.6 Aging media pH is dependent on glucose concentration and has no correlation with lifespan

In the yeast CLS model, acidification of the culture medium accelerates chronological aging when cells are cultured in a SD liquid medium (Burtner *et al.* 2009b; Murakami *et al.* 2011; Murakami *et al.* 2012). The pH of a yeast aging culture is dependent on the medium composition, especially glucose concentration. Yeast cells metabolize glucose and other substrates such as amino acids to produce organic acids via glycolysis and citric acid cycle including acetic, pyruvic and succinic acids. In this study, I examined pH changes in different media in WT and *sch9*Δ (**Table 4.1**) and analysed the correlations among pH, amino acid, YNB, GLU, lifespan and

biomass (**Table 4.3**). The pH of aging cultures ranged from 2.7 to 6.8 and pH at day 2 and day 4 had no significant difference, which was consistent with a previous study (Burtner *et al.* 2009b). In addition, the pH of WT cultures had a similar trend except *sch9*Δ strain, which might indicate that pH changes of different media were independent of deletion of *SCH9*. Furthermore, the pH of the two strains at two age-points had a strong correlation with the GLU content in the media, but had no correlation with lifespan or biomass. This result suggested that nutrient composition could offset the effect of extracellular pH decrease to influence yeast CLS under the current experimental conditions, possibly due to intracellular buffering capacity (Thomas *et al.* 2002). The pH as one determinant of CLS was observed only in a few cases in this study (media 7 versus media 8). It should be noted that buffering the pH of standard SD medium (CBS) could result in longer CLS than any of the 15 media compositions (**Table 4.1**) in WT strain. For un-buffered conditions, previous studies focused on glucose percentage in media and did not consider amino acids and YNB composition. Thus it was concluded that low pH accelerates chronological aging and pH buffering increases CLS under standard SD medium (Murakami *et al.* 2011; Murakami *et al.* 2012). In this study, I compared the lifespan of yeast in various media with changes in YNB and amino acids, which likely affected the chronological viability by alleviating the negative impact of media acidification and acetic acid toxicity.

4.3.7 The optimal SD medium for yeast

Based on the four strains used in this study, the media 12 would be the best one for yeast since it produced the maximal biomass and lifespan (**Table 4.5**). However, media 12 resulted in a shorter lifespan of WT yeast than that in the YPD and pH

buffered media (**Figure 4.2**, **Table 4.1**). In contrast, media 12 has only a slight influence on cell growth in *sch9*Δ (**Figure 4.7, 4.8**). In addition, our results showed the WT cultured in YPD (2% GLU) had a remarkable longevity (**Figure 4.1**). The other three strains (data not shown) also showed lifespan extension. All four strains grew well in YPD and there was no aggregation in *sch9*Δ (**Figure 4.7**). However, not all the chemicals included in YPD are known, thus YPD was not an ideal medium for investigating the effects of components on aging.

Table 4.5 Membership function value f(x) and ranking for the 15 media according the two criteria of lifespan and biomass in the four yeast strains

	WT		*sch9*Δ		*tor1*Δ		*sir2*Δ			
Run	lifespan	Biomass	lifespan	Biomass	lifespan	Biomass	lifespan	Biomass	Mean	Ranking
1	0.48	0.00	0.05	0.00	0.00	0.00	0.00	0.00	0.07	15
2	0.43	0.09	0.01	0.17	0.10	0.10	0.05	0.09	0.13	13
3	0.06	0.04	0.90	0.17	0.38	0.16	0.45	0.21	0.30	10
4	0.77	0.91	0.16	0.92	0.86	0.94	1.00	0.82	0.80	2
5	0.17	0.05	0.00	0.07	1.00	0.01	0.80	0.05	0.27	11
6	1.00	0.08	1.00	0.14	0.29	0.14	0.72	0.14	0.44	6
7	0.64	0.13	0.20	0.18	0.94	0.08	0.71	0.14	0.38	8
8	0.23	0.62	0.20	0.40	0.26	0.67	0.09	0.61	0.39	7
9	0.99	0.04	0.01	0.08	0.78	0.00	0.85	0.03	0.35	9
10	0.20	0.12	0.01	0.12	0.75	0.03	0.74	0.07	0.26	12
11	0.00	0.08	0.09	0.19	0.17	0.10	0.02	0.08	0.09	14
12	0.89	1.00	0.87	1.00	0.76	1.00	0.81	1.00	0.92	1
13	0.77	0.54	0.09	0.43	0.65	0.59	0.54	0.51	0.51	5
14	0.80	0.60	0.09	0.49	0.64	0.60	0.61	0.51	0.54	3
15	0.79	0.56	0.09	0.47	0.64	0.60	0.55	0.49	0.52	4

$f(x) = (x - x_{min})/(x_{max} - x_{min})$, x is the lifespan and biomass among 15 runs respectively, ranking based on means of f(x) values of lifespan and biomass in three strains, the number of ranking is smaller, indicating the medium for yeast culture is better for longevity and biomass production.

The standard SD medium is better suited for yeast aging study, and the amino acid compositions can be conveniently modified to identify optimal amino acid requirements of specific mutants. For yeast aging study, development of an ideal SD

medium mimicking YPD that can meet cell growth requirements and achieve longevity for most strains would be interesting but challenging to achieve. In this study, I found that not only glucose and amino acids but also YNB played a significant role in regulating lifespan and biomass production of yeast strains, especially of *sch9*Δ. Thus, modification of amino acids and YNB composition was important for development of a better SD medium for yeast aging study.

4.4 Discussion

In this Chapter, I used a high throughput screening assay to comprehensively evaluate the relationships between nutrients (GLU, AA and YNB) and lifespan as well as biomass production in four yeast strains (WT BY4742, *sch9*Δ, *tor1*Δ, and *sir2*Δ). Experimental design based on the classical RSM with a total of 1024 treatments (4 strains × 16 media × 16 repeats) was applied to show that different strains cultured in various media had similar response surface trends in biomass production and viability at day 2, but very different trends in lifespan. All the three groups of nutrients and their interactions seemed to play different roles in regulation of lifespan of different strains. In addition, I propose that viability at day 2 might represent the biomass production of the medium since it had a good correlation with measured biomass based on the OD660 values of the medium. Furthermore, these findings indicate that lifespan extension by DR regime was dependent on nutrients in medium and that nutrient composition was a key factor for longevity of yeast.

Recent studies have revealed that nutrition influences the biological aging process in different model organisms, especially the macronutrients including carbohydrates, fats, proteins, and water (Meydani 2001; Lee *et al.* 2008; Fanson *et al.* 2009; Ja *et al.* 2009). This information is particularly important because of its

potential for developing interventions to prevent age-related diseases and promote healthy aging.

The common medium for yeast aging study is the SD medium containing a limited amount of nutrients, which mimics yeast survival in the wild (Fabrizio & Longo 2003). The SD medium contains glucose, YNB, ammonium sulphate, and amino acid mixture. YNB contains salts, vitamins and trace elements (**Table 3.1**). For the standard SD medium, it has been shown that DR (0.5% glucose) can extend yeast RLS and CLS in various strains, as compared to the normal condition (2% glucose). Recent studies on flies also suggest that the traditional observation on DR-induced longevity was mainly due to nutrient balance. This indicates that the imbalance between dietary and other nutrients resulted in lifespan reduction under normal conditions (Skorupa *et al.* 2008; Fanson *et al.* 2009; Piper *et al.* 2011). In addition, DR in mammals is commonly defined as reduction in dietary intake without malnutrition by 10% to 50% of *ad libitum* (Mair & Dillin 2008; Fontana *et al.* 2010). However, DR in yeast is modeled by glucose restriction and reducing the glucose level in the SD medium from 2% (normal condition) to 0.5% (moderate DR) or to 0.05% (severe DR) can extend lifespan of different yeast stains (Bishop & Guarente 2007).

Recent studies suggested that the low glucose induced longevity in yeast was partially due to decreased production of acetic acid and reduced medium acidification for two possible reasons. First, acetic acid was identified as an extracellular mediator of cell death during yeast chronological aging. It was demonstrated that environmental interventions by reducing or eliminating acetic acid increased CLS, such as via DR, using non-fermentable carbon source, or transferring cells to water (Burtner *et al.* 2009b). Second, pH neutralization was demonstrated to protect against

reduction in RLS and CLS in yeast (Fabrizio *et al.* 2004; Murakami *et al.* 2011; Murakami *et al.* 2012). Extracellular acidification of the culture medium could cause intracellular damage, which subsequently limited the cell replicative potential. The reduced RLS and CLS could be extended by buffering the pH of medium to 6.0 (Murakami *et al.* 2012). In this study, I also examined impact of DR, growth on a non-fermentable carbon source, transferring yeast to water (unpublished data), deletion of *SCH9* and *RAS2*, and growth in high osmolarity or buffered media. Consistent with previous observations, I found that these factors could also extend yeast CLS. However, the results also showed that low glucose level media (low acetic acid content and high pH) resulted in CLS reduction (**Figure 4.1, 4.2, 4.3**), and that the relatively high glucose medium (high acetic acid content and low pH) extended CLS (media 6 versus media 5 or media 12 versus media 10). In addition, I measured the acetic acid contents of different cultures of WT and *sch9*Δ at day 2 and found the acetic acid concentration was relatively low (< 10 mM) and could only be detected in a few high glucose media (unpublished data). This indicates that acetic acid might not always be the key determinant of CLS, which is supported by others (Longo *et al.* 2012). It is likely that the effect of acetic acid on yeast survival is condition-dependent, such as media composition, nutrient composition, and buffering capacity of both extracellular and intracellular media (Thomas *et al.* 2002).

Due to the complexity of the factors impacting yeast ageing, at present, it is still not clear why the observations differ from prior studies (low glucose, GLU < 0.5%). One possibility might be that this study focused on the effects of nutrients (not only glucose, but also YNB and amino acids) on CLS of yeast in the SD medium. YNB and the initial amino acid composition could alter the intracellular pH of the aging culture, affect the yeast cell survival, and negate acetic acid toxicity. Another

possibility might be that the conditions were not optimized for CLS extension by low glucose (< 0.5%). It should be noted that the different results were also likely attributable to differences in the medium composition and culture conditions. For example, I modified the amino acid composition of SD medium (**Table 3.1**), which is different from prior studies, Although I followed similar composition of some amino acids such as adenine, L-arginine, L-methionine, L-serine, L-tryptophan, and L-tyrosine (Murakami *et al.* 2008), I used a shaker incubator with a high capacity of 600 aging culture vials (4 mL, 15 x 45 mm, with plastic caps) with a relatively small medium volume of 1 mL, which is greatly different from other laboratories, where bigger culture containers with more liquid medium, are used. This could result in different cell population, culture aeration and oxidative metabolism (Longo *et al.* 2012). Furthermore, yeast CLS is influenced by additional factors, including strain auxotrophies, the way the cultures are aerated, the use of 96-well microplates, the use of spectrophotometric vs. CFU-based methods for quantifying viability. All these factors may have contributed to the different observations. The current work did not necessarily disprove previous findings of acetic acid/pH as one important factor for yeast aging, although cautions should be exercised in interpretation of data (e.g. experimental conditions applied). The findings from this study need to be validated by different laboratories and further work is needed to understand the reasons for these different observations about the effect of pH on lifespan, for example, using buffered media with different nutrient compositions.

YPD would be a good medium for cell growth and longevity study since it contains yeast extract and peptone, which are rich in many types of nutrients. It has applications in diverse yeast strains (Aragon *et al.* 2008; Goldberg *et al.* 2009). YPD medium was chosen for the DR study in yeast chronological aging model mainly due

to two factors. Firstly, it allows isolation of quiescent and non-quiescent cells from stationary phase cultures grown in YPD medium (Allen *et al.* 2006; Aragon *et al.* 2008). Secondly, the shape of mortality curves for yeast grown in the nutrient-rich YPD medium was similar to the mortality patterns observed in multicellular eukaryotes (Minois *et al.* 2009). Thirdly, yeast grown in YPD medium containing 0.2% or 0.5% glucose lived significantly longer than that grown at 0.05%, 1% or 2% glucose (Goldberg *et al.* 2009), which suggests that the glucose level affects lifespan of yeast as observed in many higher eukaryotes.

It has been reported that amino acid balance plays a critical role in regulation of lifespan in rat, fly and yeast, independent of DR (Koc *et al.* 2004; Miller *et al.* 2005; Malloy *et al.* 2006; Alvers *et al.* 2009a; Grandison *et al.* 2009; Elshorbagy *et al.* 2010). Methionine restriction can decrease visceral fat mass, preserve insulin action, and prolong lifespan in rats independent of DR (Malloy *et al.* 2006). In *Drosophila*, adding methionine alone to DR condition increased fecundity as much as that under regular feeding and without reducing lifespan (Grandison *et al.* 2009). In *S. cerevisiae*, a few studies have shown that reduction in methionine increased the RLS (Koc *et al.* 2004) and removal of either asparagine or glutamate can significantly increase CLS (Powers *et al.* 2006). Furthermore, addition of isoleucine, threonine, valine, and leucine can extend CLS (Alvers *et al.* 2009a). However, these studies focused only on amino acids and did not consider other nutrients present in the medium. Thus, the relationship between glucose and amino acids in regulation of lifespan was still not established. In this study, I found that not only glucose and amino acids, but also YNB, played a significant role in regulation of yeast lifespan and biomass production. The three groups of nutrients and their interactions played different roles in regulation of lifespan of different strains. The objective of this study was not to produce an

optimal medium for yeast aging studies, but to demonstrate the fact that optimizing culture media by single nutrient variation is not sufficient to maximize the lifespan or biomass of yeast. Some previous studies have confirmed that glucose or a few amino acids are important for longevity of yeast and simple modification of one of these nutrients can greatly extend lifespan (Powers *et al.* 2006; Alvers *et al.* 2009a). With a suitable experimental design, an optimal SD medium to maximize the lifespan for a specific yeast strain can be obtained.

For lifespan, *sch9*Δ strain seemed to be more sensitive to nutrients, since more terms had significant ($P < 0.001$) effects on lifespan in *sch9*Δ than in the other strains (**Table 4.2**). The AGC kinase Sch9 is a substrate of multiprotein complex TORC1. Its function may be similar to the mammalian TORC1 substrate S6K1 (Urban *et al.* 2007). In yeast, Sch9 regulates cell growth and cell size, the absence of Sch9 activity causes a small size phenotype and distinct growth defect, while increasing lifespan by seven-fold (Fabrizio *et al.* 2001; Jorgensen *et al.* 2002; Kaeberlein *et al.* 2005b). The Tor-Sch9 pathway was thought previously to be a nutrient-sensing pathway (Mieulet *et al.* 2009; Fontana *et al.* 2010). In this study, I have confirmed and extended previous works by showing that deletion of *TOR1* regulate yeast CLS subjected to amino acids and glucose (**Table 4.2**). While *sch9*Δ strain is more sensitive to nutrients than the other three strains, Sch9 protein kinase was proposed previously as a central coordinator of protein synthesis (Huber *et al.* 2009) in promoting ribosome biogenesis and ribosomal protein gene expression (Huber *et al.* 2011). Thus, it is possible that Sch9 as a major nutrient-sensing factor to regulate cell growth, cell size, and stress resistance through control of protein synthesis. However, further experiments on quantifying Sch9 activity in different media are warranted to delineate the role of *SCH9* plays in this system.

4.5 Conclusion

These findings indicate that lifespan extension by DR may be partially dependent on nutrient composition and may be abolished by providing yeast with different nutrient compositions. Furthermore, the results show that *sch9*Δ is more nutrient-sensitive than the other three strains tested. Modification of amino acids and YNB compositions is an important factor to consider if one were to develop an optimal SD medium that can meet the cell growth requirements and enable longevity of most yeast strains for aging studies and evaluation of anti-aging activity of small molecules. My results also document that nutrient composition is an important factor for yeast CLS. Different yeast strains cultured in various media exhibited similar response surface trends in biomass production, but showed greatly different trends in lifespan. The three nutrients (glucose, amino acids and YNB) and their interactions played different roles in affecting lifespans of different strains. Taken together, these findings suggest that nutrient composition is an effective way to optimize lifespan and biomass production in yeast.

Chapter 5

INDEPENDENT AND ADDITIVE EFFECTS OF GLUTAMIC ACID AND METHIONINE ON YEAST LONGEVITY

5.1 Introduction

Reduction of 10-40% in food intake extends lifespan in diverse animals, including spiders, beetles, fish, and dogs, as well as the commonly used laboratory-model organisms: yeast, worms, fruit flies, and mice. CR is frequently reported as the most robust non-genetic intervention to extend lifespan and health span. In 2009, the results of a 20-year caloric restriction study in rhesus monkeys at the Wisconsin National Primate Research Center (WNPRC) published and suggested that CR might ameliorate human aging, because the monkeys with 70% of *ad libitum* food supply had fewer age-related deaths and lower incidence of diabetes, cancer, cardiovascular disease, and brain atrophy (Colman *et al.* 2009). However, a recent publication reported that diet composition may significantly affect the longevity of calorie restricted rhesus monkeys at the National Institute on Aging (NIA). In later study, CR reduced the incidence of diabetes and cancer but did not lower rates of cardiovascular disease and age-related death (Mattison *et al.* 2012). The differences in results and experimental design of the two CR-monkey studies were discussed adequately. A notable difference between the two studies is diet composition, the NIA study diet had relatively diverse and balanced nutrients, unlike the WNPRC study which used purified components and high sucrose (Mattison *et al.* 2012).

In addition to the two studies in primates, the idea that balance of nutrients in the diet might be a better way than simple dietary restriction for healthy lifespan was reported in other organisms (Lee *et al.* 2008; Fanson *et al.* 2009; Grandison *et al.* 2009; Greer & Brunet 2009; Ja *et al.* 2009). However, this emerging idea is not well substantiated in yeast. The benefits of dietary restriction have been generally suggested to arise from intake of fewer calories (termed caloric restriction). Thus, influences of nutrients on the biological aging process might be more dependent on the macronutrients including carbohydrates, fats and proteins (Simpson & Raubenheimer 2009). In addition to carbohydrates and fats, proteins (amino acids) in the diet as another energy contributor was shown to mediate lifespan significantly in commonly used aging model organisms, namely yeast (Jiang *et al.* 2000; Alvers *et al.* 2009a), fruit flies (Fanson *et al.* 2009; Grandison *et al.* 2009), and mice (Zimmerman *et al.* 2003; Miller *et al.* 2005). Notably, methionine may be a special one among various amino acids to regulate lifespan, since restriction of methionine by 80% was reported to increase medium and maximal lifespan by 30% and 40% in rats (Orentreich *et al.* 1993).

The budding yeast (*S. cerevisiae*) serves as a leading model organism for studying evolutionarily conserved mechanisms relevant to human aging and age-related diseases (Bishop & Guarente 2007; Steinkraus *et al.* 2008; Fontana *et al.* 2010; Kaeberlein 2010a; Longo *et al.* 2012). There are two aging models in the budding yeast: replicative aging and chronological aging (Longo *et al.* 2012). Although both types of yeast aging are influenced by nutrient composition of media, the relationship between nutrition and lifespan is unclear. It is widely known that moderate glucose restriction slows yeast chronological and replicative aging significantly, but my previous study suggested that the CLS extension by a typical glucose restriction

regime was dependent on the nutrients in media and that medium composition was a key determinant for yeast longevity (**Chapter 4**). The three nutrients (glucose, amino acids and YNB) and their interactions played important roles in affecting lifespans of different strain. In **Chapter 4**, I just investigated the effect of total amino acid on CLS. Modification of the composition of amino acids in a medium has been also reported to change yeast lifespan (Powers *et al.* 2006; Gomes *et al.* 2007; Boer *et al.* 2008; Alvers *et al.* 2009a). Yet, comprehensive studies are still lacking with regard to evaluate the influence of individual amino acids on yeast CLS in standard SD medium condition. Reported herein is my finding.

5.2 Materials and methods

5.2.1 Materials

The materials were as described in **Chapter 3** (**3.2.1**).

5.2.2 Lifespan, biomass and yeast cell growth assay

The lifespan, biomass and yeast cell growth assays have been described in **Chapter 3** (**3.2.3**).

5.2.3 Acetic acid analysis

The aging culture (2 day) was centrifuged at 4,000 g for 10 min at room temperature. The supernatant was collected and stored at –20 °C before analysis of acetic acid and pH. The pH of supernatant was measured using a Eutech Ion 6+ pH meter with a micro-tip pH electrode (Eutech Instruments, Singapore). The supernatant was filtered through a Sartorius Minisart polytetrafluoroethylene (PTFE) membrane (0.2 μm) before HPLC analysis. The acetic acid analysis was performed on a Waters

HPLC system (Milford, MA, USA) with an Alliance 2659 separation module, a 2996 photodiode array (PDA) detector. The detection wavelength was set at 210 nm. The column used was a Supelcogel C-610H column (300 × 7.8 mm, Supelco) with 0.1% sulphuric acid as mobile phase. Each sample was run 60 min at a flow rate of 0.4 ml/min at room temperature.

5.2.4 Data analysis

The data analysis on lifespan has been described in **Chapter 3** (**3.2.4**).

5.3 Results

5.3.1 Amino acids regulate lifespan and biomass changes in yeast

The EAA and NEAA contents from 0.2-fold to 5-fold of normal conditions were tested. There are usually 14 amino acids and two bases, adenine and uracil, in a standard SD medium (**Table 3.1**), only histidine, leucine, lysine and uracil are essential for WT yeast strain BY4742 (MATα *his3*Δ1 *leu2*Δ0 *lys2*Δ0 *ura3*Δ0) (Sherman 1991). I first examined whether ratio of EAA to NEAA caused CLS alteration. The EAA and NEAA contents from 0.2-fold to 5-fold of normal conditions were tested.

The ratio of EAA and NEAA changed lifespan significantly. The composition of 1-fold EAA and 5-fold NEAA had an optimal lifespan under normal glucose condition (2%, **Figure 5.1A, C**). However, this composition produced significantly shorter CLS under CR condition (0.5% glucose), and the standard composition (1E1N, 1-fold EAA and 1-fold NEAA) had an optimal lifespan (**Figure 5.1B, C**).

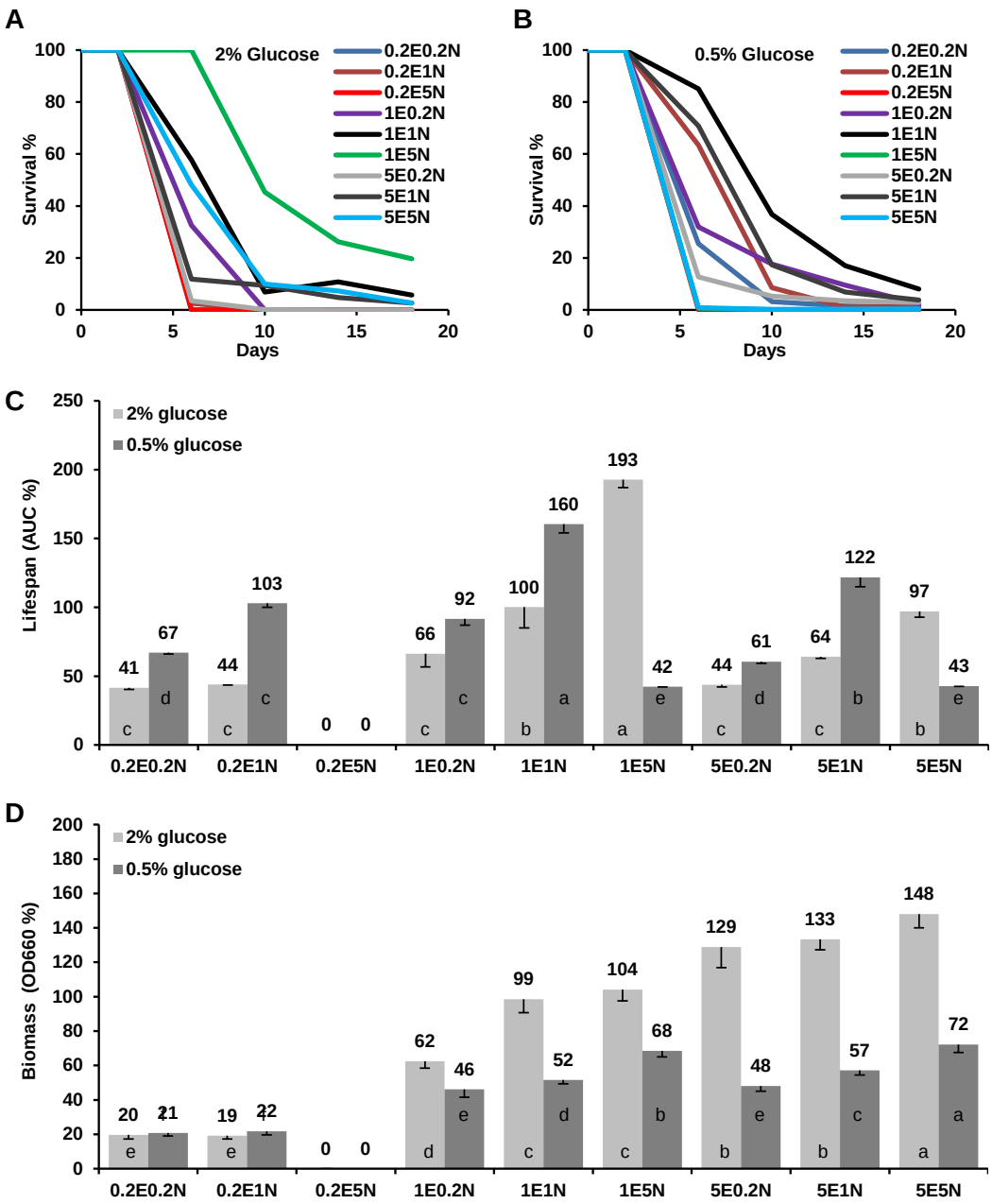

Figure 5.1 Ratio of essential and non-essential amino acids regulates lifespan and biomass changes

Survival curves of WT yeast (BY4742) were cultured in SD media with different ratios of EAA and NEAA in normal (2% glucose, **A**) and glucose restriction (0.5% glucose, **B**) conditions. For the lifespan and biomass comparison were presented in **C** and **D**, respectively. The EAA and NEAA compositions were listed in **Table 3.1**, and their concentrations were tested from 0.2-fold to 5-fold of normal conditions. AUC% represents the survival integral for lifespan comparison. The control (1E1N with 2% glucose) was defined as 100%. Biomass production was measured as the average values at OD660 of each medium from day 6 to day 10 and the biomass of SD (1E1N with 2% glucose) medium was defined as 100%. Lifespan and biomass: mean, n = 4 ± s.e.m; compared using Duncan's multiple range test at $P < 0.01$ and different lowercase letters in columns indicate significant difference.

These results suggest that the EAA and NEAA mediated lifespan alteration is influenced by glucose content in the medium (**Figure 5.1C**), and this is consistent

with the previous finding that total amino acids content has close interaction with glucose to regulate yeast CLS (**Chapter 4**). Similarly, the ratio of protein and carbohydrate was able to significantly change lifespan in *D. melanogaster* (Lee *et al.* 2008; Simpson & Raubenheimer 2009). Furthermore, it looks like high NEAA could suppress the CR effect on CLS, since I observed that CR extended CLS under conditions of 0.2 and 1 fold NEAA with 0.2 to 5 fold EAA, while CR did not appear to extend CLS in the presence of 5-fold NEAA (**Figure 5.1C**). Moreover, the cell biomass was not optimized by the ratios under 2% or 0.5% glucose conditions, because high EAA and NEAA (5E5N) promoted high cell biomass production (**Figure 5.1D**), which is similar to the observation that lifespan but not biomass/reproduction is optimized by CR in yeast and other high organisms (Mair & Dillin 2008; Fontana *et al.* 2010).

In addition, 0.2-fold EAA and 5-fold NEAA totally inhibited cell growth (**Figure 5.2A**), and the other ratios produced different amounts of cell biomass but did not interrupt cell proliferation. Although the mechanism is unknown, this result might indicate that amino acid composition was significant for cell growth. For example, removal of non-essential serine could even inhibit proliferation of p53-deficient cancer cells (Maddocks *et al.* 2012).

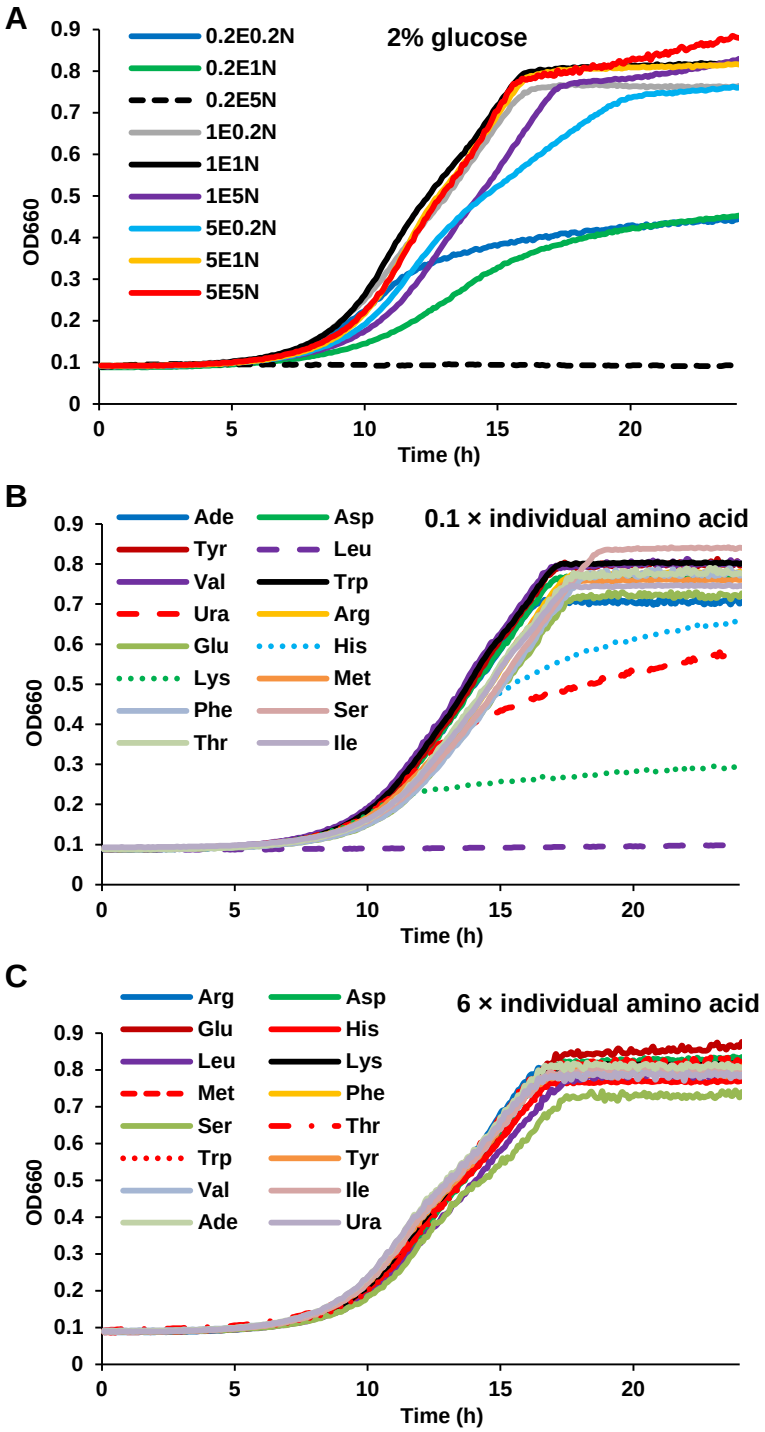

Figure 5.2 Growth curves of WT yeast were cultured in media with diverse amino acids compositions

(**A**) Ratio of EAA and NEAA was able to prevent yeast proliferation. (**B**) Reduction of EAAs (leucine, lysine, uracil, histidine) inhibit cells growth and biomass production. (**C**) Increase of individual amino acids slightly affected yeast growth. All tests were based on SD media with 2% glucose and 1E5N represents SD medium containing 1-fold EAA and 5-fold NEAA.

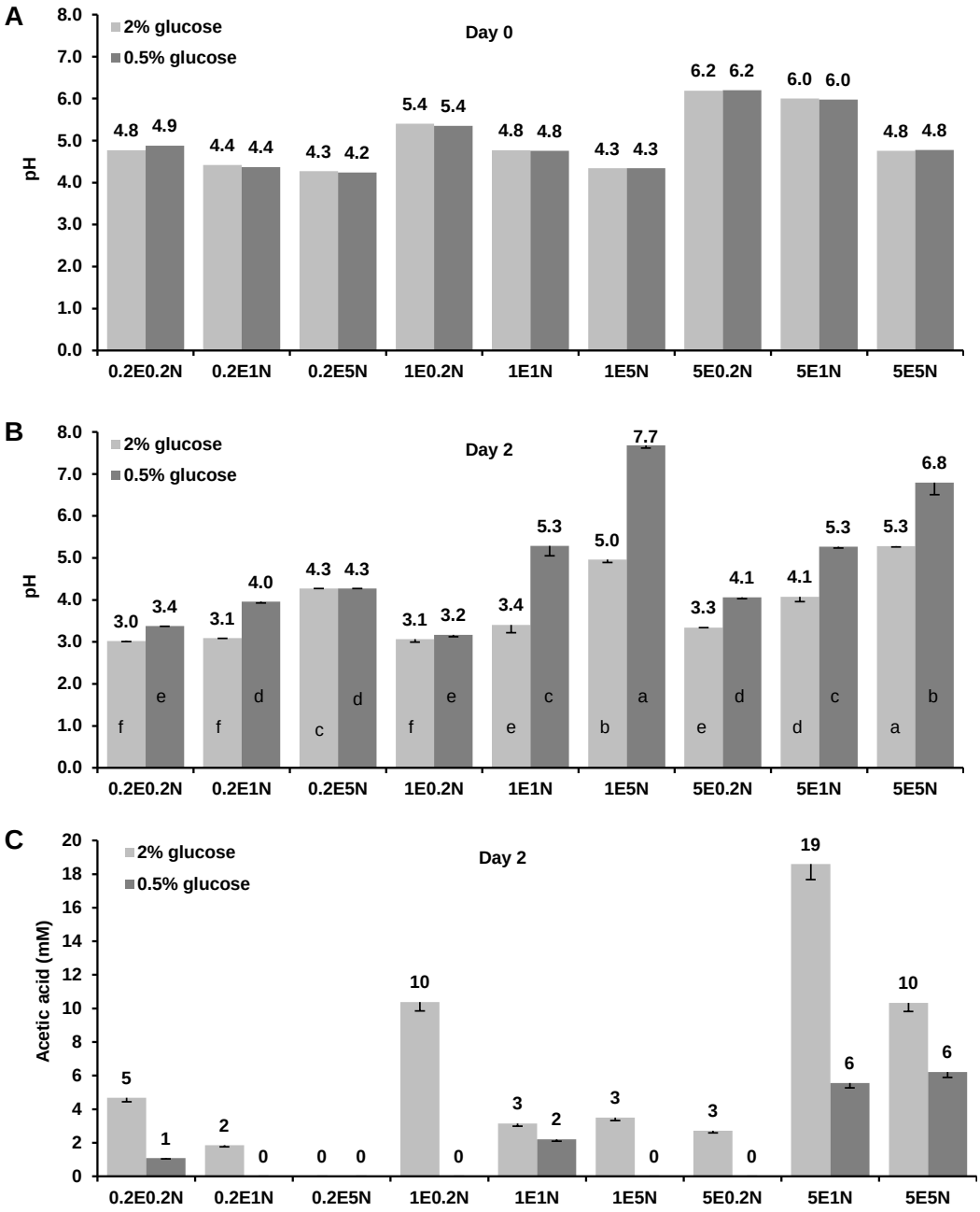

Figure 5.3 EAA and NEAA change pH value and acetic acid production of aging media
(**A**) EAA and NEAA composition slightly altered the pH of media. (**B**) The pH of aging media at stationary phase (day 2) was dependent on glucose, EAA and NEAA in media. Differences in means of the pH values of different media under normal and CR conditions were determined by Duncan's multiple range test at $P < 0.01$. (**C**) Acetic acid accumulation in aging medium (day 2) was changed by modifications of glucose, EAA and NEAA in media. Data 0.0 means not detectable or not applicable. The pH values of the different fresh media (day 0) were measured only once. Acetic acid and pH (day 2): mean ± s.d., n = 3.

The pH and acetic acid in aging medium were reported to mediate yeast chronological aging (Burtner *et al.* 2009b; Murakami *et al.* 2012). I measured the pH (**Figure 5.3A, B**) and acetic acid (**Figure 5.3C**) of the stationary phase culture (day 2).

The pH was slightly affected by the ratio of EAA and NEAA. High EAA increased pH value of medium; in contrast, high NEAA reduced the pH value (**Figure 5.3A**). After 2 day of culture, the pH of medium changed obviously (**Figure 5.3B**). For example, 1E5N had the highest pH value under CR conditions, but it did not produce longer CLS (**Figure 5.1C**). In most case, CR induced higher pH value, longer CLS, lower biomass production and acetic acid accumulation than the normal conditions. However, acidification and acetic acid of aging medium had a low correlation with lifespan and biomass, and the medium with lower acidification did not always produce longer lifespan, which could be due to the influence of amino acid composition in the SD medium.

5.3.2 Methionine and glutamic acid cause lifespan and biomass alterations in yeast

I next tested whether reduction or supplementation of individual amino acids was able to change yeast CLS. To my surprise, methionine restriction (reduced to 10% or 8 mg/L) was sufficient and more powerful to extend lifespan than the other amino acids (**Figure 5.4A**). The reduction of essential leucine and lysine could cause low biomass production and fast loss of cell viability (**Figure 5.4A, C**). Conversely, an increase of non-essential glutamic acid (6-fold, 600 mg/L) prolonged lifespan and improved biomass production, whereas the other EAA or NEAA had no much significant effects on lifespan and biomass (**Figure 5.4B, D**). Although restriction of the four individual EAA impaired biomass production and inhibited cell growth (**Figure 5.2B**), an increase of individual AA or decrease of individual NEAA could not alter biomass (**Figure 5.4**) and cell proliferation (**Figure 5.2B, C**). Overall,

methionine and glutamic acid were showed to be more efficient than the other amino acid to extend yeast CLS.

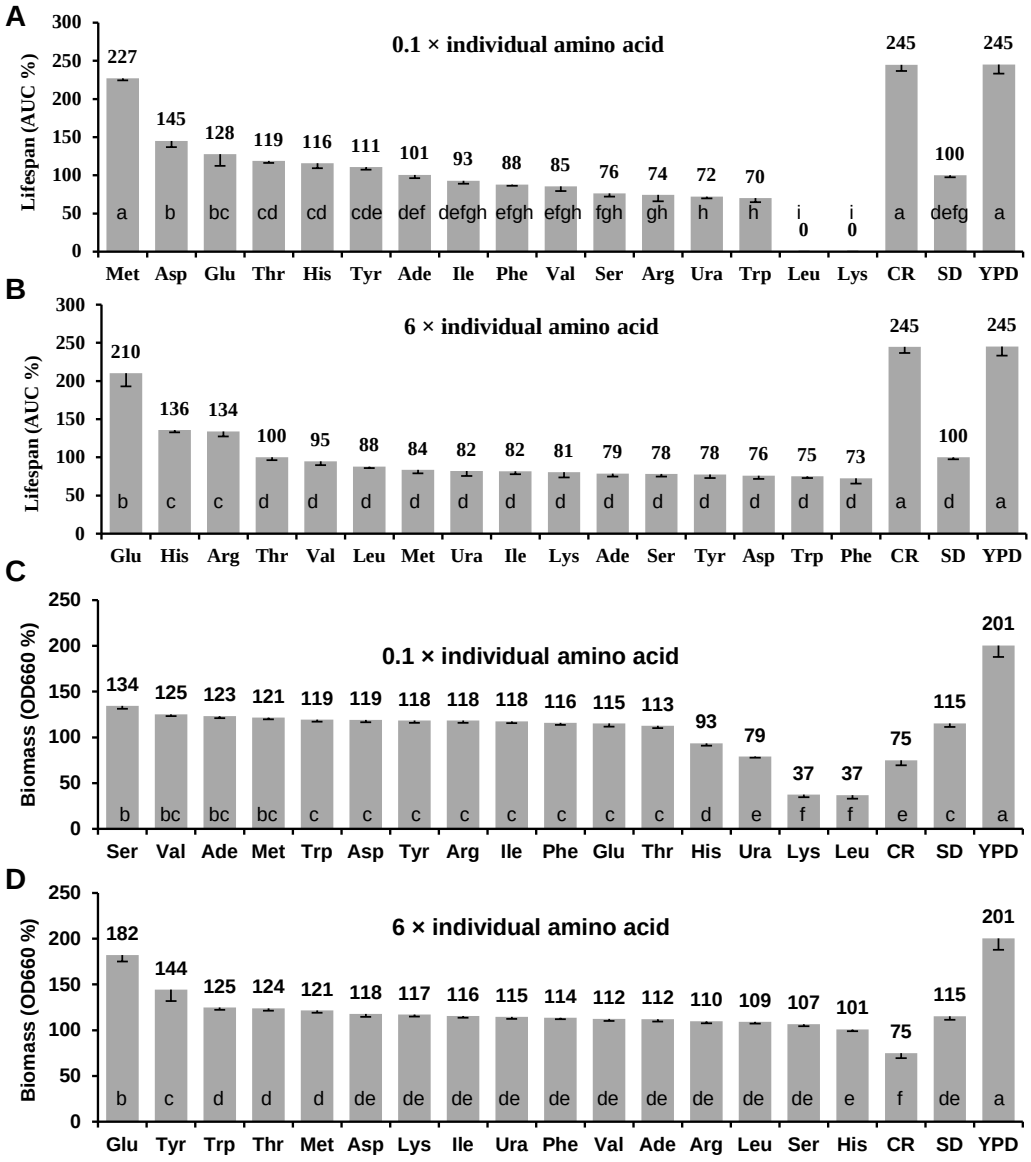

Figure 5.4 Effect of individual amino acids on yeast lifespan and biomass production
Lifespan of WT yeast was grown in SD media with individual amino acid reduction (**A**) or increase (**B**), and their biomass productions were shown in **C** and **D**, respectively. To reduce (0.1-fold) or increase (6-fold) single amino acids in SD medium, the other amino acids concentrations were held constant. SD is standard medium with 2% glucose as the normal conditions in this study (**Table 3.1**); CR is SD medium with 0.5% glucose as the CR conditions; YPD is a commonly used nutrient-rich medium with 1% yeast extract, 2% peptone and 2% dextrose. AUC% represents the survival integral for lifespan comparison. The control (1E1N with 2% glucose) was defined as 100%. Biomass production was measured as the average values at OD660 of each medium from day 6 to day 10 and the biomass of SD (1E1N with 2% glucose) medium was defined as 100%. Lifespan and biomass: mean ± s.e.m., n = 6; compared using Duncan's multiple range test at $P < 0.05$ and different lowercase letters in columns indicate significant difference.

I subsequently determined the dose-response relationship of methionine and glutamic acid in lifespan extension capacity. Depletion (0) or restriction (0.1× or 0.2×) of methionine extended CLS, whereas high doses shortened CLS under normal (2% glucose) or CR (0.5% glucose) conditions (**Figure 5.5A-C**). It indicates that methionine extended lifespan independent of CR. Methionine restriction had little effect on yeast biomass (**Figure 5.5D**), cell growth (**Figure 5.6**), pH, and acetic acid of aging media (**Figure 5.7**). However, high doses of methionine lessened biomass and enhanced slightly acetic acid production of aging culture under normal conditions.

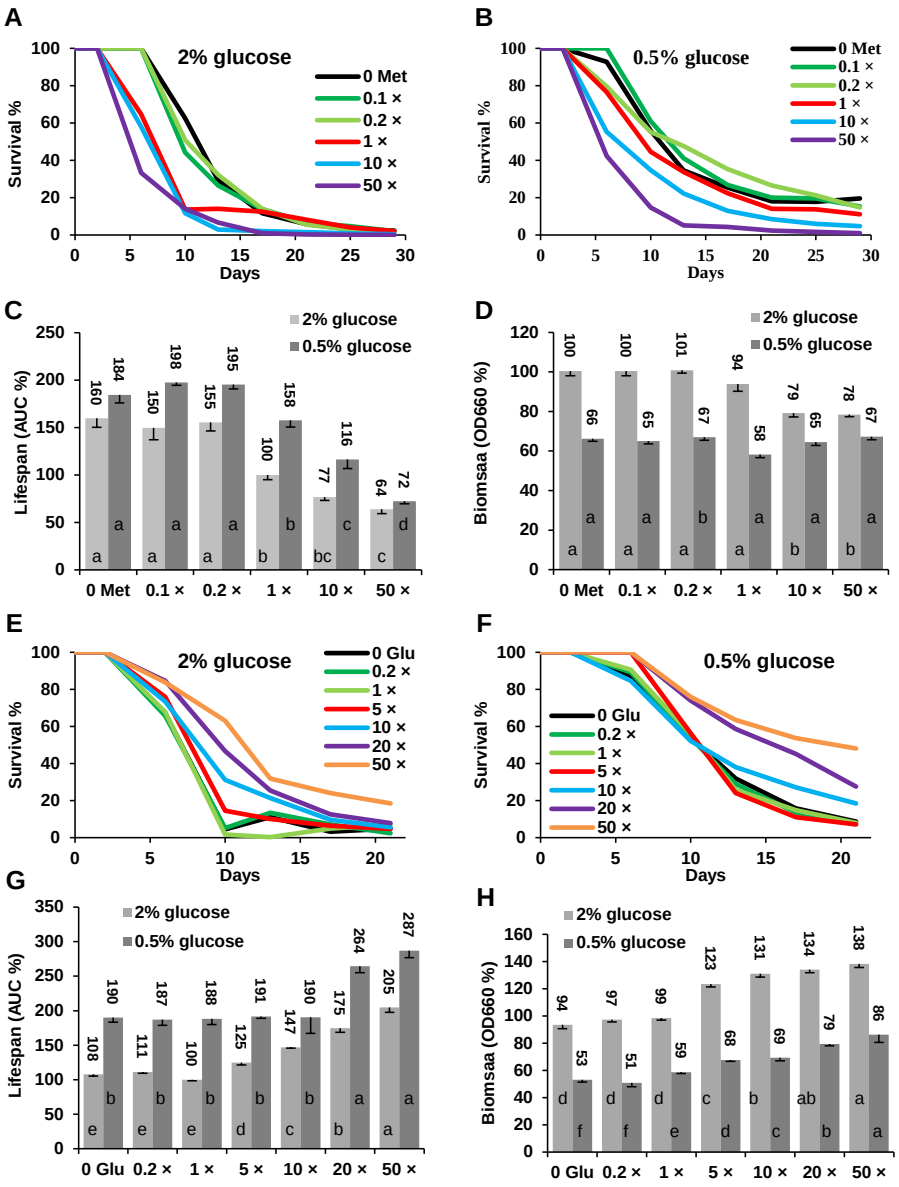

Figure 5.5 Methionine and glutamic acid cause lifespan and biomass alterations in yeast
(**A** and **B**) Survival curves of WT yeast (BY4742) were cultured in normal conditions (**A**) and glucose restriction (**B**) containing different methionine levels. (**C**) Restriction of methionine extended yeast CLS independent of CR and high levels of methionine shortened CLS. (**D**) Methionine restriction had little effect on biomass production, while high dose of methionine reduced cell biomass in normal conditions. (**E** and **F**) Survival curves of WT yeast grown in normal conditions (**E**) and glucose restriction (**F**) containing different glutamic acid levels. (**G**) Glutamic acid extended CLS in a dose-response manner independent of CR. (**H**) Low glutamic acid did not change cell biomass and high glutamic acid increased biomass. AUC% represents the survival integral for lifespan comparison. The control (1E1N with 2% glucose) was defined as 100%. Biomass of SD (1E1N with 2% glucose) medium was defined as 100%. Lifespan and biomass: mean ± s.e.m., n = 4 (**C** and **D**), n = 6 (**G** and **H**); compared using Duncan's multiple range test at $P < 0.05$ and different lowercase letters in columns indicate significant difference.

In contrast, addition of glutamic acid elevated CLS extension and biomass production in a dose-response manner independently of CR (**Figure 5.5E-H**).

Importantly, depletion of glutamic acid did not shorten CLS and high concentrations did not interrupt cell growth (**Figure 5.6** and unpublished data). Although glutamic acid addition impaired acetic acid production, the pH of aging media only changed slightly (**Figure 5.7**). High doses of acetic acid is toxic to yeast cells and shorten lifespan (Burtner *et al.* 2009b). It seems that glutamic acid addition and methionine restriction had low acetic acid production (**Figure 5.7**), while the higher acetic acid level in glutamic acid restricted media did not result in shorter lifespan. The low correlation between acetic acid, pH and lifespan was observed (**Figure 5.5, 5.7**), suggesting acetic acid and acidification might be not the key factor to mediate yeast longevity caused by methionine and glutamic acid.

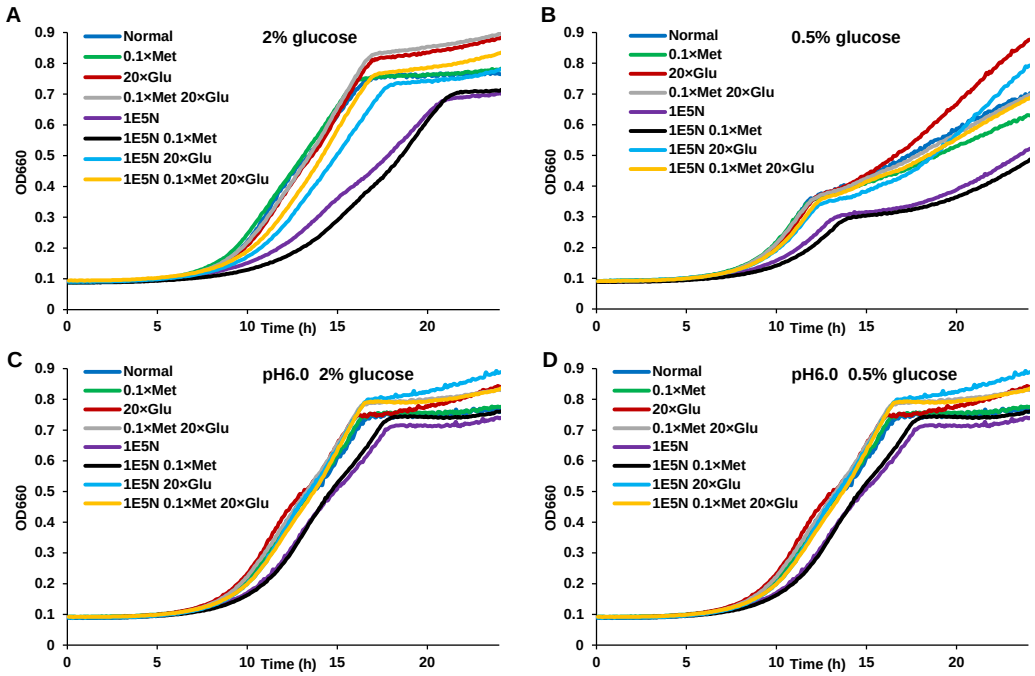

Figure 5.6 Glutamic acid addition, methionine and glucose restriction not inhibit yeast growth
WT yeast (BY4742) (≈ 1×10^4 cells) cells were grown in each well of 96-well microplate containing 100 µL of different media. The cell population was monitored with a microplate reader by recording the OD every 5 min at 660 nm. The pH neutralization was prepared by buffering the pH of medium using citrate phosphate buffer solution (64.2 mM Na_2HPO_4 and 17.9 mM citric acid, pH 6.0). All tests were based on SD media with 2% glucose. 1E5N represents SD medium containing 1-fold EAA and 5-fold NEAA.

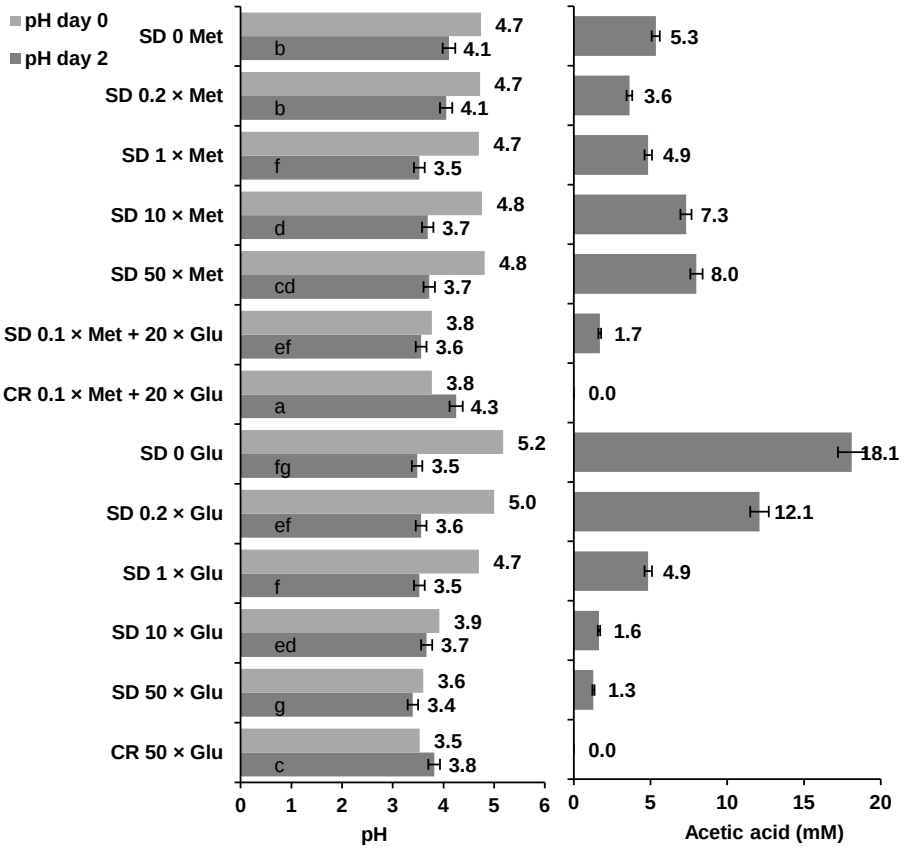

Figure 5.7 Comparison of pH and acetic acid in media containing various levels of methionine and glutamic acid

The pH of aging media (day 2) had only little change among various media. Acetic acid was increased by adding methionine and reducing glutamic acid in media. Acetic acid and pH: mean ± s.d., n = 3.

5.3.3 Independent and additive effects of glutamic acid, methionine and glucose on lifespan extension

I have shown the longevity effects of methionine restriction and glutamic acid addition. Therefore, it is possible that the two interventions have additive effects on yeast lifespan. I first tested yeast grown in normal and CR conditions with 0.1-fold methionine, 20-fold glutamic acid or a combination of both. As shown in **Figure 5.8**, yeast CLS was greatly extended by the combination in normal condition and could be further enhanced by CR (**Figure 5.8A**, **B**), indicating there is an additive effect of glutamic acid, methionine and CR on yeast longevity extension.

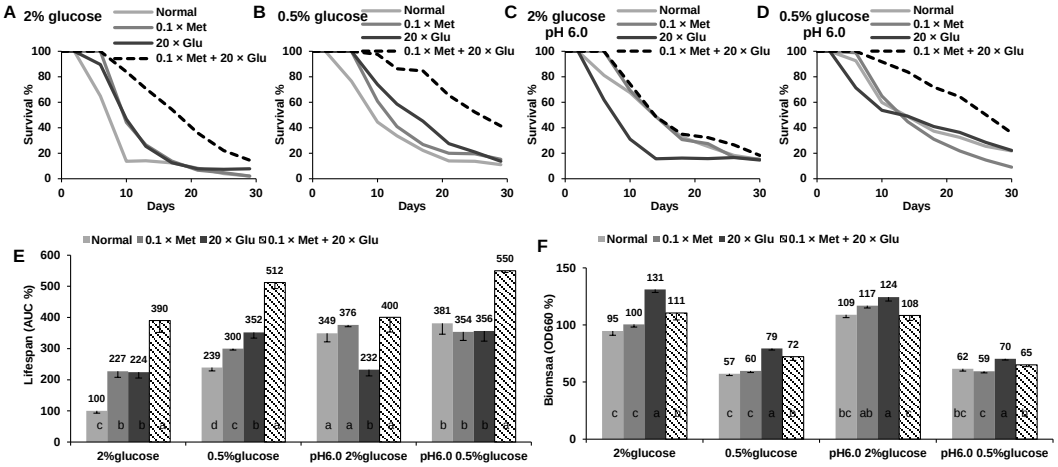

Figure 5.8 Independent and additive effects of glutamic acid, methionine and glucose on lifespan extension

(**A**) Methionine restriction and glutamic acid addition extended lifespan and the combination of both could extend the longevity under normal conditions. (**B**) CR further increased the longevity induced by low methionine, high glutamic acid or the combination. The pH neutralization could not extend the combined longevity and glutamic acid induced longevity in normal conditions (**C**) and CR conditions (**D**). CLS (**E**) and biomass (**F**) comparison of WT yeast were incubated in different media. The pH neutralization was prepared by buffering the pH of medium using citrate phosphate buffer solution (64.2 mM Na_2HPO_4 and 17.9 mM citric acid, pH 6.0). AUC% represents the survival integral for lifespan comparison. The control (1E1N with 2% glucose) was defined as 100%. Biomass of SD medium (1E1N with 2% glucose) was defined as 100%. Lifespan and biomass: mean ± s.e.m., n = 6; compared using Duncan's multiple range test at $P < 0.05$ and different lowercase letters in columns indicate significant difference.

It was known that buffering the pH of the aging medium or neutralizing the pH with NaOH to 6.0 could greatly protect against yeast lifespan reduction (Burtner *et al.* 2009b). Thus, acidification of aging medium was proposed as a major factor to accelerate yeast aging (Burtner *et al.* 2009b; Murakami *et al.* 2011; Longo *et al.* 2012; Mirisola & Longo 2012; Murakami *et al.* 2012). I examined whether pH neutralization could further elevate yeast longevity induced by methionine and glutamic acid, found that the pH buffered medium (pH 6.0) prevented CLS reduction significantly in the 2% glucose medium, but the extended longevity effects of the combination were not observed in buffered media. The additive effects of both low methionine plus high glutamic acid in buffered media were only observed in low glucose (CR) not in normal glucose (**Figure 5.8C, D, E**). Furthermore, the pH buffered medium caused shorter lifespan in glutamic acid addition. It should be also noted that the lifespan extending capacity of CR was diminished by the buffered

conditions (**Figure 5.8C, D**), because buffering was more powerful to increase yeast longevity in the normal condition than in CR condition.

I also examined CLS of yeast cultured in media with 1-fold EAA and 5-fold NEAA (1E5N), since this composition increases CLS and thus possibly has additive effects with glutamic acid, methionine and CR on yeast longevity. The results revealed that under this composition, methionine and glutamic acid still extended CLS in normal and CR conditions, but the combination of both could not promote the longevity in normal (2% glucose), CR (0.5% glucose) and pH buffered conditions (**Figure 5.9A-D**). In addition, the 1E5N composition caused significant lifespan reduction in CR conditions (**Figure 5.9B**) and the combination has longer CLS extension in 1E1N than in 1E5N (**Figure 5.10**). Altogether, methionine and glutamic acid had no additive effect on longevity extension under 1E5N composition. However, it was still sufficient to significantly extend lifespan independently of CR, 1E5N and pH neutralization (**Figure 5.10**).

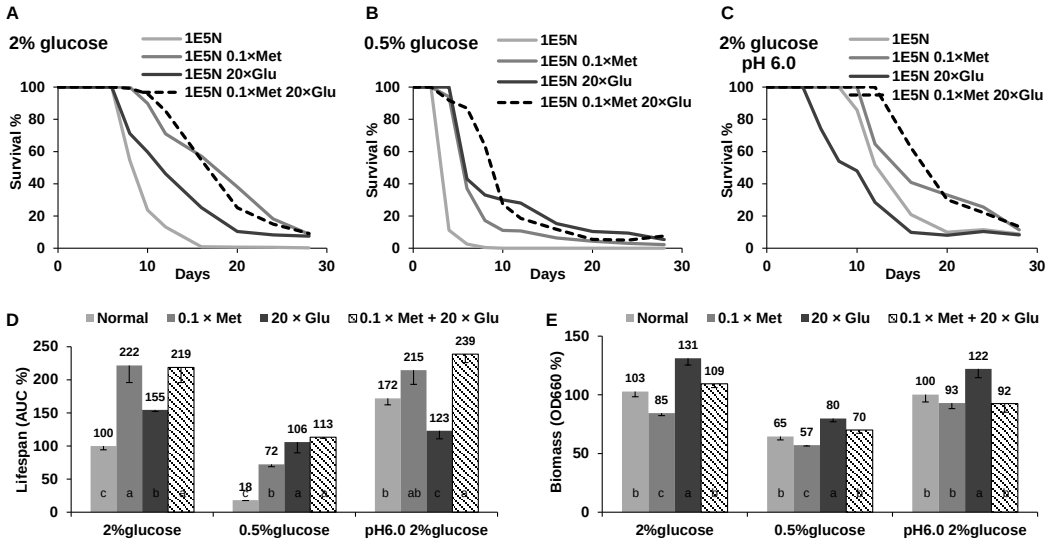

Figure 5.9 Lifespan extending capacity of the combination of glutamic acid and methionine was impaired by the medium supplying with 5-fold NEAA

(**A - C**) The combination of methionine and glutamic acid could not enhance substantially the longevity under normal (**A**), CR (**B**) and pH buffered (**C**) conditions. CLS (**D**) and biomass (**E**) comparison of WT yeast were cultured in different media. AUC% represents the survival integral for lifespan comparison. The control (1E5N with 2% glucose) was defined as 100%. All tests are based on SD

media with 2% glucose. 1E5N represents SD medium containing 1-fold EAA and 5-fold NEAA. Biomass of SD medium was defined as 100%. Lifespan and biomass: mean ± s.e.m., n = 6.

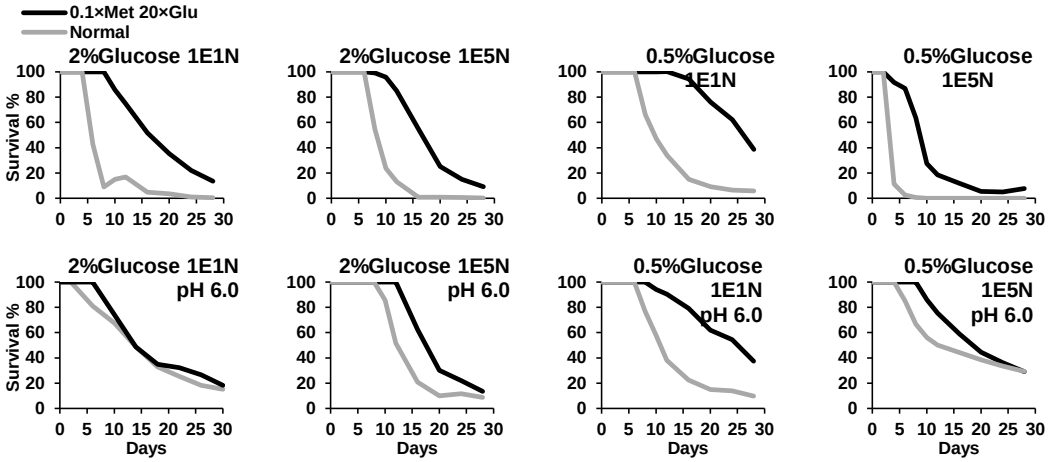

Figure 5.10 The combination is sufficient to extend lifespan in glucose restriction, 1E1N (standard), 1E5N and pH buffered conditions
All tests were based on SD media with 2% glucose and 1E5N represents SD medium containing 1-fold EAA and 5-fold NEAA.

I then evaluated biomass production (**Figure 5.8F, 5.9E**), cell growth (**Figure 5.6**), pH (**Figure 5.11, 12**) and acetic acid of aging media (**Figure 5.7, 11**). The combination of methionine and glutamic acid produced less biomass than glutamic acid addition, which had the highest biomass among the four interventions with or without pH buffering under 1E1N condition (**Figure 5.8F**) as well 1E5N condition (**Figure 5.9E**). I found that the combination not inhibited cell growth, while 1E5N or 1E5N with low methionine slight delayed cell growth (**Figure 5.6**). Interestingly, addition of glutamic acid could eliminate this phenomenon, suggesting high glutamic acid, not low methionine, might repair the amino acids imbalance induced by 1E5N.

For the pH buffered media, the four interventions did not cause apparent pH change under normal or CR conditions (**Figure 5.10A**), but their lifespans were different (**Figure 5.8E**), indicating that nutrient composition is still an important factor to influence yeast CLS in the pH buffered media. In the unbuffered media, the combination caused lower pH than that of high glutamic acid intervention in 1E1N and 1E5N media under normal condition (**Figure 5.12**). However, this not means the

longevity additive of glutamic acid and methionine is mainly due to the prevention of acidification of aging medium, because the longevity additive was observed in 1E1N media under CR condition without pH change (**Figure 5.8**, **12**). Moreover, higher pH did not result in longer CLS among the four interventions in 1E5N media under normal and CR condition (**Figure 5.9**, **12**). Acetic acid production in aging media of the four interventions was showed to depend on nutrient composition and increased by the pH neutralization (**Figure 5.11B**, **C**). The combination intervention not caused substantial more acetic acid production than high glutamic acid intervention, while significant difference in CLS of both was observed. Overall, these results further confirmed that pH and acetic acid were not the major determinants of methionine and glutamic acid induced longevity.

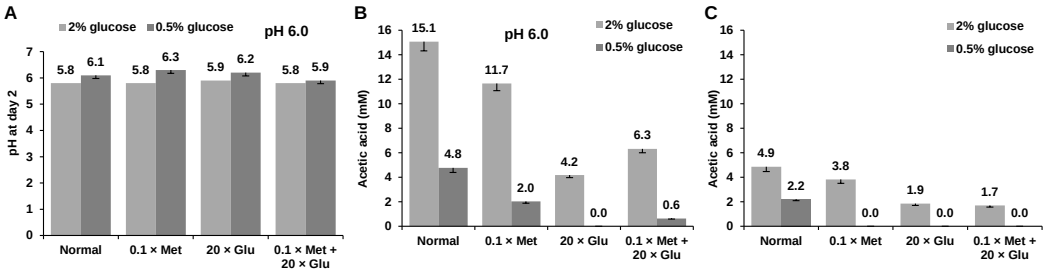

Figure 5.11 Acetic acid may be not the cause of lifespan shortening in buffered media (pH 6.0)
(**A**) The pH of the four buffered media (day 2) under normal and CR conditions have little change. Acetic acid accumulation in the four aging media under normal and CR conditions with (**B**) or without pH buffering (**C**). Data 0.0 means not detectable. Acetic acid and pH: mean ± s.d., n = 3.

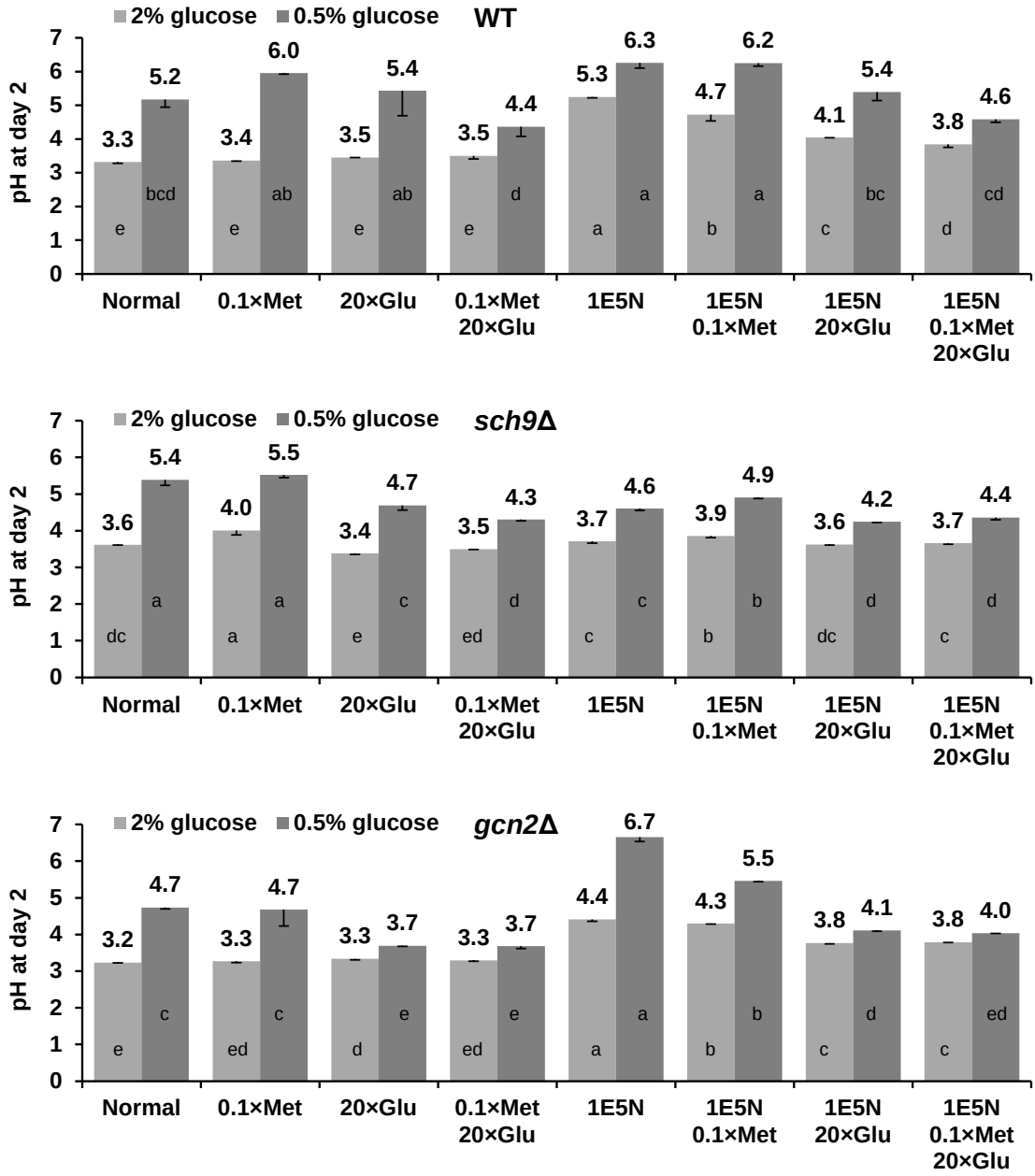

Figure 5.12 Comparative evaluation of the pH of aging media in WT, *sch9*Δ and *gcn2*Δ
All tests are based on SD media with 2% glucose. 1E5N represents SD medium containing 1-fold EAA and 5-fold NEAA. pH: mean ± s.d., n = 3, compared using Duncan's multiple range test at $P < 0.01$ and different lowercase letters in columns indicate significant difference.

5.3.4 Conserved protein kinase Gcn2 mediates amino acids induced lifespan extension

To explore the possible genetic mechanisms on how methionine, glutamic and glucose prompt longevity independently. I screened a number of genes that are evolutionarily conserved from yeast to human, and their lifespan comparison and

survival curves in different media are presented in **Figure 5.13** and **Figure 5.14**, respectively. Mitochondrial manganese superoxide dismutase (SOD2) was proposed as a downstream target of Tor/Sch9 nutrient signaling pathway for longevity extension by decreasing in part ROS levels in yeast, and deletion of *SOD2* has a shorter lifespan (Fabrizio *et al.* 2003; Fontana *et al.* 2010; Pan *et al.* 2011). In accordance with previous studies, *sod2*Δ showed shorter lifespan than WT yeast in standard SD medium, I also observed that high NEAA (1E5N), low methionine, and high glutamic acid were able to extend lifespan of *sod2*Δ significantly (**Figure 5.13A, 13B, 14A, 14B**), which indicate the amino acid composition in SD medium plays an important role in regulation of lifespan in *sod2*Δ mutant.

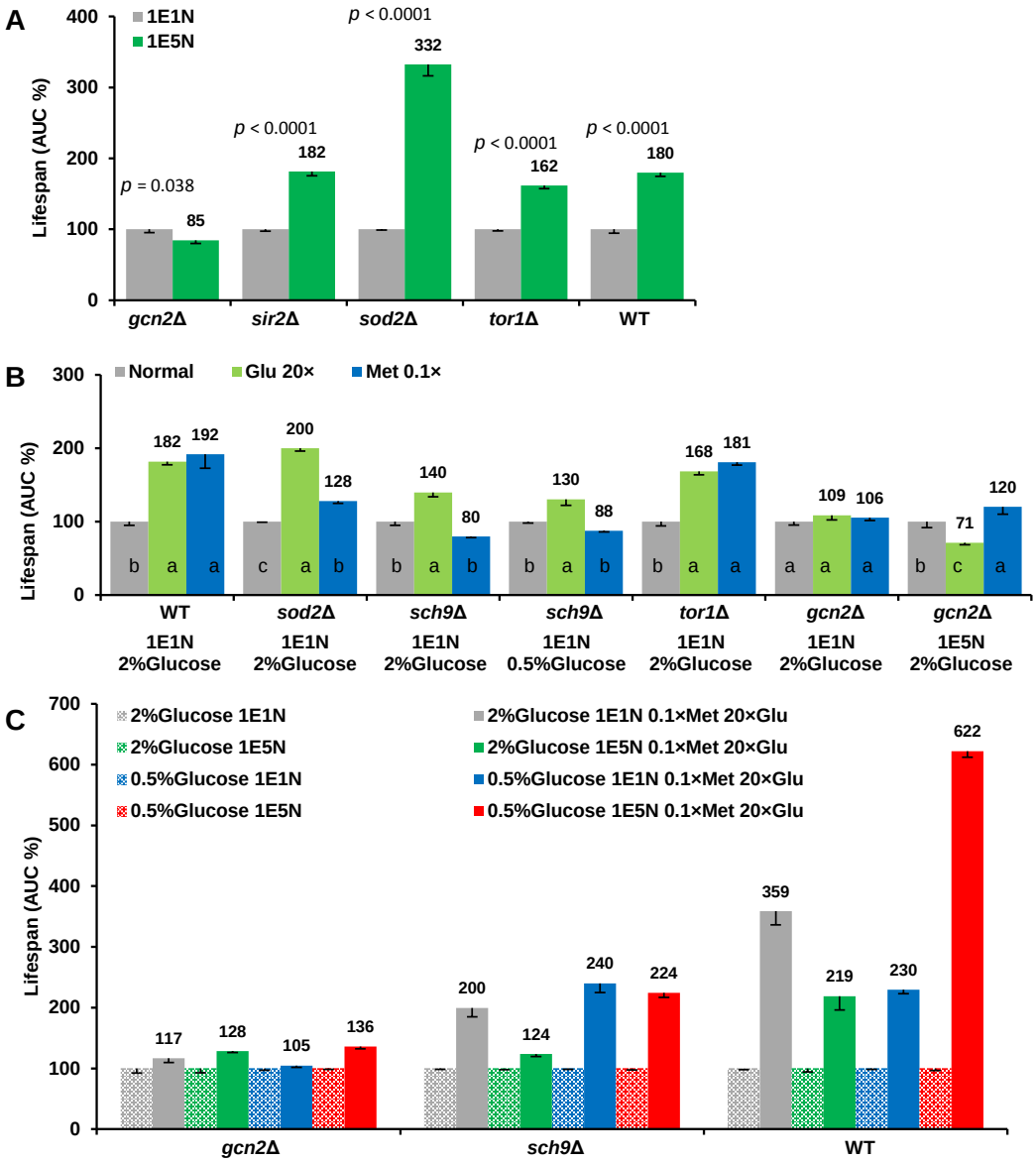

Figure 5.13 Conserved protein kinase Gcn2 mediates amino acids induced lifespan extension
(**A**) Deletion of *GCN2* rather than other genes prevented 1E5N induced lifespan extension. Lifespan of 1E5N showed in AUC% and 1E1N was defined as 100%. Differences of the means of AUC% between 1E1N and 1E5N were determined by t-test. (**B**) Methionine and glutamic acid had distinct effects on lifespan regulation in *gcn2*Δ and *sch9*Δ. Lifespan of high glutamic acid and low methionine showed in AUC% and the normal (1E1N) was defined as 100%. Differences of the means of AUC% among normal, high glutamic acid or low methionine were determined by Duncan's multiple range test at $P < 0.01$. (**C**) Deletion of *GCN2* was more effective than that of *SCH9* to impaired lifespan extension by the combination. Lifespan of high glutamic acid plus low methionine showed in AUC% and the four basic conditions (1E1N or 1E5N with 0.5 or 2 % glucose) were defined as 100%, respectively. In most cases, significant difference was achieved between the combination and the control. 1E5N represents SD medium containing 1-fold EAA and 5-fold NEAA and 1E1N is the normal conditions. CLS: mean ± s.e.m., n = 6. The survival curves are presented in **Figure 5.14**.

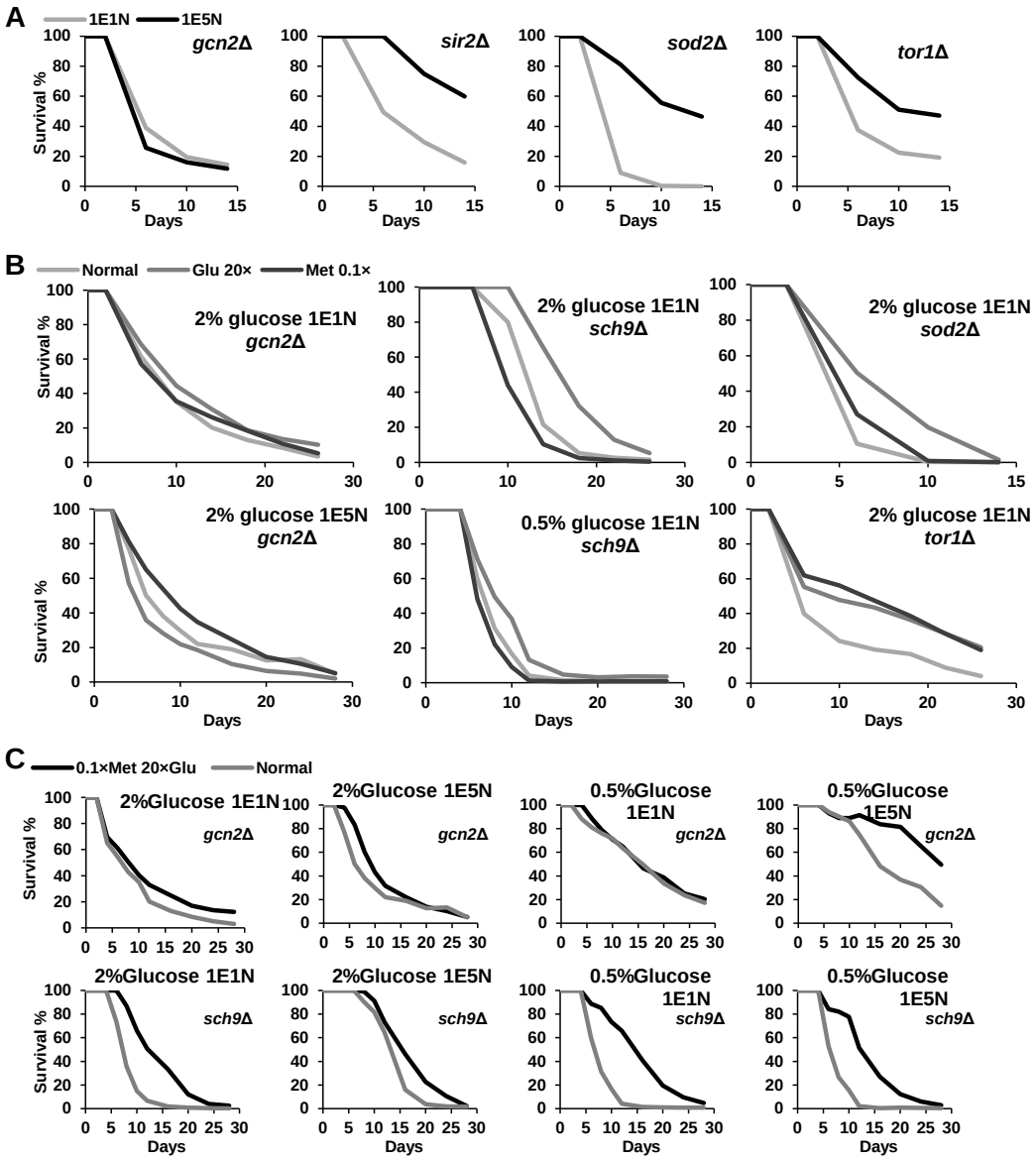

Figure 5.14 Comparative evaluation of the amino acids induced longevity in different single gene deletion strains.

(**A**) Survival curves of *gcn2*Δ, *sir2*Δ, *sod2*Δ, and *tor1*Δ were cultured in 1E1N or 1E5N with 2% glucose medium. (**B**) Survival curves of *gcn2*Δ, *sch9*Δ, *sod2*Δ, and *tor1*Δ were grown in different media with high glutamic acid or low methionine. (**C**) Survival curves of *gcn2*Δ, and *sch9*Δ were grown in different media with the combination of glutamic acid and methionine. 1E5N represents SD medium containing 1-fold EAA and 5-fold NEAA and 1E1N is the normal condition. Survival curves: mean, n = 6. The statistical analysis of significant difference for the CLS comparison is presented in **Figure 5.13**.

Silent Information Regulator 2 (Sir2) has been proposed to mediate lifespan extension (Lin *et al.* 2000b; Lamming *et al.* 2005). Deletion of *SIR2* decreases RLS, whereas over-expression of *SIR2* increases RLS (Kaeberlein *et al.* 1999). In contrast, deletion of *SIR2* was reported to extend CLS under control conditions (Smith *et al.*

2007; Murakami *et al.* 2008). Consistent with prior reports, I found that CLS of *sir2*Δ was extended in standard SD medium and could be enhanced by supplying with high NEAA (**Figure 5.13A, 14A**), suggesting that Sir2 is not sensitive to NEAA increase.

Several studies have indicated that TOR signalling may play a conserved role in mediating beneficial health and longevity effects associated with CR (Fontana *et al.* 2010; Kaeberlein 2010a; Johnson *et al.* 2013). Deletion of *TOR1* increased lifespan significantly under normal condition but not CR condition (Kaeberlein *et al.* 2005b; Powers *et al.* 2006). Herein I showed that *tor1*Δ extend lifespan in SD medium, and the longevity could be further prolonged by the NEAA, methionine, and glutamic acid (**Figure 5.13A, 13B, 14A, 14B**). Altogether, lifespan extension induced by high NEAA, methionine restriction, and glutamic acid addition could be independent of deletion of *SIR2, SOD2* and *TOR1* (**Figure 5.13, 14**).

Remarkably, Gcn2 was shown to impair lifespan extension induced by these amino acids interventions (**Figure 5.13, 14**). Gcn2 is one of major evolutionarily conserved protein kinases. It regulates amino acid homeostasis and protein synthesis through modulating amino acid biosynthesis in response to different amino acid deprivation in yeast (Wilson & Roach 2002). Therefore, deletion of *GCN2* could result in cell function deficiency in modulating amino acids imbalance caused by methionine restriction, glutamic acid addition, and 1E5N. The lifespan extending capacity of these interventions was impaired by the absence of *GCN2* (**Figure 5.13A, 13B, 14A, 14B**). The combination of methionine and glutamic acid produced significant longevity, whereas the data presented that deletion of *GCN2* was more effective than that of *SCH9* to impair the longevity capacity by the combination in different media (**Figure 5.13C**). This indicated that Gcn2 might be a major target to regulate amino acid metabolism and then influence yeast chronological aging.

It is well known that the longevity of *sch9*Δ strain is CR-dependent. For example, deletion of *SCH9* extended lifespan in normal condition but not CR condition (**Figure 5.13B**). Sch9 was proposed as a highly conserved nutrient-sensing factor to regulate aging, cell growth, cell size, and stress resistance through controlling protein synthesis (Fabrizio *et al.* 2001; Kaeberlein *et al.* 2005b; Huber *et al.* 2009). Interestingly, methionine restriction could not extend CLS of *sch9*Δ strain under normal and CR conditions, which means methionine induced longevity required Sch9 activity. However, glutamic acid extended CLS in *sch9*Δ mutant but not in *gcn2*Δ mutant (**Figure 5.13B, 5.14B**). Altogether, the longevity via modification of amino acids required, in part, Gcn2 activity, while Sch9 was necessary for methionine and glucose restriction induced longevity. Thus, the distinct mechanisms could somewhat explain the additive longevity effect of methionine restriction, glutamic acid addition and CR.

In some cases, methionine, glutamic acid or a combination of both caused significant changes in the pH of aging media in WT, *sch9*Δ and *gcn2*Δ that cultured in normal (1E1N) and high NEAA (1E5N) conditions with 2% or 0.5% glucose, but the pH had no good correlation with CLS (**Figure 5.12**), which was also consistent with results in **Chapter 4**. I also found that acetic acid was not key determinants of CLS in *sch9*Δ and *gcn2*Δ, since higher acetic acid had longer lifespan was observed in some cases (**Figure 5.14**). It is well known that CR shortens lifespan of *sch9*Δ, which was also observed in this study (**Figure 5.13B**). However, CR resulted in less acetic acid production (**Figure 5.15**). Thus these data might imply that deletion of *SCH9* and *GCN2* mediate CLS independently of acetic acid and acidification of aging medium, (Longo *et al.* 2012).

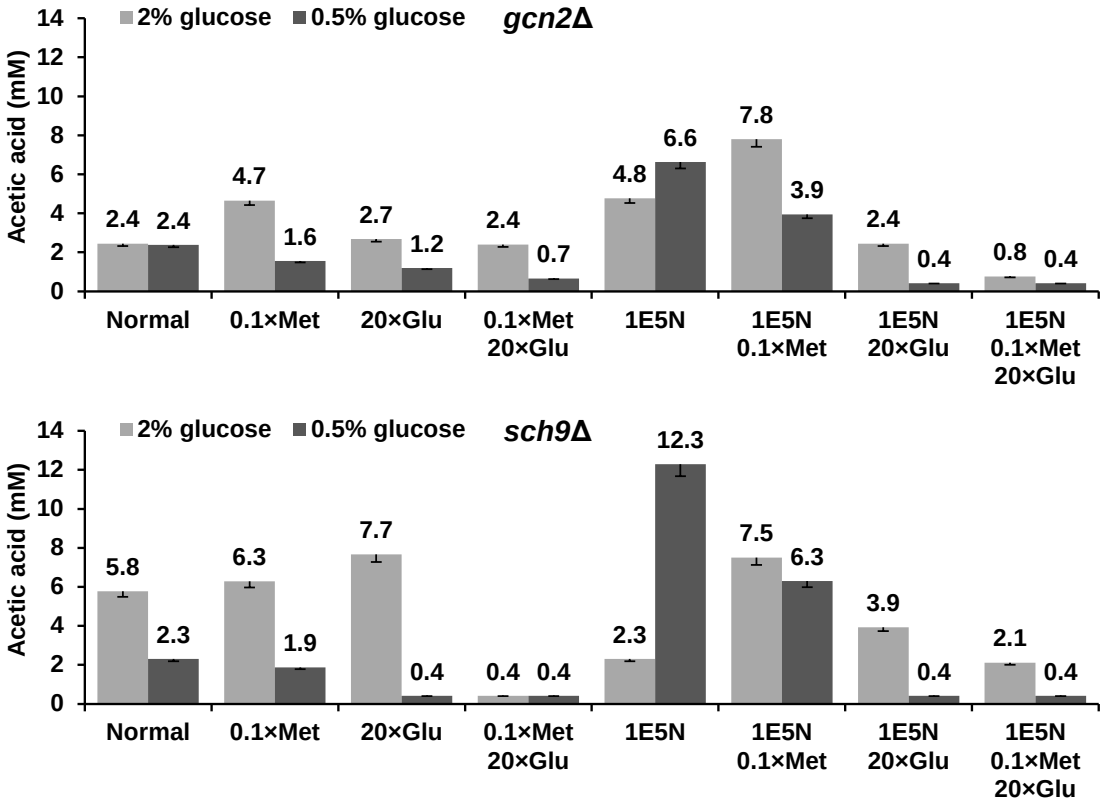

Figure 5.15 The acetic acid production of aging media in *sch9*Δ and *gcn2*Δ
All tests were based on SD media with 2% glucose and 1E5N represents SD medium containing 1-fold EAA and 5-fold NEAA. Acetic acid: mean, n = 3.

5.4 Discussion

In this Chapter, the high throughput screening assay was used to comprehensively evaluate the CLS-extending capacity of amino acids. The ratio of NEAA and EAA caused greatly changes in CLS, biomass production, cell growth, pH and acetic acid of aging medium. Increase or decrease of individual amino acids had little effect on CLS change in most cases. Interestingly, methionine restriction and glutamic acid addition resulted in CLS extension more substantially. Furthermore, current data showed that the two NEAAs could CR-independently extended yeast CLS through distinct mechanisms that in part required evolutionarily conserved protein kinase, such as Sch9 and Gcn2.

Methionine has been reported to play a critical role in regulation of lifespan in rat, fly and yeast (Koc *et al.* 2004; Miller *et al.* 2005; Malloy *et al.* 2006; Alvers *et al.* 2009a; Grandison *et al.* 2009; Elshorbagy *et al.* 2010). Methionine restriction (by 80%) was shown to increase medium and maximum lifespan of rats by 30% and 40%, respectively (Orentreich *et al.* 1993). Later studies indicated that methionine restriction delayed the onset of age-dependent pathologies and extended lifespan through control of adiposity and insulin resistance in rats and mice independently of CR (Miller *et al.* 2005; Malloy *et al.* 2006). Although the mechanisms of methionine restriction induced lifespan extension was not fully understood, a few studies suggested that it was different to CR at the molecular level in mammals. For example, CR increased the phosphorylation of ERK, JNK2, p38, mTOR and 4EBP1, while no such effect was observed from methionine restriction (Sun *et al.* 2009).

In *Drosophila*, methionine restriction (by 67%) extended maximum and mean lifespan by 2.4% and 10.5%, respectively. Severe restriction (by 88%) did not further extend maximum and mean lifespan (Troen *et al.* 2007). In *S. cerevisiae*, a study reported that reduction in methionine (0.1 ×) increased average RLS, and high methionine (10 ×) slightly shortened RLS (Koc *et al.* 2004). Altogether, these results were partly similar to current observation that methionine restriction caused CLS extension and high level of methionine shortened CLS (**Figure 5.5A-D**).

It should be noted that intake of high amount of methionine is very toxic to both young and adult mammals, and this toxicity far exceeds that produced by the excess intake of any other amino acid (Harper *et al.* 1970). In addition, this study suggested that methionine restriction may share some of the effects with CR, i.e. either methionine restriction or CR caused lifespan reduction in *sch9*Δ strain (**Figure 5.13**), which indicate they induce longevity via diminishing Sch9 activity. Overall, those

data partially supported that methionine was able to mediate some of evolutionarily conserved longevity signalling pathways to induce lifespan extension among different species. For example, methionine restriction induced CLS extension seemed to require Sch9 and Gcn2 activity (**Figure 5.13B**).

Glutamic acid (physiologically glutamate) is the most abundant free amino acid in brain, the key excitatory neurotransmitter of central nervous system, and primarily linked to the pathogenesis of many neurological diseases or disorders, such as Alzheimer's disease, amyotrophic lateral sclerosis, autism, cerebral ischemia, depression, epilepsy, Huntington disease, multiple sclerosis, Parkinson's disease, schizophrenia and traumatic brain injury (Danbolt 2001; Javitt *et al.* 2011).

In the yeast *S. cerevisiae*, glutamate plays fundamental roles in amino acid metabolism, tricarboxylic acid (TCA) cycle, and glutathione synthesis. It can be degraded by a $NADP^+$-dependent glutamate dehydrogenase (GLDH) encoded by *GDH2* to α-ketoglutarate and ammonia, as well be biosynthesized from α-ketoglutarate and ammonia by two NAD^+-dependent GLDH Gdh1 and Gdh3 (Miller & Magasanik 1990). Gdh1 was proposed to be more suitable for regulation of glutamate production during exponential phase, while Gdh3 might be more important to mediate glutathione biosynthesis for resistance to stress-induced apoptosis and chronological aging during stationary phase (Lee *et al.* 2012).

In both yeast and mammalian cells, glutathione is a crucial metabolite for stress resistance and its biosynthesis requires glutamate. It was also shown that glutamate could suppress reactive oxygen species (ROS) accumulation to prevent thermal and oxidative stress-induced apoptosis in the stationary cells of *GDH3* deletion strain (Lee *et al.* 2012). In this study, it is the first to report the lifespan-extending activity of glutamic acid. Glutamic acid caused WT yeast CLS extension in a dose-response

manner (**Figure 5.5E-H**), as well protected against the fast loss of viability during chronological aging in *SOD2*-null strain (**Figure 5.13B**).

Yeast has two SOD genes, cytoplasmic copper-zinc superoxide dismutase (*SOD1*) and mitochondrial manganese superoxide dismutase (*SOD2*). The lack of either of the two SODs causes attenuation in replicative and chronological aging due to highly oxidative damage induced by ROS in the cell (Longo *et al.* 1996b; Unlu & Koc 2007). Hence, glutamic acid extends CLS probably via enhancing the stress resistance of yeast cells. In addition, high glutamic acid appears to significantly increase biomass under conditions in which it extends CLS (**Figure 5.5, 5.8, 5.9**). This suggests that high glutamic acid plays a role in biosynthesis that may be important during extension of CLS. However, either further investigations of lifespan extending activity of glutamic acid in other aging models or in-depth studies of the longevity mechanisms in yeast were important for us to fully evaluate the anti-aging capacity of glutamic acid.

Recent studies suggested that the low glucose prompted yeast lifespan extension was primarily due to decreased production of acetic acid and reduced acidification of medium for two possible reasons: (1) acetic acid was identified as an extracellular mediator of cell death during chronological aging, and it was demonstrated that environmental interventions by reducing or eliminating acetic acid increased CLS, such as via DR, using non-fermentable carbon source, or transferring cells to water (Burtner *et al.* 2009b); (2) pH neutralization was demonstrated to protect against reduction in RLS and CLS in yeast (Fabrizio *et al.* 2004; Murakami *et al.* 2011; Murakami *et al.* 2012), extracellular acidification of the culture medium could cause intracellular damage that subsequently limited the cell replicative potential, and the

reduced RLS and CLS could be extended by buffering the pH of medium to 6.0 (Murakami *et al.* 2012).

Therefore, the amino acid induced CLS alterations could be due to the changes in acetic acid and pH of aging media. In this study, I measured acetic acid production and pH of stationary phase media. The data showed that ratio of EAA/NEAA, methionine and glutamic acid extended CLS were not always with lower acetic acid concentration and higher pH of medium. On the other hand, CLS of WT, *sch9*Δ and *gcn2*Δ had poor correlation with the acetic acid production and acidification of medium. Those results suggested that the amino acid induced longevity not primarily benefited from the two factors. Moreover, these amino acid interventions also caused significant CLS changes in pH buffered media, which indicate that the pH might be not a primary factor to limit CLS under those not only glucose varied media.

Glutamic acid addition coupled with methionine and glucose restriction resulted in an optimal medium for yeast lifespan extension, which could not be further enhanced by buffering the pH of the media, modifying EAA and NEAA composition, or deleting the longevity gene *SCH9*. Methionine and glucose restriction were also reported to cause lifespan extension in other organisms, including mammals (Orentreich *et al.* 1993; Miller *et al.* 2005). The three nutrients are also important for organism's physiological activities and human health. Furthermore, current data suggested the three interventions individually functioned on highly evolutionarily conserved kinases, such as Sch9 and Gcn2, which have been implicated in nutrients metabolism, cell development, stress resistance and aging (Wilson & Roach 2002; Kaeberlein *et al.* 2005b). Thus, these results imply that the extraordinary yeast lifespan extension capacity of the combination of glutamic acid addition, methionine and glucose restriction may also be realized in mammals.

5.5 Conclusion

Glutamic acid addition coupled with methionine and glucose restriction resulted in an optimal medium for yeast lifespan extension, which could not be further enhanced by buffering the pH of the media, modifying EAA and NEAA composition, or deleting the longevity gene *SCH9*. Methionine and glucose restriction were also reported to cause lifespan extension in other organisms, including mammals (Orentreich *et al.* 1993; Miller *et al.* 2005). The three nutrients are also important for organism's physiological activities and human health. Furthermore, present data suggested the three interventions individually functioned on highly evolutionarily conserved kinases, such as Sch9 and Gcn2, which have been implicated in nutrients metabolism, cell development, stress resistance and aging (Wilson & Roach 2002; Kaeberlein *et al.* 2005b). Thus, present results imply that the extraordinary yeast lifespan extension capacity of the combination of glutamic acid addition, methionine and glucose restriction may also be realized in mammals.

Chapter 6

CRYPTOTANSHINONE EXTENDS CHRONOLOGICAL LIFESPAN IN THE BUDDING YEAST

6.1 Introduction

Natural products with anti-aging capacity have been receiving great attention in the academic community. Compare to the compound that targeted at single age-related diseases, the compound could have more benefit to quality of life if it extends health lifespan by delaying or reducing the onset of aging-associated diseases, such as cardiovascular disease, cancer, osteoporosis, diabetes, hypertension and Alzheimer's disease (Fontana *et al.* 2010). So far a few natural products such as resveratrol (Howitz *et al.* 2003; Baur & Sinclair 2006) and rapamycin (Harrison *et al.* 2009) target conserved longevity mechanisms and have been proposed to act as dietary restriction mimetics to slow aging in multiple model organisms (Steinkraus *et al.* 2008; Kaeberlein 2010b). Resveratrol, an induced phytoalexin found in yeast infected grape skin, can extend the RLS of budding yeast *S. cerevisiae*, worms *C. elegans* and fruit flies *D. melanogaster* but not that of mice (Baur *et al.* 2006; Strong *et al.* 2012). Rapamycin, isolated from bacterium *Streptomyces hygroscopicus*, has potent immunosuppressive and antiproliferative properties, while can extends median and maximal lifespan of mice even when they were fed at 20 months of age (Harrison *et al.* 2009). Remarkably, longevity effect of resveratrol and rapamycin is first identified and characterized in yeast aging model as well as the most promising longevity

factors (e.g. Sir2, Tor1, Sch9, Ras2) (Fabrizio *et al.* 2001; Howitz *et al.* 2003; Powers *et al.* 2006). Irrefutably, the budding yeast is serving as a leading model organism for studying evolutionarily conserved mechanism relevant to human aging and age-related disease (Kaeberlein 2010a; Longo *et al.* 2012).

Danshen, the dried roots of *Salvia miltiorrhiza* Bunge, is a commonly used traditional Chinese medicine (TCM) for the treatment of coronary heart disease, hyperlipidemia, cerebrovascular diseases, angina pectoris and acute ischemic stroke (Zhou *et al.* 2005). Recently, Compound Danshen dripping pill, a product of Danshen from Tasly Pharmaceutical Group Co. Ltd. (Tianjing, China), has passed FDA phase II clinical trials for cardiovascular conditions (Xu 2011). Previous investigations have shown that cryptotanshinone, a major tanshinones in Danshen, possesses multiple biological activities relevant to late-life diseases, such as stroke (Adams *et al.* 2006; Yu *et al.* 2007; Zhang *et al.* 2009a; Kaneko *et al.* 2010), Alzheimer disease (Adams *et al.* 2006; Yu *et al.* 2007; Mei *et al.* 2009), atherosclerosis (Zhou *et al.* 2005; Suh *et al.* 2006), cancer (Shin *et al.* 2009; Chen *et al.* 2010; Chen *et al.* 2012), inflammatory (Jin *et al.* 2006; Tang *et al.* 2011), obesity and type 2 diabetes (Kim *et al.* 2007). Moreover, studies in the mechanism of action indicated that cryptotanshinone involves mediation of several signaling pathways that are highly conserved in multiple species, such as mTOR pathway (Chen *et al.* 2010), AMP activated protein kinase (AMPK) pathway (Kim *et al.* 2007; Chen *et al.* 2012), and phosphatidylinositol 3-kinase (PI3K) pathway (Don *et al.* 2007; Mei *et al.* 2010). Interestingly, recent studies suggested that these pathways are involved in regulation of aging among different species (Steelman *et al.* 2011; Zoncu *et al.* 2011; Salminen & Kaarniranta 2012). Thus, it is presumable that cryptotanshinone could act as an anti-aging compound via targeting these conserved longevity pathways. To address

whether cryptotanshinone induce longevity, I used a high throughput assay in the yeast chronological aging model and demonstrated that cryptotanshinone is the key compound from Danshen to extend CLS, I also elucidated a evolutionarily conserved longevity mechanism on CLS extension by cryptotanshinone in budding yeast.

6.2 Experimental Procedures

6.2.1 Materials

Tanshinone IIA, tanshinone I and cryptotanshinone were from Sigma-Aldrich Chemical Company (St. Louis, MO, USA). Other materials were as described in **Chapter 3** (**3.2.1**).

6.2.2 Lifespan and yeast cell growth assay

The lifespan, biomass and yeast cell growth assays have been described in **Chapter 3** (**3.2.3**).

6.2.3 HPLC chromatogram analysis of compounds from Danshen

Dried Danshen root was purchased from Hubei Jingui Chinese Traditional Medicine Electuary Co., Ltd. (Hubei, China). Approximately 10 g of the dried root was ground and extracted three times using 100 mL acetone/ethanol/water (AEW; 2:2:1, v/v/v) on a shaking incubator at 200 rpm and room temperature for 2 h at each time. The extract was centrifuged at 4000 rpm for 10 min, and the supernatant was concentrated in a rotary evaporator at 50 °C. The concentrated residue was transferred to a LH-20 column (35 × 6 cm, Sephadex™, GE Healthcare, Piscataway, NJ, USA) pre-equilibrated with water. Successive elution with water and water/ methanol/ acetone mixture at a flow rate of 5 mL/min gave many fractions (each fraction volume

was 100 mL). HPLC analysis of each fraction was carried out on a Waters HPLC system (Milford, MA, USA) with an Alliance 2659 separation module and a 2996 photodiode array (PDA) detector with detection wavelength set at 260 nm. The separation was accomplished on a Waters C18 column (3 μm, 4.6 × 150 mm, Atlantis T3, Wexford, Ireland) with water (A), acetonitrile (B) and 2% acetic acid in water (C) as mobile phase. The column temperature was 30 °C. The injection volume was 5 μL. Solvent C composition was maintained at an isocratic 5% for 60 min. Solvent A and B gradient was as follows: 0 – 2 min, A 90%; 2 – 10 min, A from 90% to 70%; 10 – 30 min, A from 70% to 50%; 30 – 50 min, A from 50% to 5%; 50 – 52 min, A 5%; 52 – 55 min, A from 5% to 90%; 55 – 60 min, A 90%. The flow rate was 0.5 mL/min. MS spectra were acquired using a Finnigan/MAT LCQ ion trap mass spectrometer (San Jose, CA, USA) equipped with an electrospray ionization (ESI) source. The capillary temperature and spray voltage were maintained at 250 °C and 4.5 kV, respectively.

6.2.4 Intracellular ROS quantification and fluorescence images of yeast cells

To quantify intracellular ROS level of yeast cells, 2 μL of H_2DCFDA (Invitrogen Molecular Probes, Eugene, OR, USA) from a fresh 5 mM of stock solution in DMSO was added into 1 mL of yeast aging culture at 30 °C for 1 hour. The culture was then washed twice in sterile distilled water and resuspended in 1 mL of 50 mM Tris/Cl buffer (pH 7.5). 20 μL of chloroform and 10 μL of 0.1% (w/v) SDS were added and the cells were incubated at 200 rpm for 30 min to allow the dye to diffuse into the buffer. The culture was centrifuged at 5,000 rpm for 5 min and the fluorescence of the supernatant was measured using a Synergy HT microplate reader (Bio-tek, Winooski, VT, USA) with excitation at 480 nm and emission at 520 nm.

6.2.5 Data analysis

The data analysis on lifespan has been described in **Chapter 3** (**3.2.4**).

6.3 Results

6.3.1 A high throughput assay identifies cryptotanshinone as the key compound from Danshen to extend yeast lifespan in a concentration and the time of addition dependent manner

Taking the advantage of yeast chronological aging model, a high throughput assay was developed recently in different labs for quick and easy quantification of CLS (Murakami *et al.* 2008; Burtner *et al.* 2009b). Subsequently, I applied this assay to screen about 150 plant materials for their anti-aging activity (unpublished data). From these results, we singled out the root extract of Salvia miltiorrhiza Bunge, a very commonly used TCM, which showed the highest activity (**Figure 6.1A**). I further fractionated the crude extract (using solvents) and, using the HTS as a guide, pinpointed the active compound such as tanshinones (i.e. cryptotanshinone, tanshinone I, and tanshinone IIA), which turned out to be commercially available. Therefore, to investigate the mechanisms we purchased these compounds from a commercial supplier. We determined the longevity efficacy of tanshinones in a range of doses and at different addition times. As shown in **Figure 6.1B**, there is a dose-response relationship between yeast survival (day 8) and the extract concentrations, optimized concentration for maximum survival is between 128 and 512 mg/L, while higher or lower concentrations reduce or cannot enhance cell survival. However, It is found as well that delayed addition (day 2) of Danshen extract cannot enhance yeast survival (**Figure 6.1C**).

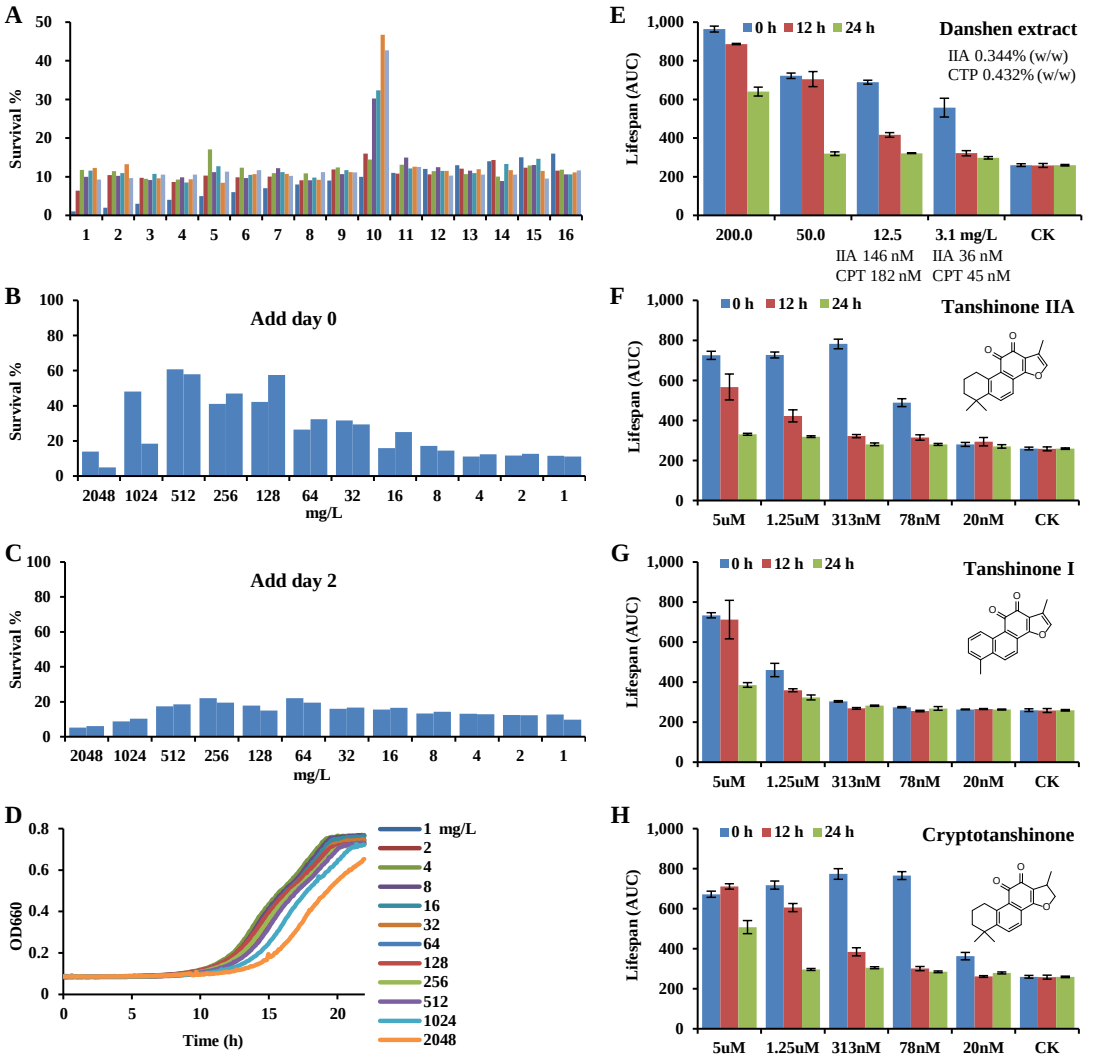

Figure 6.1 A high throughput assay identifies cryptotanshinone as the key compound from Danshen to extend yeast lifespan in a concentration and the time of addition dependant manner

(A) Danshen root raw extract extends yeast survival at day 8. Approximately 1×10^4 WT yeast strain BY4742 are transferred to 1.0 mL of SD medium and maintained at 30˚C with constant agitation (200 rpm) for the entire experiment. TCM raw extracts are added into the culture at initial incubation, 16 extract with 3 dilutions (duplicate) are tested survival at day 8 in a 96-well plate using a microplate reader. No. 10 is Danshen raw extract.

(B and C) Survival of yeast cell is tested at day 6. Twelve concentrations (duplicate) of Danshen raw extract are added at day 0 (B) and day 2 (C), respectively.

(D) Danshen extract has little effect on yeast cell growth. Yeast (≈ 1×10^4 cells) treated with different doses of Danshen extract. The extract is dissolved in methanol/acetone/water (2:2:1) and added into YPD medium (5 µL compound: 100 µL medium) in a 96-well plate inoculated at 30˚C for 22 h.

(E, F, G and H) Compounds from Danshen root extract extend yeast CLS is dependent on concentration and the time of addition into growth medium. Danshen extract (E), compounds tanshinone IIA (F), tanshinone I (G) and cryptotanshinone (H) in methanol or DMSO with several concentrations (2 µL) are added into 1 mL SD medium (≈ 1×10^4 cells) at initial inoculation (0 h), or 12 h and 24 h after inoculation. Percentage composition (w/w) of tanshinone IIA (IIA) and cryptotanshinone (CPT) in Danshen extract are shown as well as their concentrations in 3.1 and 12.5 mg/L the extract. AUC represents the survival integral for lifespan comparison and error bars represent SEM within 4 replicates.

Then, I tested whether the extract inhibit yeast cell growth, the results shows that Danshen extract has relatively low toxicity to suppress yeast cells growth even at a high concentration of 2,048 mg/L (**Figure 6.1D**). According to above data, I propose that there are some highly activity compounds in the extract could be served as a novel candidates to extend yeast CLS.

Next, I separated the compounds using a LH-20 column chromatography. Fractions containing from hydrophilic to lipophilic compounds were collected and tested their capacity on enhancing yeast survival. I found that the 13th fraction has the highest activity, and HPLC chromatogram (260 nm) of this fraction indicates the major compounds are cryptotanshinone, methylenetanshinone and tanshinone IIA (**Figure 6.2**). This result suggests that the main functional compounds may be cryptotanshinone and tanshinone IIA since previous studies suggested the major bioactive components are lipophilic (tanshinone IIA, cryptotanshinone) and hydrophilic (danshensu, protocatechuic aldehyde, Salvianolic acid B) compounds (Zhou *et al.* 2005). Then I determined the longevity efficacy of cryptotanshinone, tanshinone I and tanshinone IIA from Sigma Company, as well as Danshen extract at a range of dose and different addition time (**Figure 6.1E-H**). I also quantified the concentration of cryptotanshinone (45 nM and 182 nM) and tanshinone IIA (36 nM and 146 nM) in the 3.1 mg/L and 12.5 mg/L extract (**Figure 6.1E**). Comparing the lifespan extension capacity of the two doses of Danshen extract with cryptotanshinone, tanshinone I and tanshinone IIA at 78 nM, cryptotanshinone and tanshinone IIA are proved to be major contributors in Danshen extract for longevity, and cryptotanshinone shows stronger capacity on CLS extension than tanshinone IIA (**Figure 6.1F, H**).

Cell growth phase seems to be a critical factor for modulating nutrient signaling influenced CLS. Consistent with this hypothesis, current data showed that tanshinones extend CLS only when it is applied to cells that are entering stationary phase, not when applied to cells that are already in stationary phase (**Figure 6.1**). It is similar to the effect reported for caffeine (Wanke *et al.* 2008), rapamycin (Powers *et al.* 2006; Pan *et al.* 2011), spermidine (Eisenberg *et al.* 2009) and lithocholic acid (Goldberg *et al.* 2010; Burstein *et al.* 2012) in promotion of longevity of yeast chronological aging. All these compounds, as well as CR and other nutrients with anti-aging property are added before yeast cell entering stationary phase (day 2). In laboratory mice and rats, CR and other nutrients can achieve maximal benefit for longevity only if they are applied during the rapid growth period (Weindruch & Walford 1982; Yu *et al.* 1985). Previous studies indicated that they prolonged lifespan via nutrient signaling pathways (Fontana *et al.* 2010). In fact, compounds targeting nutrient signaling pathways are an effective mechanism in regulating longevity of an organism, since cells require nutrients in response to the compound induced physiological change in the organism (Howitz & Sinclair 2008; Fontana *et al.* 2010). Overall, these results may implicate that these tanshinones prolong CLS via a nutrient-dependent regime.

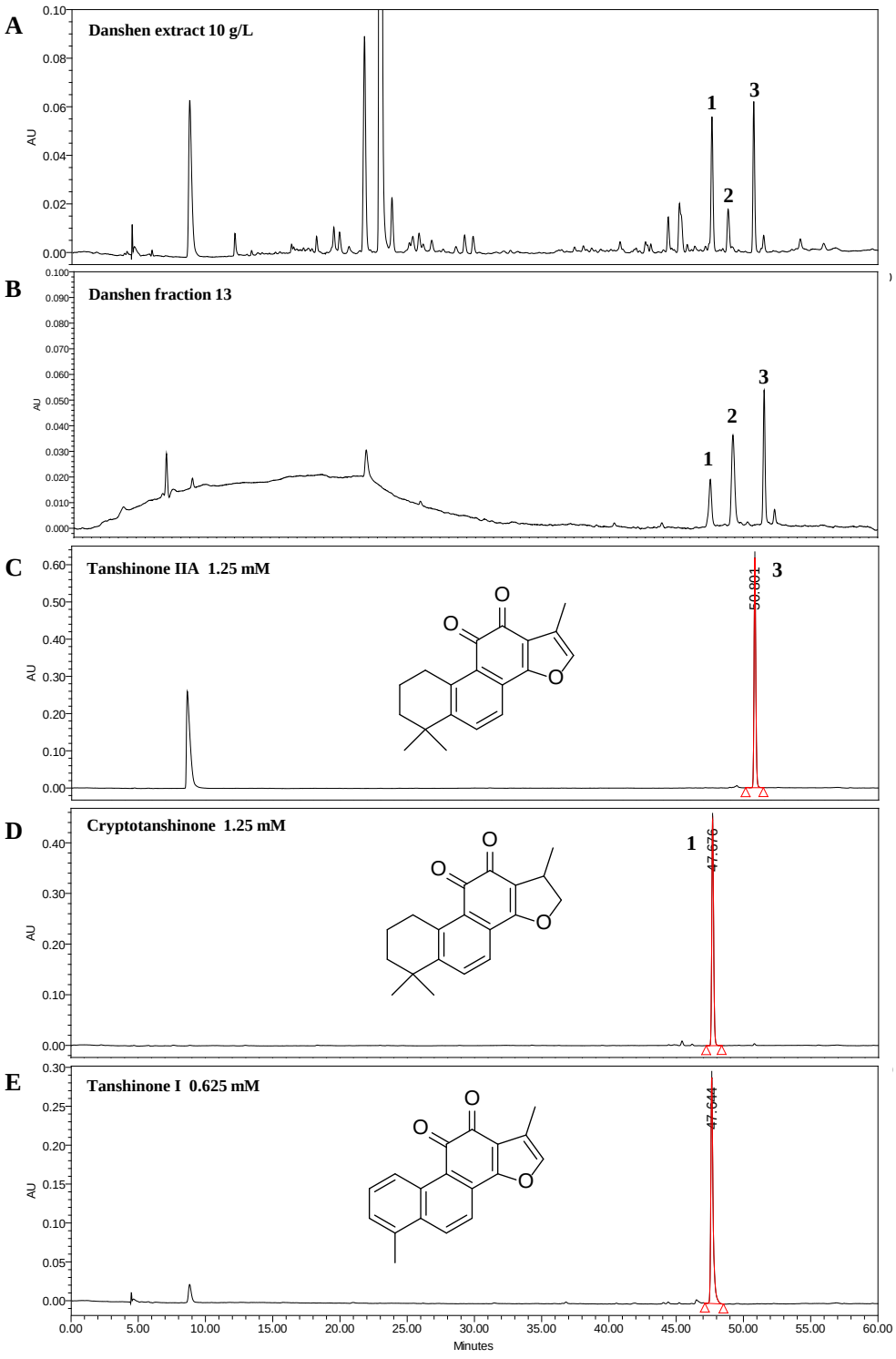

Figure 6.2 HPLC chromatogram analysis compounds from Danshen

(A) HPLC chromatogram (260 nm) of 10 g/L Danshen root extract. Danshen root is extracted by acetone/methanol/water (2:2:1). Peak 1, 2 and 3 are cryptotanshinone, methylenetanshinone and tanshinone IIA, respectively.

(B) HPLC chromatogram (260 nm) of the 13th fraction from a LH-20 column chromatography for isolation of the Danshen extract. The extract was transferred to a LH-20 column (35 × 6 cm, Sephadex LH-20) pre-equilibrated with water. Successive elution with water, methanol and acetone mixture at a flow rate of 5 mL/min gave many fractions (each fraction volume was 100 mL).

(C, D, E) HPLC chromatogram (260 nm) and structures of tanshinone IIA, cryptotanshinone and tanshinone I standard compounds from Sigma-Aldrich company.

6.3.2 Cryptotanshinone induced CLS extension is prevented by amino acid restriction

To determine which nutrient factors alter tanshinones induced longevity, I tested CLS extension capacity of cryptotanshinone at 78 nM in different media (**Figure 6.3**). The concentration was chosen because at the low concentrations the compounds are able to extend CLS but unable to inhibit cell growth and reduce biomass production. To my surprise, the data showed that cryptotanshinone extended CLS in several media (**Figure 6.3A-G**), especially in the low glucose (0.5%, CR condition, **Figure 6.3B**), high glucose (8%, **Figure 6.3D**), and buffered media (pH 6.0) (**Figure 6.3E, F**). However, it could not extend lifespan in a medium in which the total amino acid amount was reduced (**Figure 6.3H**). This finding suggests that cryptotanshinone might extend lifespan in a wide range of environmental conditions. Overall, these results indicate that cryptotanshinone induced longevity greatly depends on media composition, and amino acids are an important factor to affect the lifespan extension capacity of cryptotanshinone. It is already established that CLS is severely compromised if cells are grown on SD medium that causes starvation for EAA (Gomes *et al.* 2007; Boer *et al.* 2008). In the measurements presented here this effect appears to be overriding any CLS-extending effect of cryptotanshinone.

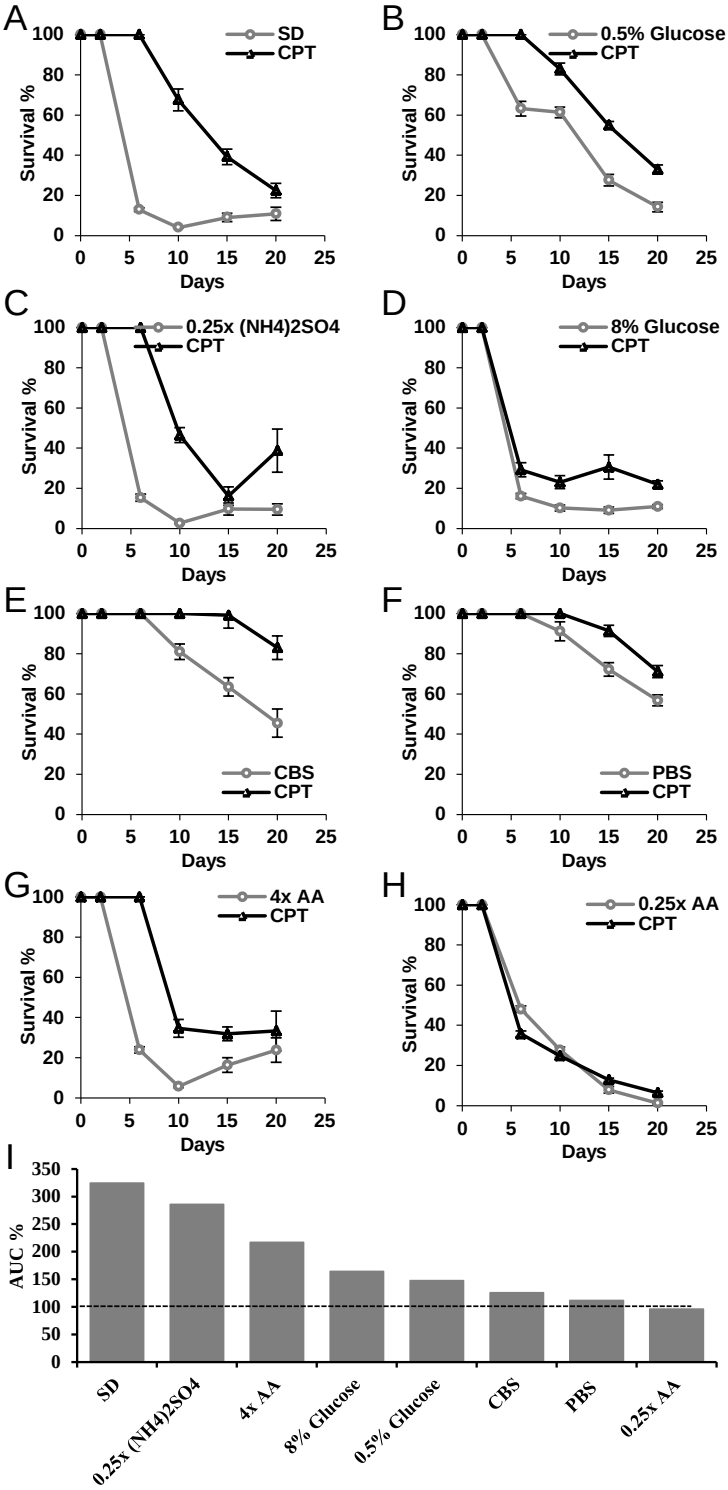

Figure 6.3 Cryptotanshinone (CPT) induced CLS extension is prevented by amino acids restriction

(A-H) Survival curve (mean + SEM, n = 8) of WT strain BY4742 cultured in 8 SD based media with or without cryptotanshinone (78 nM, 0.2% methanol). They are SD medium with 2% glucose **(A)**, 0.5% glucose as CR condition **(B)**, 0.25-fold ammonium sulphate **(C)**, 8% glucose **(D)**, SD medium prepared with citrate phosphate buffer solution (CBS, Na_2HPO_4 and citric acid, pH 6.0; **E**) or phosphate buffer solution (PBS, Na_2HPO_4 and NaH_2PO_4, pH 6.0; **F**), 4-fold total amino acids **(G)** and 0.25-fold total amino acids **(H)**. **(I)** Relative AUC comparison (AUC of compound / AUC of untreated × 100%) in the 8 media. Cryptotanshinone dissolved in methanol, 2 µL of 39 µM compounds was added in 1 mL growth medium at the time of cell inoculation.

6.3.3 Essential amino acid sufficiency is required for cryptotanshinone induced longevity

In order to examine how the amino acid composition affects cryptotanshinone lifespan extending activity, seven media with different proportions of EAA and NEAA were designed and tested (**Figure 6.4**, **6.5A, B**). A standard SD medium normally contains 14 amino acids and two bases, adenine and uracil (Sherman 1991; Murakami *et al.* 2008). Among these compounds, only histidine, leucine, lysine and uracil are essential as auxotrophy-complementing amino acid for the WT yeast strain *S. cerevisiae* BY4742 (MATα *his3*Δ1 *leu2*Δ0 *lys2*Δ0 *ura3*Δ0) (**Table 3.1**). The medium with 1-fold EAA and 5-fold NEAA (1E5N) produced longer CLS than the other media in WT strain and 5E5N has the shortest CLS (**Figure 6.4**, **6.5A, B**). However, this observation changed greatly when cryptotanshinone was added to these media. These results clearly showed that EAA sufficiency was required for cryptotanshinone induced CLS extension in WT based on the following observations: (1) Cryptotanshinone could not extend CLS in low EAA media (0.2E0.2N or 0.2E1N); (2) Increasing NEAA did not improve the efficacy of cryptotanshinone when the EAA was maintained at the same level (e.g. 1E0.2N, 1E1N, 1E5N); (3) Although CLS changed slightly when EAA increased, the efficacy of cryptotanshinone improved significantly (e.g. 0.2E1N, 1E1N, 5E1N); (4) The ratio of EAA and NEAA concentrations could alter CLS, but the addition of cryptotanshinone changed this consequence and led to longer CLS in higher EAA media (e.g. 0.2E, 1E, 5E) (**Figure 6.4A**). Moreover, cryptotanshinone did not suppress cell growth and biomass production in different media (**Figure 6.4B**).

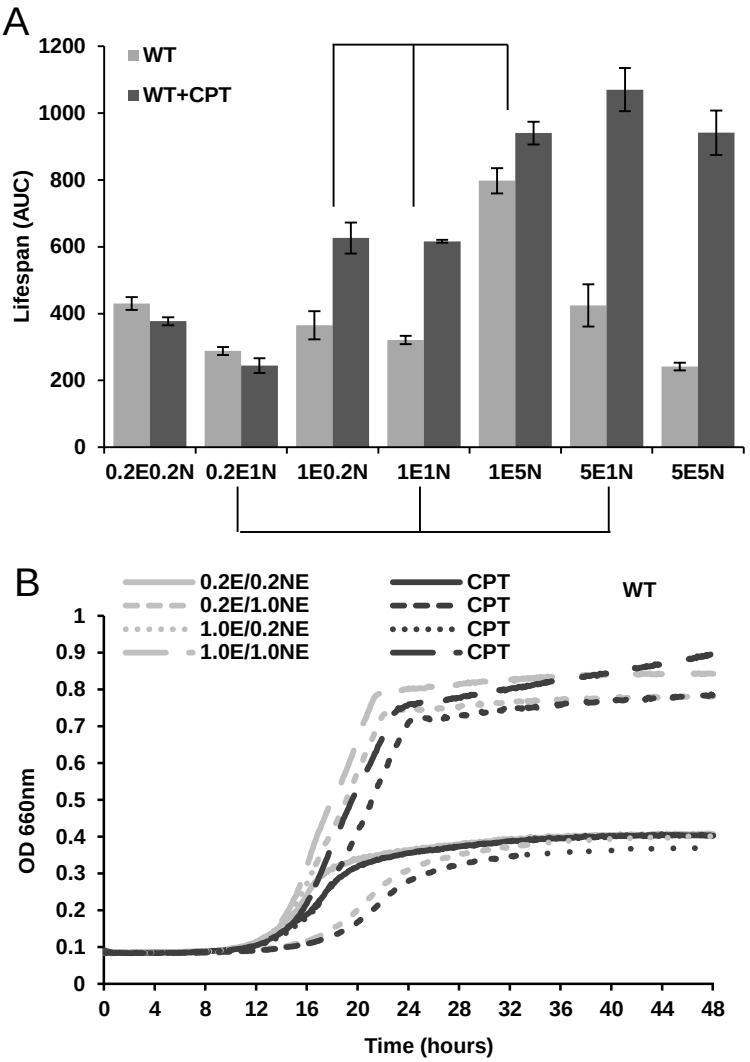

Figure 6.4 EAA sufficiency was required for cryptotanshinone induced CLS extension
Yeast was grown in the 7 media with or without cryptotanshinone (78 nM) and error bars represent SEM within 6 replicates. The growth curve of yeast cultured in 4 SD based media with different amount of EAA and NEAA. The growth curves showed that yeast cells could proliferate well with cryptotanshinone (CPT, 78 nM) in different media since the lag time (≈ 12 h) of each curve had no significant changes. 0.2E0.2N represents SD medium containing 0.2-fold EAA and 0.2-fold NEAA.

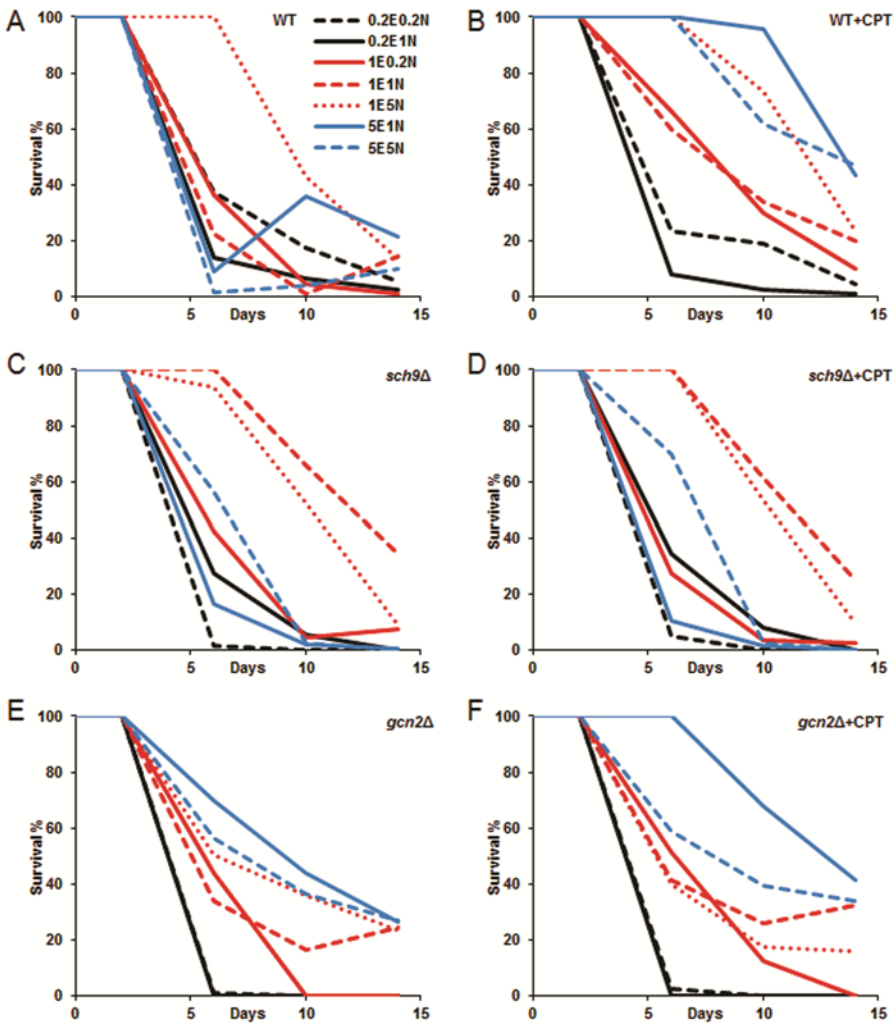

Figure 6.5 Survival curves (mean, n = 6) of the WT, sch9Δ and gcn2Δ yeast cultured in 7 SD based media with different amount of EAA and NEAA with or without cryptotanshinone (78 nM)
0.2E0.2N represents SD medium containing 0.2-fold EAA and 0.2-fold NEAA.

Next, I examined the effect of individual amino acids on the efficacy of cryptotanshinone (**Figure 6.6**). Consistent with the analysis above that restriction of EAA prevents cryptotanshinone induced longevity, the addition of cryptotanshinone in the media with 0.1-fold histidine (**Figure 6.6E**) and uracil (**Figure 6.6M**) showed little CLS extension, which was not observed in NEAA (**Figure 6.6O**). It should be highlighted that leucine and lysine were not shown here as the low concentration of these two amino acids led to low biomass production and an accelerated loss of viability.

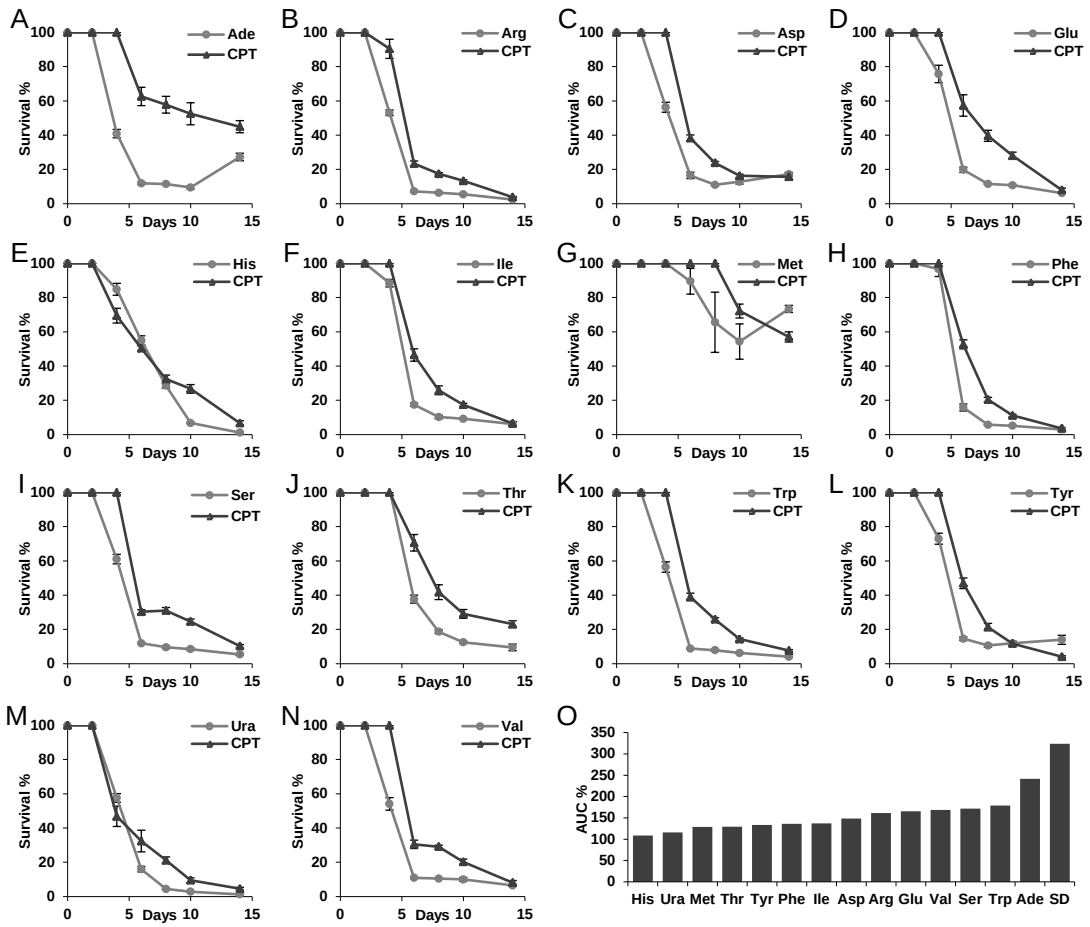

Figure 6.6 Effect of individual amino acid restriction on cryptotanshinone induced CLS extension (A - N) Survival curve (mean, n = 6) of WT strains cultured in SD based media containing 0.1-fold individual amino acid with/without cryptotanshinone. **(O)** Relative AUC comparison (AUC of compound / AUC of untreated × 100%) in different media.

6.3.4 Cryptotanshinone requires Tor1 and Sch9 for CLS extension

To elucidate the genetic mechanism of cryptotanshinone induced CLS extension, I focused on those evolutionarily conserved and nutrient-sensing longevity pathways from yeast to humans. In yeast, the Tor/Sch9 pathway was thought previously to be a highly conserved nutrient-sensing pathway that regulates longevity among different species (Fontana *et al.* 2010). Sch9 is proposed as a major nutrient-sensing factor to regulate cell growth, cell size, and stress resistance through controlling protein synthesis. Absence of Sch9 activity causes a small-sized phenotype and distinct growth defect, while increasing the lifespan (Fabrizio *et al.* 2001; Kaeberlein *et al.* 2005b; Urban *et al.* 2007; Huber *et al.* 2009). I previously demonstrated that *sch9*Δ is

more responsive to nutrients than WT, *tor1*Δ, and *sir2*Δ (**Chapter 5**). Thus, I first examined the effect of cryptotanshinone on *sch9*Δ lifespan in SD media with different ratios of EAA and NEAA. Similar to the observation in WT, the amino acid composition changed CLS of *sch9*Δ, but cryptotanshinone did not increase the lifespan significantly even in the media containing a high content of EAA (**Figure 6.7A, 6.5C, D**). It implicates that cryptotanshinone induced longevity requires Sch9 activity.

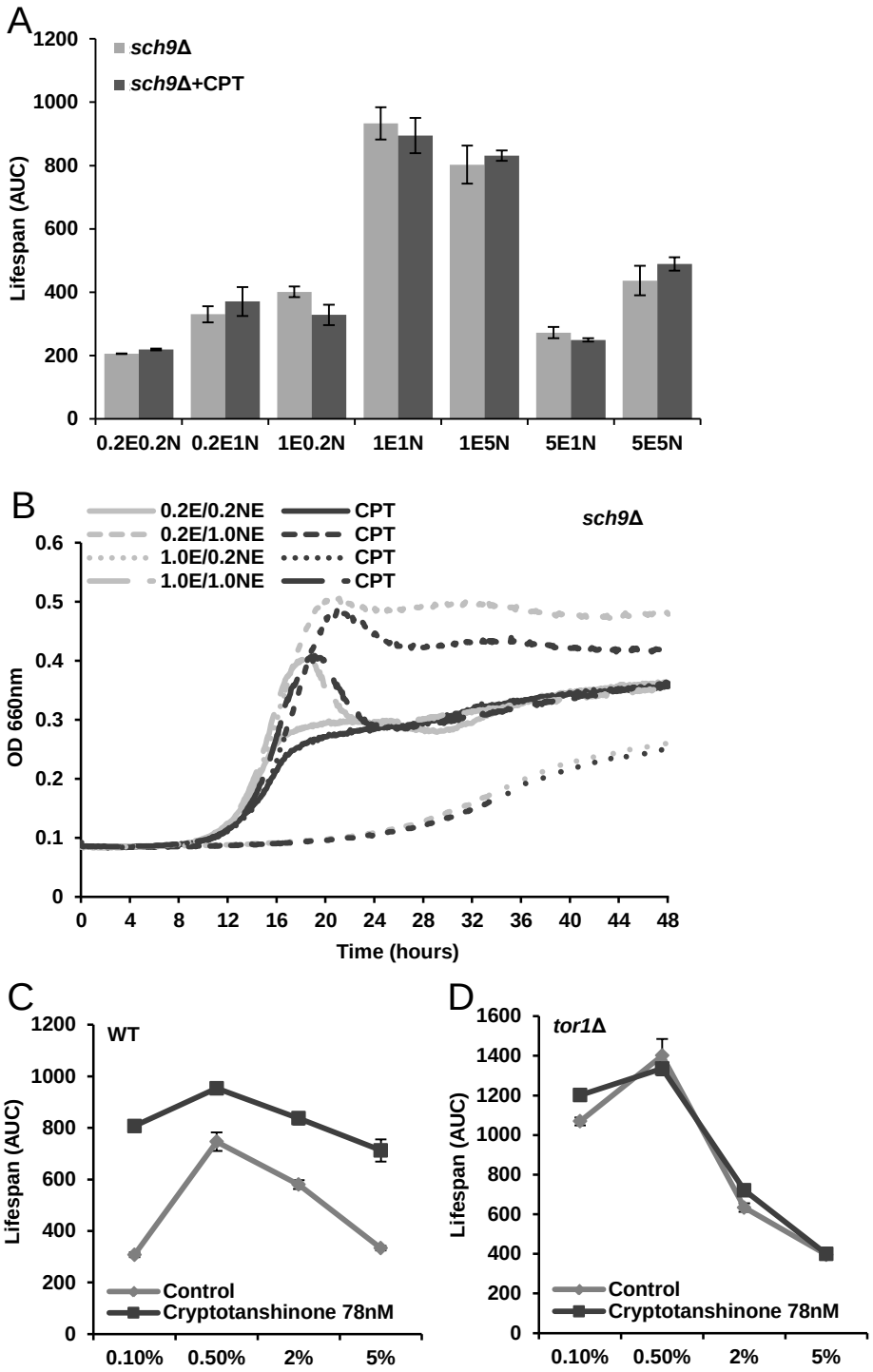

Figure 6.7 Cryptotanshinone induced lifespan extension depends on Sch9 and Tor1 activity
(A) Deletion of *SCH9* prevented cryptotanshinone induced CLS extension in different media. The yeast was grown in the 7 media with or without cryptotanshinone (78 nM; mean ± SEM, n = 6). **(B)** Cryptotanshinone did not inhibit cell growth in *sch9*Δ strain. (**C** and **D**) Cryptotanshinone induced longevity was independent of glucose levels and was prevented by deletion of *TOR1*. WT and *tor1*Δ cultured in SD medium containing 0.1%, 0.5%, 2% and 5% glucose with or without cryptotanshinone (78 nM; mean ± SEM, n = 6). 0.2E0.2N represents SD medium containing 0.2-fold EAA and 0.2-fold NEAA.

Next, I tested the effect of cryptotanshinone on *tor1*Δ strain cultured in SD medium containing 0.1%, 0.5%, 2%, and 5% glucose. The data showed that cryptotanshinone prolonged lifespan in media with different levels of glucose (**Figure 6.7C, 6.8A**), indicating further that cryptotanshinone induced lifespan extension was not dependent on glucose concentration. Although this result suggests that the action of cryptotanshinone is independent of CR (0.5% glucose), it is possible that cryptotanshinone could enhance the resistance of yeast against the toxicity of metabolites (e.g. ROS, and organic acids) at high glucose levels. In contrast, cryptotanshinone could not prolong lifespan of *tor1*Δ strain (**Figure 6.7D, 6.8B**). Overall, these results suggest that the CLS-extending effect of cryptotanshinone is overridden by loss of either Sch9 or Tor1.

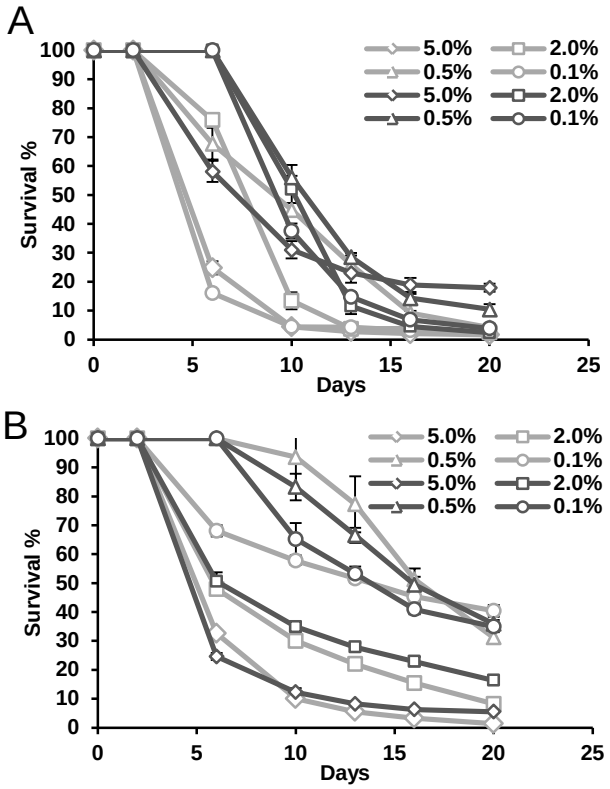

Figure 6. 8 Survival curves of WT yeast (A) and tor1Δ (B) cultured in SD medium containing 0.1%, 0.5%, 2% and 5% glucose with (red line) or without (blue line) cryptotanshinone (78 nM; mean ± SEM, n = 6)

6.3.5 Tanshinones extend yeast lifespan via similar mechanisms

To determine whether the tanshinones induce longevity via other mechanisms, tanshinone IIA (1.25 μM), cryptotanshinone (78 nM) and a mixture containing tanshinone I (1.7 μM), tanshinone IIA (0.42 μM), cryptotanshinone (26 nM) were chosen, and their effects on CLS of WT BY4742, *sch9*Δ, and *sir2*Δ cultured in the standard SD medium were evaluated (**Figure 6.9**). Tanshinone IIA (1.25 μM) and cryptotanshinone (78 nM) extended lifespan by equal amounts (**Figure 6.9A**), but the mixture did not show a longer lifespan compared with that of individual compounds, which means that tanshinones have no additive or synergistic effect on yeast longevity. In addition, the three selected compounds could not extend CLS in *sch9*Δ, while they prolonged the *sir2*Δ lifespan significantly (**Figure 6.9B, C**). Altogether, these observations indicate that tanshinones require Sch9 for CLS extension and they may act on similar mechanisms.

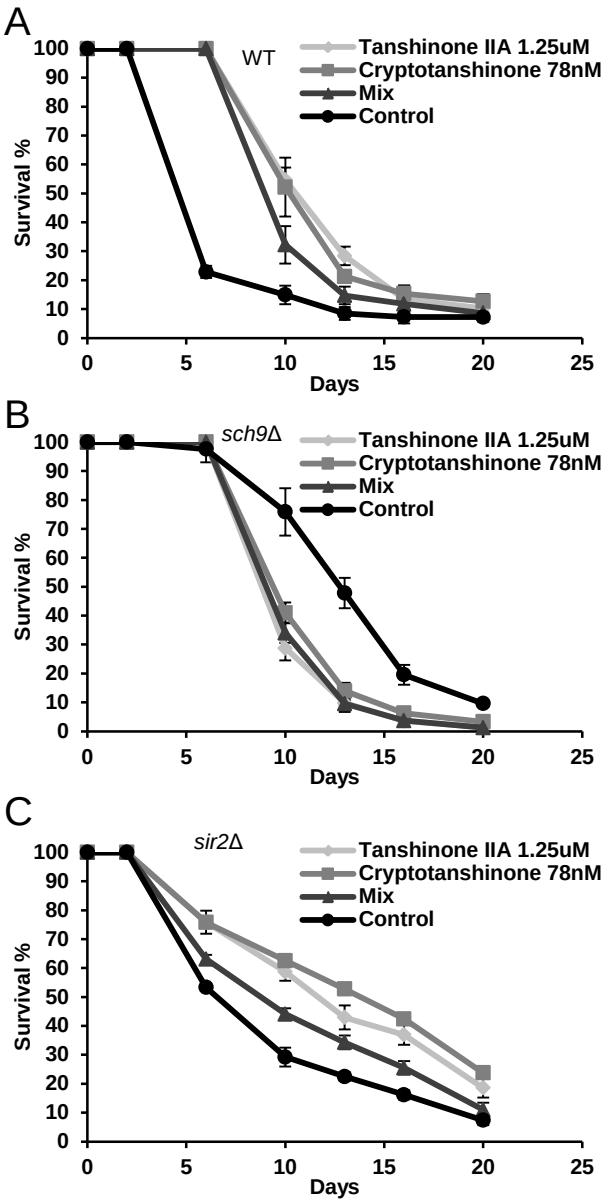

Figure 6.9 Tanshinones have no synergetic effect on yeast longevity via similar mechanisms
(A) Tanshinones had no synergetic effect on CLS extension. Tanshinone IIA (1.25 μM), cryptotanshinone (78 nM) and a mixture containing tanshinone I (1.7 μM), tanshinone IIA (0.42 μM), cryptotanshinone (26 nM) were tested in WT BY4742 grown in standard SD medium. **(B)** Deletion of *SCH9* prevented CLS extension by the Danshen compounds. **(C)** Tanshinones extended CLS in dependent of deletion of *SIR2*. **(D)** Comparison of CLS of WT, *sch9*Δ, and *sir2*Δ treated with tanshinones. AUC represents the survival integral for lifespan comparison (mean ± SEM, n = 6).

6.3.6 Gcn2 regulates essential amino acids and cryptotanshinone induced CLS extension

In addition to the Tor-Sch9 nutrient-sensing pathway, general amino acid control (GAAC) is an important nutrient-sensing pathway in the regulation of yeast growth and metabolism. It is also noteworthy that GAAC could be a major factor of the

Tor/Sch9 pathway, and Gcn2 may play a central role in the integration of GAAC and Tor/Sch9 pathways (Staschke *et al.* 2010). Gcn2 is one of the major evolutionarily conserved protein kinases in response to nutritional cues, especially amino acid starvation (Wilson & Roach 2002). The starvation causes activation of Gcn2, which subsequently phosphorylates eukaryotic initiation factor-2 (eIF2). As a result, initiation of general protein synthesis is repressed. This change enables cells to conserve resources and have time to reconfigure the transcriptome to alleviate nutrient stress (Staschke *et al.* 2010). Concomitantly, Gcn2 phosphorylation also elevates Gcn4 activity, a transcription activator of a large number of genes subject to the GAAC, many of which are involved in amino acid biosynthesis (Hinnebusch 2005).

Based on the above reasoning, it is possible that Gcn2 could be involved in regulation of cryptotanshinone induced CLS extension. I measured CLS of *gcn2*Δ in the seven media, and found that a higher EAA concentration had longer CLS and NEAA had less contribution to CLS extension than EAA (**Figure 6.10A, 6.5E, F**), which means Gcn2 mainly regulated EAA and may partly prevent CLS extension in WT and *sch9*Δ strains grown in the media with a high level of EAA (**Figure 6.4A, 6.7A**). I also found that cryptotanshinone are more effective to extend lifespan of WT in 5E1N than that in 1E5N (**Figure 6.4A**), while cryptotanshinone cannot extend lifespan of *gcn2*Δ in 1E5N and slight increase in 5E1N. Obviously, 1E5N and 5E1N are greatly different in amino acids composition. Cryptotanshinone extends CLS in WT and the efficacy is mainly dependent on EAA concentration (**Figure 6.4A**). Thus, this observation is consistent with the conclusion that EAA is a key determinant for cryptotanshinone activity. Furthermore, current data showed that deletion of *GCN2* could impair the efficacy of cryptotanshinone relative to WT in normal and high EAA

media (**Figure 6.4A, 6.10A**). Thus, I conclude that the CLS-extending effect of cryptotanshinone is partly overridden by loss of Gcn2 in EAA sufficient media.

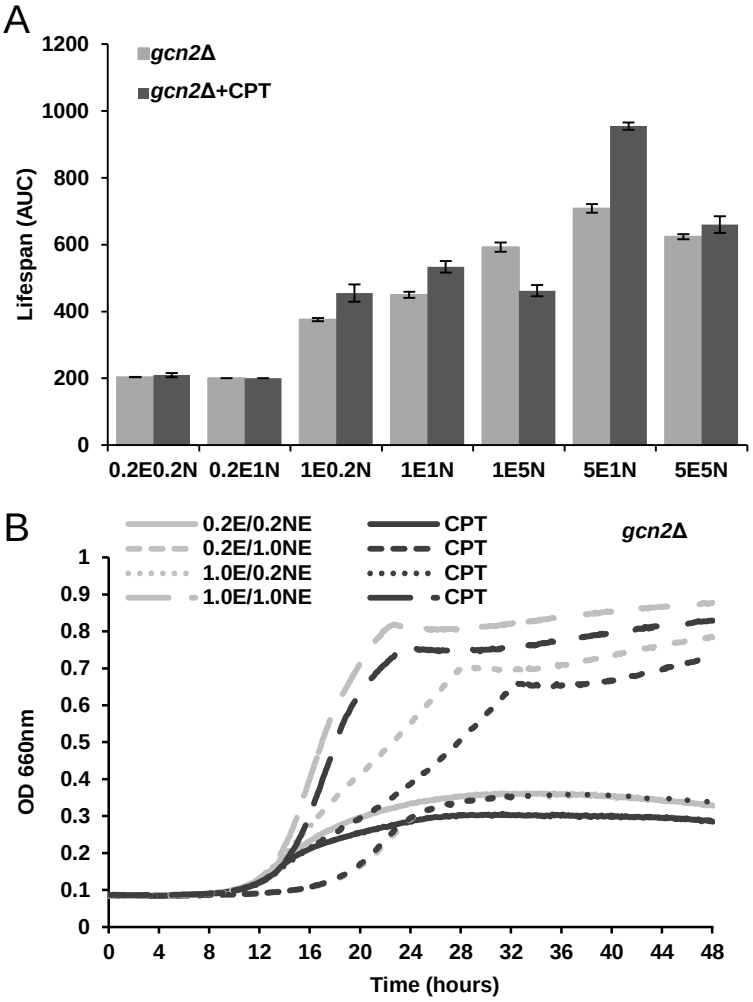

Figure 6.10 Gcn2 regulated amino acids homeostasis to extend lifespan and impaired cryptotanshinone induced longevity in different media
(A) The yeast were grown in the 7 media with or without cryptotanshinone (78 nM; mean ± SEM, n = 6). **(B)** Cryptotanshinone did not inhibit cell growth in *gcn2*Δ strain. 0.2E0.2N represents SD medium containing 0.2-fold EAA and 0.2-fold NEAA.

6.3.7 Cryptotanshinone extend lifespan without reduce in ROS level in *sod2*Δ

Reactive oxygen species (ROS)-initiated irreversible cellular damage is the cornerstone of free radical theories of aging and enzymatic antioxidants, particularly superoxide dismutase (SOD), are critical in protection from ROS damage to cells (Harman 1956; Finkel & Holbrook 2000). Yeast has two SOD genes, cytoplasmic

copper-zinc superoxide dismutase (*SOD1*) and mitochondrial manganese superoxide dismutase (*SOD2*). The lack of either of the two SODs resulted in decreased lifespan enormously, and deletion of *SOD2* has a shorter lifespan than deletion of *SOD1* (Unlu & Koc 2007). *SOD2* was proposed as a downstream target of Tor/Sch9 nutrient signaling pathway for longevity extension by decreasing in part ROS levels in yeast (Fabrizio *et al.* 2003; Fontana *et al.* 2010; Pan *et al.* 2011). Thus, it is interesting to ascertain whether cryptotanshinone reduces ROS stress to extend CLS. Surprisingly, although cryptotanshinone could not reduce the intracellular ROS level in *sod2*Δ mutant at early stationary phase day 2, it extended CLS in the *sod2*Δ strain that has shortened lifespan significantly in the standard SD medium due to impaired superoxide detoxification in the cell (**Figure 6.11A, B**) (Pan *et al.* 2011). Additionally, this was not due to the SOD mimicking activity of cryptotanshinone in cells because *in vitro* assays showed that cryptotanshinone had no superoxide anion scavenging activity (unpublished data). The observation that cryptotanshinone had no effect on ROS production in *sch9*Δ, might further indicated that *SCH9* deletion eliminated the cryptotanshinone effect.

6.4 Discussion

In this study, I used a high throughput assay in yeast chronological aging model to screen anti-aging compounds from diverse natural sources, and discovered that a novel compound cryptotanshinone from Danshen, a notable traditional Chinese medicine because of its widespread medicinal use in treatment of cardiovascular

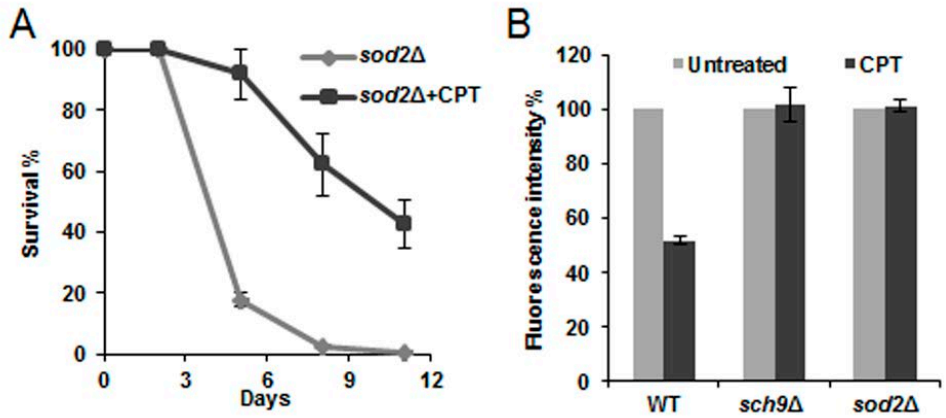

Figure 6.11 Cryptotanshinone mediates reactive oxygen species (ROS) production
(A) Cryptotanshinone extends CLS of *sod2*Δ strain (mean ± SEM, n = 6). **(B)** Intracellular ROS levels of WT, *sch9*Δ and *sod2*Δ strains grown in standard SD medium with/without cryptotanshinone were quantified by a Bio-Tek plate reader. The ROS probe H_2DCFDA (2',7'-dichlorodihydrofluorescein diacetate) was used. DCF (dichlorofluorescein) fluorescence was measured at 520 nm with excitation at 480 nm. Relative fluorescence intensity (fluorescence intensity of compound / fluorescence intensity of untreated × 100%) at day 2 was presented. Error bars are mean ± SD, n = 4.

diseases has strong lifespan extending activity in relatively low concentrations (e.g. 78 nM). I found that cryptotanshinone has a stronger efficacy than tanshinone IIA and tanshinone I. Compared to other reported anti-aging compounds, such as resveratrol, rapamycin, lithocholic acid and spermidine (Howitz *et al.* 2003; Powers *et al.* 2006; Eisenberg *et al.* 2009; Pan *et al.* 2011; Burstein *et al.* 2012), cryptotanshinone is a novel candidate for anti-aging medicine based on four reasons:

(1) **Ideal pharmaceutical properties**. Cryptotanshinone meets Lipinski's rule of five including molecular weight 296 g/mol, molecular formula $C_{19}H_{20}O_3$, octanol-water partition coefficients (XLogP3-AA) 3.8, H-bond donor 0 and H-bond acceptor 3. As shown in Fig. 1, the three tanshinones have little structural differences, but have significant activity difference, indicating a strong structure-activity relationship for this compound that warrants further chemical structure modification for drug development.

(2) **High activity**. Cryptotanshinone can extend yeast CLS more than three times in a standard SD medium at only 78 nM, in which concentration it does not inhibit

cell growth nor supress biomass production (**Figure 6.4B, 6.7B, 6.10B**). In contrast, resveratrol extends yeast RLS at least 10 μM but does not extend CLS even at 100 μM (Howitz *et al.* 2003); rapamycin prolongs yeast CLS at 200 nM whereas it greatly inhibits cell growth (Pan *et al.* 2011).

(3) **Multifunctionality**. Cryptotanshinone not only exerts longevity extension in diverse media and strains as shown in this study, but also processes numerous other bioactivities assessed in different models including human cells (Don *et al.* 2007; Chen *et al.* 2010; Mei *et al.* 2010; Chen *et al.* 2012; Park *et al.* 2012a). Aging is a very complex and dynamic process involving multiple factors and their interactions, thus a compound that is multi-targeting of these factors or pathways might be desired as an anti-aging candidate. Resveratrol is such an example but it has low efficacy (Park *et al.* 2012b).

(4) **Action on evolutionarily conserved genetic pathway.** Present data documented that EAA, rather than other nutrients, is the key nutrient factor that is required for cryptotanshinone to induce lifespan extension. This result is of considerable interesting since almost all living cells require EAA for protein synthesis and survival. Therefore it is reasonable that cryptotanshinone could be applied in diverse cell lines for lifespan extension via targeting the highly conserved nutrient-sensing Tor/Sch9 pathway, which is a control point of lifespan of in higher organisms (Fontana *et al.* 2010). Moreover, cryptotanshinone was reported to inhibit mTORC1 mediated phosphorylation of ribosomal p70 S6K1 (having similar functionality to Sch9) and eukaryotic initiation factor 4E binding protein 1 (4EBP1) in a concentration and time dependent manner (Chen *et al.* 2010).

I have shown that deleting Tor/Sch9 signaling pathway in yeast eliminates CLS extension by cryptotanshinone. Sod2 was proposed as a downstream of Sch9, double

deletion of *SCH9* and *SOD2* abolished CLS extension in *sch9*Δ (Fabrizio *et al.* 2003; Fontana *et al.* 2010). In this study, removing of mitochondrial Sod2 cannot prevent cryptotanshinone induced lifespan extension, and cryptotanshinone does not diminish the intracellular ROS level in *sod2*Δ mutants based on the fluorescence intensity of the redox sensitive probe (**Figure 6.11**), but significantly reduce the oxidative stress status in WT strain. For the WT strain, cryptotanshinone may inhibit the activity of Tor/Sch9 signaling, and subsequently reduce total ROS production (**Figure 6.12**) (Fontana *et al.* 2010). Consistently, there is no change in the ROS level in *sch9*Δ strain with/without cryptotanshinone treatment (**Figure 6.11B**). The Tor/Sch9 signalling downregulate many stress response and the antioxidant enzymes Sod1 and Sod2 or catalase involving ROS regulation. In yeast, overexpression of these antioxidant enzymes results in no significant lifespan extension, indicating that many other systems are important in lifespan modulation (Fontana *et al.* 2010). This might be why CPT extended CLS in *sod2*Δ but not in *sch9*Δ or *tor1*Δ. On the other hand, it is possible that H_2DCFDA (2',7'-dichlorodihydrofluorescein diacetate) detects general ROS stress (including superoxide, hydrogen peroxide and hydroxyl radicals) but not specifically superoxide radical, which is a major signaling ROS mediated by Sod1 and Sod2. The change of superoxide stress level in *sod2*Δ is thus not possible to be distinguished by fluorescence intensity for the general ROS status of the cells. The other possibility is that cryptotanshinone may extend CLS of *sod2*Δ via other mechanism. Previous studies have revealed that cryptotanshinone mediates the AMPK pathway, PI3K pathway and endoplasmic reticulum (ER) stress (Kim *et al.* 2007; Mei *et al.* 2010; Park *et al.* 2012a), which might contribute to lifespan extension. Furthermore, given the similar effective treatment window between rapamycin and CPT, it should be interesting to measure superoxide with DHE

(dihydroergotamine) and/or Mitosox and peroxide with H_2DCFDA in log phase and stationary phase. It would be worthwhile to confirm or eliminate mitohormesis as a mechanism underlying CPT extension of CLS (Ristow & Zarse 2010; Pan 2011).

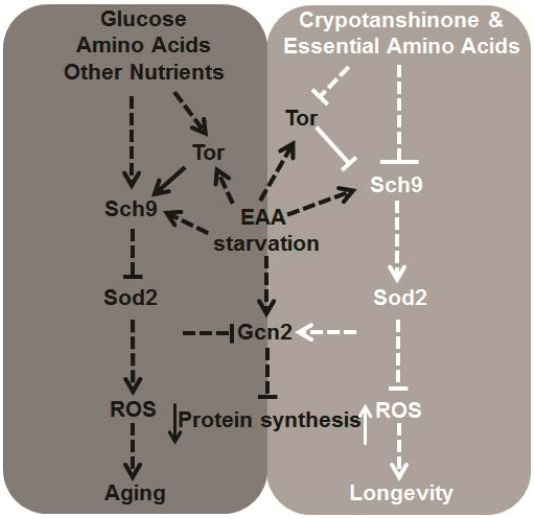

Figure 6.12 A proposed pathway induced by cryptotanshinone for longevity in yeast
The left part shows a conserved aging pathway regulated by Tor, Sch9 and Sod2 in yeast under normal condition. The right part presents the conserved longevity pathway induced by cryptotanshinone when yeast grown in a medium with sufficient EAA.

The EAA concentration in a medium is a key nutrient parameter affecting lifespan extending capacity of cryptotanshinone in WT yeast and determining CLS of *gcn2*Δ. I have demonstrated that EAA and NEAA composition changes lifespan of WT and *sch9*Δ significantly (**Figure 6.4**, **6.7**) and EAA is a determining factor for biomass production in different strains (**Figure 6.4B, 6.7B, 6.10B**). On the other hand, EAA restriction (0.2-fold EAA of normal) greatly decreases biomass and restriction of both EAA and NEAA (0.2EAA/0.2NEAA) do not inhibit cell growth in comparison to that under normal conditions, while EAA and NEAA imbalance (0.2EAA/1NEAA) delays cell growth in WT, *sch9*Δ, and *gcn2*Δ strains (**Figure 6.4B, 6.7B, 6.10B**). To our knowledge, only few previous studies reported that a higher EAA concentration causes a longer CLS and higher biomass production in yeast chronological aging model (Gomes *et al.* 2007; Boer *et al.* 2008; Alvers *et al.* 2009a).

Although the individual EAA composition and concentration differ from ours, the results are similar to present observation.

Gcn2 regulates amino acid homeostasis and protein synthesis by modulating amino acid biosynthesis in response to different amino acids deprivation in yeast (Hinnebusch & Natarajan 2002). So far, there are two known ways to regulate Gcn2 activity. Firstly, amino acid starvation causes accumulation of uncharged tRNAs that bind to Gcn2 protein kinase and subsequently activates Gcn2. Secondly, rapamycin activates Gcn2 by inhibiting TORC1 even in amino acid depleted cells (Hinnebusch 2005). In this study, I document for the first time that Gcn2 regulates EAA and NEAA homeostasis to alter lifespan, deletion of *GCN2* causes yeast cells to become amino acid insensitive, which leads to longer lifespan and prevents cryptotanshinone induced lifespan extension in EAA sufficient media (**Figure 6.10**).

Although it is not clear whether cryptotanshinone affects Gcn2 directly, current data suggest that cryptotanshinone appears to reduce Tor/Sch9 pathway activity, and in turn elevate Gcn2 activity (**Figure 6.12**). It is consistent with previous studies shown that Gcn2 is at downstream of TOR and upstream of Gcn4 linking TOR pathway and GAAC pathway (Steffen *et al.* 2008; Staschke *et al.* 2010). Growth in media with amino acid imbalance can elicit the pathway. Activation of GAAC decreases CLS while suppression of GAAC prolongs CLS in minimal medium (Alvers *et al.* 2009a). Testing CLS of *gcn4*Δ strain cultured in the different media I used with or without cryptotanshinone would be informative to find out if Gcn4 is indeed a potential longevity factor for CLS and RLS and a master regulator of gene expression for GAAC in yeast (Steffen *et al.* 2008; Alvers *et al.* 2009a). Gcn2 was examined herein because my aim was to delineate genes that are conserved aging factors. The domain structure of Gcn2 is highly conserved and it functions as both

general and gene-specific translational control in fungi, insects and mammals (Hinnebusch 2005). Altogether, I demonstrated a novel longevity-regulating function of Gcn2.

6.5 Conclusion

My findings demonstrate that cryptotanshinone-induced lifespan extension is dependent on the nutrient composition of media, especially EAA concentration. Restriction of total amino acids or EAA, and deletion of *TOR1*, *SCH9* or *GCN2* prevent longevity extension by cryptotanshinone. An increased lifespan of *sod2*Δ by cryptotanshinone and intracellular ROS level analysis suggests that the compound might mediate ROS stress resistance. Altogether, I propose that cryptotanshinone targets partly Tor1, Sch9, Gcn2 and Sod2, evolutionarily conserved longevity kinases mediated by nutrients from yeast to human, to greatly prolong lifespan of yeast at nanomolar concentrations. The highly conserved mechanism merits future investigation of longevity activity of cryptotanshinone in higher organisms and its molecular mechanisms. The structure and activity dependency of the tanshinones is noteworthy and warrants more investigation in order to establish a correlation and discovery of even more potent anti-aging compounds.

Chapter 7

HORMESIS OF GLYCEOLLIN I, AN INDUCED PHYTOALEXIN FROM SOYBEAN, ON BUDDING YEAST CHRONOLOGICAL LIFESPAN EXTENSION

7.1 Introduction

Hormesis is an adaptive response of cells and organisms to a moderate stress. It describes the dose-response relationships of stressors (e.g., chemical, thermal, or radiological) that are noxious at higher levels but can exert a beneficial effect on cells at low doses by inducing a response that results in stress resistance (Mattson 2008; Marques *et al.* 2010). Rapamycin and resveratrol are also antifungal natural products and can induce defense responses at low doses in fungi, nematodes, flies, fish, and mice (Howitz & Sinclair 2008). CR is probably one of the most well recognized hormetic phenomenon capable of increasing mammalian lifespan. These stressors, in large part via activation of conserved stress-response signal transduction pathways, decrease risks of common age-related conditions, such as cancer, cardiovascular diseases, type 2 diabetes, and neurological diseases, hence lengthening the lifespan (Gems & Partridge 2008).

Previous work has shown that food grade microbial-stressed (*R. oligosporus*) germination of living soybeans leads to generation of a group of oxooctadecadienoic acids and their glyceryl esters in addition to glyceollins, a known phytoalexins present in wild and stressed soybeans. In addition, the nutritional values of the soybean foods

made from the bean seeds may be particularly beneficial with higher content of total isoflavones (Feng *et al.* 2008). Interestingly, after screening a number of natural products, I found that an induced phytoalexin, glyceollin I, could similarly function as hormesis in yeast and extend their lifespan through CR-dependent regime at low doses.

7.2 Experimental Procedures

7.2.1 Materials

Food grade fungus, *Rhizopus oligosporus*, was bought from PT. Aneka Fermentasi Industri (Bandung, Indonesia), and black soybean (Glycine max (L.) Merr., China) was bought from a supermarket in Singapore. Other materials were as described in **Chapter 3** (**3.2.1**).

7.2.2 Isolation of glyceollins

The soybean seeds (2.0 kg) were germinated with *R. oligosporus* stress at 25 °C in the dark for 3 days. The resulting germinated beans were homogenized in methanol, and then extracted three times on a shaking incubator at 200 rpm and room temperature for 6 h each time. The extraction solutions were concentrated in a rotary evaporator at 50 °C. The concentrated residue was transferred to a silica gel column (35 × 6 cm, silica gel 60 (0.040-0.063 mm)) pre-equilibrated with hexane. Successive elution with hexane and hexane/ ethyl acetate (7:3) mixture at a flow rate of 5 mL/min gave many fractions (each fraction volume was 100 mL). After HPLC analysis, the fractions containing the glyceollins were combined and the three isomers: glyceollin I, II, III (**Figure 7.1A**) were obtained and their identity confirmed by UV/Vis spectrum (**Figure 7.1B**), ESI-MS and ^{1}H NMR spectroscopy. HPLC analysis was carried out on

a Waters HPLC system (Milford, MA) with an Alliance 2659 separation module and a 2996 photodiode array (PDA) detector with detection wavelength set at 285 nm. The separation was accomplished on a Waters C18 column (5 μm, 4.6 × 250 mm, Atlantis T3, Ireland) with water (A), acetonitrile (B) and 2% acetic acid in water (C) as mobile phase. The column temperature was 30 °C. The injection volume was 20 μL. Solvent C composition was maintained at an isocratic 5% for 40 min. Solvent A and B gradient was as follows: 0 – 1 min, A 95%; 1 – 5 min, A from 95% to 50%; 8 – 36 min, A from 50% to 50%; 36 – 39 min, A from 50% to 90%; 39 – 40 min, A from 90% to 95%. The flow rate was 1.0 mL/min. MS spectra were acquired using a Finnigan/MAT LCQ ion trap mass spectrometer (San Jose, CA, USA) equipped with an electrospray ionization (ESI) source. The capillary temperature and spray voltage were maintained at 250 °C and 4.5 kV, respectively. ^{1}H NMR spectra were recorded in $CDCl_3$ with a Bruker AC300 spectrometer (Karlsruhe, Germany) operating at 300 MHz.

7.2.3 Lifespan and yeast cell growth assay

The lifespan, biomass and yeast cell growth assays have been described in **Chapter 3** (**3.2.3**).

7.2.4 Data analysis

The data analysis on lifespan has been described in **Chapter 3** (**3.2.4**).

7.3 Results and Discussion

7.3.1 Antiproliferation activity of glyceollins

The glyceollin I, II, and III were isolated by Silica gel column chromatography (**Figure 7.1**) and the structures were confirmed by ^{1}H NMR, UV–Vis, and MS spectra. Glyceollins, one type of induced phytoalexins from soybean, were released in much higher concentrations during plants in response to a number of stress factors such as wounding, freezing, ultraviolet light exposure, chemical and exposure to microorganisms. Several studies had shown that their biological activities included antiproliferation/antitumor, antiestrogenic, antibacterial, and antifungal activities (Ng *et al.* 2011).

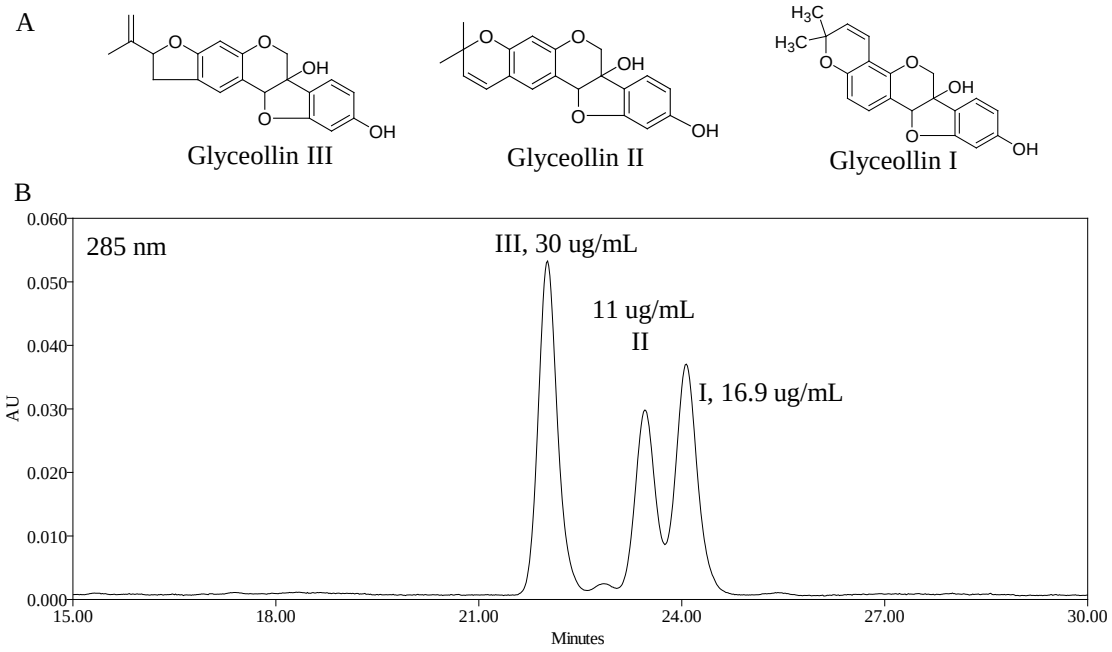

Figure 7.1 Structure (A), and HPLC chromatogram at 285 nm (B) of glyceollin isomers I, II, and III obtained from black soybean sprouts with food grade fungus *R. oligosporus* stress

To test the antiproliferation activity of glyceollins on budding yeast, approximately 2×10^{4} 2-day YPD cultured yeast cells in each well of a 96-well plate were treated with different concentrations of glyceollins, which were compared with methanol-treated controls (defined as 100% viability). The results showed that all three glyceollin isomers could inhibit yeast proliferation (**Figure 7.2**), and 50% growth inhibition (GI_{50}) of glyceollin I, II and III were 85, 139 and 150 μM

respectively. These GI_{50} values were consistent with previous reports that glyceollin I at 10 µM can reduce cell viability by 86% on MCF-7 breast cancer cells and by 90.32% on BG-1 ovarian cancer cells based on an assay of 1000 cells per well (Zimmermann *et al.* 2010).

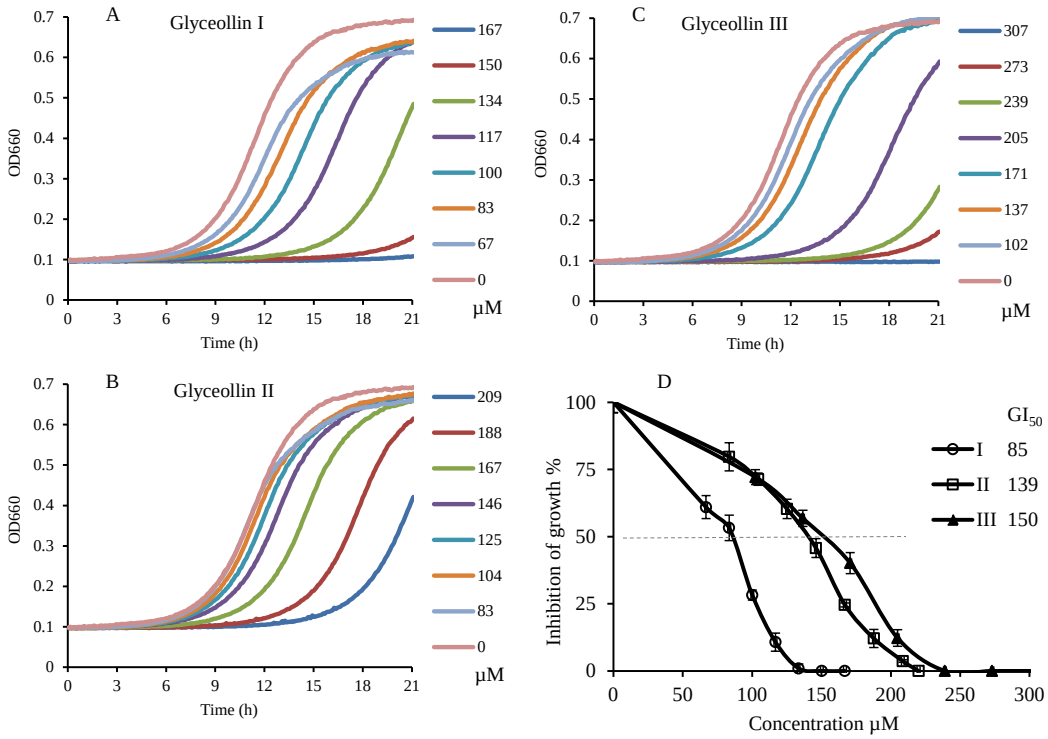

Figure 7.2 Influence of glyceollin I, II, and III on proliferation of yeast
These compounds were dissolved in methanol and added into YPD medium (5 µL compound: 100 µL medium) inoculated at 30˚C for 21 h. Growth curves of *S. cerevisiae* BY4742 at different concentrations of glyceollin I (A), II (B) and III (C) were monitored with a microplate reader by recording the optical density every 5 min at 660 nm. Relative inhibition of growth of yeast at different concentrations of glyceollins was calculated and the GI_{50} was the concentration that glyceollins inhibited 50% yeast cell growth. Error bars represent SEM within four replicates.

Glyceollin I (⁻) has GI_{50} in the low to mid µM range for human breast, ovarian, and prostate cancer cell lines (< 5000 cells/well) (Khupse *et al.* 2011). In this assay, glyceollin I was more effective to reduce yeast viability than its isomers II and III. This result also agrees with a previous finding that glyceollin isomer I had stronger bioactivity than isomers II and III on cancer cell line models (Payton-Stewart *et al.* 2010; Zimmermann *et al.* 2010). According to a recent study, mechanism of the

inhibitory effects of glyceollins on platelet-derived growth factor (PDGF)-induced abnormal proliferation might be due to the influence on signal transduction events in the G_0/G_1-S interphase arrest. Glyceollins significantly reduce DNA synthesis in a dose-dependent manner without cytotoxicity and change the expression of cell cycle-regulatory proteins such as phosphorylated retinoblastoma protein (pRB), cyclin-dependent kinase (CDK)2 and cyclin D1, CDK inhibitor proteins $p21^{cip1}$ and $p27^{kip1}$, and tumor suppressors p53 (Payton-Stewart *et al.* 2009; Kim *et al.* 2011). Therefore, it is possible that the antiproliferation assay on budding yeast could be used as a simple and rapid method for screening candidates with antifungal and anticancer activities, because the basic cellular processes among eukaryotes have a high degree of conservation (Simon & Bedalov 2004).

7.3.2 Glyceollin I extends yeast CLS by CR-dependent regime

To test the antiaging activity of glyceollins, they were dissolved in methanol and added into yeast culture at day 2 of the stationary phase, and the initial age-point (day 2) was defined to be 100% viability. As can be seen in **Figure 7.3**, under normal condition, glyceollin I in the range of 5 nM to 1.25 μM can extend lifespan ($P < 0.05$). The optimum concentration is at 12.5 nM with the maximum lifespan extension by 40% relative to the control. However, I found that glyceollin I could not extend CLS even at the optimal concentration (12.5 nM) under CR conditions that could significantly extend yeast CLS. This suggests that glyceollin I mediates CLS extension and does not prevent lifespan extension through CR.

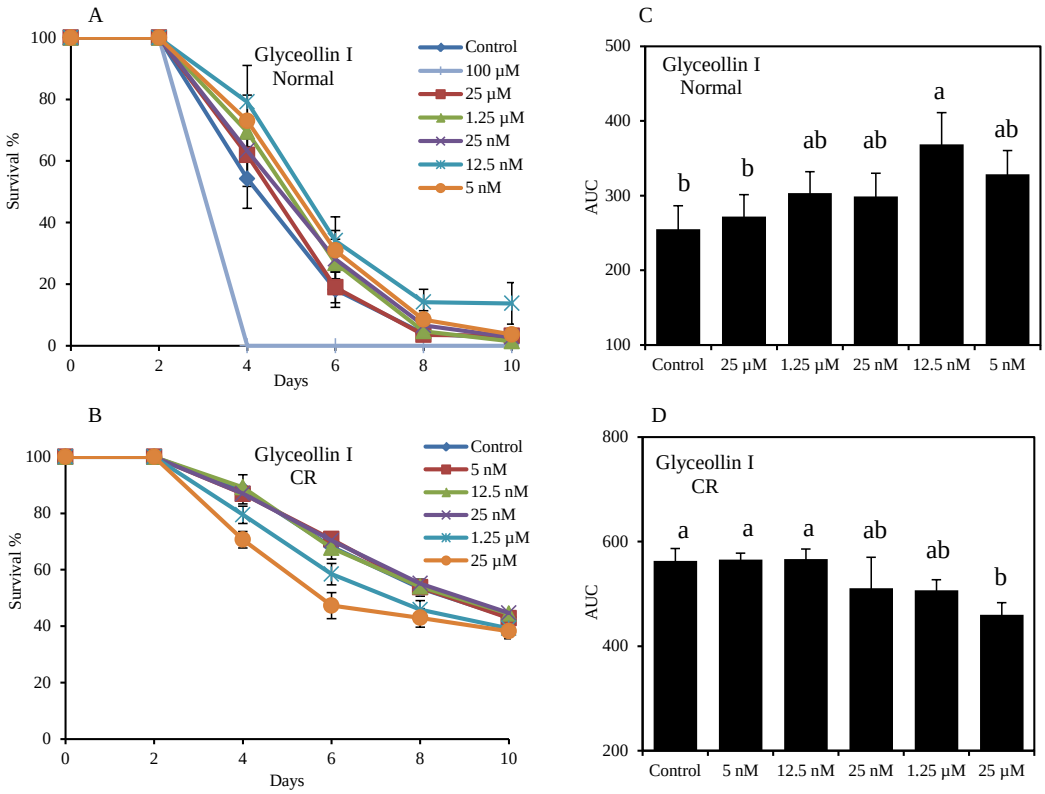

Figure 7.3 Glyceollin I as a CRM extends the budding yeast CLS
Glyceollin I was dissolved in methanol at different concentrations and added into the medium (5 μL compound: 1 mL medium) at day 2. (A) Survival curves of WT BY4742 cultured in SD2D (SD medium containing 2% dextrose, normal condition) for 10 days, the control was added methanol without compound. (B) Survival curves of yeast in SD0.5D medium (0.5% dextrose, CR condition). Error bars represent SEM within 8 replicates. (C) AUC of different treatments under control and (D) CR condition; AUC represents the survival integral, the variance of AUC (mean + SEM, n = 8) between treatments was compared using the Duncan's multiple range test at $P < 0.05$, different letters (a–b) show significant differences.

Despite the fact that many natural small molecules such as caffeine, rapamycin, methionine sulfoximine, spermidine and lithocholic acid have been reported to extend yeast CLS, up to now, most of these compounds are not confirmed as candidate CRM (Powers *et al.* 2006; Eisenberg *et al.* 2009). A desired feature of a CRM should mimic the metabolic, hormonal, and physiological effects of CR under the normal calorie intake. CRM should activate stress response pathways observed under CR, provide protection against a variety of stressors, and produce CR-like effects on longevity with reduction of age-related diseases (Ingram *et al.* 2006). In comparison, glyceollin II and III had no effects on CLS (**Figure 7.4**) over a wide range of concentrations (5 nM to 150 μM). Glyceollin II reduced CLS at high doses. It is remarkable that the

subtle structural variations of glyceollin I and II can result in such a dramatic difference in bioactivity. This indicates that structurally specific binding of the glyceollin I to yeast target is the critical event to exert bioactivity.

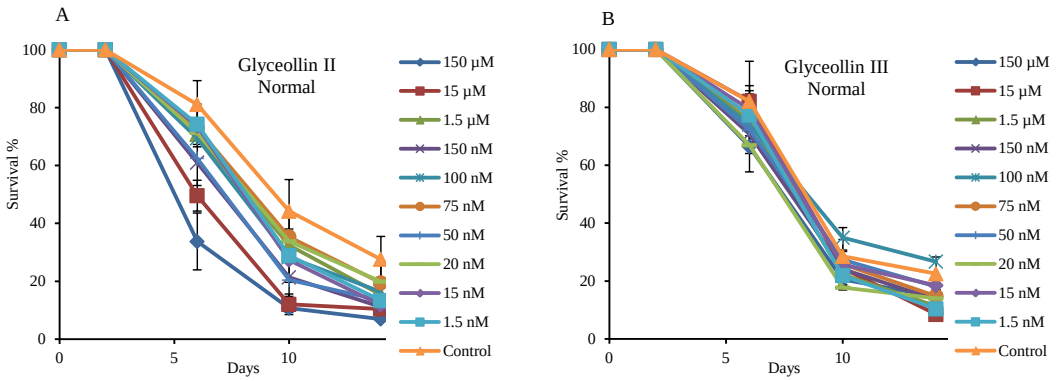

Figure 7.4 Glyceollin II (A) and III (B) do not extend yeast CLS
These compounds were dissolved in methanol at different concentrations and added into the medium (5 µL compound: 1 mL medium) at day 2. The control was methanol without compounds. Error bars represent SEM within 8 replicates.

7.3.3 Hormetic effect of glyceollin I on yeast lifespan

I measured the CLS extension activity of glyceollin I at a wide range of concentrations and found a dose-response curve of glyceollin I on CLS with a hormetic effect (**Figure 7.5**). At low doses (10 to 100 nM), glyceollin I resulted in yeast CLS extension. From 100 nM to 1.0 µM, there were negligible effects of glyceollin I on yeast CLS. Doses higher than 1.0 µM led to reduced CLS and toxicity (100 µM). Hormesis indicates that low concentrations of a toxin might have long-term beneficial consequences as a way of conditioning the organism toward enhanced stress responses. In this case, glyceollin I had the maximum CLS extension of only 40% relative to the control (**Figure 7.5**) In fact, because the positive effects of a toxin occur at low doses, it has been reported that the benefits are typically only 30%–60% greater than controls (Calabrese & Baldwin 2003). Glyceollins are induced phytoalexins from soybean in response to stress factors. Therefore, I propose that

glyceollin I would serve as stress-response hormesis to yeast and trigger specific physiological response of the fungus to extend their lifespan by a CRM regime. The validity of my hypothesis if proven may have a significant impact on aging-related research, and provide critical evidence on stress-response hormesis, CRM as well as other aging related theories.

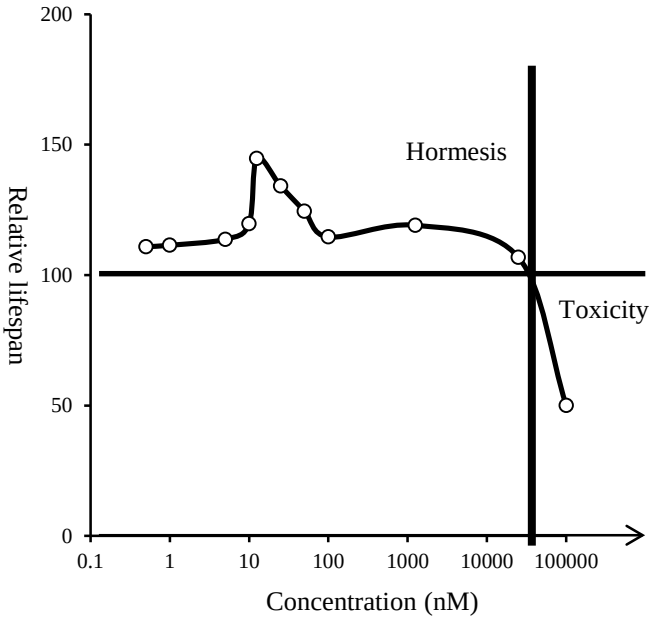

Figure 7.5 Dose-response curve of glyceollin I on yeast CLS with a hormetic effect
The testing concentrations were 0.5, 1, 5, 10, 12.5, 25, 50, 100, 1250, 25,000, 100,000 nM, respectively. Low doses resulted in lifespan extension, whereas higher doses resulted in lifespan reduction. The control with 100% lifespan was defined as adding methanol without glyceollin I, and the relative lifespan was based on AUC comparison of different doses relative to the control.

7.4 Conclusion

I presented the antiproliferation and antiaging activities of induced phytoalexin glyceollin I, II and III from soybean on the budding yeast model. The three glyceollin isomers showed strong antiproliferation activity at μM levels and glyceollin I had lower GI_{50} than the other isomers. Interestingly, it was found that glyceollin I could extend yeast lifespan at nM levels. Furthermore, the longevity effect was a CR-dependent regime. However, glyceollin II and III did not have hormetic effects on

yeast lifespan. Glyceollin I has been reported to have more potent activity on wider range of bioactivities including anti-bacterial, anti-nematode, anti-fungal, anti-estrogenic and anti-cancer, antioxidant, anti-inflammatory, insulin sensitivity enhancing, and attenuation of vascular contractions (Ng *et al.* 2011). This discovery adds glyceollin I on to the list as a unique candidate of CRM. The biological mechanism of glyceollin I bioactivity awaits to be elucidated so that I can rationally alter the structures of glyceollins to improve the CRM effects.

Chapter 8

CONCLUSIONS AND FUTURE OUTLOOK

In the Part I, I have successfully developed a high throughput screening assay for determination of yeast lifespan based on the chronological aging model and applied in evaluating several factors that mediate lifespan, including inoculum size, cellular state in nutrient-rich medium, and calorie level. Using this assay, I confirmed the previously reported genetic mimics of CR, including deletion of *TOR1*, *SCH9* or *RAS2*. In contrast, deletion of *SIR2* had longevity effect but seems produced only small beneficial effect on the response to CR. Overall, this new high throughput screening assay may facilitate identification of CRMs with a rapid and simple protocol, uncomplicated data analysis, and high sensitivity. In addition, the assay also provides quantifiable data including lag-time, growth rate, doubling time, and survival percentage (**Chapter 3**).

Furthermore, present results indicate that lifespan extension by a typical dietary restriction regime was dependent on the nutrients in media and that nutrient composition was a key determinant for yeast longevity. Four different yeast strains were cultured in various media, which showed similar response surface trends in biomass production and viability at day two but greatly different trends in lifespan. The pH of aging media was dependent on glucose concentration and had no apparent correlation with lifespan under conditions where amino acids and YNB were varied widely, and simply buffering the pH of media could extend lifespan significantly. Furthermore, the results showed that strain *sch9*Δ was more sensitive to nutrients than *tor1*Δ, *sir2*Δ and WT strains, suggesting that Sch9 (serine-threonine kinase pathway)

is a major nutrient-sensing factor that regulates cell growth, cell size, metabolism, stress resistance and longevity. Overall, these findings support the notion that nutrient composition might be a more effective way than simple dietary restriction to optimize lifespan and biomass production from yeast to other organisms (**Chapter 4**).

In addition, I showed that amino acid composition greatly altered yeast CLS. NEAA methionine and glutamic acid had the most significant impact on yeast CLS extension, and restriction of methionine and/or increase of glutamic acid caused longevity that was not the cause of low acetic acid production and acidification in aging medium. Remarkably, low methionine, high glutamic acid and glucose restriction extended lifespan additively and independently, and the longevity could not be further extended by buffering the medium (pH 6.0). These preliminary findings demonstrate that glutamic acid addition, methionine and glucose restriction prompt yeast longevity through distinct mechanisms (**Chapter 5**).

On the other hand, I reported a new anti-aging compound, cryptotanshinone. It could greatly extend yeast CLS (up to 2.5 times) in a dose and the-time-of-addition dependent manner at nanomolar concentrations without disruption of cell growth. I demonstrated that cryptotanshinone prolonged CLS via a nutrient-dependent regime, especially essential amino acid sensing, and three conserved protein kinases Tor1, Sch9 and Gcn2 were required for cryptotanshinone induced lifespan extension. In addition, cryptotanshinone significantly increased lifespan of *SOD2* deleted mutants. Altogether, those data suggest that cryptotanshinone might be involved in the regulation of Tor1, Sch9, Gcn2 and Sod2, these highly conserved longevity proteins modulated by nutrients from yeast to humans (**Chapter 6**).

Interestingly, glyceollin I had hormesis extended yeast lifespan at low dose (nM) in a CR-dependent manner, while reduced lifespan and inhibited yeast cell

proliferation at higher doses (μM). In contrast, the other two glyceollin isomers II and III could not extend yeast lifespan and only showed lifespan reduction and antiproliferation at higher doses. The result in anti-aging activity indicates that glyceollin I is a unique candidate of CRM (**Chapter 7**).

Altogether, current data demonstrate that the high throughput assay is a very powerful tool for studying the mechanism of aging and developing anti-aging factors. In the future study, there are several research areas that need further study:

1. As many studies claim that extreme glucose restriction (<0.5% glucose) extend yeast lifespan (Lamming *et al.* 2006; Burtner *et al.* 2009b; Mesquita *et al.* 2010; Lu *et al.* 2011; Longo *et al.* 2012), it is interesting to find out why the low glucose shorten yeast lifespan in this assay. Is the mechanism relevant to starvation since the similar observation exists in higher organism?
2. Sch9 seems to be a key nutrients sensor in the budding yeast, however, it is still unclear that the complex functions or mechanisms of action of Sch9 in regulation of aging (Fabrizio *et al.* 2001; Kaeberlein *et al.* 2005b; Urban *et al.* 2007; Huber *et al.* 2011). Further experiments on quantifying Sch9 activity in different media are warranted to delineate the role of Sch9 plays in chronological aging.
3. Gcn2 plays a key role in controlling amino acid homeostasis and protein synthesis by modulating amino acid biosynthesis in response to different amino acids deprivation (Dever & Hinnebusch 2005; Staschke *et al.* 2010; Murguia & Serrano 2012; Gallinetti *et al.* 2013; Rousakis *et al.* 2013). I report Gcn2 function in yeast chorological aging. Thus, it is important to elucidate mechanisms of regulating network between the highly conserved protein kinase Gcn2 and TOR/Sch9, and also *GCN2* function in regulation of lifespan in fruit fly model or higher organisms.

4. Methionine restriction extends lifespan in mammal, but significantly decreases bodyweight gain (Orentreich *et al.* 1993; Sun *et al.* 2009; Perrone *et al.* 2013). Current data show that glutamic acid extends yeast lifespan independently of methionine, and increases yeast biomass production. Therefore, it is possible to apply the combination of methionine restriction and glutamic acid addition in higher organisms to induce longevity without reduces body size.
5. Cryptotanshinone seems as a novel anti-aging compound, further study on the anti-aging activity of cryptotanshinone in higher organisms is highly interesting and necessary.

Part II

ANTIOXIDANTS FROM GERMINATED LEGUME SEEDS

Chapter 9

INTRODUCTION

9.1 Introduction

9.1.1 Grain legume is important for human diet

Seeds of well-known grain legumes are used for human and animal consumption or for the production of oils for industrial uses. Grain legumes are also known as pulses or food legumes include beans, lentils, lupins, peas, and peanuts. Pulses contain high concentrations of proteins, complex carbohydrates, dietary fibers, essential amino acid, folate and other B-vitamins and contribute greatly to human diet. Pulses are 20 to 25% protein by weight, which is twice as much protein as wheat and three times as much as rice. In total, they provide about 10% of the total dietary protein in the world. In addition, pulses contain several polyphenolic compounds, which are considered to be natural antioxidants, representing an important group of bioactive compounds in foods, and may reduce the risk of cardiovascular disease and cancer (Arts & Hollman 2005).

Recent studies have suggested that legumes especially soybean and peanuts could be good functional foods for health promotion (Francisco & Resurreccion 2008; Boue *et al.* 2009). Furthermore, Germination as an inexpensive and effective technology can significantly enhance bioavailability and digestibility of their nutrients (Ghavidel & Prakash 2007), improve the nutritional quality of legumes by increasing amino acids contents, total dietary fibers, and total soluble sugars, while reducing antinutrients levels such as α-galactosides (Khattak *et al.* 2008; Martín-Cabrejas *et al.* 2008). It is also a convenient process to enhance phenolic antioxidants (Cevallos-

Casals & Cisneros-Zevallos 2009). Germination of legume seed (mainly mung bean and yellow soybean) is widely conducted in many regions and countries in which legume sprouts have great demand for consumers.

9.1.2 Phytochemical profiling is significant for quality and safety control

Recent technological advances in chemistry help to investigate structure-activity relationships and food quality control, rapid and reliable method for the analysis and identification of complex phytochemicals. The instrumentation method include reversed-phase high-performance liquid chromatography (RP-HPLC) with photodiode array (PDA) detection system, mass spectrometer with electrospray ionization (ESI) and tandem mass spectrometry (MS/MS) or time-of-flight mass spectrometry (TOF-MS), and nuclear magnetic resonance (NMR) spectroscopy. These advances have led to phytochemical profiling of common food products.

In the past few years, characterization and quantification of bioactive metabolites by HPLC/PDA/ESI/MS system was used in dry beans (Lin *et al.* 2008b), peanuts (Sales & Resurreccion 2010) and soybeans (Correa *et al.* 2010). Only a few studies have investigated germinated legumes (Paucar-Menacho *et al.* 2010). Microbe-infected germination of soybean has been studied from our laboratory and other groups, which suggested that the production of glyceollin-enriched soy milk, soy yogurt and other traditional soy food were feasible (Feng *et al.* 2008), while a comprehensive phytochemical profile was not investigated. However, no study has been reported on microbe-stressed germination of other food legume, including mung bean and peanuts, two of the most popular traditional foods.

9.1.3 Antioxidant capacity is a popular criterion of functional food

Oxidative stress is an imbalance between oxidants and antioxidants in favor of the oxidants, leading to a disruption of redox signaling and control and/or molecular damage. Disturbances in the normal redox state of tissues can cause toxic effects through the production of free radicals that damage all components of the cell, including proteins, lipids, and DNA. In humans, oxidative stress is believed to be the causative factor of many diseases. Examples include atherosclerosis, Parkinson's disease, heart failure, myocardial infarction, Alzheimer's disease, schizophrenia, bipolar disorder, fragile X syndrome and chronic fatigue syndrome, but short-term oxidative stress may also be important in prevention of aging by induction of a process named mitohormesis (Finkel & Holbrook 2000; Gems & Partridge 2008).

A large number of studies have shown an inverse correlation between the intake of fruits and vegetables and the occurrence of diseases such as inflammation, cardiovascular disease, cancer, and aging-related disorders. Phytochemicals possess those beneficial properties, are referred to as chemopreventers. One of the predominant mechanisms of their protective action is due to their capacity to scavenge free radicals. Among the most investigated chemopreventers are some vitamins, plant polyphenols, and pigments such as carotenoids, chlorophylls, flavonoids, and betalains. Thus, resolution of the potential protective roles of specific antioxidants and other constituents of fruits and vegetables deserves major attention.

Many methods are available for determining food antioxidant capacity, which is an important topic in food and nutrition research. In fact, antioxidant activities in complex systems cannot be evaluated satisfactorily using a single test, and several test procedures may be required. In this project, I planned to measure two antioxidant-related phytochemical compositions (total phenolic content (TPC) and total flavonoids content (TFC)) and other kinds of free radical scavenging capacity

(peroxyl radical, hydroxyl radical, superoxide anion, hypochlorite, peroxynitrite and 2,2-diphenyl-1-picryhydrazyl) in order to provide a comparative information for total antioxidant capacity of my samples, for meaningful comparisons of other foods or commercial products, as well as for provision of quality standards for regulatory issues and health claims (Prior *et al.* 2005).

9.2 Objectives

The **main objective of Part II of this thesis** is to explore the phytochemical changes during germination or fungus-stressed germination of legume seeds. The **specific objectives of Part II study** are to:

- Determine the effect of germination or fungus-stressed germination on the antioxidant capacity, phytochemicals and phytoalexins in different legume seeds (**Chapter 10**).
- Study the isoflavonoids changes during germination in chickpea (**Chapter 11**).
- Investigate the effect of food grade fungus-stressed germination on phytoalexins production and antioxidant capacity in peanut seeds (**Chapter 12**).

In the Part II project, I focus on the development of novel process of legumes and study the bioactive metabolites for their bioactivity. Overall, the prospect of success of this project will lead to the creation of relatively fundamental knowledge on food legumes via two major contributions:

- ✓ Providing a comprehensive data on antioxidant capacity, phytochemicals and phytoalexins changes during germination or fungus-stressed germination in

diverse legume seeds, which could be useful information for developing food products or other applications of the germinated legume seeds.

- ✓ A new discovery that chickpea greatly increases isoflavonoids production and food grade fungus-stress induce stilbenoid phytoalexins in peanut, which could extend the nutritional values of chickpea and peanut seeds in terms of their bioactive constituents.

Although other nutrients or secondary metabolites may be changed during germination, which could contribute to the change in antioxidant capacity of legume seeds, my study concentrates on polyphenolic antioxidants that have been studied to process many health benefits for human.

Chapter 10

POLYPHENOLIC ANTIOXIDANTS AND PHYTOALEXINS CHANGES IN GERMINATING LEGUME SEEDS WITH FOOD GRADE FUNGAL *RHIZOPUS OLIGOPORUS* STRESS

10.1 Introduction

Plants possess both constitutive and inducible mechanisms to resist stress from wounds, freeze, ultraviolet light, and microorganisms (e.g. oomycetes, fungi, bacteria, viruses). In the past few years, a large number of reports have been published on identification of phytoalexins, and the effects of stress on gene expressions, transcription factors, signaling pathways, metabolic pathways against both compatible and incompatible plant-pathogen (van Loon *et al.* 2006). Nevertheless, there is a paucity of literatures on the changes of such treatments in nutritional values, antioxidant capacity as well as phenolic composition. Phytoalexin concentration can be produced at much higher level when plants responses to the stress (López-Amorós *et al.* 2006). Their functions in plant mainly include antimicrobe and antioxidant activities which are some of the beneficial activities to human health and disease prevention (Hammerschmidt 1999; Boue *et al.* 2009). Resveratrol is a well-studied polyphenolic phytoalexin and has received tremendous attention because of its broad range of health benefits in a variety of human disease models (Pervaiz & Holme 2009). Logically, it is an emerging field of functional food research by introducing phytoalexins through bioprocesses (Boue *et al.* 2009).

Probiotics are food grade microorganisms, some of them used in starters such as *Rhizopus oligosporus* for tempeh fermentation and *Bacillus subtilis* in natto fermentation. They are attractive stresser to induce phytoalexins from legume seeds. A previous work has shown that food grade microbial-stressed germination of living soybeans leads to generation of a group of oxooctadecadienoic acids and their glyceryl esters in addition to glyceollins, a known phytoalexins present in wild and stressed soybeans (Feng *et al.* 2007). Furthermore the nutritional values of the soybean foods made from the bean seeds may be particularly beneficial with higher content of total isoflavones (Feng *et al.* 2008). To expand the research into other legumes seeds, the present study investigated 13 well known and used legume seeds. The aim to evaluate the influence of germination and *R. oligosporus* stressed germination process on phytochemicals, phytoalexins, and antioxidant capacity changes. This study will also provide comparative information for further identification of phytoalexins in legumes.

10.2 Materials and Methods

10.2.1 Materials

Food grade fungus, *Rhizopus oligosporous*, was bought from PT. Aneka Fermentasi Industri (Bandung, Indonesia). Sword bean (*Canavalia gladiata* (Jacq.) DC., Indonesia), kidney bean (*Phaseolus vulgaris* L., China), Black-eyed pea (*Vigna unguiculata* subsp. *unguiculata*, Myanmar), yardlong bean/cowpea (*Vigna unguiculata* subsp. *sesquipedalis*, China), azuki bean (*Vigna angularis* (Willd.) Ohwi & H. Ohashi, China), hyacinth bean (*Lablab purpureus* (L.) Sweet, India), mung bean (*Vigna radiata* (L.) R. Wilczek, Thailand), broad bean (*Vicia faba* L., China), yellow soybean (*Glycine max* (L.) Merr., Canada), black soybean (*Glycine max* (L.) Merr.,

China), big peanut (*Arachis hypogaea* L., China), small peanut (*Arachis hypogaea* L., India) and chickpea (*Cicer arietinum* L., Turkey) from supermarket in and the origins of production were obtained from Singapore Trade Statistics. Other materials were the same as **Chapter 3** (**3.2.1**).

10.2.2 Germination and fungal inoculations

Legume seeds were allowed to imbibe distilled water for 24 h at room temperature. The skins of the legume seeds were peeled off afterwards without destroying radicals. The legumes seeds were divided equally into five kinds, namely non-germinated (UG), germinated with/without stress (GS/G), and deactivated seed with/without fungal stress (DS/D). The seeds prepared for germination were put into petri dishes. The petri dishes were covered with filter papers that were sprayed with distilled water or the fungal suspension. Those dishes were placed at room temperature under dark condition and germinated for four days. The deactivated seeds were prepared by putting them into oven at 150°C for twenty minutes and then germinated in the petri dishes for four days. Approximately two to four seeds of each legume sample were collected and accurately weighed in a 15 mL screw-cap tube, then extracted with 5 mL acetone/ethanol/water (2: 2: 1; v/v) mixture containing 0.1% acetic acid on a shaking incubator at 200 rpm and room temperature for 12 h. The supernatant was collected and stored at –20°C for analysis.

10.2.3 Quantification of antioxidant capacity and total phenolics

Three antioxidant capacity related values including total phenolics content (TPC), total flavonoid content (TFC) and oxygen radical absorbance capacity (ORAC) values were measured. TPC was measured based on Folin-Ciocalteau method according to

Wu et al (Wu *et al.* 2004). Gallic acid (50, 25, 12.5, 6.25, 3.12, 1.56 mg/L, correlation coefficient, r = 0.999) was used to establish the standard curve. These results were expressed as gallic acid equivalents (mg GAE/100 g fresh weight sample). TFC was determined using a colorimetric method described previously (Heimler *et al.* 2005). The results were calculated and expressed as catechin equivalents (mg CAE/100 g fresh weight sample). Hydrophilic ORAC procedure based on previous report (Huang *et al.* 2002). The results were expressed as Trolox equivalents (μmol TE/100 g fresh weight sample).

10.2.4 Phytochemicals and phytoalexins identification

HPLC analysis was carried out on a Waters HPLC system (Milford, MA) with a Alliance 2659 separation module, a 2996 photodiode array detector (PDA), and a Waters C18 column (5 μm, 4.6×250 mm, Atlantis, Ireland). The detection wavelength was set from 210 to 800 nm. The separation was accomplished with water (A), acetonitrile (B) and 2% acetic acid in water (C) as mobile phase. The column temperature was 30°C. The injection volume was 20 μL. Solvent C composition was maintained at an isocratic 5% for 60 min. Solvent A and B gradient was as follows: 0 – 1 min, A 95%; 1 – 8 min, A from 95% to 85%; 8 – 24 min, A from 85% to 70%; 24 – 34 min, A from 70% to 40%; 34– 50 min, A from 40% to 20%; 50 – 55 min, A from 20 % to 5%; 55 – 58 min, A from 5% to 95 %; 58 – 60 min, A 95%. The flow rate was 1.0 mL/min. The gradient was identical to those used for HPLC analysis above. The injection volume of each sample was 20 μL.

10.2.5 Data analysis

The data analysis on lifespan has been described in **Chapter 3** (**3.2.4**).

10.3 Results and Discussion

10.3.1 Comprehensive evaluation of antioxidant contents of fungal-stressed sprouts

TPC of ungermination (UG, 0 day), germination (G, 1-4 day) and germination with fungal stress (GS, 1-4 day) of 13 selected legume seeds are presented in **Table 10.1**. Germination improves TPC in most cases except yellow soybean that has less changes during 4-day germination, and this result is similar with the investigations on phenolic contents of germinated edible seeds (Cevallos-Casals & Cisneros-Zevallos 2009) and 9 selected legumes (Lin & Lai 2006). Meanwhile, legume seeds with food grade fungi *R. oligosporous* stress have much higher ($P < 0.01$) TPC than that of without fungal-stressed germination. Overall, these data suggest that fungal-stressed germination could greatly increase the TPC in legume seeds.

TFC ranges from the minimum 3.19 (chickpea) to the maximum 19.68 (yardlong bean) mg CAE/100g FW in UG seeds (**Table 10.1)**. Germination significantly improves TFC in broad bean by 9.69 times, 2.57 times for yellow soybean and 2.42 times for chickpea. In sharp contrast, TFC reduce in germinated yardlong, azuki, hyacinth and mung beans. Majority of germinated legume seeds with fungal-stress have higher ($P < 0.05$) TFC than that of without fungal-stress.

Table 10.1 Comparative evaluation of total phenolic content (TPC), total flavonoid content (TFC) and oxygen radical absorbing capacity (ORAC) of 13 legume seeds

	TPC			TFC			ORAC		
	UG	G	GS	UG	G	GS	UG	G	GS
Sword bean	42.0g	42.3	63.3	10.11d	10.82	12.99	614g	1298	1903
Kidney bean	33.2h	48.5	77.6	6.20g	8.89	12.07	888e	1855	2145
Black-eyed pea	28.1i	59.6	68.2	9.17e	10.70	12.63	753f	1708	2195
Yardlong bean	54.8f	60.0	67.3	19.68a	12.38	12.88	1139d	1863	2601
Azuki bean	43.1g	54.2	57.2	11.68b	10.33	9.56	858e	1495	1682
Hyacinth bean	15.0j	34.2	45.0	4.26h	3.61	5.63	682g	1186	2021
Mung bean	42.0g	70.6	85.7	8.78e	7.70	9.79	456h	1759	2705
Broad bean	60.6e	129.6	147.0	7.80f	56.73	59.13	679g	2816	2679
Yellow soybean	107.2b	106.5	110.0	6.10g	12.95	13.85	2805a	4003	5038
Black soybean	69.2d	76.9	86.4	4.78h	7.65	14.48	1667c	2434	3632
Big peanut	97.8c	125.4	151.6	8.15f	9.21	9.77	762f	2428	3157
Small peanut	116.5a	153.9	152.4	10.80c	13.19	30.92	1768b	2249	3484
Chickpea	54.6f	91.7	98.6	3.19i	6.03	6.54	874e	1997	2352
Minimum	15.0	34.2	45.0	3.19	3.61	5.63	456	1186	1682
Maximum	116.5	153.9	152.4	19.68	56.73	59.13	2805	4003	5038
Mean	58.8C	81.0B	93.1A	8.52C	13.09B	16.17A	1073C	2084B	2738A

TPC expressed as mg GAE/100g FW; data present as mean, n = 4, RSD < 5%. TPC of 13 legume seeds are determined at three different treatments: UG = ungermination at 0 day, G = germination for 1 to 4 day without fungal stress, GS = germination with stress of food grade fungus *R. oligosporous* for 1 to 4 day. Means of UG (lowercase letters in the UG column) or among UG, G and GS (uppercase letters in the last row) were compared with Duncan's multiple range test ($P < 0.05$), different letters showed significant differences. TFC expressed as mg CAE/100g FW; data present as mean, n = 4, RSD < 7%. ORAC value expressed as µmol TE/100 g FW, data present as mean, n = 4, RSD < 8%.

ORAC is a method of measuring antioxidant capacities in biological samples *in vitro*. A wide variety of foods has been tested using this assay. Different legume seeds have very large differences ($P < 0.05$) of ORAC values ranging from 456 (mung bean) to 2805 (yellow soybean) (**Table 10.1)**. Germination significantly increases ORAC in all legumes. Fungal stress results in higher ORAC value than that of without fungal-stressed germination. The sprouts from mung bean and yellow soybean are the most popular traditional food. ORAC of mung bean and yellow soybean sprout from supermarket in Singapore are 1606 and 3126 µmol TE/100g FW respectively (Isabelle, et al. 2010), while soybean sprout is 962 µmol TE/100g FW from USDA Database for the ORAC of Selected Foods (Release 2, 2010). In this study, the ORAC of mung

bean sprouts are 1759 μmol TE/100g FW, and yellow soybean sprouts are 4003 μmol TE/100g FW.

In order to rank antioxidant capacity of 13 GS samples based on TPC, TFC and ORAC, the three criteria are given same priority and ranking of antioxidant capacity based on means of membership function values f(x) of TPC, TFC and ORAC, and the order from largest to smallest is listed in **Table 10.2**. Interestingly, broad bean has the highest antioxidant capacity. This might be germination of broad bean significantly increase the production of catechin derivatives, since USDA Flavonoid Database (2003) shows the concentration of (-)-epicatechin, (-)-epigallocatechin and (+)-catechin in immature raw broad bean seeds are 22.51, 14.03, 12.83 mg/100 g FW respectively. From **Table 10.1**, the change of broad bean on TFC is much higher than TPC and ORAC. Additionally, present results indicate that the antioxidant capacity of soybean, peanut and mung bean are ranked top.

Table 10.2 Ranking of antioxidant capacity based on three criteria of TPC, TFC and ORAC under GS

Samples	Mean [a]			membership function value f(x) [b]				
	TPC	TFC	ORAC	TPC	TFC	ORAC	Mean	Ranking
Sword bean	63.3	12.99	1903	0.17	0.14	0.07	0.12	11
Kidney bean	77.6	12.07	2145	0.30	0.12	0.14	0.19	9
Black-eyed pea	68.2	12.63	2195	0.22	0.13	0.15	0.17	10
Yardlong bean	67.3	12.88	2601	0.21	0.14	0.27	0.21	8
Azuki bean	57.2	9.56	1682	0.11	0.07	0.00	0.06	12
Hyacinth bean	45.0	5.63	2021	0.00	0.00	0.10	0.03	13
Mung bean	85.7	9.79	2705	0.38	0.08	0.30	0.25	6
Broad bean	147.0	59.13	2679	0.95	1.00	0.30	0.75	1
Yellow soybean	110.0	13.85	5038	0.61	0.15	1.00	0.59	3
Black soybean	86.4	14.48	3632	0.39	0.17	0.58	0.38	5
Big peanut	151.6	9.77	3157	0.99	0.08	0.44	0.50	4
Small peanut	152.4	30.92	3484	1.00	0.47	0.54	0.67	2
Chickpea	98.6	6.54	2352	0.50	0.02	0.20	0.24	7

[a] TPC (mg GAE/100g FW), TFC (mg CAE/100g FW) and ORAC (μmol TE/100g FW) values are expressed as mean of GS in four days. [b] $f(x) = (x - x_{min})/(x_{max} - x_{min})$, x is the mean of TPC, TFC and

ORAC respectively, ranking based on means of f(x) values in TPC, TFC and ORAC, the number of ranking is smaller indicates the antioxidant capacity of sample is stronger.

10.3.2 Phytochemical and phytoalexin changes in germinating legume seeds

To determine phytochemicals changes in different legume samples, HPLC analysis was carried out. HPLC chromatograms of the 13 legumes under different conditions were then collected and analyzed. The numbers of peaks at three wavelengths 260, 300 and 340 nm were counted respectively. The AU of peaks that were counted is above 0.002 AU. After the data of the numbers of peaks were collected, the thirteen legume seeds were then divided into four different classes (**Table 10.3**).

Table 10.3 Comparison of the number of peaks in HPLC chromatograms for the thirteen legume seeds under non-germination (UG), germination (G) and germination and fungal stress (GS)

Categories	Legumes	Number of Peaks								
		260 nm			300 nm			340 nm		
		UG	G	GS	UG	G	GS	UG	G	GS
Rich phytoalexins & enhanced phytochemicals	Small peanut	30	52	83	28	58	69	19	49	55
	Big peanut	32	69	75	26	64	75	14	54	65
	Sword bean	43	55	65	39	55	72	27	42	52
	Black soybean	35	70	75	30	59	71	16	36	51
	Azuki bean	18	32	37	13	18	36	1	15	33
	Broad bean	38	52	59	18	43	58	9	30	45
Low phytoalexins & enhanced phytochemicals	Kidney bean	23	73	75	21	73	77	14	53	55
	Black-eyed bean	17	58	63	20	60	62	12	35	40
	Hyacinth bean	17	50	55	13	37	39	5	22	25
	Chickpea	18	64	67	9	55	60	3	35	40
Less phytochemicals under GS	Mung bean	9	50	46	5	36	30	3	15	12
	Yardlong bean	26	50	26	37	46	19	20	30	11
Less phytochemicals under G	Yellow soybean	49	48	60	47	42	47	34	26	32

The difference in the numbers of peaks between the chromatograms under UG and those under G indicates the change in the phytochemical contents in the legumes

during germination. Whereas, the difference in the numbers of peaks between G and GS shows the increase or decrease in the phytoalexins that are released after fungal stress germination. The legume seeds were divided into the four classes so that it will be very helpful in determining which legume seeds will produce more or less phytochemicals when they are germinated and which will synthesize more phytoalexins when they are germinated under fungal stress.

Rich phytoalexins and enhanced phytochemicals are the legume seeds that show high difference in the numbers of peaks between the chromatograms under UG and G, as well as between the chromatograms under G and GS. High difference means that the difference in the numbers of peaks between UG and G or G and GS are greater than 10 in average of the three wavelengths. For example, peanut is one of the most widely used legumes because of their high nutritional value and good taste. After GS, there are 69 compounds observed at 300 nm, more than 11 of which may be phytoalexins. As can be seen from **Figure 10.1,** there are more peaks that observed from HPLC chromatogram under GS compared to that of G. This shows that fungal stress can induce the production of phytoalexins in peanuts during germination. From the LC-MS spectral data, 45 compounds were identified in the peanut sprouts (see **Chapter 12**). Small peanut sprouts produced the highest amount of phytoalexins after GS with 55 compounds detected. Forty five of these compounds were stilbenoid phytoalexins, 3 flavonoids, 4 oxooctadecadienic acids, 1 pterocarpanoid phytoalexin – aracarpene and 2 unknown compouds (see **Chapter 12**).

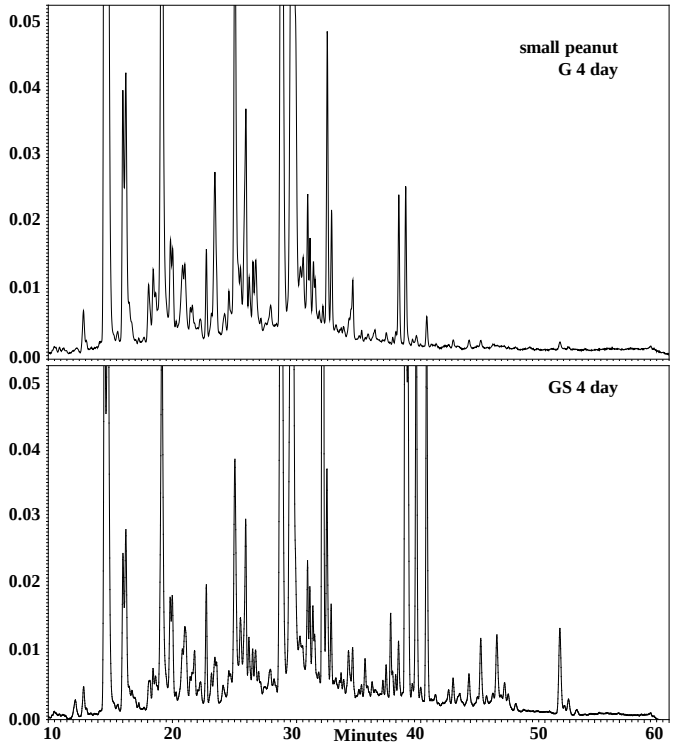

Figure 10.1 HPLC chromatogram (300 nm) of small peanut after 3 days germination without R. oligosporous stress (G3d) and 3 days with the fungal stress (GS3d)

Low phytoalexins but enhanced phytochemicals are the legume seeds that show low difference in the numbers of peaks between G and GS, but high difference in the numbers of peaks between UG and G. Low difference means that the difference between the numbers of peaks concerned are below 10 in average. From **Table 10.3** and **Figure 10.2,** after germination, the phytochemicals in kidney beans increase quite significantly by 50 at 260 nm, by 52 at 300 nm and by 39 at 340 nm. The large difference in the numbers of peaks between UG and G indicates that kidney beans synthesize many new compounds during germination. While slight difference in the numbers of peaks between chromatograms under G and GS indicates that germinating kidney beans with *R. oligoporus* stress may not be an effective way to induce phytoalexins.

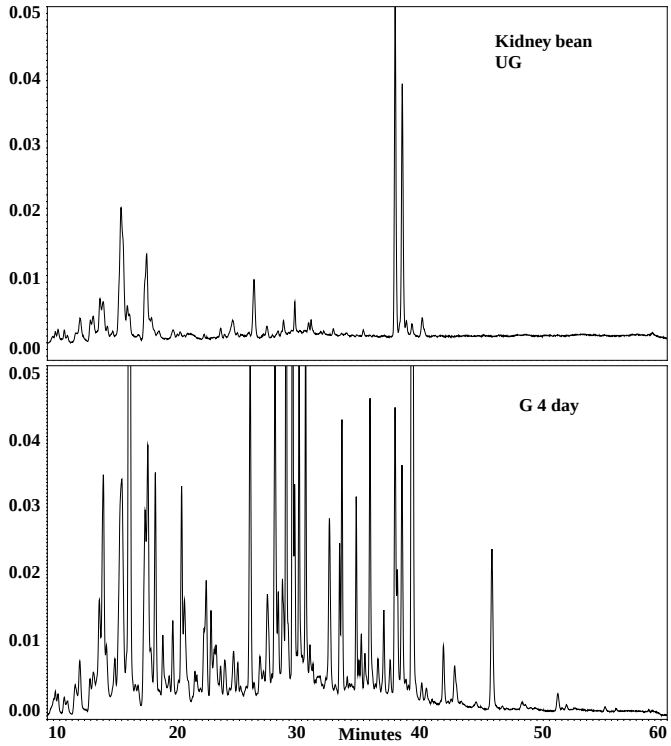

Figure 10.2 HPLC chromatogram (300 nm) of kidney bean (UG) after 4 days germination without R. oligosporous stress (G 4 day)

Less phytochemicals under GS means that the legume seeds show lesser peaks in GS chromatograms when they are compared with G chromatograms. For example, yardlong bean has been reported that contains many anthocyanin derivatives (Ha *et al.* 2010). The phytochemicals in yardlong bean decrease significantly by 24 at 260 nm, by 27 at 300 nm and by 19 at 340 nm (**Figure 10.3**). However, mung bean shows less decrease in the numbers of peaks between GS and G compared to yardlong bean.

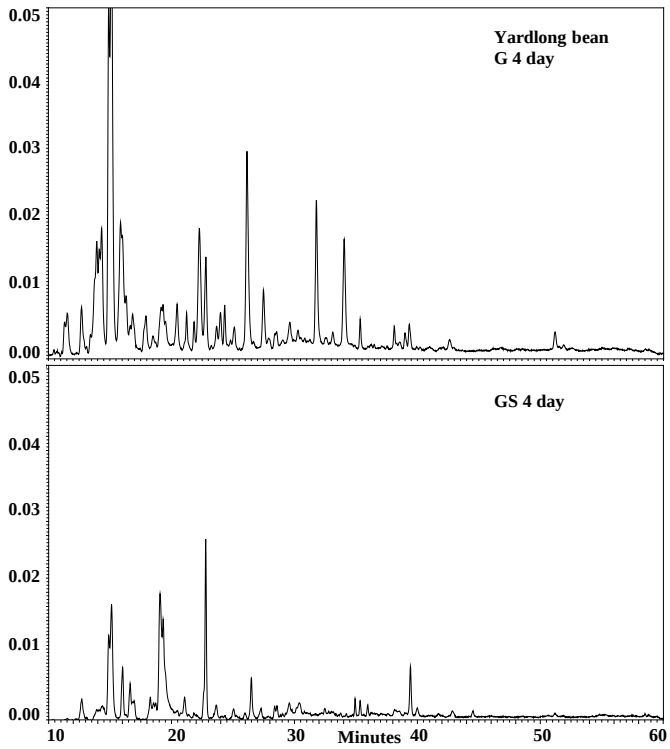

Figure 10.3 HPLC chromatogram (300 nm) of yardlong bean after 4 days germination without R. oligosporous stress (G 4 day) and 4 days with the fungal stress (GS 4 day)

Less phytochemicals under G means that the legume seeds show lesser peaks in G chromatograms when they are compared with UG. Yellow soybean is rich in isoflavones. The phytochemicals slightly reduced by 1 at 260 nm, by 5 at 300 nm and by 8 at 340 nm after germination (**Figure 10.4**), which represents that germination might not be an effective way to enhance the production of phytochemicals in yellow soybeans.

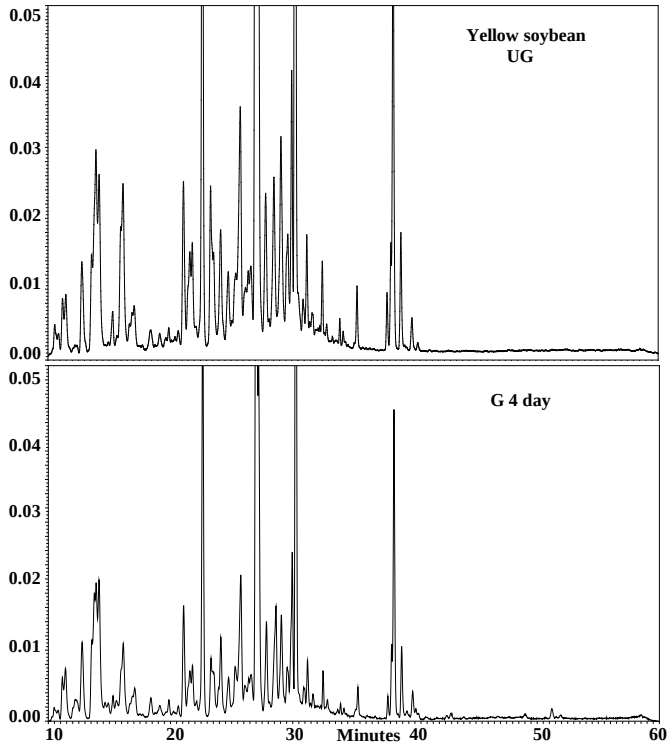

Figure 10.4 HPLC chromatogram (300 nm) of yellow soybean bean (UG) after 4 days germination without R. oligosporous stress (G 4 day)

Overall, different legume seeds have different responses towards germination and fungal-stress germination. Although some legume seeds belong to the same species, they still have different responses towards germination and fungal stress germination. In this experiment, the two peanuts also show a slight difference in their responses towards germination and fungal stress germination. Both peanuts have produced many phytochemicals and are rich in phytoalexins after fungal stress germination. However, big peanuts produced more phytochemicals upon germination compared to small peanuts. Although black soybeans and yellow soybeans are the same species, the phytochemicals contents in both soybeans are quite different as well as the response towards fungal stress. Black soybeans produce more phytochemicals as well as phytoalexins under fungal-stressed germination, while yellow soybeans do not.

10.4 Conclusion

The food grade fungus *R. oligosporus* infected sprout can greatly improve antioxidant capacity, enhance production of phytochemicals and induce phytoalexins of 13 selected food legumes. This study proposes that I may develop a new kind of functional food using a novel process of germinated legume seed with stress of food grade microorganisms such as probiotics. It is possible that these functional foods contain significantly higher concentration of phytochemicals (such as flavonoids, phenolic acids, saponins and also phytoalexins) that may lead to many health enhancing benefits (e.g. antioxidant, anti-inflammation, anti-cancer, anti-obesity, cholesterol-lowering and anti-aging). However, I would firstly establish a relatively comprehensive metabolite profiling of the stressed sprouts and analyze the safety of these food in future study to develop this novel food and validate my hypothesis.

Chapter 11

GERMINATION DRAMATICALLY INCREASES ISOFLAVONOID CONTENT AND DIVERSITY IN CHICKPEA (*CICER ARIETINUM* L.) SEEDS

11.1 Introduction

Chickpea (*Cicer arietinum* L.) is an important grain legume crop in the world. Due to the high protein contents (25.3–28.9% after dehulling), they are consumed as a meat substitute particularly by vegetarian in developing countries. Studies of germinated chickpea seeds are mostly focused on protein content, amino acid composition, polysaccharides and mineral composition. Isoflavonoids have been reported as the main bioactive components of chickpea plant. The major compounds in chickpea seed are formononetin (4'-*O*-methyl ether of daidzein), biochanin A (4'-*O*-methyl ether of genistein), ononin (formononetin glucoside), and sissotrin (biochanin A glucoside) (**Figure 11.1**) (Lv *et al.* 2009). In a study on sprouted chickpea seeds, seven isoflavonoids were isolated and identified, i.e. biochanin A, calycosin, formononetin, genistein, trifolirhizin, ononin and sissotrin (Zhao *et al.* 2009).

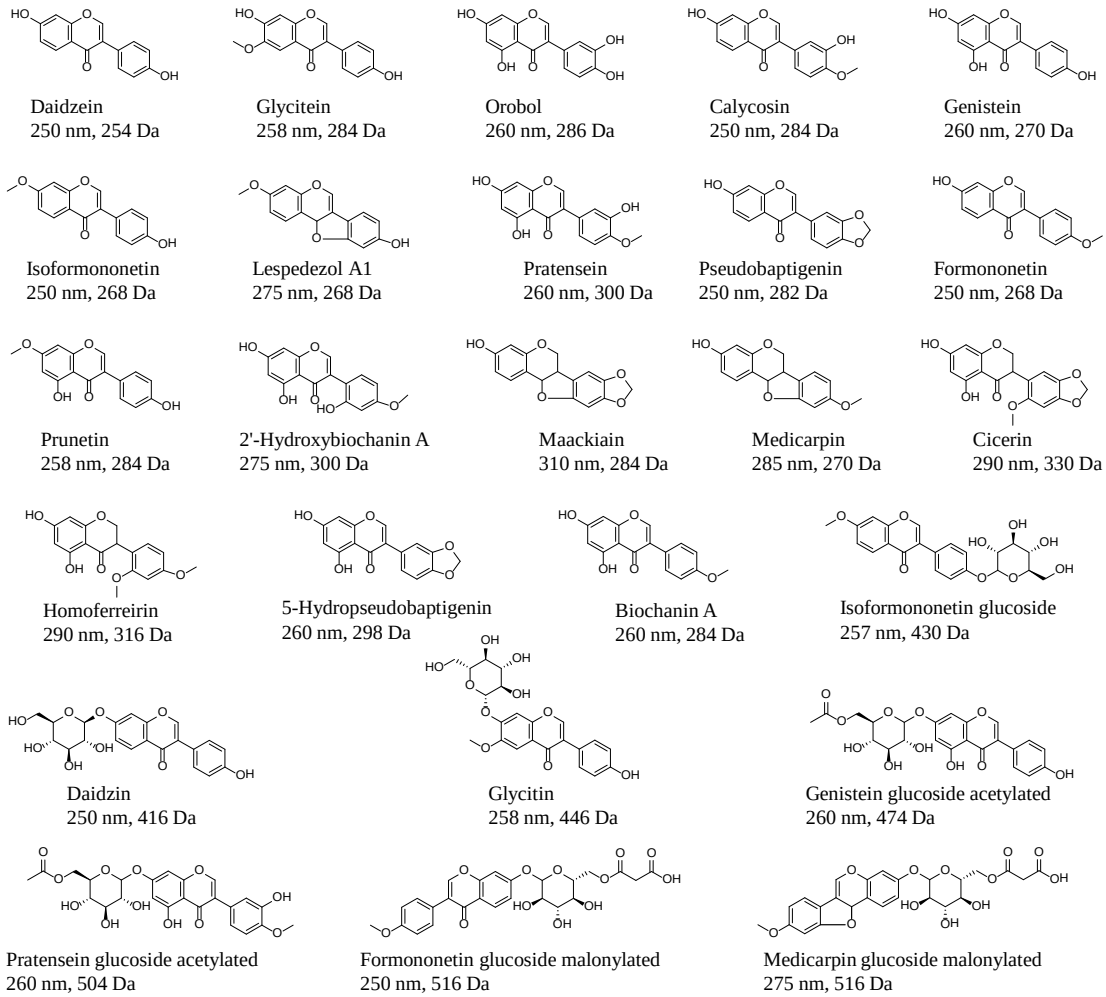

Figure 11.1 Structures, maximum UV absorptions and molecular weights of major isoflavonoids aglycones and a few representatives of their glycoside conjugates identified from germinated chickpea and soybean in this study

Isoflavonoids are a large group of plant secondary metabolites; they play important roles in plant defense as antimicrobial phytoalexins. Over the past decades, isoflavonoids have received considerable attention for their diverse biological activities, including antiestrogenic, anticancer, antioxidative, antimicrobial, anti-cardiovascular diseases and anti-osteoporosis properties (McCue & Shetty 2004). Up to now, there are more than 1600 known isoflavonoids and the subclass of isoflavonoid includes isoflavan, isoflav-3-ene, isoflavone, isoflavanone, isoflavanquinone, pterocarpan, pterocarpene, rotenoid, etc (Veitch 2007; Veitch 2009). Interestingly, the majority of isoflavonoids are isolated from Faboideae, a subfamily

of the flowering plant family Leguminosae, and are synthesized through the central phenylpropanoid pathway and the specific isoflavonoid branch pathways in legumes (Du *et al.* 2010; Wang 2011).

Previous work has shown that germination of chickpea results in increase of TPC and phytochemical production (**Chapter 10**). In this Chapter, the isoflavonoids profiles of chickpea were characterized.

11.2 Materials and Methods

11.2.1 Materials

All materials were as described in **Chapter 3** (**3.2.1**) and **Chapter 10** (**10.2.1**).

11.2.2 Instruments

A Synergy HT microplate reader (Bio-tek, Winooski, VT, USA) was used in antioxidant capacity assays. HPLC analysis was carried out on a Waters HPLC system (Milford, MA, USA) with an Alliance 2659 separation module, a 2996 PDA detector, and the column used was a 250 mm x 4.6 mm i.d., 5 µm, Atlantis T3 C_{18} with a 4 mm x 4 mm i.d. guard column of the same materials (Waters, Ireland). LC-MS spectra were acquired using a Finnigan/MAT LCQ ion trap mass spectrometer (San Jose, CA, USA) equipped with a TSP 4000 HPLC system and an ESI source, which consisted of a P4000 quaternary pump, a UV6000LP PDA detector, and an AS3000 autosampler. The capillary temperature and spray voltage were maintained at 250 °C and 4.5 kV, respectively. ^{1}H NMR spectra were recorded in CD_3OD with a Bruker AC300 spectrometer (Karlsruhe, Germany) operating at 300 MHz.

11.2.3 Seed germination

Germination of the nine legume seeds was carried out according to the method described previously (**Chapter 10**). In brief, seeds were surface sterilized with 70% ethanol for 3 min and then rinsed with water before they were imbibed for 24 h at room temperature (25 °C). The inoculated seeds were placed on a sterile plastic petri dishes (90 mm × 13 mm) lined with two autoclaved filter papers moistened with 5 mL of sterile water. The petri dishes were sealed with parafilm and incubated for 4 days at 25 °C in the dark. Two mL sterile water was added into the petri dishes each day. Four replicates were conducted for each sample.

11.2.4 Sample preparation procedures

Two to ten germinated seeds of each sample were collected from day one to day four and weighed in a 15 mL screw-cap tube, and then extracted with 5.0 mL acetone/ethanol/water (2: 2: 1; v/v) containing 0.1% acetic acid on a shaking incubator at 200 rpm and at room temperature for 12 h. The mixture was centrifuged at 5,000 rpm for 10 min. The supernatant was collected and stored at –20 °C before analysis of antioxidant capacity and TPC. The supernatant was filtered through a Sartorius Minisart polytetrafluoroethylene (PTFE) membrane (0.45 μm) before phytochemical HPLC and LC-ESI-MS analysis.

11.2.5 Quantification of antioxidant capacity and TPC

Assays for hydrophilic antioxidant capacity was carried out using automated oxygen radical absorbing capacity (ORAC) procedure based on previous reports (Huang *et al.* 2002). AAPH was used as the peroxyl generator and Trolox as the antioxidant standard with concentration ranging from 100 to 6.25 μM. Fluorescein solution (160 μL) (9.57×10^{-5} mM), 20 μL of AAPH (81 mM), and 20 μL of sample

were mixed in each well, fluorescence (excitation at 485 nm and emission at 525 nm) readings were taken every 2 min for 2 h, and the area under the curve was calculated. The results were expressed as Trolox equivalents (µmol TE/100 g fresh weight sample). TPC was measured based on Folin-Ciocalteau method according to previous reports (Wu *et al.* 2004). Gallic acid (50, 25, 12.5, 6.25, 3.125, 1.5625 mg/L, correlation coefficient, r = 0.999) was used to establish the standard curve. FCR (100 µL) was diluted ten times from the original reagent, mixed with 80 µL of Na_2CO_3 (75 g/L), and 20 µLof sample in each well. Absorbance was measured at 765 nm after standing for 30 min at 37 °C. These results were expressed as gallic acid equivalents (mg GAE/100 g fresh weight sample).

11.2.6 Detection of isoflavonoids by PDA and MS

HPLC analysis was performed on a Waters apparatus equipped with PDA detector. The detection wavelength was set from 210 to 800 nm. The column used was a 250 mm x 4.6 mm i.d., 5 µm, Atlantis T3 C_{18} with a 4 mm x 4 mm i.d. guard column with water (A), acetonitrile (B) and 2% acetic acid in water (C) as mobile phase. The column temperature was 35 °C. The injection volume was 20 µL. Solvent C composition was maintained at 5% for the entire run. Solvent A and B gradient was as follows: 0 – 1 min, A 95%; 1 – 8 min, A from 95% to 85%; 8 – 24 min, A from 85% to 70%; 24 – 34 min, A from 70% to 40%; 34– 50 min, A from 40% to 20%; 50 – 55 min, A from 20 % to 5%; 55 – 58 min, A from 5% to 95 %; 58 – 60 min, A 95%. The flow rate was 1.0 mL/min. The LC conditions for LC-MS analysis used solvent A (water with 0.05% acetic acid) and B (acetonitrile with 0.05% acetic acid) as mobile phase. The gradient was identical to those used for HPLC analysis above. The injection volume of each sample was 20 µL. For ESI-MS, both the positive and

negative ion modes were used for further characterization of the phytochemicals. The capillary temperature and spray voltage were maintained at 250 °C and 4.5 kV, respectively. Nitrogen was supplied at 80 psi as sheath gas, and at 20 psi as auxiliary gas. Full scan mass spectra from m/z (mass-to-charge ratio) 50 to 2000 were recorded with a scan speed of one scan per second.

11.2.7 Isolation and identification of biochanin A and formononetin

Chickpea seeds (1.0 kg) were germinated at 25 °C in the dark for 3 days. The resulting germinated seeds were homogenized in methanol, and then extracted three times on a shaking incubator at 200 rpm and at room temperature for 6 h each time. The extraction solutions were concentrated in a rotary evaporator at 50 °C. The concentrated residue was transferred to a silica gel column (35 × 6 cm, silica gel 60 (0.040-0.063 mm)) pre-equilibrated with hexane. Successive elution with hexane/ ethyl acetate (9:1, 9:2, 8:2, 8:3, 7:3) mixture at a flow rate of 5 mL/min gave many fractions (each fraction volume was 50 mL). After HPLC analysis, the fractions containing biochanin A and formononetin were combined and the two compounds were obtained and their identities confirmed by UV/vis, ESI-MS and ^{1}H NMR spectra. ^{1}H NMR spectra were recorded in deuterated methanol with a Bruker AC300 spectrometer operating at 300 MHz.

11.2.8 Identification and quantification of isoflavonoids from chickpea and soybean

Identification of isoflavones was achieved by comparing their retention times, UV/vis and MS spectra with those of the standards. For those compounds without commercially available standards, the compounds were tentatively identified by using

HPLC retention times, UV/vis and MS fragments information, and assigned by matching with compounds reported in literatures and existing metabolite databases, such as PubChem, Kegg Ligand database, Massbank, Scifinder Scholar. Five isoflavone standards including biochanin A, daidzein, formononetin, genistein and glycitein were used to obtain the standard curves of major isoflavones. Quantifications of individual and total isoflavones in chickpea and soybean were performed. The concentrations of those isoflavones without standards were calculated by using the standard curve of genistein at 260 nm.

11.2.9 Statistical analysis

The data analysis on lifespan has been described in **Chapter 3** (**3.2.4**).

11.3 Results and Discussion

11.3.1 Antioxidant capacity and TPC

In this study, I examined TPC and antioxidant capacity in nine legume seeds that are most commonly consumed and available at Singapore food markets. Data presented in **Figure 11.2A** show that germination could significantly increase TPC in the nine legume seeds. Furthermore, ungerminated (0 day) black soybean has the highest TPC (69.2 mg GAE/100g FW) among the 9 selected legume seeds, but after germination, its value is less than that of chickpea (76.9 vs 91.7 mg GAE/100g FW). Meanwhile, chickpea has the highest TPC among the geminated seeds.

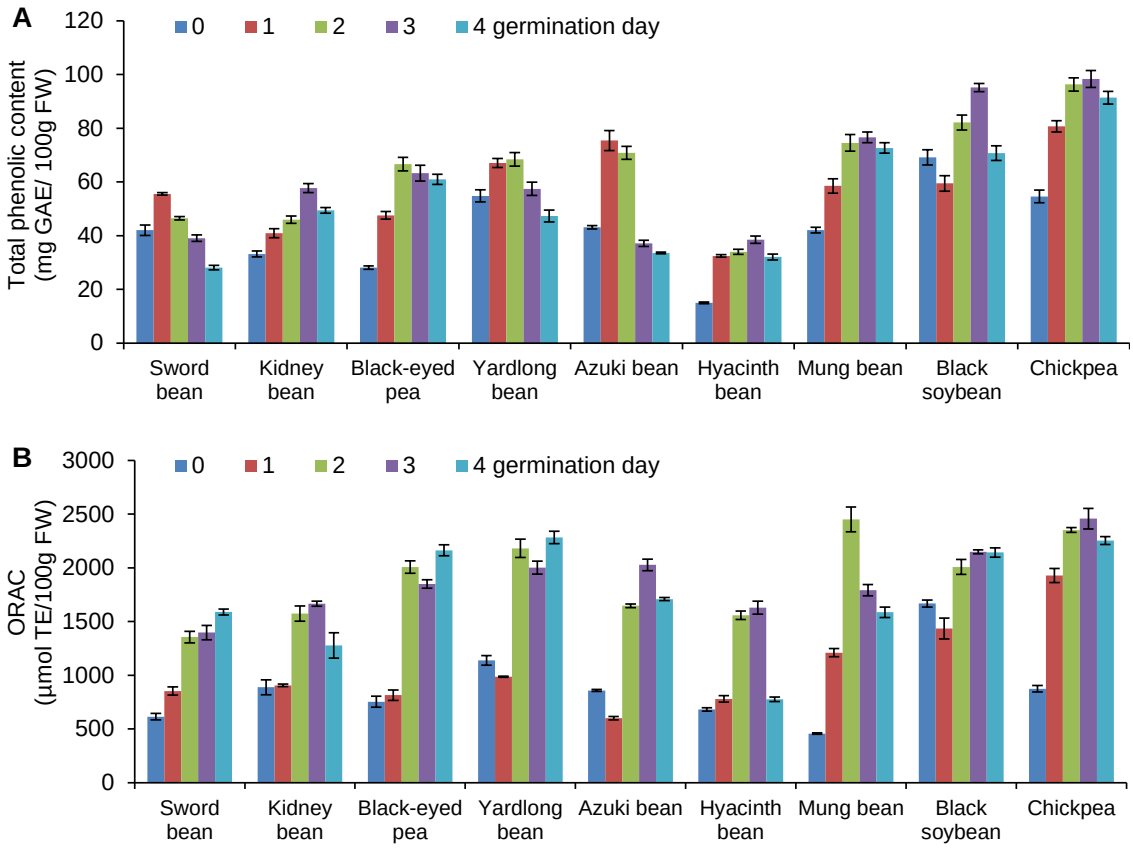

Figure 11.2 TPC and ORAC values of ungerminated seed (0 day) and germinated seed (1–4 days) in nine legumes (also see Table 10.1)
TPC expressed as milligrams of gallic acid equivalents per 100 gram fresh weight basis (mg GAE/100g FW); ORAC value expressed as micromoles of Trolox equivalents per 100 gram fresh weight basis (µmol TE/100 g FW), data is presented as mean, n = 4.

Antioxidant capacity was evaluated by ORAC assay and the ORAC values of ungerminated and germinated legume seeds are shown in **Figure 11.2B**. Overall, the results are similar with that of TPC in **Figure 11.2A**. The nine legumes undergo a significant increase in antioxidant activity after germination. For ungerminated seeds, black soybean possesses the highest ORAC value (1667 µmol TE/100 g FW) than other legumes, however, germination process of the soybean only slightly improve ORAC value. In contrast, germination lead to an almost three times increase in the ORAC of chickpea (874 in 0 day vs 2457 in 3 day, µmol TE/100 g FW). Present results are similar to previous investigations on phenolic contents and antioxidant capacity of germinated some edible seeds (Cevallos-Casals & Cisneros-Zevallos 2009) and selected legumes (Lin & Lai 2006). In addition, current data clearly indicate that

chickpea not only produces great change in phenolic contents and antioxidant capacity during germination but also processes the highest values among the nine germinated legume seeds.

11.3.2 Profiles of isoflavonoids in germinated chickpea seeds

To elucidate the identities of phytochemicals that produce the significant increase in phenolic antioxidants, HPLC analysis was carried out to detect the phytochemicals change during the germination of chickpea. HPLC chromatograms (260 nm) of acetone/ethanol/water (2:2:1) extracts of chickpea seeds during the germination are given in **Figure 11.3**. The HPLC-PDA detector provided UV/vis spectra in the range of 210–800 nm for the peaks. The chromatograms at 260 nm are presented in this study since most compounds have absorbance at this wavelength. As shown in **Figure 11.3**, there are a number of new peaks produced during germination; in addition, there are increased concentrations of several compounds, especially those at retention time between 30 to 40 min.

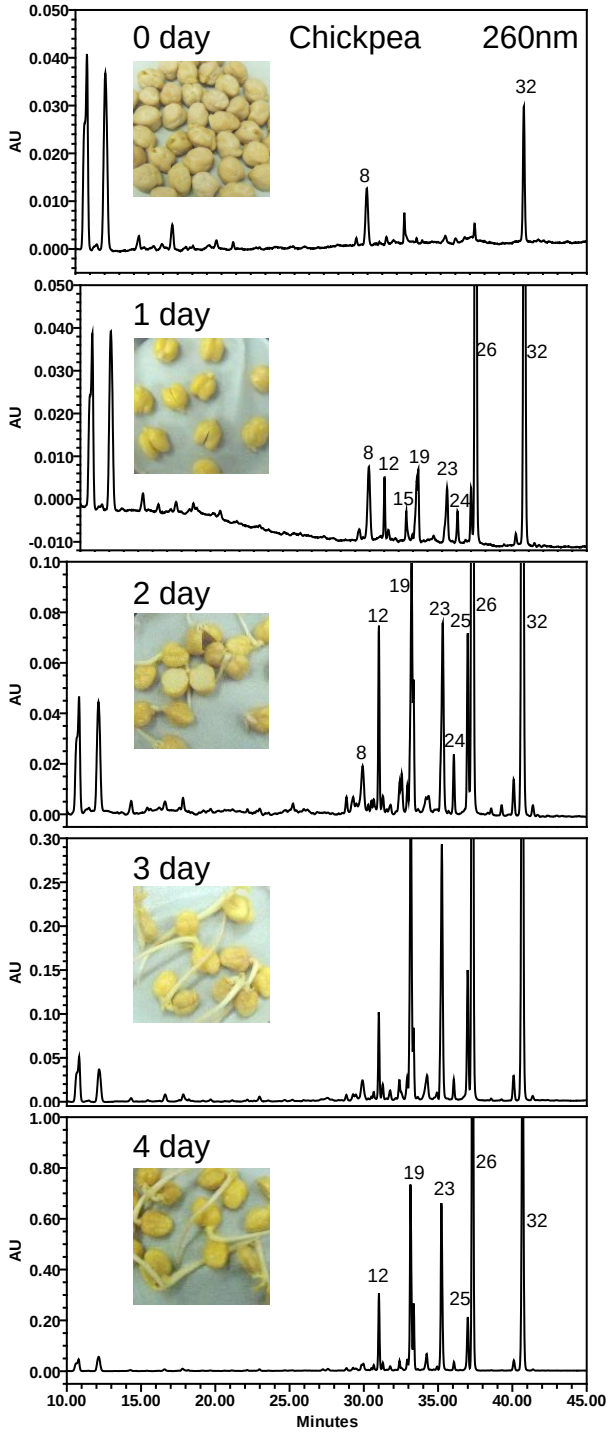

Figure 11.3 Effect of germination time on phytochemicals production in chickpea
The germinated chickpea seeds are extracted by acetone/methanol/water (2:2:1) and the HPLC chromatogram are shown at 260 nm. Tentative identifications of compounds are listed in **Table 11.1**.

Previous studies on chickpea seeds and sprouts suggested that the major constituents are isoflavonoids including biochanin A, formononetin, genistein and their glycoside conjugates (**Figure 11.1**) (Lv *et al.* 2009; Zhao *et al.* 2009). In agreement with this finding, I isolated two major compounds (peak 26 and 32) by

silica column chromatography and confirmed their structures by ^{1}H NMR, UV–Vis, and MS spectra (**Table 11.1, Figure 11.1**) to be formononetin (peak 26) and biochanin A (peak 32).

Table 11. 1 Peak assignments of isoflavonoids in germinated chickpea and soybean presented according to retention time, maximum UV absorption, and molecular ions

Peak	LC-RT (min)	Compounds	UVmax (nm)	ESI+ $[M+H]^{+}$	ESI- $[M+H]^{-}$
1	22.65	Daidzin	250	417	475, 253
2	23.31	Glycitin	258	285	505, 283
3	25.72	Glycitein glucoside malonylated	256	447, 285	445
4	27.00	Daidzein glucoside malonylated	249	503, 417, 255	415, 253
5	27.22	Genistin	261	433	431, 269
6	28.27	Genistein glucoside malonylated	262	473, 271	269
7	28.79	Formononetin glucoside	251	593, 269	591, 447, 267
8	29.22	Garbanzol	277	273	271
9	29.94	Glycitein glucoside acetylated	256	285	547, 283
10	30.25	Genistein glucoside malonylated	261	519	517, 271
11	30.73	Orobol glucoside malonylated	259	535, 287	533
12	30.99	Isoformononetin glucoside malonylated	258	553, 431, 269	489, 267
13	31.55	Lespedezol A1 glucoside malonylated	276	269, 255	267, 253
14	31.84	Prunetin glucoside	259	285	283
15	32.45	Formononetin glucoside malonylated	249	269	267
16	32.49	Daidzein	249	255	253
17	32.85	Glycitein	258	285	283
18	32.89	Maackiain glucoside	286	285	445, 283
19	33.33	Biochanin A glucoside	260	447, 285	283
20	34.40	Biochanin A glucoside malonylated	261	285	533, 283
21	34.73	Maackiain/Medicarpin glucoside acetylated	275	475, 285, 271	487, 283, 269
22	35.06	5-Hydroxypseudobaptigenin glucoside acetylated	261	503, 299	297
23	35.36	Genistein	262	271	269
24	36.00	Pratensein	261	301	299
25	36.98	Pseudobaptigenin	249	283	281
26	37.31	Formononetin	250	269	267
27	38.36	2'-Hydroxybiochanin A	275	301	299
28	38.58	Maackiain	310	285	283
29	39.10	Medicarpin	287	271	269
30	39.81	Cicerin/Homoferreirin	291	331/317	329/315
31	40.10	5-Hydroxypseudobaptigenin	263	299	297
32	40.69	Biochanin A	261	285	283

In order to identify the other compounds, LC-ESI-MS^n analysis was carried out to obtain the molecular masses or their fragmentation information of those peaks. The m/z values of molecular masses or fragments in chickpea were matched with known phytochemicals reported in literatures (Lin *et al.* 2000a; Armero *et al.* 2001; Klejdus *et al.* 2001; Stevenson & Aslam 2006), and supported by UV absorption maxima, HPLC relative retention time, and standards, including biochanin A, formononetin, daidzein, genistein and glycitein, as well as online metabolite databases including KNApSAcK, PubChem, Kegg Ligand database, Massbank and Scifinder Scholar™. For instance, there are mainly two steps to identify maackiain (peak 28), medicarpin (peak 29), cicerin (peak 30), and homoferreirin (peak 30) in this study. Based on literature, the elution times for the four compounds were likely to be in between that of formononetin and biochanin A in reversed-phase HPLC system (column: 4 × 250 mm, RP-C_{18}, 5 μm) (Armero *et al.* 2001). I then checked the MS and UV absorption of the four compounds in literatures and matched with those of peaks in between formononetin (peak 26) to biochanin A (peak 32). Overall, twenty-five isoflavonoids and a flavanonol (garbanzol, peak 8) were identified in the germinated chickpea seeds (**Figure 11.4**). HPLC retention time, maximum UV absorption, fragment ion masses in positive-ion ($[M+H]^+$) and negative-ion ($[M–H]^–$) modes of compounds assigned are listed in **Table 11.1**.

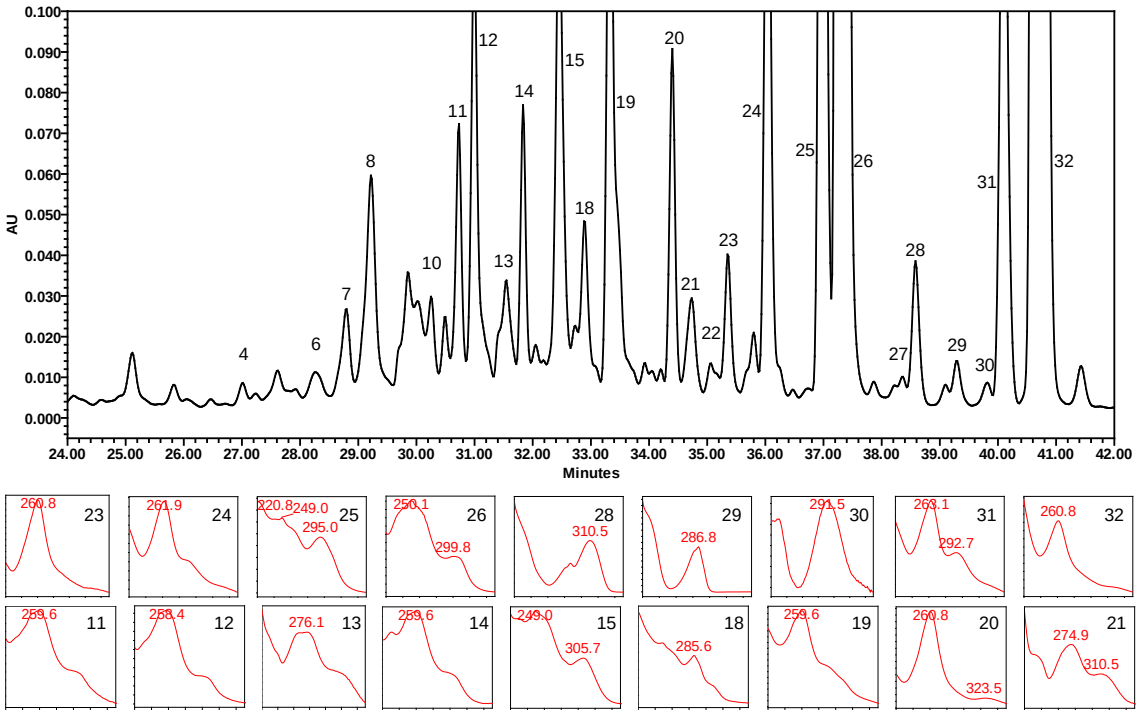

Figure 11.4 HPLC chromatogram (260 nm) and UV absorption spectra of isoflavonoids in germinated chickpea

The sample are concentrated from the raw acetone/methanol/water (2:2:1) extracts in order to detect the lower concentration isoflavonoids. Tentative identifications of compounds are listed in **Table 11.1**.

The UV absorption maximum of individual compound was presented in **Figure 11.1** and **Table 11.1**, as well as the UV spectra of major isoflavonoids in germinated chickpea (**Figure 11.4**). The UV absorption spectra have been used as a complementary method in identifying isoflavonoids, especially daidzein, genistein, glycitein and their conjugates (Rice-Evans *et al.* 1996). Isoflavonoids have a characteristic UV absorption band-II with maxima in the 240 to 280 nm range due to absorption of the A-ring benzoyl system. The UV absorption maxima of individual isoflavonoids mainly depend on the number of present aglycone hydroxyl groups, their relative positions, the glycosidic substitution pattern, and aromatic acyl groups (Mabry *et al.* 1970). A recent study suggested that glucuronidation on 5-hydroxyl group resulted in a UV absorption maxima blue shift of 5-10 nm. In contrast, glucuronidation on 7-hydroxyl group did not cause any change in UV absorption,

whereas glucuronidation on 6-hydroxyl group did not cause predictable changes in UV maxima values (Singh *et al.* 2010).

As shown in **Figure 11.3** and **11.4**, the major compounds in germinated chickpea seed are biochanin A (peak 32), formononetin (peak 26), pseudobaptigenin (peak 25), pratensein (peak 24), genistein (peak 23), biochanin A glucoside (peak 19), formononetin glucoside malonylate (peak 15), and isoformononetin glucoside malonylate (peak 12). Remarkably, these compounds belong to isoflavones, the largest subgroup of isoflavonoids. Biochanin A and formononetin were the first phytochemicals found in the sprouted germs of *Cicer arietinum* in 1945 (Stevenson & Aslam 2006). Subsequently daidzein, pratensein, sissotrin (biochanin A 7-*O*-glucoside), genistein, genistin (genistein-7-*O*-glucoside), ononin (formononetin-7-*O*-glucoside), 2'-hydroxyformononetin, calycosin, pseudobaptigenin, and other isoflavones and their glycoside conjugates were identified in seedlings, germinated cotyledons, roots or other parts of *Cicer* spp (Stevenson & Aslam 2006).

In this Chapter, twenty isoflavones and conjugates were detected and identified in germinated chickpea, and the majority of them are 4'-*O*-methylated isoflavones. In addition, two pterocarpans maackiain and medicarpin, as well as two isoflavanones, cicerin and homoferreirin, were detected. Maackiain and medicarpin were proposed as phytoalexins produced in response to elicitor's induction and infection in chickpea roots, seedlings and cell cultures (Cherif *et al.* 2007). They may be important compounds in chickpea defense of microbial infection, since it was reported that their potent antifungal activity could fight against several pathogens causing Ascochyta blight in chickpea (Stevenson & Aslam 2006). However, their bioactivity for animal and human is less studied than the other pterocarpan phytoalexin glyceollins, primarily from soybean.

11.3.3 Quantification of isoflavonoids in chickpea and soybean

I compared the HPLC chromatogram (**Figure 11.5**) of isoflavonoids between black soybean, chickpea, and their germinated seeds at day 4 in acetone/methanol/water (2:2:1) extracts. It illustrated clearly that the changes of isoflavonoids production after germination was more significant in chickpea than that in black soybean. I also examined the two major isoflavones biochanin A and formononetin productions during germination in chickpea seed (**Figure 11.6A**). It was remarkable that the content of biochanin A and formononetin changed from 19 and 1.0 (μg/g FW) of ungerminated seeds (0 day) to 702 and 1484 (μg/g FW) of germinated seeds at day 4 (G4d), respectively, an increase of approximately 40 and 1400 times. Soybean germination has much less impact on the total flavonoids, with increase of only 43.6% (1132 μg/g FW in ungerminated seeds to 1626 μg/g FW after germination). In comparison, approximately 90 times increase in total flavonoids was found in chickpea (83 μg/g FW in ungerminated seeds to 7568 μg/g FW in germinated seeds) (**Figure 11.6B**).

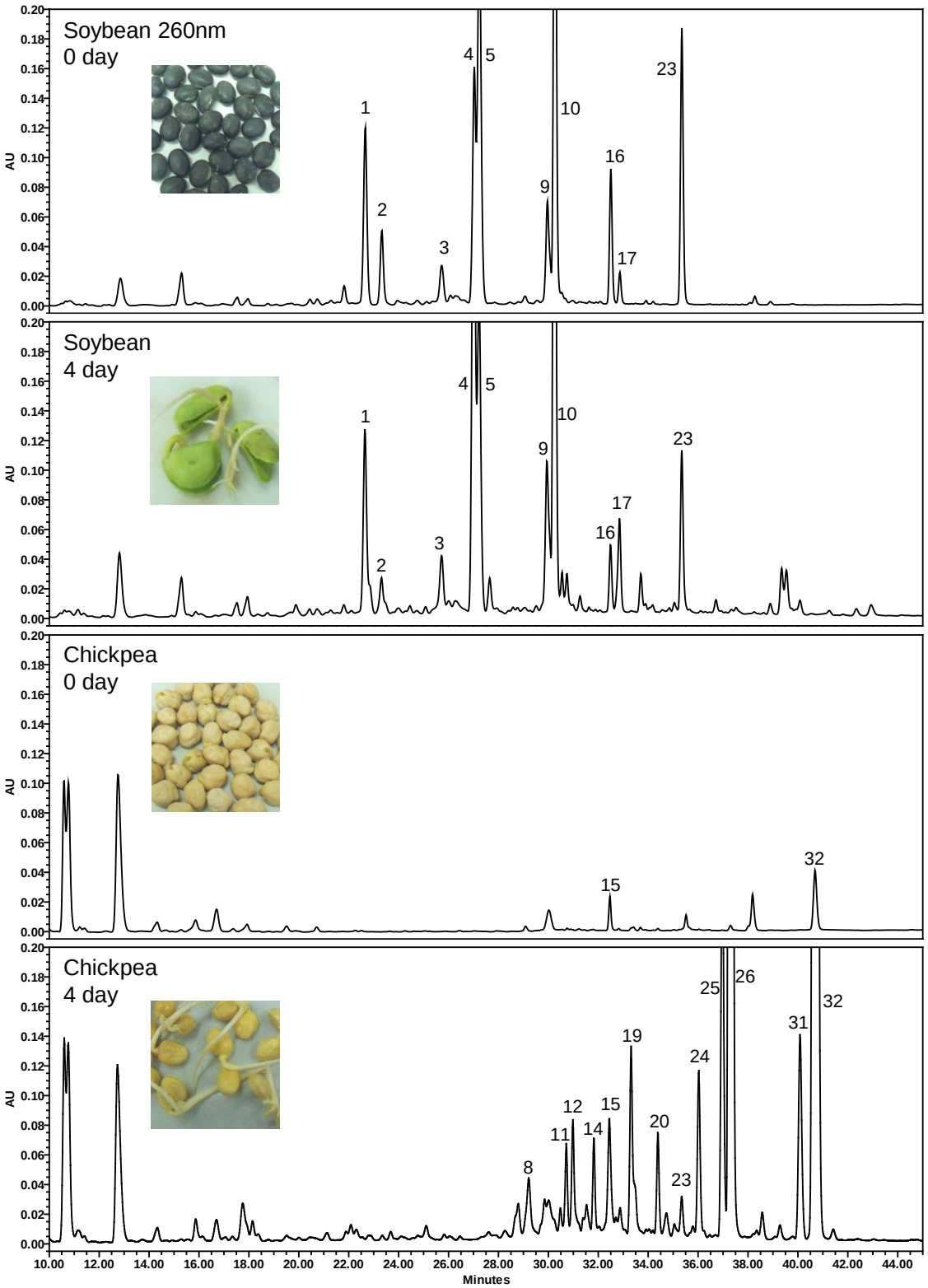

Figure 11.5 Comparative HPLC chromatogram (260 nm) of isoflavonoids between black soybean, chickpea, and their germinated seeds at day 4 in acetone/methanol/water (2:2:1) extracts
Tentative identifications of compounds are listed in **Table 11.1**.

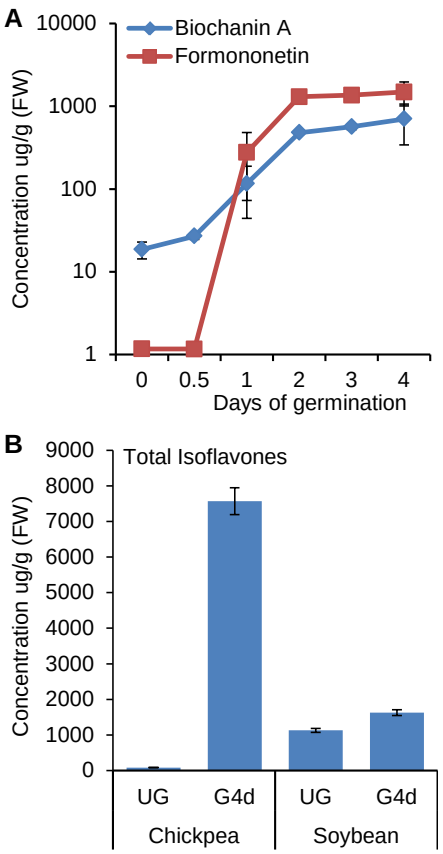

Figure 11.6 Quantitative analysis of isoflavonoids in chickpea and black soybean
(A) Production of the two major isoflavones biochanin A and formononetin during the germination of chickpea seed. (B) Total isoflavonoids content in ungerminated (UG) black soybean, chickpea, and their germinated seeds at day 4 (G4d).

Antioxidant capacity of germinated chickpea (2253 µmol TE/100 g FW) and germinated soybean (2142 µmol TE/100 g FW) are comparable, while the total isoflavonoids content for germinated chickpea was approximately 4-fold higher than for germinated soybean. This may be due to the weaker antioxidant activity of 4'-*O*-methylated isoflavones biochanin A and formononetin than that of genistein and daidzein (Rufer & Kulling 2006). The health benefits of chickpea seed received much less attention. It has been reported that these 4'-*O*-methylated isoflavones can be converted by 4'-*O*-demethylation to the more potent phytoestrogens daidzein and genistein in human (Tolleson *et al.* 2002), and the resulting daidzein and genistein would be further metabolized to other metabolites including equol (Tham *et al.* 1998). Moreover, germination of chickpea could produce 4-fold higher total isoflavonoids

content than soybean in addition to a few of pterocarpan phytoalexins, such as maackiain and medicarpin. Recent investigation has shown that red clover, another leguminous plant not used as a food source, also contains significantly high concentrations of biochanin A, formononetin and other isoflavones (Lin *et al.* 2000a; Klejdus *et al.* 2001; Tsao *et al.* 2006); total isoflavone content of more than 7500 µg/g FW was measured in this study, and this amount could be comparable to that of 10 red clovers cultivars ranged between 8.92 and 12.75 mg/g of dry matter (Sivesind & Seguin 2005). Germination also improves phytic acid, ascorbic acid, folic acid, β-carotene content, protein solubility and in vitro protein digestibility of chickpea seeds. Thus, the germinated chickpea seed would serve as a promising functional food rich in isoflavonoids.

Isoflavonoids are synthesized by the central phenylpropanoid pathway and the specific isoflavonoid branch pathways in legumes (**Figure 11.7**). The central phenylpropanoid pathway is common to all plant species and it produces lignin, coumarins, benzoic acids, stilbenes, and flavonoids/isoflavonoids (Dixon *et al.* 2002). Chalcone is the first step in the production of flavonoids and isoflavonoids that requires the enzyme chalcone synthase (CHS). In the isoflavonoid biosynthetic pathway, the branch-point enzyme of isoflavonoid specific branch is introduced by 2-hydroxyisoflavanone synthase (isoflavone synthase, IFS), and yields an immediate product 2-hydroxyisoflavanone. The immediate product is then dehydrated to daidzein and genistein through catalysis by 2-hydroxyisoflavanone dehydratase (HID) (Wang 2011). In soybean, the daidzein is a precursor to the major phytoalexin glyceollins. In chickpea, 2-hydroxyisoflavanone is methylated by 2,7,4'-trihydroxyisoflavanone 4'-O-methyl transferase (HI4'OMT) to form methoxyisoflavanones which are further dehydrated by HID to form biochanin A and

formononetin (Wang 2011). Chickpea constitutively accumulates biochanin A and formononetin, mainly as 7-0-glucoside-6''-O-malonate esters stored in cell vacuoles (Du *et al.* 2010). Under environmental stress, the two pterocarpan phytoalexins medicarpin and maackiain are induced (Daniel *et al.* 1990). It is known that several subgroups of isoflavonoids are represented in chickpea. Generally, aglycones are represented more frequently than glycosides and are substituted most frequently by glucose, which is consistent with my finding that the major compounds are aglycone isoflavones biochanin A (peak 32), 5-hydroxypseudobaptigenin (peak 31), formononetin (peak 26), pseudobaptigenin (peak 25), pratensein (peak 24) and genistein (peak 23) in germinated chickpea seeds (**Figure 11.3, 11.4, 11.5**). Many isoflavonoids in *Cicer* occur as glycosides and often in larger quantities than the aglycones, which is probably for storage purposes since the glycosides appear to occur most abundantly in the roots and stems but only the aglycones occur in other parts of the plant tissues (Stevenson & Aslam 2006).

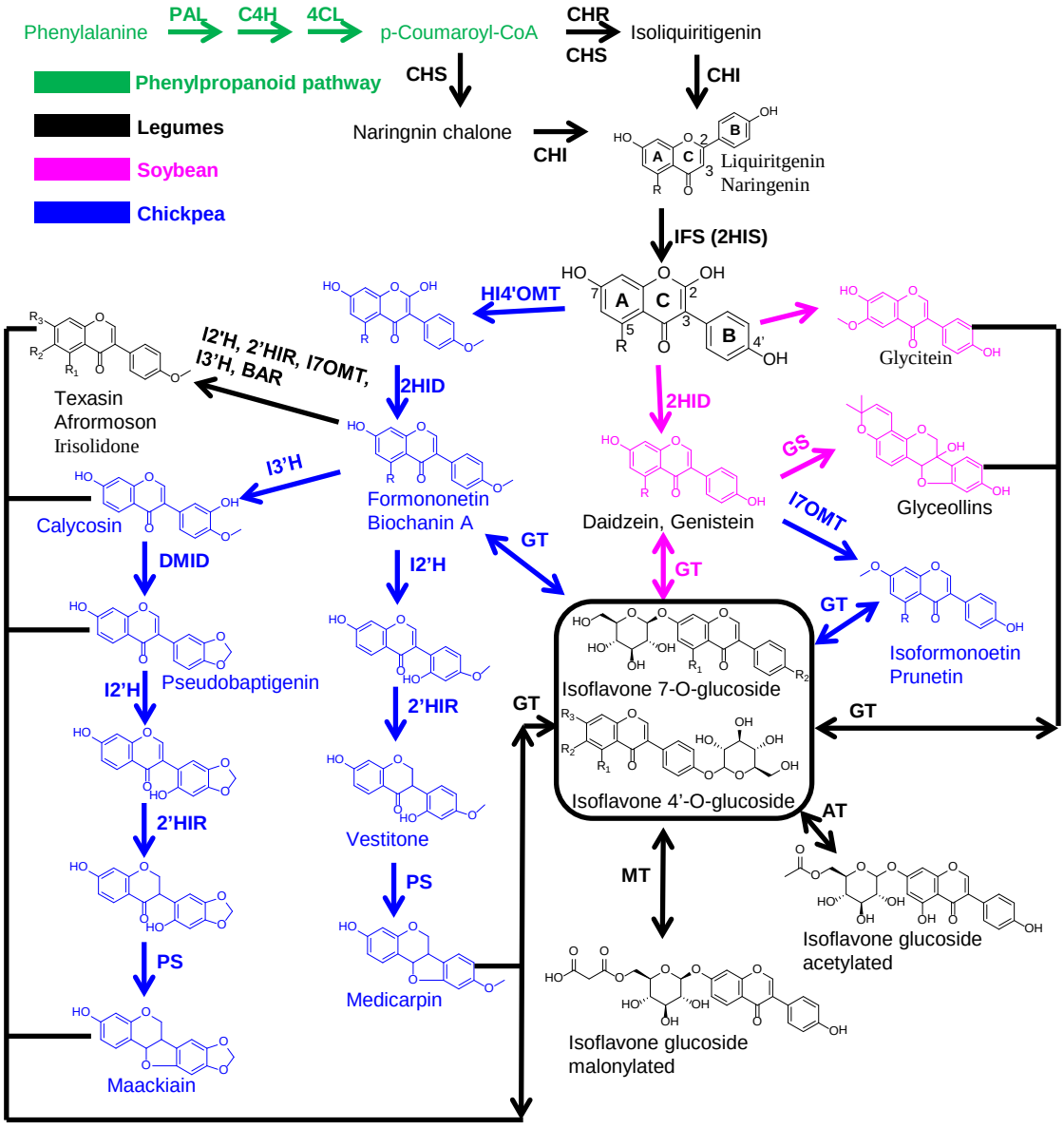

Figure 11.7 Proposed isoflavonoids biosynthesis pathway in legumes
PAL, phenylalanine ammonialyase; C4H, cinnamate-4-hydroxylase, 4CL, 4-coumarate CoA ligase; CHS, chalcone synthase; CHR, chalcone reductase; CHI, chalcone isomerase; IFS, isoflavone synthase; 2HIS, 2-hydroxyisoflavanone synthase; HI4′OMT, 2,7,4′-trihydroxyisoflavanone 4′-O-methyl transferase; I7OMT, isoflavone 7-O-methyltransferase; 2HID, 2-hydroxyisoflavanone dehydratase; GS, glyceollin synthase; I2′H, isoflavone 2′-hydroxylase; 2'HIR, 2'-hydroxyisoflavone reductase; VR, vestitone reductase; DMID, 7,2′-dihydroxy,4′-methoxyisoflavanol dehydratase; PS, pterocarpin synthase; I3'H, isoflavone 3'-hydroxylase; BAR, biochanin A reductase; GT, uridine diphosphoglucose-isoflavone 7-O-glucosyltransferase; MT, isoflavone-7-O-beta-glucoside 6"-O-malonyltransferase; AT, isoflavone-7-O-beta-glucoside 6"-O-acetyltransferase.

11.4 Conclusion

Germinated chickpea seed has higher TPC and antioxidant capacity than the other eight germinated seeds. In total, 31 isoflavonoids in chickpea and soybean are tentatively identified, based on their chromatographic retention time, UV spectra,

positive and negative MS fragments patterns in comparison to known compounds and the literature. Remarkably, germination greatly increases isoflavonoid diversity and content in germinated chickpea, which has more than 4-fold higher total isoflavonoid content than soybean. The findings in this Chapter provide important information for further studies on the utilization of germinated chickpea seeds as a source for nutraceuticals and functional foods.

Chapter 12

FOOD GRADE FUNGAL STRESS ON GERMINATING PEANUT SEEDS INDUCED PHYTOALEXINS AND ENHANCED POLYPHENOLIC ANTIOXIDANTS

12.1 Introduction

Phytoalexins are secondary metabolites that plants synthesize for self-defense against microbial infections; they have shown great promises in chronic disease prevention. The most well-known example is resveratrol, an induced phytoalexin found in yeast infected grape skin. Resveratrol may have interesting potential as a CRM. Furthermore, it has been shown to be a good antioxidant and anti-inflammatory agent (Jang *et al.* 1997; Pervaiz & Holme 2009). However, foods containing significant levels of resveratrol are limited to red grape wine / juice (Baur & Sinclair 2006). Glyceolin is another induced phytoalexin in soybean, which has many health benefits. I have demonstrated that germinating soybeans stressed with tempeh starter led to great enrichment of glyceollins among other isoflavones biosynthesized by the beans (**Chapter 7**). I extended this food grade bioprocessing technology to peanut seeds and reported herein is my findings.

Peanuts are widely consumed food. They have recently attracted greater attention because of its health promoting properties attributed to the numerous bioactive components such as unsaturated fatty acids, vitamin E, folate, phytosterols, phenolic acids, procyanidins, and selenium (Francisco & Resurreccion 2008). Peanut seeds,

when induced by pathogenic infections, fungal elicitors, and UV light, could produce inducible phytoalexins such as stilbenoid derivatives (resveratrol, arachidins, 3'-isopentadienyl-3,5,4'-trihydroxystilbene, SB-1, chiricanine A, arahypins), and pterocarpanoid derivatives (e.g. aracarpene-1 and aracarpene-2) (Sobolev *et al.* 2006; Sobolev *et al.* 2007; Sobolev *et al.* 2009; Sobolev *et al.* 2010a; Sobolev *et al.* 2010b). Stress-induced stilbenoid phytoalexins from peanuts are of considerable interest because of their biological activities and possible therapeutic value for chronic diseases. Resveratrol derivatives and their oligomers are less studied but have demonstrated some potential as disease preventing ingredients (Shen *et al.* 2009; Fulda 2010). There is no report on stressing germinating peanuts by using *R. oligoporus*, a popular food grade microbe for food fermentation in Southeast Asia region.

12.2 Materials and Methods

12.2.1 Reagents

The reagents were as described in **Chapter 3** (**3.2.1**) and **Chapter 10** (**10.2.1**).

12.2.2 Instruments

The instruments were as described in **Chapter 11** (**11.2.2**).

12.2.3 Peanut germination and fungal inoculations

Peanut (*Arachis hypogaea* L.) seeds with three classes of skin colors (reddish brown, red and black) were collected from the supermarket in China (BEYOND ORGANIC, Bejing, China). The seeds germination and fungal inoculations have been described in **Chapter 10** (**10.2.2**).

12.2.4 Sample preparation procedures

The sample preparation procedures have been described in **Chapter 11** (**11.2.4**).

12.2.5 Quantification of antioxidant capacity and total phenolics

Six antioxidant capacity related values including total phenolics content (TPC), total flavonoid content (TFC), oxygen radical ($ROO^{\cdot}$) absorbance capacity (ORAC), hydroxyl radical ($HO^{\cdot}$) absorbance capacity (HORAC), superoxide radical ($O_2^{\cdot-}$) absorbance capacity (SORAC), DPPH (2,2-Diphenyl-1-picrylhydrazyl) radical scavenging capacity values were measured. TPC was measured based on Folin-Ciocalteau method according to Wu et al (Wu *et al.* 2004). Gallic acid (50, 25, 12.5, 6.25, 3.125, 1.5625 mg/L, correlation coefficient, r = 0.999) was used to establish the standard curve. These results were expressed as gallic acid equivalents (mg GAE/100 g FW). TFC was determined using a colorimetric method described previously (Heimler *et al.* 2005). Twenty μL sample or (+)-catechin standard solution (50, 25, 12.5, 6.25, 3.125, 1.56, 0.78 mg/L) were mixed with 80 μL distilled water in each well of 96-well polypropylene plate, followed by adding 6 μL of 5(w/v)% $NaNO_2$ solution. After 5 min, 6 μL 10(w/v)% $AlCl_3$ solution were added and allowed to stand for another 1 min before adding 40 μL 1 M NaOH. The mixture was toped up to 200 μL with distilled water. The absorbance was measured immediately against the blank (the same mixture without the sample) at 510 nm. The results were calculated and expressed as catechin equivalents (mg CAE/100 g FW). Hydrophilic ORAC procedure was based on previous report (Huang *et al.* 2002). The results were expressed as Trolox equivalents (μmol TE/100 g FW). HORAC assay was based on previous report (Ou *et al.* 2002). Gallic acid was used to establish the standard curve,

and results were expressed as mg GAE/100 g FW. SORAC protocol was based on Zhang et al. report (Zhang *et al.* 2009b), and results were expressed as units SOD equivalent/100 g FW. DPPH scavenging capacity determined as previously described (Gorinstein *et al.* 2006). Gallic acid was used to establish the standard curve, and results were expressed as mg GAE/100 g FW.

12.2.6 Detection of phytochemical by PDA and MS

HPLC analysis was performed on a Waters apparatus equipped with PDA detector. The detection wavelength was set from 210 to 800 nm. The separation was accomplished on a Waters C_{18} column (5 μm, 4.6×250 mm) with water (A), acetonitrile (B) and 2% acetic acid in water (C) as mobile phase. The column temperature was 30 °C. The injection volume was 20 μL. Solvent C composition was maintained at an isocratic 5% for 60 min. Solvent A and B gradient was as follows: 0 – 1 min, A 95%; 1 – 8 min, A from 95% to 85%; 8 – 24 min, A from 85% to 70%; 24 – 34 min, A from 70% to 40%; 34– 50 min, A from 40% to 20%; 50 – 55 min, A from 20 % to 5%; 55 – 58 min, A from 5% to 95 %; 58 – 60 min, A 95%. The flow rate was 1.0 mL/min. The LC conditions for LC-MS analysis used solvent A (water with 0.05% acetic acid) and B (acetonitrile with 0.05% acetic acid) as mobile phase. The gradient was identical to those used for HPLC analysis above. The injection volume of each sample was 20 μL. For ESI-MS, both the positive and negative ion modes were used for further characterization of the phytochemicals. The capillary temperature and spray voltage were maintained at 250 °C and 4.5 kV, respectively. Nitrogen was supplied at 80 psi as sheath gas, and at 20 psi as auxiliary gas. Full scan mass spectra from m/z 50 to 2000 were recorded with a scan speed of one scan per second.

12.2.7 Phytoalexin extraction and detection by HPLC and LC-MS

The reddish brown peanut seeds (500 g) were germinated with *R. oligosporus* stress at 25 °C in the dark for 3 day. The peanut samples were homogenized in acetone/ethanol/water (2: 2: 1; v/v), then extracted with the same solvent mixture for three times on a shaking incubator at 200 rpm and room temperature for 12 h at each time. The extraction solutions were concentrated in a rotary evaporator at 50 °C. The concentrated residue was transferred to a silica gel column (35 × 6 cm, silica gel 60) for fractionation. The column was pre-equilibrated with hexane and then successively eluted with hexane and hexane/ ethyl acetate (7:3) mixture at a flow rate of 5 mL/min. Each fraction was collected (100 mL). After HPLC detection, the fractions containing the phytoalexins are combined and further analyzed by LC-ESI-MS. Ths LC-ESI-MS conditions were similar with those used for phytochemical detection above, except the LC mobile phase gradient. The gradient was as follows: 0 – 1 min, A 95%; 1 – 8 min, A from 95% to 65%; 8 – 15 min, A from 65% to 55%; 15 – 50 min, A from 55% to 40%; 50 – 55 min, A from 40% to 10%; 55 – 58 min, A from 10 % to 95%; 58 – 60 min, A 95%.

12.3 Results and Discussion

Peanut skin color varies usually from light brown to deep red. However, peanuts with different skin colors have been cultivated and consumed widely during the past decade in China, such as black, purple black, white, red, and multi-colored, although most of them are rarely seen in the marketplace worldwide. In order to investigate the difference between phytochemicals in peanut seeds with different skin colors, three of

the types of peanut were studied; for future comparison purpose, samples of each peanut seeds were kept at -80 °C freezer in our lab.

Stressed peanuts can produce a wide range of phytoalexins. Using *R. oligosporus* as food grade elicitor, the germinating peanuts of three different skin colors were processed and their phytoalexin profiles were extracted, fractionated, and characterized by HPLC and LC-MS. I applied an analytical method for the comprehensive profiling of semi-polar metabolites in the acetone/ethanol/water (2: 2: 1; v/v) extract of the three cultivars of peanuts. HPLC-PDA and ESI-MS detectors were used to tentatively identify the secondary metabolites. The masses or MS fragments information were matched with compounds reported in literatures, and supplemented by UV, HPLC retention time, and reference compounds, including caffeic acid, catechin, *p*-coumaric acid, ferulic acid, genistein, hydroxybenzoic acid, *trans*-resveratrol and sinapic acid, as well as existing metabolite databases including PubChem, Kegg Ligand database, Massbank and Scifinder Scholar^{TM}.

12.3.1 Profiles of phenolic acids in peanut seeds

For ungerminated peanut seeds, HPLC chromatograms (310 nm) of acetone/ethanol/water extracts of three different types of peanut seeds are given in **Figure 12.1**. The HPLC-PDA detector allowed us to record the UV/Vis spectrum in the range of 210-800 nm, but only the chromatograms at 310 nm are presented in this study since the most number of peaks are observed at this wavelength in all peanut samples. LC-MS analysis reveals that phenolic acids are the major group of phenolic compounds in ungerminated seeds. LC retention time, maximum UV absorption, fragment ion masses in positive-ion ($[M+H]^+$) and negative-ion ($[M–H]^–$) mode of compounds identified tentatively are listed in **Table 12.1**.

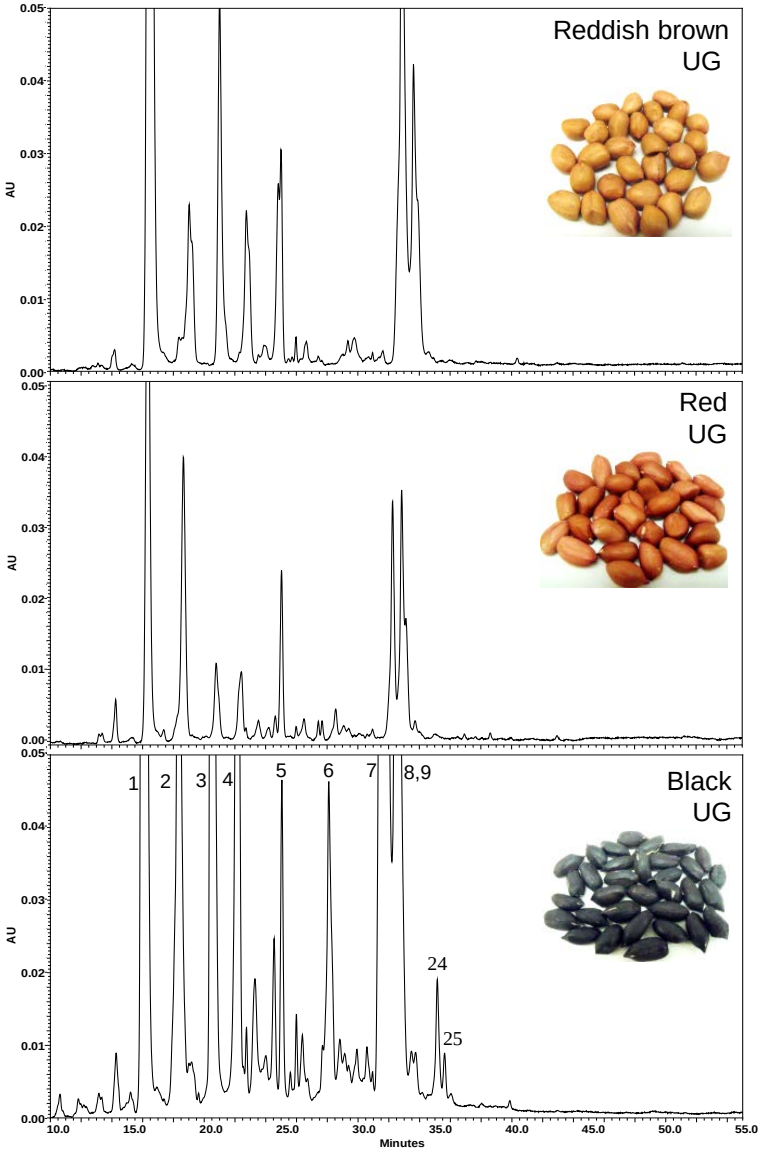

Figure 12.1 HPLC chromatograms (310 nm) of three types of peanut seeds in acetone/ethanol/water (2:2:1) extracts

Tentative identification of compounds can be seen in **Table 12.1**.

Table 12.1 Peak assignment of compounds in GS peanut sprouts presented according to retention time, maximum UV absorption and molecular ions

Peak	LC-RT (min)	Tentative identification	PDA UV bands (nm)	ESI+ $[M+H]^+$	ESI– $[M–H]^-$
1	9.1	Coumaric acid derivative 1	314	147, 165	163, 295
2	10.6	Coumaric acid derivative 2	314	147, 297	163, 277
3	12.6	Coumaric acid derivative 3	314	147	163, 295
4	13.0	Coumaric acid derivative 4	314	251	163, 295
5	16.2	Coumaric acid derivative 5	314	309	163
6	18.9	Coumaric acid derivative 6	314	291	163, 289
7	21.8	Coumaric acid derivative 7	314	147, 309	163, 277, 441
8	23.2	Sinapinic acid derivative 1	318	207	223
9	23.7	Feruloyl malic acid derivative 1	318	177, 291	193, 307
10	12.0	Hydroxybenzoic acid derivative 1	260, 302		137
11	14.1	Coumaric acid derivative 8	313		132, 163, 307
12	14.7	Coumaric acid derivative 9	311	134,	132, 163, 307
13	16.0	Sinapinic acid derivative 2	305	207	205
14	10.1	Coumaric acid derivative 10	314	147, 297	163, 277
15	19.4	Coumaric acid derivative 11	313	133	163
16	19.5	Catechin	282	291, 245	203, 245, 289
17	19.8	Feruloyl malic acid derivative 2	318	291	193
18	20.0	Sinapinic acid derivative 3	305	207	223
19	20.4	Caffeic acid derivative 1	240, 324	163	179, 135
20	21.0	Hydroxybenzoic acid derivative 2	260, 302	152	137
21	26.3	Sinapinic acid derivative 4	318	165,207	223
22	26.7	Feruloyl malic acid derivative 3	327	177, 291	193
23	27.4	Piceid derivative 1	307	391	389, 227
24	29.2	Coumaric acid derivative 12	314		277, 441
25	29.4	Coumaric acid derivative 13	315	147	163, 295
26	29.5	*cis*-Resveratrol	309	229	227
27	36.4	3'-Isopentadienyl-3,5,4'-trihydroxystilbene derivative 1	297	295	293
28	36.5	3'-Isopentadienyl-3,5,4'-trihydroxystilbene derivative 2	298	295	293
29	37.8	Arachidin-3 derivative 1	336	297, 923, 241	921, 239, 295
30	27.9	*trans*-Resveratrol	306, 318	229	227, 453
31	36.5	Arachidin-1 derivative 1	323	313	311
32	37.1	Arachidin-2 derivative 1	325	297	
33	30.8	Arahypin-3 derivative 2	337	229	227, 329
34	31.3	Coumaric acid derivative 14	314	147	145, 163
35	32.5	Genistein	260	271	269
36	34.2	SB-1 derivative 1	325	345	343
37	34.7	SB-1 derivative 2	322	343	341
38	35.1	Arahypin-4 derivative 1	310	229, 313	311, 227
39	35.6	3'-Isopentadienyl-3,5,4'-trihydroxystilbene derivative 3	295	295	
40	39.3	Arahypin-5 derivative 1	341	295	293
41	39.5	Arahypin-1 derivative 2	326	281	279
42	40.6	Chiricanine A derivative 1	317		279
43	41.6	Chiricanine A derivative 2	316	281	279
44	42.8	KODE glyceryl esters	282	351, 355, 369	353, 367
45	47.5	KODEs	280	295	293

Majority of the phenolic acids are found to be coumaric acid derivatives (peak 1 to 7), sinapinic acid (peak 8) and ferulic acid (peak 9). This result is consistent with previous reports that *p*-coumaric acid accounted for 40–68% of the total phenolic acids in all peanut protein products, and roasted peanuts contain *p*-coumaric acid greater than 100 mg/kg (Talcott *et al.* 2005). Coumaric acid derivatives are characterized by common maximal UV absorption at 309-314 nm (Abad-Garcia *et al.* 2009) and by MS peak at 147 ($[M+H–H_2O]^+$ from dehydration of the coumaric acid ion ($[M–H]^–$, 163). Meanwhile, sinapinic acid derivatives are identified by main product ions at ($[M+H–H_2O]^+$, 207), ($[M–H–H_2O]^–$, 205) and ($[M–H]^–$, 223); and ferulic acid at ($[M+H–H_2O]^+$, 177) and ($[M–H]^–$, 193) (**Figure 12.2**, **12.3**).

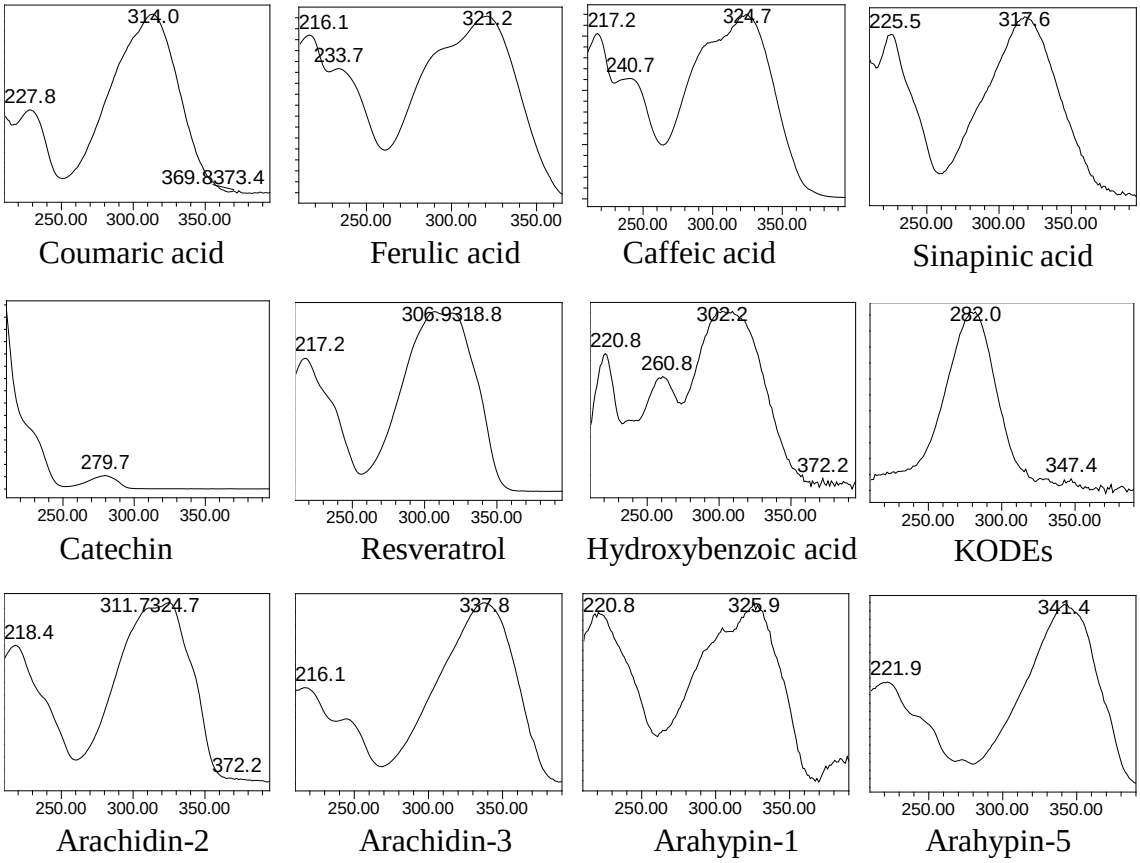

Figure 12.2 UV spectra of major phytochemcials in peanut sprouts under food grade fungus *R. oligosporus* stress

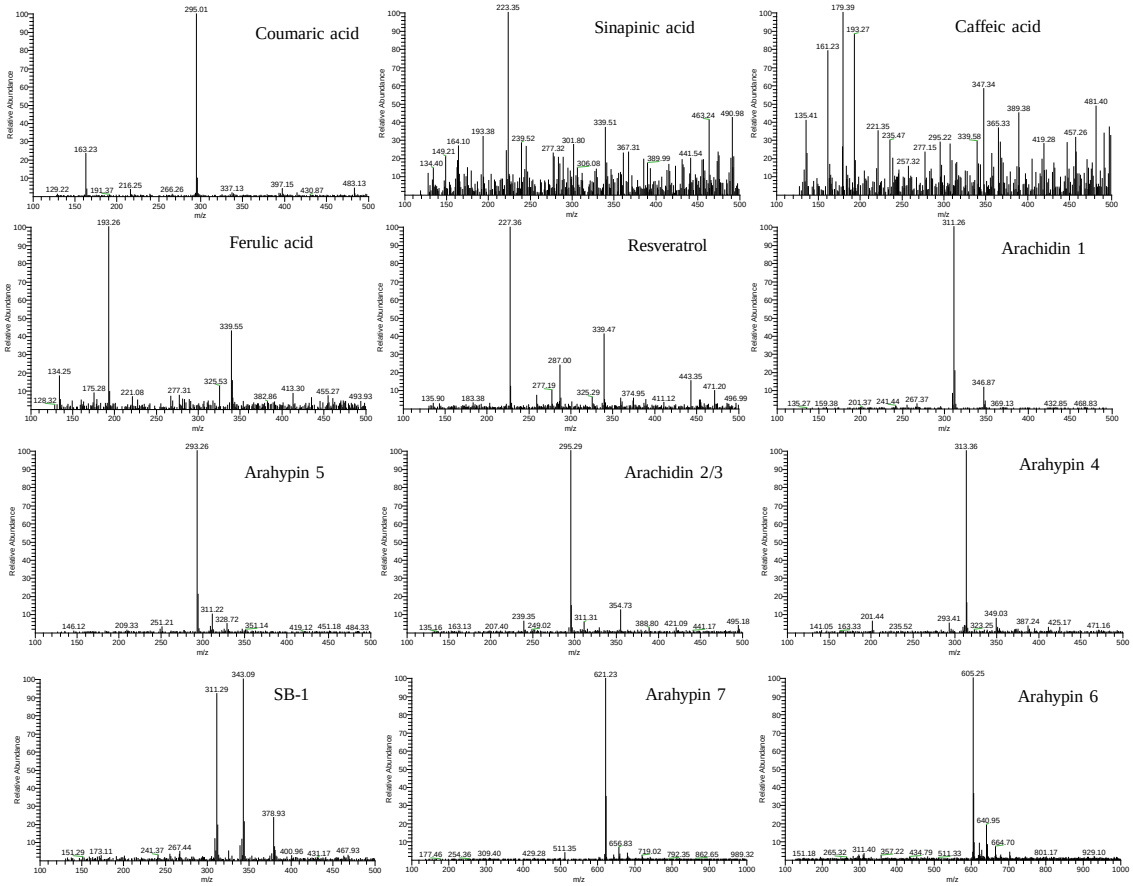

Figure 12.3 ESI (negative ion) mass spectra of major phytochemicals in peanut sprouts under food grade fungus *R. oligosporus* stress

These phenolic acids are potent scavengers of free radicals that may reduce the risk of several chronic diseases such as cancer, cardiovascular disease, and diabetes. For higher plants, these phenolic acids are covalently bound to polysaccharides in cell walls, acting as crosslinkers between the lignins polymers and the hemicellulose and cellulose. Coumaric acid plays a central role in the phenylpropanoid biosynthetic pathway (**Figure 12.4**) which starts from the conversion of phenylalanine to *trans*-cinnamic acid, which subsequently hydroxylates to form *p*-coumaric acid. *p*-Coumaric acid is a precursor of 4-coumaroyl-CoA, which serves as a substrate to form the basic skeleton of all flavonoid derivatives (Nishiyama *et al.* 2010). Coumaric acid could also be used as a precursor in the production of resveratrol in microorganisms (e.g. food-grade yeast *S. cerevisiae*) genetically modified with genes of the phenylpropanoid pathway (Shin *et al.* 2011).

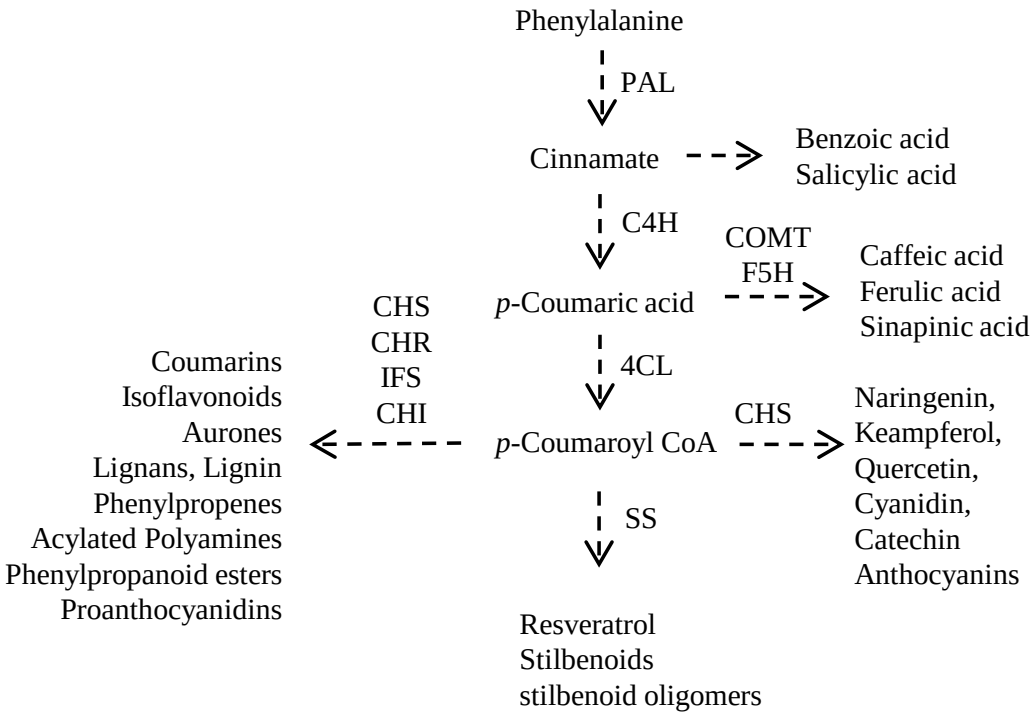

Figure 12.4 Proposed phenylpropanoid biosynthetic pathway in peanut sprouts under food grade fungus *R. oligosporus* stress
PAL, phenylalanine ammonialyase; C4H, cinnamate 4-hydroxylase; F5H, ferulic acid 5-hydroxylase; COMT, caffeic acid *O*-methyltransferase; COA, coenzyme A; 4CL, 4-coumarate:CoA ligase; SS, stilbene synthase; CHS, chalcone synthase; CHR, chalcone reductase; IFS, isoflavone synthase; CHI, chalcone isomerase.

As can be seen in **Figure 12.1** and **Table 12.2**, black peanuts have higher content of phenolic acids, total phenolic (TPC), total flavonoids (TFC) than reddish brown and red peanuts. These translate to its higher ORAC and hydroxyl radical absorbing capacity (HORAC). However, the superoxide radical absorbing capacity (SORAC) and DPPH radical scavenging capacity do not show proportional increase (**Table 12.2**). For ORAC and HORAC values, black peanut (2335 μmol TE/100 g, 651 mg GAE/100 g) has much higher value than that of reddish (1384 μmol TE/100 g, 229 mg GAE/100 g) and red peanuts (690 μmol TE/100 g, 126 mg GAE/100 g). In addition, black peanuts is reported to be rich in mineral elements, such as potassium (7136 μg/g), iron (58.16 μg/g), selenium (14.24 μg/g), and zinc (38.92 μg/g), which are higher than the levels in red peanut (Xin *et al.* 2009). Therefore, black peanuts may have a potential as a new functional food due to its rich mineral contents. The

measured values are found to be smaller than USDA database for TPC and ORAC of peanut raw (U.S. Department of Agriculture 2010). However, these results may be different if the sample is the whole seeds.

Table 12.2 TPC, TFC, ORAC, HORAC, SORAC and DPPH values of ungerminated seed (UG), germinated seed (G) and germinated seed with fungal-stress (GS)

Peanut	Treatment	TPC		TFC		ORAC		HORAC		SORAC		DPPH	
		mean	SD	mean	SD	mean	SD	mean	SD	mean	SD	mean	SD
Black	UG0d	144.8k	3.6	18.54j	0.40	2335.5hi	16.3	651.3b	19.5	54.9h	2.0	3.54n	0.10
	G1d	184.7f	5.6	24.23i	0.89	2279.1i	99.0	594.3c	14.1	30.0k	2.1	6.96hi	0.06
	G2d	165.6hi	6.6	24.58i	1.29	2892.3f	83.4	663.6b	33.7	20.4l	1.1	6.16ijk	0.21
	G3d	174.2gh	7.1	18.93j	0.91	2984.2f	123.6	690.5ab	61.1	12.5l	1.8	5.09kl	0.26
	Mean	174.9		22.64		2718.5		649.5		21.0		6.11	
	GS1d	194.1e	8.6	14.80kl	0.55	2439.6gh	20.3	663.2b	25.1	33.6jk	2.8	6.28ij	0.37
	GS2d	165.8hi	6.2	15.22kl	0.75	3313.3e	122.0	568.8c	31.5	13.9l	0.4	7.69gh	0.62
	GS3d	158.5ij	5.0	15.69kl	0.80	3288.7e	125.9	687.4ab	20.3	14.1l	0.1	5.55jkl	0.20
	Mean	172.8		15.21		3013.9		639.8		20.5		6.52	
Red	UG0d	126.9l	3.4	13.59l	0.51	690.4n	0.9	126.8i	2.3	36.4ijk	1.3	4.87lm	0.21
	G1d	155.8j	2.7	27.25h	0.23	1339.4m	28.9	216.7h	10.8	55.6h	1.1	6.46ij	0.30
	G2d	174.3gh	4.4	36.89f	0.39	1685.2l	54.9	337.0g	23.3	66.3g	3.5	10.36ef	0.10
	G3d	194.1e	8.6	24.77i	0.91	2084.4j	84.9	364.2fg	29.1	37.6ijk	1.3	10.53ef	0.71
	Mean	174.8		29.61		1703.0		306.0		53.1		9.15	
	GS1d	160.1ij	4.8	33.80g	1.61	1393.3m	47.6	235.5h	12.1	42.1ij	2.2	8.71g	0.13
	GS2d	181.1gf	5.7	57.34d	1.16	3580.2d	86.2	381.1f	16.4	250.1b	6.7	18.47c	0.99
	GS3d	228.0b	10.9	75.73c	2.11	4670.6b	155.9	520.6d	41.8	142.0d	12.8	11.44e	0.33
	Mean	189.7		55.67		3214.7		379.1		144.7		12.92	
Reddish brown	UG0d	130.1l	3.0	17.06jk	0.37	1383.6m	60.9	229.5h	5.5	94.3f	4.7	3.90mn	0.08
	G1d	160.6ij	4.0	34.45g	0.89	1914.5k	32.6	357.2fg	29.3	104.6e	5.9	9.78f	0.40
	G2d	194.7e	8.2	44.42e	0.64	2502.4g	18.2	451.9e	16.6	45.5i	2.9	18.79bc	2.00
	G3d	208.4d	5.8	45.98e	0.67	3384.0e	97.9	586.1c	20.2	40.7ij	4.1	12.50d	1.23
	Mean	187.9		41.65		2600.3		465.0		63.6		13.77	
	GS1d	218.5c	10.1	35.96fg	0.61	3360.8e	103.0	369.5fg	25.5	144.1d	6.0	10.86ef	1.03
	GS2d	220.0bc	12.2	95.31b	4.18	3859.2c	134.5	530.9d	17.8	318.5a	18.2	19.70b	1.33
	GS3d	253.2a	5.1	113.35a	4.73	5031.6a	155.9	713.2a	38.8	196.6c	16.1	23.67a	1.26
	Mean	230.5		81.52		4083.9		537.9		219.7		18.13	

The data are expressed as mean ± standard deviation (n = 4), G and GS are measured during the 3 days. The means of treatments are compared by Duncan's multiple range test at $P < 0.05$, different letters show significant differences. TPC values are expressed as gallic acid equivalents (mg GAE/100 g fresh weight sample); TFC values are expressed as catechin equivalents (mg CAE/100 g FW); ORAC values are expressed as Trolox equivalents (μmol TE/100 g FW); HORAC are expressed as mg GAE/100 g FW; SORAC values are expressed as units SOD equivalent/100 g FW; DPPH scavenging capacity values are expressed as mg GAE/100 g FW.

12.3.2 Polyphenolic profiles in germinated peanuts

In this study, a total of 45 compounds (**Table 12.1**) are identified tentatively in the raw GS sprouts (germinating seeds with fungal stress); these include 14 coumaric acid derivatives, 3 ferulic acids, 4 sinapinic acids, 2 hydroxybenzoic acids, 1 caffeic acid, 2 flavonoids and 19 stilbenoids derivatives. Among the metabolites detected, the most abundant compounds are phenolic acid compounds (10 to 32 min, **Figure 12.5, 12.6**) and stilbenoid phytoalexins (32 to 55 min). Both classes of secondary metabolites are receiving considerable attention from producers and consumers due to their antioxidant activity and anti-inflammation activity.

Figure 12.5 presents a comparative HPLC chromatogram between red and black peanuts after 3 days of germination with or without fungal inoculation (G or GS). There are several compounds proposed as phytoalexins that are generated under GS and G such as peak 27 and 28 (isopentadienyl-3,5,4'-trihydroxystilbene), peak 29 (trans-arachidin-3), and peak 30 (trans-resveratrol). In addition, some new phenolic acid derivatives are also produced during G and GS, such as peak 19 (caffeic acid), peak 10 and 20 (hydroxybenzoic acids), as well as catechin (peak 16) and genistein (peak 35) (UV and MS spectra see **Figure 12.2**, **12.3**).

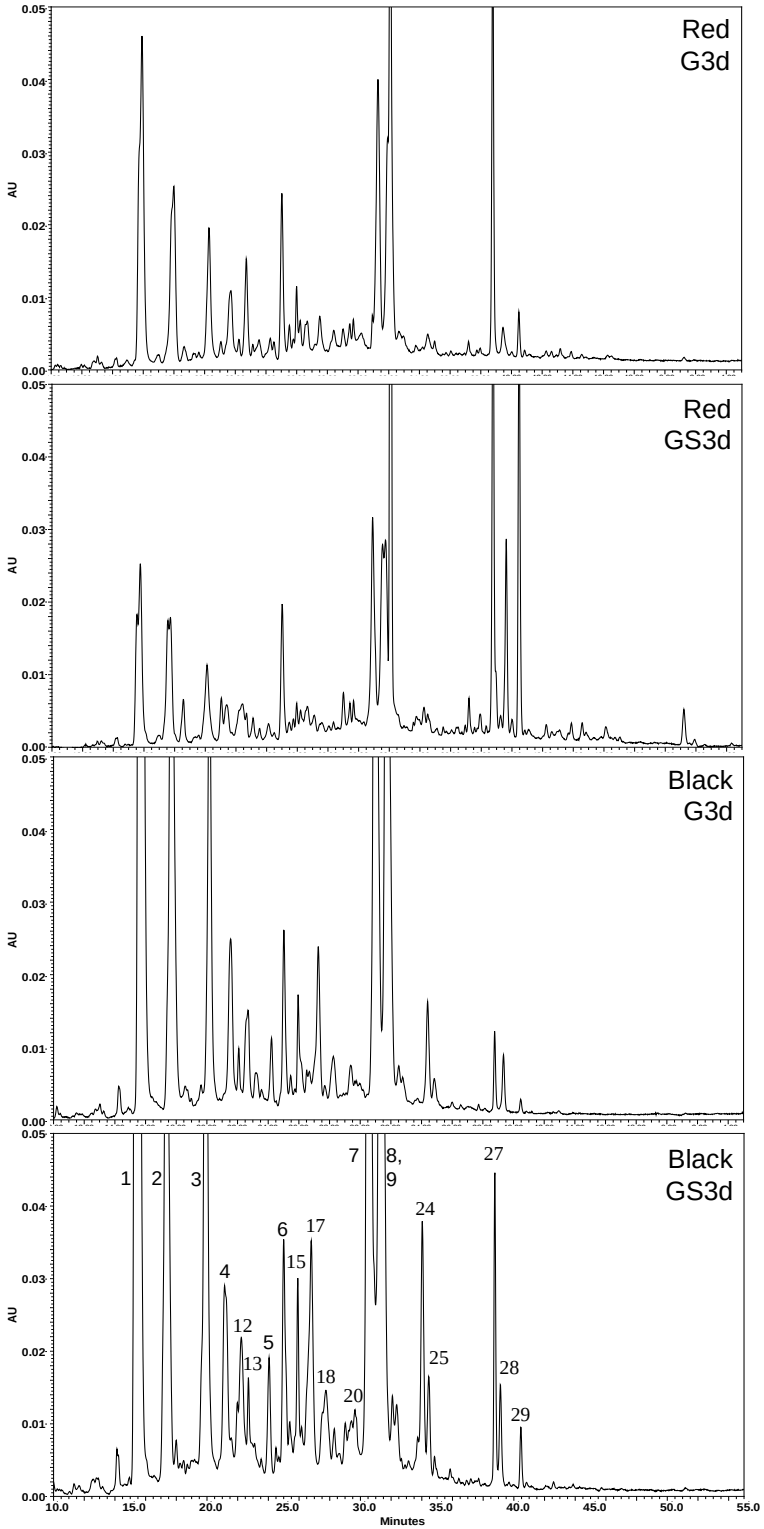

Figure 12.5 Comparative HPLC chromatograms (310 nm) between red and black peanuts after 3 days germination with or without fungal inoculation (G or GS)
The peak assignment of corresponding compounds is presented in **Table 12.1**.

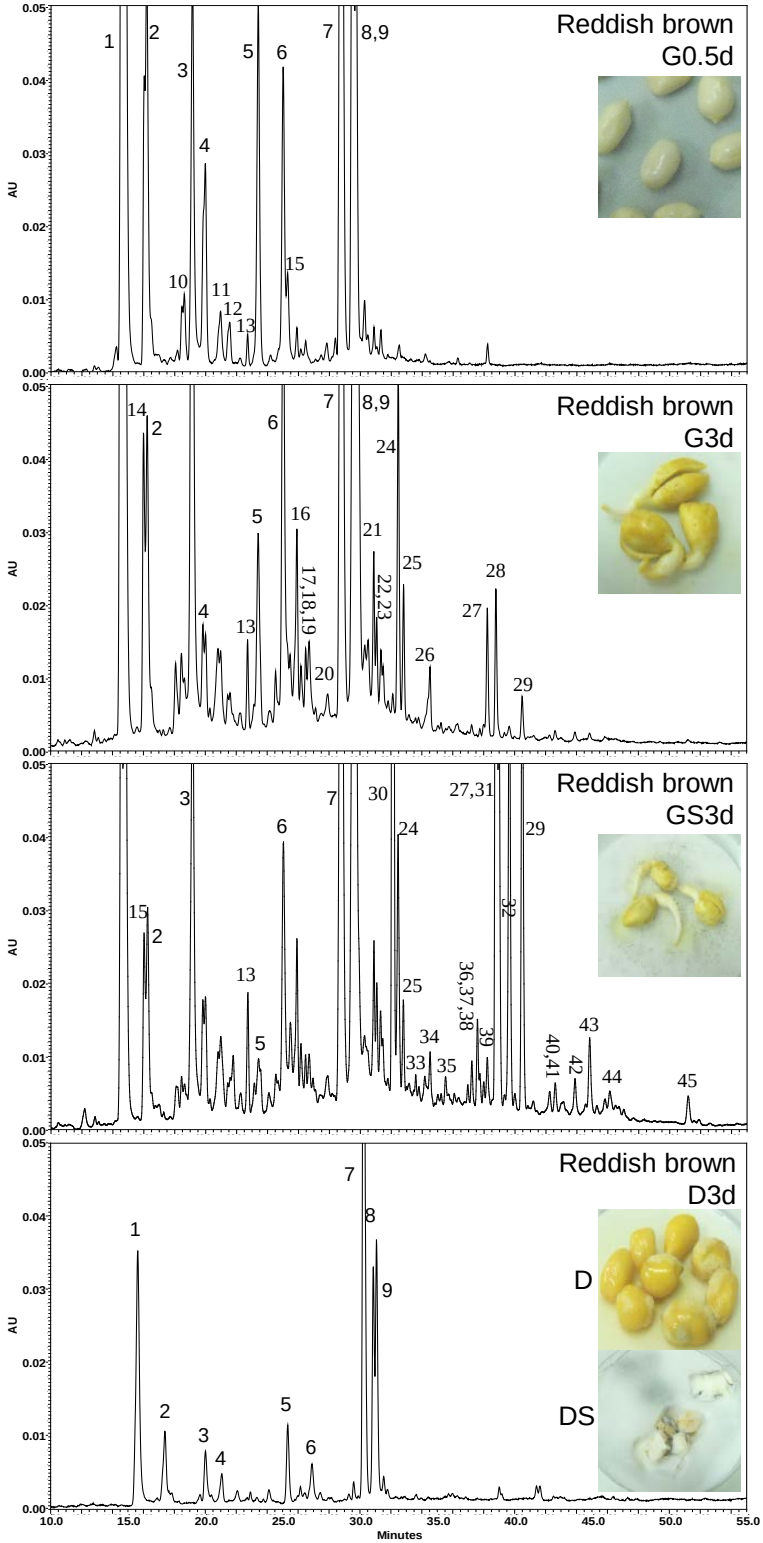

Figure 12.6 HPLC chromatogram (310 nm) of germinated reddish peanut after 12 hours (G0.5d) and 3 days (G3d) without *R. oligosporus* stress, 3 days with the fungal stress (GS3d), and thermal-deactivated seeds inoculated without (D) or with (DS) fungal stress for 3 days.
The peak assignment is shown in **Table 12.1**.

Figure 12.6 shows HPLC chromatogram of germinated reddish peanut after 12 hours (G0.5d) and 3 days (G3d) without *R. oligosporus* stress, 3 days with the fungal

stress (GS3d), and thermal-deactivated seeds inoculated without (D) or with (DS) fungal stress for 3 days (D3d). To confirm whether these newly released compounds are produced by fungi themselves or by peanuts in response to the fungal action, the D3d peanuts are analysed and it is found that these compounds are not present. Thus, I conclude that the 19 stilbenoids are phytoalexins produced by the peanuts during the germination under fungal stress. In addition, I found that there is a significant decrease in phenolic acid compounds in deactivated peanut after 3 days (**Figure 12.6**) in comparison to the ungerminated seeds. However, not much difference is found in the phytochemicals between the deactivated peanut with or without fungal inoculation (data not shown). This suggests that thermal processing could reduce phenolic acid compounds.

Overall, among the three peanuts, the maximum changes in the production of phytochemicals are observed in reddish brown peanuts during G and GS, followed by red peanuts, while black peanuts seemed to have little change from the HPLC analysis as shown in **Figure 12.1**, **12.5**, **12.6**. For red peanuts, G and GS could increase polyphenolic compounds and concentrations, which may be responsible for the significant increase in TPC, TFC, ORAC, HORAC, SORAC and DPPH values in the corresponding seeds (**Table 12.2**). For TPC in GS reddish peanut, the maximum value is 230 mg GAE/100 g FW, which is 1.8 times higher than that of ungerminated seed. Similarly, TFC maximum value is 81 mg CAE/100g FW in GS reddish peanut, an increase of 4.8 times, ORAC is 4084 μmol TE/100 g FW or 2.9 times, SORAC is 220 units SOD equivalent/100 g FW or 2.3 times, and DPPH is 18 mg GAE/100 g FW or 4.6 times. However, for HORAC, the maximum value belongs to ungerminated black peanut (651 mg GAE/100 g FW) which is higher than that of GS reddish peanut (538 mg GAE/100 g FW).

The sprouts from mung bean and yellow soybean are the most popular traditional food. ORAC of mung bean and yellow soybean sprout obtained from a supermarket in Singapore were 1606 and 3126 µmol TE/100g FW respectively (Isabelle *et al.* 2009), and soybean sprout is 962 µmol TE/100g FW (U.S. Department of Agriculture 2010). In this study, the ORAC of GS peanut sprouts was 4084 µmol TE/100 g FW. Peanut sprouts are not a typical food item in this part of the world although they may have some health benefits due to the unique phytoalexin contents.

12.3.3 Phytoalexins in germinated peanuts

In order to identify the possible phytoalexins generated, the phenolic acids and fats are removed by a traditional silica column chromatography with hexane and ethyl acetate (see method section). The HPLC chromatogram of phytoalexins is shown in **Figure 12.7** and their LC retention time, maximum UV absorption, fragment ion masses in positive-ion ($[M+H]^+$) and negative-ion ($[M–H]^-$) mode are listed in **Table 12.3**.

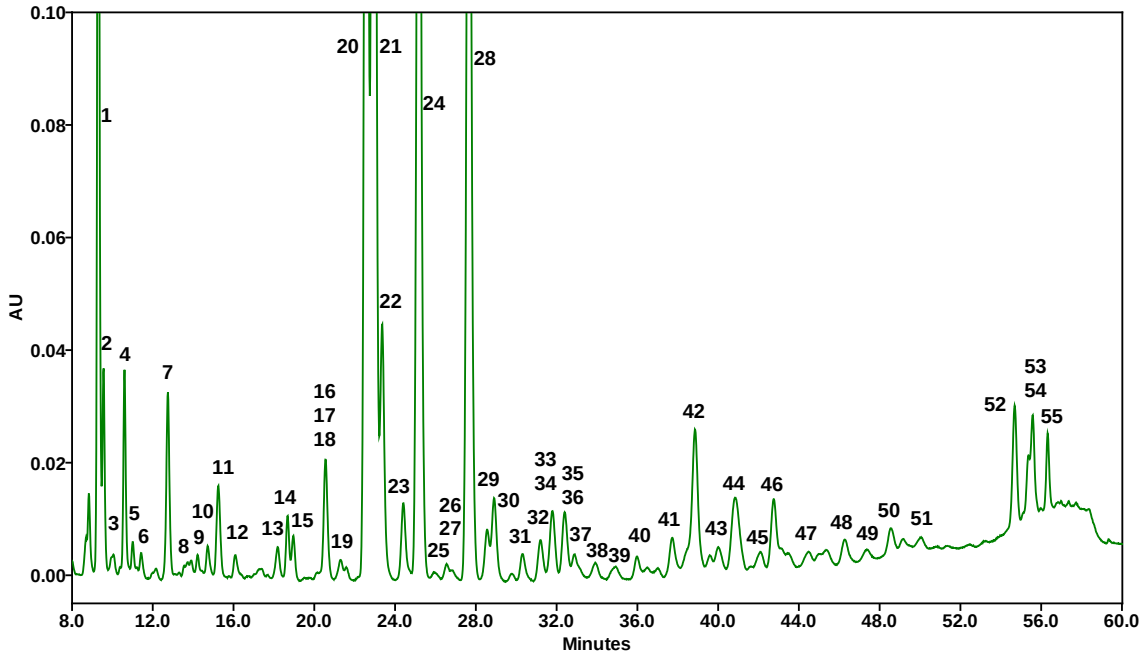

Figure 12.7 HPLC chromatogram (310 nm) of peanut phytoalexins in peanut sprouts under food grade fungus *R. oligosporus* stress
The tentative identification of corresponding compounds is listed in **Table 12.3**.

Table 12.3 Peak assignment of proposed phytoalexins in GS peanut sprouts presented according to retention time, maximum UV absorption and molecular ions

Peak	LC-RT (min)	Tentative identification	PDA UV bands (nm)	ESI+ $[M+H]^+$	ESI– $[M–H]^-$
1	8.92	*trans*-Resveratrol	307, 320		227
2	9.12	Arachidin 2 derivative 1	326	297	295, 457
3	9.5	Arahypin 2 derivative 1		331	329
4	10.1	Arachidin 3 derivative 1	338	297	295, 457
5	10.4	Arahypin 4 derivative 1		311, 313	295, 315, 325
6	10.8	Cyanidin	280	287	285
7	12.1	Naringenin	277		271
8	12.8	Arahypin 2/3 derivatives 1		331	329
9	13.5	Hesperetin	289		301
10	14.0	Chiricanine A derivative 1	308	225, 281	223, 227, 279, 453
11	14.6	Unknown	260		299
12	15.3	Arahypin 1 derivative 1		281	225, 279
13	17.4	SB 1 derivative 1	260, 357	345	299, 329, 343, 389
14	17.8	SB 1 derivative 2	262, 360	465	299, 343, 361
15	18.2	Arahypin 3 derivative 1	300		329
16	19.8	Arachidin 2 derivatives 2	322	297	295
17	19.8	Aracarpene	322	301	299
18	19.8	Arachidin 1 derivatives 3	322	313	311
19	20.6	Acacetin	332		283
20	21.8	Arachidin 1 derivative 4	343	313	311
21	22.2	3'-Isopentadienyl-3,5,4'-trihydroxystilbene derivative 1	296	295	293
22	22.6	Arachidin 2 derivatives 3	324	297	295
23	23.6	Arachidin 1 derivatives 5	346	309, 311, 313	309
24	24.4	Arachidin 2 derivative 4	326	297	295
25	25.1	Arahypin 7 derivatives 1		623	621
26	25.8	Arachidin 2 derivatives 5		297	295
27	25.8	Arachidin 1 derivatives 6		313	311
28	26.9	Arachidin 3 derivative 2	337	297, 591	295, 589
29	27.7	Unknown	345		325
30	28.1	3'-Isopentadienyl-3,5,4'-trihydroxystilbene derivative 2	296		295, 355
31	29.5	Arahypin 7 derivative 2	331	311	311, 621
32	30.4	Arahypin 6 derivative 1	276, 320	607	605
33	31.1	Arahypin 5 derivative 1	341	238	293
34	31.1	Arahypin 4 derivative 2	341	238	313
35	31.6	Arachidin 1 derivatives 7	328	313	311
36	31.6	SB 1 derivatives	328		343
37	32.3	Arahypin derivatives 1	340	394, 667	313, 619
38	33.3	Arahypin 7 derivatives 3	335	623	621
39	34.4	Dimeric stilbenoids derivatives 1	330	605	311, 603, 621
40	35.5	Dimeric stilbenoids derivatives 2	333	603, 621, 623	311, 619, 621
41	37.4	Dimeric stilbenoids derivatives 3	335	311, 621, 623	309, 311, 603, 619, 621
42	38.5	Arahypin 7 derivative 4	262, 347	623	621
43	39.6	Arahypin 6 derivatives 2		607	605
44	40.4	Arahypin derivatives	324	621, 623	295, 327, 619, 621
45	42.0	Arahypin 6 derivatives 3		607	605
46	42.6	Arahypin 6 derivative 4	269, 345	607	605
47	44.0	Arahypin 6 derivatives 5		311	605
48	46.2	Arachidin 2 derivatives 6	324	589, 591	295, 587, 592
49	47.0	Dimeric stilbenoids derivatives 4		299	297, 621, 653
50	48.6	Dimeric stilbenoids derivatives 5	341	623	311, 621, 657
51	50.1	Arachidin 2 derivatives 7		399, 631	295, 587
52	54.4	13-Z,E-KODE	279	195, 249, 295	293
53	55.2	13-E,E-KODE	279	195, 249, 296	293
54	55.2	9-E,Z-KODE	279	199, 249, 295	293
55	56	9-E,E-KODE	276	199, 249, 295	293

In total, there are 55 compounds detected. 45 of these compounds are suggested to be stilbenoid phytoalexin derivatives, 3 flavonoids (cyanidin, peak 6; naringenin, peak 7; hesperetin, peak 9), 2 unknown compounds (peak 11 and 29), 4 oxooctadecadienic acids (KODEs, peak 52–55) and 1 peanut pterocarpanoid phytoalexin – aracarpene (peak 17) (Sobolev *et al.* 2010b). Furthermore, resveratrol (peak 1), arachidin 1 (peak 20), isopentadienyl-3,5,4'-trihydroxystilbene (peak 21), arachidin 2 (peak 24) and arachidin 3 (peak 28) are at concentrations that are among the most abundant in GS peanuts.

It has been reported that Georgia Green peanut kernel, when challenged by *Aspergillus flavus* produced the highest level of resveratrol (2.91 mg/g) at 48 h, while SB-1 concentration (4.51 mg/g) peaked at 72 h (Sobolev *et al.* 2006), higher phytoalexin concentrations are accumulated with longer incubation times (Sobolev *et al.* 2007). Prior reports showed that germination increased amino acids, sucrose and glucose contents of peanut kernels. This might improve sprout taste and flavor preference (Wang *et al.* 2005). Peanut sprout are prone to be colonized by *A. flavus* and *A. parasiticus* since the germinating condition is generally under high temperature and moisture. The fungi can generate aflatoxins, thus, rendering the resulting peanut toxic, a major concern to consumers. *In vivo* toxicological and nutraceutical assessments of peanut sprouts revealed no obvious growth hazard or health toxicity in female Sprague-Dawley rats, which were fed with basal diets supplemented with different amounts of peanut sprouts for 18 weeks (Lin *et al.* 2008a).

Peanuts are prone to form stilbenoid phytoalexins under stresses. Reported phytoalexins include arachidin 1-3, 3'-isopentadienyl-3,5,4'-trihydroxystilbene, SB-1, chiricanine A, arahypin 1-7 (Sobolev *et al.* 2006; Sobolev *et al.* 2007; Sobolev *et al.*

2009; Sobolev *et al.* 2010a). However, more than 1000 stilbenoids including monomeric stilbenes, bibenzyls, bisbibenzyls, phenanthrenoids, stilbene oligomers and other stilbenoids have been found in plants. Over 400 monomeric and oligomeric stilbenes have been isolated (Shen *et al.* 2009). These stilbenoid phytoalexin resveratrol and their derivatives have received marvelous attention over the past decade because of the tremendous number of reports highlighting their benefits. *In vitro* and *in vivo* studies of using various human disease models have demonstrated diverse bioactivities, including antioxidant, antimicrobial, antimalarial, anti-inflammatory properties, cardio- and neuroprotection, immune regulation, cancer chemoprevention and lifespan extension (Baur *et al.* 2006; Baur & Sinclair 2006; Pervaiz & Holme 2009; Fulda 2010). Furthermore, its potential therapeutic value has significantly promoted the study of this class of compounds in various plants around the world.

12.4 Conclusion

The HPLC-PDA and LC-ESI-MS based approach is important in the metabolic profiling of peanuts due to the highly diverse phytochemicals present. The objective of a 'non-targeted' metabolic profiling analysis is to determine the most detectable metabolites in the acetone/ethanol/water extracts of the three peanuts. A total of 45 compounds in raw sprouts (mainly phenolic acids) and approximately 50 phytoalexins in re-extracted GS reddish brown peanut are detected on the basis of their chromatographic retention, UV absorption, positive and negative MS fragments, and data from the literature. In addition, G or GS peanut sprouts produce much higher concentrations of phenolic acids, their derivatives and phytoalexins, along with higher TPC, TFC, ORAC, HORAC, SORAC and DPPH values than peanut seeds. Present

results form a basis for further study to examine the potential of stress germinated peanuts as source of complex phytoalexins that are otherwise hard to obtain in large quantity.

Chapter 13

CONCLUSIONS AND FUTURE OUTLOOK

In the Part II, I investigated the phytochemical changes in food legume seeds under ungermination, germination, and germination with fungus *R. oligoporus* stress. Thirteen selected legumes are studied, including sword bean, big red bean, black-eyed bean, brown bean, small red bean, white bean, green bean, broad bean, yellow bean, black bean, big peanut, small peanut and chick pea. The results showed that germination could enhance the generation of phytochemicals in most legumes and fungus-stressed germination can release some novel phytoalexins in several legume sprouts, such as sword bean, soybeans and peanuts (**Chapter 10**).

Furthermore, germination increased TPC and antioxidant capacity of most seeds. Particularly in chickpea seeds, the isoflavone contents increased by over 100 fold, mainly due to increase of formononetin and biochanin A level. Germination could significantly increase isoflavonoids diversity. Twenty-five isoflavonoids were detected and identified tentatively. These include 20 isoflanones, 2 isoflavanones and 3 pterocarpan phytoalexins. Total isoflavonoid content of germinated chickpea was approximately 5-fold of that of germinated soybean (**Chapter 11**).

In addition, the effects of food grade fungus *R. oligosporus* stress on phytochemicals and phytoalexins of germinating peanut seeds were investigated by comparing the metabolic profiles of ungerminated (UG), germinated (G) and germinated seeds under fungal stress (GS). Current results showed that phenolic acids (coumaric, sinapinic and ferulic acids derivatives) were the major group of phenolic compounds in ungerminated seeds. G or GS increased the level of phenolic acids,

phytoalexins, and antioxidant capacity values in reddish and red peanuts, but not in black peanuts. 45 compounds were identified tentatively in the peanut sprouts, including 14 coumaric acids, 3 ferulic acids, 4 sinapinic acids, 2 hydroxybenzoic acids, 1 caffeic acid, 2 flavonoids and 19 stilbenoids derivatives. Reddish brown peanut sprouts produced the highest amount of phytoalexins after GS with 55 compounds detected. Forty five of these compounds were suggested as stilbenoid phytoalexins derivatives (**Chapter 12**).

Overall, this study suggested that germination or food grade fungal stressed germination of legume seeds might be used as a processing method to induce phytoalexins and enhance production of polyphenolic antioxidants, which are proven to have many health enhancing benefits (e.g. antioxidant, anti-inflammation, anti-cancer, anti-obesity, and anti-aging).

In the future study, more plant seeds, not only the legume seeds can be investigated by the novel processing method. Furthermore, food grade probiotics including bacteria (*Lactobacillus plantarum*, *Bacillus subtilis var natto*, *lactobacillus. acidophilus*) and fungus (*S. cerevisiae*, *R. oligosporus*) are promising inducer. The probiotic when administered in adequate amounts confer a health benefit for human, and also be found as part of a variety of naturally fermented legume foods, such as soy yogurt, natto, tempeh and kefir. With potential bioactivities associated with the generated phytoalexins in the seeds, it is promising to explore new pathways for functional food and nutritional supplement development, as well as for food waste utilization.

BIBLIOGRAPHY

Abad-Garcia B, Berrueta LA, Garmon-Lobato S, Gallo B, Vicente F (2009). A general analytical strategy for the characterization of phenolic compounds in fruit juices by high-performance liquid chromatography with diode array detection coupled to electrospray ionization and triple quadrupole mass spectrometry. *Journal of Chromatography A*. **1216**, 5398-5415.

Adams JD, Wang R, Yang J, Lien EJ (2006). Preclinical and clinical examinations of *Salvia miltiorrhiza* and its tanshinones in ischemic conditions. *Chinese Medicine*. **1**, 1-15.

Aguilaniu H, Gustafsson L, Rigoulet M, Nystrom T (2003). Asymmetric inheritance of oxidatively damaged proteins during cytokinesis. *Science*. **299**, 1751-1753.

Allen C, Buttner S, Aragon AD, Thomas JA, Meirelles O, Jaetao JE, Benn D, Ruby SW, Veenhuis M, Madeo F, Werner-Washburne M (2006). Isolation of quiescent and nonquiescent cells from yeast stationary-phase cultures. *Journal of Cell Biology*. **174**, 89-100.

Alvers AL, Fishwick LK, Wood MS, Hu D, Chung HS, Dunn WA, Jr., Aris JP (2009a). Autophagy and amino acid homeostasis are required for chronological longevity in *Saccharomyces cerevisiae*. *Aging Cell*. **8**, 353-369.

Alvers AL, Wood MS, Hu D, Kaywell AC, Dunn WA, Jr., Aris JP (2009b). Autophagy is required for extension of yeast chronological lifespan by rapamycin. *Autophagy*. **5**, 847-849.

Anderson RM, Bitterman KJ, Wood JG, Medvedik O, Sinclair DA (2003). Nicotinamide and PNC1 govern lifespan extension by calorie restriction in *Saccharomyces cerevisiae*. *Nature*. **423**, 181-185.

Anisimov VN, Berstein LM, Egormin PA, Piskunova TS, Popovich IG, Zabezhinski MA, Kovalenko IG, Poroshina TE, Semenchenko AV, Provinciali M, Re F, Franceschi C (2005). Effect of metformin on life span and on the development of spontaneous mammary tumors in HER-2/neu transgenic mice. *Experimental Gerontology*. **40**, 685-693.

Anisimov VN, Berstein LM, Egormin PA, Piskunova TS, Popovich IG, Zabezhinski MA, Tyndyk ML, Yurova MV, Kovalenko IG, Poroshina TE, Semenchenko AV (2008). Metformin slows down aging and extends life span of female SHR mice. *Cell Cycle*. **7**, 2769-2773.

Anisimov VN, Berstein LM, Popovich IG, Zabezhinski MA, Egormin PA, Piskunova TS, Semenchenko AV, Tyndyk ML, Yurova MN, Kovalenko IG, Poroshina TE (2011a). If started early in life, metformin treatment increases life span and postpones tumors in female SHR mice. *Aging (Albany NY)*. **3**, 148-157.

Anisimov VN, Egormin PA, Piskunova TS, Popovich IG, Tyndyk ML, Yurova MN, Zabezhinski MA, Anikin IV, Karkach AS, Romanyukha AA (2010a). Metformin extends life span of HER-2/neu transgenic mice and in combination with melatonin inhibits growth of transplantable tumors in vivo. *Cell Cycle*. **9**, 188-197.

Anisimov VN, Piskunova TS, Popovich IG, Zabezhinski MA, Tyndyk ML, Egormin PA, Yurova MV, Rosenfeld SV, Semenchenko AV, Kovalenko IG, Poroshina TE, Berstein LM (2010b). Gender differences in metformin effect on aging, life span and spontaneous tumorigenesis in 129/Sv mice. *Aging (Albany NY)*. **2**, 945-958.

Anisimov VN, Zabezhinski MA, Popovich IG, Piskunova TS, Semenchenko AV, Tyndyk ML, Yurova MN, Antoch MP, Blagosklonny MV (2010c). Rapamycin extends maximal lifespan in cancer-prone mice. *American Journal of Pathology*. **176**, 2092-2097.

Anisimov VN, Zabezhinski MA, Popovich IG, Piskunova TS, Semenchenko AV, Tyndyk ML, Yurova MN, Rosenfeld SV, Blagosklonny MV (2011b). Rapamycin increases lifespan and inhibits spontaneous tumorigenesis in inbred female mice. *Cell Cycle*. **10**, 4230-4236.

Aragon AD, Rodriguez AL, Meirelles O, Roy S, Davidson GS, Tapia PH, Allen C, Joe R, Benn D, Werner-Washburne M (2008). Characterization of differentiated quiescent and nonquiescent cells in yeast stationary-phase cultures. *Molecular Biology of the Cell*. **19**, 1271-1280.

Armero J, Requejo R, Jorrin J, Lopez-Valbuena R, Tena M (2001). Release of phytoalexins and related isoflavonoids from intact chickpea seedlings elicited with reduced glutathione at root level. *Plant Physiology and Biochemistry*. **39**, 785-795.

Arts I, Hollman P (2005). Polyphenols and disease risk in epidemiologic studies. *American journal of clinical nutrition*. **81**, 317S.

Baş D, Boyacı İH (2007). Modeling and optimization I: Usability of response surface methodology. *Journal of Food Engineering*. **78**, 836-845.

Bass TM, Weinkove D, Houthoofd K, Gems D, Partridge L (2007). Effects of resveratrol on lifespan in *Drosophila melanogaster* and *Caenorhabditis elegans*. *Mechanisms of Ageing and Development*. **128**, 546-552.

Bauer JH, Goupil S, Garber GB, Helfand SL (2004). An accelerated assay for the identification of lifespan-extending interventions in *Drosophila melanogaster*. *Proceedings of the National Academy of Sciences of the United States of America*. **101**, 12980-12985.

Baur JA, Pearson KJ, Price NL, Jamieson HA, Lerin C, Kalra A, Prabhu VV, Allard JS, Lopez-Lluch G, Lewis K, Pistell PJ, Poosala S, Becker KG, Boss O, Gwinn D, Wang M, Ramaswamy S, Fishbein KW, Spencer RG, Lakatta EG, Le Couteur D, Shaw RJ, Navas P, Puigserver P, Ingram DK, de Cabo R, Sinclair DA (2006). Resveratrol improves health and survival of mice on a high-calorie diet. *Nature*. **444**, 337-342.

Baur JA, Sinclair DA (2006). Therapeutic potential of resveratrol: the in vivo evidence. *Nature Reviews Drug Discovery*. **5**, 493-506.

Bishop NA, Guarente L (2007). Genetic links between diet and lifespan: shared mechanisms from yeast to humans. *Nature Reviews Genetics*. **8**, 835-844.

Bjedov I, Toivonen JM, Kerr F, Slack C, Jacobson J, Foley A, Partridge L (2010). Mechanisms of life span extension by rapamycin in the fruit fly *Drosophila melanogaster*. *Cell Metabolism*. **11**, 35-46.

Boer VM, Amini S, Botstein D (2008). Influence of genotype and nutrition on survival and metabolism of starving yeast. *Proceedings of the National Academy of Sciences of the United States of America*. **105**, 6930-6935.

Bonilla E, Contreras R, Medina-Leendertz S, Mora M, Villalobos V, Paz M, Teran R, Bravo Y (2012). Manganese toxicity in *Drosophila melanogaster*: extension of the life span by resveratrol. *Toxicological & Environmental Chemistry*. **94**, 742-747.

Boue S, Cleveland T, Carter-Wientjes C, Shih B, Bhatnagar D, McLachlan J, Burow M (2009). Phytoalexin-enriched functional foods. *Journal of Agricultural and Food Chemistry*. **57**, 2614.

Burstein MT, Kyryakov P, Beach A, Richard VR, Koupaki O, Gomez-Perez A, Leonov A, Levy S, Noohi F, Titorenko VI (2012). Lithocholic acid extends longevity of chronologically aging yeast only if added at certain critical periods of their lifespan. *Cell Cycle*. **11**, 3443-3462.

Burtner CR, Murakami CJ, Kaeberlein M (2009a). A genomic approach to yeast chronological aging. *Methods in Molecular Biology*. **548**, 101-114.

Burtner CR, Murakami CJ, Kennedy BK, Kaeberlein M (2009b). A molecular mechanism of chronological aging in yeast. *Cell Cycle*. **8**, 1256-1270.

Cabreiro F, Au C, Leung KY, Vergara-Irigaray N, Cocheme HM, Noori T, Weinkove D, Schuster E, Greene ND, Gems D (2013). Metformin Retards Aging in *C. elegans* by Altering Microbial Folate and Methionine Metabolism. *Cell*. **153**, 228-239.

Calabrese EJ, Baldwin LA (2003). Hormesis: the dose-response revolution. *Annual Review of Pharmacology and Toxicology*. **43**, 175-197.

Canuelo A, Gilbert-Lopez B, Pacheco-Linan P, Martinez-Lara E, Siles E, Miranda-Vizuete A (2012). Tyrosol, a main phenol present in extra virgin olive oil, increases lifespan and stress resistance in *Caenorhabditis elegans*. *Mechanisms of Ageing and Development*. **133**, 563-574.

Cevallos-Casals B, Cisneros-Zevallos L (2009). Impact of germination on phenolic content and antioxidant activity of 13 edible seed species. *Food Chemistry*. **119**, 1485-1490

Chalkiadaki A, Guarente L (2012). Sirtuins mediate mammalian metabolic responses to nutrient availability. *Nature Reviews Endocrinology*. **8**, 287-296.

Chen W, Liu L, Luo Y, Odaka Y, Awate S, Zhou H, Shen T, Zheng S, Lu Y, Huang S (2012). Cryptotanshinone activates p38/JNK and inhibits Erk1/2 leading to caspase-independent cell death in tumor cells. *Cancer Prevention Research*. **5**, 778-787.

Chen WX, Luo Y, Liu L, Zhou HY, Xu BS, Han XZ, Shen T, Liu ZJ, Lu Y, Huang SL (2010). Cryptotanshinone inhibits cancer cell proliferation by suppressing mammalian target of rapamycin-mediated cyclin D1 expression and Rb phosphorylation. *Cancer Prevention Research*. **3**, 1015-1025.

Cherif M, Arfaoni A, Khaiem A (2007). Phenolic compounds and their role in biocontrol and resistance of chickpea to fungal pathogenic attacks. *Tunisian Journal of Plant Protection*. **2**, 7.

Colman RJ, Anderson RM, Johnson SC, Kastman EK, Kosmatka KJ, Beasley TM, Allison DB, Cruzen C, Simmons HA, Kemnitz JW, Weindruch R (2009). Caloric restriction delays disease onset and mortality in rhesus monkeys. *Science*. **325**, 201-204.

Comas M, Toshkov I, Kuropatwinski KK, Chernova OB, Polinsky A, Blagosklonny MV, Gudkov AV, Antoch MP (2012). New nanoformulation of rapamycin Rapatar extends lifespan in homozygous p53-/- mice by delaying carcinogenesis. *Aging (Albany NY)*. **4**, 715-722.

Correa C, Li L, Aldini G, Carini M, Chen C, Chun H, Cho S, Park K, Russell R, Blumberg J (2010). Composition and stability of phytochemicals in five varieties of black soybeans (*Glycine max*). *Food Chemistry*. **123**, 1176–1184.

Couzin-Frankel J (2011). Genetics. Aging genes: the sirtuin story unravels. *Science*. **334**, 1194-1198.

Crespo JL, Hall MN (2002). Elucidating TOR signaling and rapamycin action: lessons from *Saccharomyces cerevisiae*. *Microbiology and Molecular Biology Reviews*. **66**, 579-591.

da Luz PL, Tanaka L, Brum PC, Dourado PM, Favarato D, Krieger JE, Laurindo FR (2012). Red wine and equivalent oral pharmacological doses of resveratrol delay vascular aging but do not extend life span in rats. *Atherosclerosis*. **224**, 136-142.

Danbolt NC (2001). Glutamate uptake. *Progress in Neurobiology*. **65**, 1-105.

Daniel S, Tiemann K, Wittkampf U, Bless W, Hinderer W, Barz W (1990). Elicitor-induced metabolic changes in cell-cultures of chickpea (*Cicer-Arietinum* L) cultivars resistant and susceptible to ascochyta-rabiei. 1. Investigations of enzyme-activities involved in isoflavone and pterocarpan phytoalexin biosynthesis. *Planta*. **182**, 270-278.

Defossez PA, Prusty R, Kaeberlein M, Lin SJ, Ferrigno P, Silver PA, Keil RL, Guarente L (1999). Elimination of replication block protein Fob1 extends the life span of yeast mother cells. *Molecular Cell*. **3**, 447-455.

Dever TE, Hinnebusch AG (2005). GCN2 whets the appetite for amino acids. *Molecular Cell*. **18**, 141-142.

Ding MZ, Tian HC, Cheng JS, Yuan YJ (2009). Inoculum size-dependent interactive regulation of metabolism and stress response of *Saccharomyces cerevisiae* revealed by comparative metabolomics. *Journal of Biotechnology*. **144**, 279-286.

Dixon RA, Achnine L, Kota P, Liu CJ, Reddy MS, Wang L (2002). The phenylpropanoid pathway and plant defence-a genomics perspective. *Molecular Plant Pathology*. **3**, 371-390.

Don MJ, Liao JF, Lin LY, Chiou WF (2007). Cryptotanshinone inhibits chemotactic migration in macrophages through negative regulation of the PI3K signaling pathway. *British Journal of Pharmacology*. **151**, 638-646.

Du H, Huang YB, Tang YX (2010). Genetic and metabolic engineering of isoflavonoid biosynthesis. *Applied Microbiology and Biotechnology*. **86**, 1293-1312.

Eisenberg T, Knauer H, Schauer A, Buttner S, Ruckenstuhl C, Carmona-Gutierrez D, Ring J, Schroeder S, Magnes C, Antonacci L, Fussi H, Deszcz L, Hartl R, Schraml E, Criollo A, Megalou E, Weiskopf D, Laun P, Heeren G, Breitenbach M, Grubeck-Loebenstein B, Herker E, Fahrenkrog B, Frohlich KU, Sinner F, Tavernarakis N, Minois N, Kroemer G, Madeo F (2009). Induction of autophagy by spermidine promotes longevity. *Nature Cell Biology*. **11**, 1305-1314.

Elshorbagy AK, Valdivia-Garcia M, Refsum H, Smith AD, Mattocks DA, Perrone CE (2010). Sulfur amino acids in methionine-restricted rats: hyperhomocysteinemia. *Nutrition*. **26**, 1201-1204.

Fabrizio P, Battistella L, Vardavas R, Gattazzo C, Liou LL, Diaspro A, Dossen JW, Gralla EB, Longo VD (2004). Superoxide is a mediator of an altruistic aging program in *Saccharomyces cerevisiae*. *Journal of Cell Biology*. **166**, 1055-1067.

Fabrizio P, Gattazzo C, Battistella L, Wei M, Cheng C, McGrew K, Longo VD (2005). Sir2 blocks extreme life-span extension. *Cell*. **123**, 655-667.

Fabrizio P, Hoon S, Shamalnasab M, Galbani A, Wei M, Giaever G, Nislow C, Longo VD (2010). Genome-wide screen in *Saccharomyces cerevisiae* identifies vacuolar protein sorting, autophagy, biosynthetic, and tRNA methylation genes involved in life span regulation. *PLoS Genetics*. **6**, e1001024.

Fabrizio P, Liou LL, Moy VN, Diaspro A, Valentine JS, Gralla EB, Longo VD (2003). SOD2 functions downstream of Sch9 to extend longevity in yeast. *Genetics*. **163**, 35-46.

Fabrizio P, Longo VD (2003). The chronological life span of *Saccharomyces cerevisiae*. *Aging Cell*. **2**, 73-81.

Fabrizio P, Longo VD (2008). Chronological aging-induced apoptosis in yeast. *Biochimica et Biophysica Acta*. **1783**, 1280-1285.

Fabrizio P, Pozza F, Pletcher SD, Gendron CM, Longo VD (2001). Regulation of longevity and stress resistance by Sch9 in yeast. *Science*. **292**, 288-290.

Fanson BG, Weldon CW, Perez-Staples D, Simpson SJ, Taylor PW (2009). Nutrients, not caloric restriction, extend lifespan in Queensland fruit flies (*Bactrocera tryoni*). *Aging Cell*. **8**, 514-523.

Feng S, Saw C, Lee Y, Huang D (2007). Fungal-stressed germination of black soybeans leads to generation of oxooctadecadienoic acids in addition to glyceollins. *Journal of Agricultural and Food Chemistry*. **55**, 8589-8595.

Feng S, Saw C, Lee Y, Huang D (2008). Novel process of fermenting black soybean [*Glycine max* (L.) Merrill] yogurt with dramatically reduced flatulence-causing oligosaccharides but enriched soy phytoalexins. *Journal of Agricultural and Food Chemistry*. **56**, 10078-10084.

Finkel T, Holbrook N (2000). Oxidants, oxidative stress and the biology of ageing. *Nature*. **408**, 239-247.

Fontana L, Partridge L, Longo VD (2010). Extending healthy life span--from yeast to humans. *Science*. **328**, 321-326.

Francisco M, Resurreccion A (2008). Functional components in peanuts. *Critical reviews in food science and nutrition*. **48**, 715-746.

Fulda S (2010). Resveratrol and derivatives for the prevention and treatment of cancer. *Drug Discovery Today*. **15**, 757-765.

Gallinetti J, Harputlugil E, Mitchell JR (2013). Amino acid sensing in dietary-restriction-mediated longevity: roles of signal-transducing kinases GCN2 and TOR. *Biochemical Journal*. **449**, 1-10.

Gems D, Partridge L (2008). Stress-response hormesis and aging. *Cell Metabolism*. **7**, 200-203.

Genade T, Lang DM (2013). Resveratrol extends lifespan and preserves glia but not neurons of the *Nothobranchius guentheri* optic tectum. *Experimental Gerontology*. **48**, 202-212.

Ghavidel R, Prakash J (2007). The impact of germination and dehulling on nutrients, antinutrients, in vitro iron and calcium bioavailability and in vitro starch and protein digestibility of some legume seeds. *LWT-Food Science and Technology*. **40**, 1292-1299.

Goldberg AA, Bourque SD, Kyryakov P, Gregg C, Boukh-Viner T, Beach A, Burstein MT, Machkalyan G, Richard V, Rampersad S, Cyr D, Milijevic S, Titorenko VI (2009). Effect of calorie restriction on the metabolic history of chronologically aging yeast. *Experimental Gerontology*. **44**, 555-571.

Goldberg AA, Richard VR, Kyryakov P, Bourque SD, Beach A, Burstein MT, Glebov A, Koupaki O, Boukh-Viner T, Gregg C, Juneau M, English AM, Thomas DY, Titorenko VI (2010). Chemical genetic screen identifies lithocholic acid as an anti-aging compound that extends yeast chronological life span in a TOR-independent manner, by modulating housekeeping longevity assurance processes. *Aging (Albany NY)*. **2**, 393-414.

Gomes P, Sampaio-Marques B, Ludovico P, Rodrigues F, Leao C (2007). Low auxotrophy-complementing amino acid concentrations reduce yeast chronological life span. *Mechanisms of Ageing and Development*. **128**, 383-391.

Gorinstein S, Caspi A, Libman I, Lerner HT, Huang D, Leontowicz H, Leontowicz M, Tashma Z, Katrich E, Feng S, Trakhtenberg S (2006). Red grapefruit positively influences serum triglyceride level in patients suffering from coronary atherosclerosis: studies in vitro and in humans. *Journal of Agricultural and Food Chemistry*. **54**, 1887-1892.

Grandison RC, Piper MD, Partridge L (2009). Amino-acid imbalance explains extension of lifespan by dietary restriction in Drosophila. *Nature*. **462**, 1061-1064.

Granot D, Snyder M (1991). Glucose induces cAMP-independent growth-related changes in stationary-phase cells of *Saccharomyces cerevisiae*. *Proceedings of the National Academy of Sciences of the United States of America*. **88**, 5724-5728.

Greer EL, Brunet A (2009). Different dietary restriction regimens extend lifespan by both independent and overlapping genetic pathways in *C. elegans*. *Aging Cell*. **8**, 113-127.

Gruber J, Tang SY, Halliwell B (2007). Evidence for a trade-off between survival and fitness caused by resveratrol treatment of *Caenorhabditis elegans*. *Annals of the New York Academy of Sciences*. **1100**, 530-542.

Guarente L (2011). Franklin H. Epstein Lecture: Sirtuins, aging, and medicine. *New England Journal of Medicine*. **364**, 2235-2244.

Ha TJ, Lee MH, Park CH, Pae SB, Shim KB, Ko JM, Shin SO, Baek IY, Park KY (2010). Identification and characterization of anthocyanins in yard-long beans (*Vigna unguiculata* ssp. sesquipedalis L.) by high-performance liquid chromatography with diode array detection and electrospray ionization/mass spectrometry (HPLC- DAD- ESI/MS) analysis. *Journal of agricultural and food chemistry*. **58**, 2571-2576.

Hada B, Yoo MR, Seong KM, Jin YW, Myeong HK, Min KJ (2013). D-chiro-inositol and pinitol extend the life span of *Drosophila melanogaster*. *Journals of Gerontology Series A: Biological Sciences and Medical Sciences*. **68**, 226-234.

Haigis MC, Sinclair DA (2010). Mammalian sirtuins: biological insights and disease relevance. *Annual Review of Pathology*. **5**, 253-295.

Hammerschmidt R (1999). Phytoalexins: what have we learned after 60 years? *Annual Review of Phytopathology*. **37**, 285-306.

Harman D (1956). Aging: a theory based on free radical and radiation chemistry. *Journals of Gerontology*. **11**, 298-300.

Harper AE, Benevenga NJ, Wohlhueter RM (1970). Effects of ingestion of disproportionate amounts of amino acids. *Physiological Reviews*. **50**, 428-558.

Harrison DE, Strong R, Sharp ZD, Nelson JF, Astle CM, Flurkey K, Nadon NL, Wilkinson JE, Frenkel K, Carter CS, Pahor M, Javors MA, Fernandez E, Miller RA (2009). Rapamycin fed late in life extends lifespan in genetically heterogeneous mice. *Nature*. **460**, 392-395.

Havermann S, Rohrig R, Chovolou Y, Humpf HU, Watjen W (2013). Molecular effects of baicalein in Hct116 cells and *Caenorhabditis elegans*: activation of the Nrf2 signaling pathway and prolongation of lifespan. *Journal of agricultural and food chemistry*. **61**, 2158–2164.

Heimler D, Vignolini P, Dini M, Romani A (2005). Rapid tests to assess the antioxidant activity of *Phaseolus vulgaris* L. dry beans. *Journal of Agricultural and Food Chemistry*. **53**, 3053-3056.

Helliwell SB, Wagner P, Kunz J, Deuter-Reinhard M, Henriquez R, Hall MN (1994). TOR1 and TOR2 are structurally and functionally similar but not identical phosphatidylinositol kinase homologues in yeast. *Molecular Biology of the Cell*. **5**, 105-118.

Hinnebusch AG (2005). Translational regulation of GCN4 and the general amino acid control of yeast. *Annual Review of Microbiology*. **59**, 407-450.

Hinnebusch AG, Natarajan K (2002). Gcn4p, a master regulator of gene expression, is controlled at multiple levels by diverse signals of starvation and stress. *Eukaryot Cell*. **1**, 22-32.

Howitz K, Sinclair D (2008). Xenohormesis: sensing the chemical cues of other species. *Cell*. **133**, 387-391.

Howitz KT, Bitterman KJ, Cohen HY, Lamming DW, Lavu S, Wood JG, Zipkin RE, Chung P, Kisielewski A, Zhang LL, Scherer B, Sinclair DA (2003). Small molecule activators of sirtuins extend *Saccharomyces cerevisiae* lifespan. *Nature*. **425**, 191-196.

Huang D, Ou B, Hampsch-Woodill M, Flanagan J, Prior R (2002). High-throughput assay of oxygen radical absorbance capacity (ORAC) using a multichannel liquid handling system coupled with a microplate fluorescence reader in 96-well format. *Journal of agricultural and food chemistry*. **50**, 4437-4444.

Hubbard BP, Gomes AP, Dai H, Li J, Case AW, Considine T, Riera TV, Lee JE, E SY, Lamming DW, Pentelute BL, Schuman ER, Stevens LA, Ling AJ, Armour SM, Michan S, Zhao H, Jiang Y, Sweitzer SM, Blum CA, Disch JS, Ng PY, Howitz KT, Rolo AP, Hamuro Y, Moss J, Perni RB, Ellis JL, Vlasuk GP, Sinclair DA (2013). Evidence for a common mechanism of SIRT1 regulation by allosteric activators. *Science*. **339**, 1216-1219.

Huber A, Bodenmiller B, Uotila A, Stahl M, Wanka S, Gerrits B, Aebersold R, Loewith R (2009). Characterization of the rapamycin-sensitive phosphoproteome reveals that Sch9 is a central coordinator of protein synthesis. *Gene Development*. **23**, 1929-1943.

Huber A, French SL, Tekotte H, Yerlikaya S, Stahl M, Perepelkina MP, Tyers M, Rougemont J, Beyer AL, Loewith R (2011). Sch9 regulates ribosome biogenesis via Stb3, Dot6 and Tod6 and the histone deacetylase complex RPD3L. *EMBO Journal*. **30**, 3052-3064.

Ingram DK, Zhu M, Mamczarz J, Zou S, Lane MA, Roth GS, deCabo R (2006). Calorie restriction mimetics: an emerging research field. *Aging Cell*. **5**, 97-108.

Isabelle M, Lee B, Lim M, Koh W, Huang D, Ong C (2009). Antioxidant activity and profiles of common vegetables in Singapore. *Food Chemistry*. **120**, 993-1003.

Ja WW, Carvalho GB, Zid BM, Mak EM, Brummel T, Benzer S (2009). Water- and nutrient-dependent effects of dietary restriction on Drosophila lifespan. *Proceedings of the National Academy of Sciences of the United States of America*. **106**, 18633-18637.

Jang M, Cai L, Udeani GO, Slowing KV, Thomas CF, Beecher CW, Fong HH, Farnsworth NR, Kinghorn AD, Mehta RG, Moon RC, Pezzuto JM (1997). Cancer chemopreventive activity of resveratrol, a natural product derived from grapes. *Science*. **275**, 218-220.

Jarolim S, Millen J, Heeren G, Laun P, Goldfarb DS, Breitenbach M (2004). A novel assay for replicative lifespan in *Saccharomyces cerevisiae*. *FEMS Yeast Res*. **5**, 169-177.

Javitt DC, Schoepp D, Kalivas PW, Volkow ND, Zarate C, Merchant K, Bear MF, Umbricht D, Hajos M, Potter WZ, Lee CM (2011). Translating glutamate: from pathophysiology to treatment. *Science Translational Medicine*. **3**, 102mr102.

Jia K, Chen D, Riddle DL (2004). The TOR pathway interacts with the insulin signaling pathway to regulate *C. elegans* larval development, metabolism and life span. *Development*. **131**, 3897-3906.

Jiang JC, Jaruga E, Repnevskaya MV, Jazwinski SM (2000). An intervention resembling caloric restriction prolongs life span and retards aging in yeast. *FASEB Journal*. **14**, 2135-2137.

Jin DZ, Yin LL, Ji XQ, Zhu XZ (2006). Cryptotanshinone inhibits cyclooxygenase-2 enzyme activity but not expression. *Acta Pharmacologica Sinica*. **27**, 348-349.

Johnson SC, Rabinovitch PS, Kaeberlein M (2013). mTOR is a key modulator of ageing and age-related disease. *Nature*. **493**, 338-345.

Jorgensen P, Nishikawa JL, Breitkreutz BJ, Tyers M (2002). Systematic identification of pathways that couple cell growth and division in yeast. *Science*. **297**, 395-400.

Kaeberlein M (2010a). Lessons on longevity from budding yeast. *Nature*. **464**, 513-519.

Kaeberlein M (2010b). Resveratrol and rapamycin: are they anti-aging drugs? *Bioessays*. **32**, 96-99.

Kaeberlein M, Andalis AA, Fink GR, Guarente L (2002). High osmolarity extends life span in *Saccharomyces cerevisiae* by a mechanism related to calorie restriction. *Molecular and Cellular Biology*. **22**, 8056-8066.

Kaeberlein M, Burtner CR, Kennedy BK (2007). Recent developments in yeast aging. *PLoS Genet*. **3**, e84.

Kaeberlein M, Kirkland KT, Fields S, Kennedy BK (2004). Sir2-independent life span extension by calorie restriction in yeast. *PLoS Biology*. **2**, E296.

Kaeberlein M, McDonagh T, Heltweg B, Hixon J, Westman EA, Caldwell SD, Napper A, Curtis R, DiStefano PS, Fields S, Bedalov A, Kennedy BK (2005a). Substrate-specific activation of sirtuins by resveratrol. *Journal of Biological Chemistry*. **280**, 17038-17045.

Kaeberlein M, McVey M, Guarente L (1999). The SIR2/3/4 complex and SIR2 alone promote longevity in *Saccharomyces cerevisiae* by two different mechanisms. *Genes Development*. **13**, 2570-2580.

Kaeberlein M, Powers RW, 3rd, Steffen KK, Westman EA, Hu D, Dang N, Kerr EO, Kirkland KT, Fields S, Kennedy BK (2005b). Regulation of yeast replicative life span by TOR and Sch9 in response to nutrients. *Science*. **310**, 1193-1196.

Kaeberlein M, Steffen KK, Hu D, Dang N, Kerr EO, Tsuchiya M, Fields S, Kennedy BK (2006). Comment on "HST2 mediates SIR2-independent life-span extension by calorie restriction". *Science*. **312**, 1312; author reply 1312.

Kampkotter A, Timpel C, Zurawski RF, Ruhl S, Chovolou Y, Proksch P, Watjen W (2008). Increase of stress resistance and lifespan of *Caenorhabditis elegans* by quercetin. *Comparative Biochemistry and Physiology Part B: Biochemistry and Molecular Biology*. **149**, 314-323.

Kaneko Y, Eve DJ, Yu S, Shojo H, Bae EC, Park DH, Roschek B, Jr., Alberte RS, Sanberg PR, Sanberg CD, Bickford PC, Borlongan CV (2010). Acute treatment with herbal extracts provides neuroprotective benefits in in vitro and in vivo stroke models, characterized by reduced ischemic cell death and maintenance of motor and neurological functions. *Cell Medicine*. **1**, 137-142.

Kapahi P, Chen D, Rogers AN, Katewa SD, Li PW, Thomas EL, Kockel L (2010). With TOR, less is more: a key role for the conserved nutrient-sensing TOR pathway in aging. *Cell Metabolism*. **11**, 453-465.

Kapahi P, Zid BM, Harper T, Koslover D, Sapin V, Benzer S (2004). Regulation of lifespan in Drosophila by modulation of genes in the TOR signaling pathway. *Current Biology*. **14**, 885-890.

Kennedy BK, Austriaco NR, Jr., Zhang J, Guarente L (1995). Mutation in the silencing gene SIR4 can delay aging in *S. cerevisiae*. *Cell*. **80**, 485-496.

Khattak A, Zeb A, Bibi N (2008). Impact of germination time and type of illumination on carotenoidcontent, protein solubility and in vitro protein digestibility of chickpea (*Cicer arietinum* L.) sprouts. *Food Chemistry*. **109**, 797-801.

Khupse RS, Sarver JG, Trendel JA, Bearss NR, Reese MD, Wiese TE, Boue SM, Burow ME, Cleveland TE, Bhatnagar D, Erhardt PW (2011). Biomimetic syntheses and antiproliferative activities of racemic, natural (-), and unnnatural (+) glyceollin I. *Journal of Medicinal Chemistry*. **54**, 3506-3523.

Kim EJ, Jung SN, Son KH, Kim SR, Ha TY, Park MG, Jo IG, Park JG, Choe W, Kim SS, Ha J (2007). Antidiabetes and antiobesity effect of cryptotanshinone via activation of AMP-activated protein kinase. *Molecular Pharmacology*. **72**, 62-72.

Kim HJ, Cha BY, Choi B, Lim JS, Woo JT, Kim JS (2011). Glyceollins inhibit platelet-derived growth factor-mediated human arterial smooth muscle cell proliferation and migration. *British Journal of Nutrition*, 1-12.

Klejdus B, Vitamvasova-Sterbova D, Kuban V (2001). Identification of isoflavone conjugates in red clover (*Trifolium pratense*) by liquid chromatography-mass spectrometry after two-dimensional solid-phase extraction. *Analytica Chimica Acta*. **450**, 81-97.

Koc A, Gasch AP, Rutherford JC, Kim HY, Gladyshev VN (2004). Methionine sulfoxide reductase regulation of yeast lifespan reveals reactive oxygen species-dependent and -independent components of aging. *Proceedings of the National Academy of Sciences of the United States of America*. **101**, 7999-8004.

Komarova EA, Antoch MP, Novototskaya LR, Chernova OB, Paszkiewicz G, Leontieva OV, Blagosklonny MV, Gudkov AV (2012). Rapamycin extends lifespan and delays tumorigenesis in heterozygous p53+/- mice. *Aging (Albany NY)*. **4**, 709-714.

Kunz J, Henriquez R, Schneider U, Deuter-Reinhard M, Movva NR, Hall MN (1993). Target of rapamycin in yeast, TOR2, is an essential phosphatidylinositol kinase homolog required for G1 progression. *Cell*. **73**, 585-596.

Lamming DW, Latorre-Esteves M, Medvedik O, Wong SN, Tsang FA, Wang C, Lin SJ, Sinclair DA (2005). HST2 mediates SIR2-independent life-span extension by calorie restriction. *Science*. **309**, 1861-1864.

Lamming DW, Latorre-Esteves M, Medvedik O, Wong SN, Tsang FA, Wang C, Lin SJ, Sinclair DA (2006). Response to comment on "HST2 mediates SIR2-independent life-span extension by calorie restriction". *Science*. **312**.

Lamming DW, Ye L, Katajisto P, Goncalves MD, Saitoh M, Stevens DM, Davis JG, Salmon AB, Richardson A, Ahima RS, Guertin DA, Sabatini DM, Baur JA (2012). Rapamycin-induced insulin resistance is mediated by mTORC2 loss and uncoupled from longevity. *Science*. **335**, 1638-1643.

Laplante M, Sabatini DM (2012). mTOR signaling in growth control and disease. *Cell*. **149**, 274-293.

Laun P, Rinnerthaler M, Bogengruber E, Heeren G, Breitenbach M (2006). Yeast as a model for chronological and reproductive aging - A comparison. *Experimental Gerontology*. **41**, 1208-1212.

Lebel M, Picard F, Ferland G, Gaudreau P (2012). Drugs, nutrients, and phytoactive principles improving the health span of rodent models of human age-related diseases. *Journals of Gerontology Series A: Biological Sciences and Medical Sciences*. **67**, 140-151.

Lee KP, Simpson SJ, Clissold FJ, Brooks R, Ballard JW, Taylor PW, Soran N, Raubenheimer D (2008). Lifespan and reproduction in Drosophila: New insights from nutritional geometry. *Proceedings of the National Academy of Sciences of the United States of America*. **105**, 2498-2503.

Lee KS, Lee BS, Semnani S, Avanesian A, Um CY, Jeon HJ, Seong KM, Yu K, Min KJ, Jafari M (2010). Curcumin extends life span, improves health span, and modulates the expression of age-associated aging genes in *Drosophila melanogaster*. *Rejuvenation Researchearch*. **13**, 561-570.

Lee YJ, Kim KJ, Kang HY, Kim HR, Maeng PJ (2012). Involvement of GDH3-encoded NADP+-dependent glutamate dehydrogenase in yeast cell resistance to stress-induced apoptosis in stationary phase cells. *Journal of Biological Chemistry*. **287**, 44221-44233.

Liao VH, Yu CW, Chu YJ, Li WH, Hsieh YC, Wang TT (2011). Curcumin-mediated lifespan extension in *Caenorhabditis elegans*. *Mechanisms of Ageing and Development*. **132**, 480-487.

Lin BS, Lien TF, Chao MR, Lai TY, Chang JC, Chou SJ, Liao HF, Chiou RY (2008a). Toxicological and nutraceutical assessments of peanut sprouts as daily supplements to feed Sprague Dawley rats for 18 weeks. *Journal of the Science of Food and Agriculture*. **88**, 2201-2207.

Lin L, Harnly J, Pastor-Corrales M, Luthria D (2008b). The polyphenolic profiles of common bean (*Phaseolus vulgaris* L.). *Food Chemistry*. **107**, 399-410.

Lin LZ, He XG, Lindenmaier M, Yang J, Cleary M, Qiu SX, Cordell GA (2000a). LC-ESI-MS study of the flavonoid glycoside malonates of red clover (*Trifolium pratense*). *Journal of agricultural and food chemistry*. **48**, 354-365.

Lin P, Lai H (2006). Bioactive compounds in legumes and their germinated products. *Journal of Agricultural and Food Chemistry*. **54**, 3807-3814.

Lin SJ, Defossez PA, Guarente L (2000b). Requirement of NAD and SIR2 for life-span extension by calorie restriction in *Saccharomyces cerevisiae*. *Science*. **289**, 2126-2128.

Lin SJ, Ford E, Haigis M, Liszt G, Guarente L (2004). Calorie restriction extends yeast life span by lowering the level of NADH. *Genes Development*. **18**, 12-16.

Lin SJ, Kaeberlein M, Andalis AA, Sturtz LA, Defossez PA, Culotta VC, Fink GR, Guarente L (2002). Calorie restriction extends *Saccharomyces cerevisiae* lifespan by increasing respiration. *Nature*. **418**, 344-348.

Loewith R, Jacinto E, Wullschleger S, Lorberg A, Crespo JL, Bonenfant D, Oppliger W, Jenoe P, Hall MN (2002). Two TOR complexes, only one of which is rapamycin sensitive, have distinct roles in cell growth control. *Molecular Cell*. **10**, 457-468.

Lombard DB, Pletcher SD, Canto C, Auwerx J (2011). Ageing: longevity hits a roadblock. *Nature*. **477**, 410-411.

Longo VD (1999). Mutations in signal transduction proteins increase stress resistance and longevity in yeast, nematodes, fruit flies, and mammalian neuronal cells. *Neurobiology of Aging*. **20**, 479-486.

Longo VD (2003). The Ras and Sch9 pathways regulate stress resistance and longevity. *Experimental Gerontology*. **38**, 807-811.

Longo VD, Gralla EB, Valentine JS (1996a). Superoxide dismutase activity is essential for stationary phase survival in *Saccharomyces cerevisiae* - Mitochondrial production of toxic oxygen species in vivo. *Journal of Biological Chemistry*. **271**, 12275-12280.

Longo VD, Gralla EB, Valentine JS (1996b). Superoxide dismutase activity is essential for stationary phase survival in *Saccharomyces cerevisiae*. Mitochondrial production of toxic oxygen species in vivo. *Journal of Biological Chemistry*. **271**, 12275-12280.

Longo VD, Shadel GS, Kaeberlein M, Kennedy B (2012). Replicative and chronological aging in *Saccharomyces cerevisiae*. *Cell Metabolism*. **16**, 18-31.

López-Amorós M, Hernández T, Estrella I (2006). Effect of germination on legume phenolic compounds and their antioxidant activity. *Journal of Food Composition and Analysis*. **19**, 277-283.

Lu JY, Lin YY, Sheu JC, Wu JT, Lee FJ, Chen Y, Lin MI, Chiang FT, Tai TY, Berger SL, Zhao Y, Tsai KS, Zhu H, Chuang LM, Boeke JD (2011). Acetylation of yeast AMPK controls intrinsic aging independently of caloric restriction. *Cell*. **146**, 969-979.

Lucanic M, Lithgow GJ, Alavez S (2013). Pharmacological lifespan extension of invertebrates. *Ageing Research Reviews*. **12**, 445-458.

Lv QY, Yang Y, Zhao YX, Gu DY, He DJ, Yili A, Ma QL, Cheng Z, Gao YH, Aisa HA, Ito Y (2009). Comparative study on separation and purification of isoflavones from the seeds and sprouts of chickpea by high-speed countercurrent chromatography. *Journal of Liquid Chromatography & Related Technologies*. **32**, 2879-2892.

Mabry TJ, Markham KR, Thomas MB (1970). The systematic identification of flavonoids. *The systematic identification of flavonoids.*

Maddocks OD, Berkers CR, Mason SM, Zheng L, Blyth K, Gottlieb E, Vousden KH (2013). Serine starvation induces stress and p53-dependent metabolic remodelling in cancer cells. *Nature*. **493**, 542-546.

Mair W, Dillin A (2008). Aging and survival: the genetics of life span extension by dietary restriction. *Annual Review of Biochemistry*. **77**, 727-754.

Malloy VL, Krajcik RA, Bailey SJ, Hristopoulos G, Plummer JD, Orentreich N (2006). Methionine restriction decreases visceral fat mass and preserves insulin action in aging male Fischer 344 rats independent of energy restriction. *Aging Cell*. **5**, 305-314.

Marques F, Markus M, Morris B (2010). Hormesis as a pro-healthy aging intervention in human beings? *Dose-Response*. **8**, 28-33.

Martín-Cabrejas M, Díaz M, Aguilera Y, Benítez V, Mollá E, Esteban R (2008). Influence of germination on the soluble carbohydrates and dietary fibre fractions in non-conventional legumes. *Food Chemistry*. **107**, 1045-1052.

Mattison JA, Roth GS, Beasley TM, Tilmont EM, Handy AM, Herbert RL, Longo DL, Allison DB, Young JE, Bryant M, Barnard D, Ward WF, Qi W, Ingram DK, de Cabo R (2012). Impact of caloric restriction on health and survival in rhesus monkeys from the NIA study. *Nature*. **489**, 318-321.

Mattson M (2008). Hormesis defined. *Ageing Research Reviews*. **7**, 1-7.

McCormick MA, Tsai SY, Kennedy BK (2011). TOR and ageing: a complex pathway for a complex process. *Philosophical Transactions of the Royal Society B: Biological Sciences*. **366**, 17-27.

McCue P, Shetty K (2004). Health benefits of soy isoflavonoids and strategies for enhancement: A review. *Critical reviews in food science and nutrition*. **44**, 361-367.

Medvedik O, Lamming DW, Kim KD, Sinclair DA (2007). MSN2 and MSN4 link calorie restriction and TOR to sirtuin-mediated lifespan extension in *Saccharomyces cerevisiae*. *PLoS Biology*. **5**, e261.

Mei Z, Situ B, Tan X, Zheng S, Zhang F, Yan P, Liu P (2010). Cryptotanshinione upregulates alpha-secretase by activation PI3K pathway in cortical neurons. *Brain Research*. **1348**, 165-173.

Mei ZR, Zhang FY, Tao L, Zheng WH, Cao YN, Wang ZH, Tang S, Le K, Chen SR, Pi RB, Liu PQ (2009). Cryptotanshinone, a compound from *Salvia miltiorrhiza* modulates amyloid precursor protein metabolism and attenuates beta-amyloid deposition through upregulating alpha-secretase in vivo and in vitro. *Neuroscience Letters*. **452**, 90-95.

Mesquita A, Weinberger M, Silva A, Sampaio-Marques B, Almeida B, Leao C, Costa V, Rodrigues F, Burhans WC, Ludovico P (2010). Caloric restriction or catalase inactivation extends yeast chronological lifespan by inducing H_2O_2 and superoxide dismutase activity. *Proceedings of the National Academy of Sciences of the United States of America*. **107**, 15123-15128.

Meydani M (2001). Nutrition interventions in aging and age-associated disease. *Annals of the New York Academy of Sciences*. **928**, 226-235.

Mieulet V, Yan L, Lamb RF (2009). Signalling by amino acid nutrients: mTOR and beyond. *Amino Acids*. **37**, 67-67.

Miller RA, Buehner G, Chang Y, Harper JM, Sigler R, Smith-Wheelock M (2005). Methionine-deficient diet extends mouse lifespan, slows immune and lens aging, alters glucose, T4, IGF-I and insulin levels, and increases hepatocyte MIF levels and stress resistance. *Aging Cell*. **4**, 119-125.

Miller RA, Harrison DE, Astle CM, Baur JA, Boyd AR, de Cabo R, Fernandez E, Flurkey K, Javors MA, Nelson JF, Orihuela CJ, Pletcher S, Sharp ZD, Sinclair D, Starnes JW, Wilkinson JE, Nadon NL, Strong R (2011). Rapamycin, but not resveratrol or simvastatin, extends life span of genetically heterogeneous mice. *Journals of Gerontology Series A: Biological Sciences and Medical Sciences*. **66**, 191-201.

Miller RA, Harrison DE, Astle CM, Floyd RA, Flurkey K, Hensley KL, Javors MA, Leeuwenburgh C, Nelson JF, Ongini E, Nadon NL, Warner HR, Strong R (2007). An Aging Interventions Testing Program: study design and interim report. *Aging Cell*. **6**, 565-575.

Miller SM, Magasanik B (1990). Role of NAD-linked glutamate dehydrogenase in nitrogen metabolism in *Saccharomyces cerevisiae*. *Journal of Bacteriology*. **172**, 4927-4935.

Minois N, Lagona F, Frajnt M, Vaupel JW (2009). Plasticity of death rates in stationary phase in *Saccharomyces cerevisiae*. *Aging Cell*. **8**, 36-44.

Mirisola MG, Longo VD (2012). Acetic acid and acidification accelerate chronological and replicative aging in yeast. *Cell Cycle*. **11**, 3532-3533.

Mortimer RK, Johnston JR (1959). Life span of individual yeast cells. *Nature*. **183**, 1751-1752.

Murakami C, Delaney JR, Chou A, Carr D, Schleit J, Sutphin GL, An EH, Castanza AS, Fletcher M, Goswami S, Higgins S, Holmberg M, Hui J, Jelic M, Jeong KS, Kim JR, Klum S, Liao E, Lin MS, Lo W, Miller H, Moller R, Peng ZJ, Pollard T, Pradeep P, Pruett D, Rai D, Ros V, Schuster A, Singh M, Spector BL, Vander Wende H, Wang AM, Wasko BM, Olsen B, Kaeberlein M (2012). pH neutralization protects against reduction in replicative lifespan following chronological aging in yeast. *Cell Cycle*. **11**, 3087-3096.

Murakami C, Kaeberlein M (2009). Quantifying yeast chronological life span by outgrowth of aged cells. *Journal of Visualized Experiments*.

Murakami CJ, Burtner CR, Kennedy BK, Kaeberlein M (2008). A method for high-throughput quantitative analysis of yeast chronological life span. *Journals of Gerontology Series A: Biological Sciences and Medical Sciences*. **63**, 113-121.

Murakami CJ, Wall V, Basisty N, Kaeberlein M (2011). Composition and acidification of the culture medium influences chronological aging similarly in vineyard and laboratory yeast. *PLoS One*. **6**, e24530.

Murguia JR, Serrano R (2012). New functions of protein kinase Gcn2 in yeast and mammals. *IUBMB Life*. **64**, 971-974.

Ng TB, Ye XJ, Wong JH, Fang EF, Chan YS, Pan W, Ye XY, Sze SC, Zhang KY, Liu F, Wang HX (2011). Glyceollin, a soybean phytoalexin with medicinal properties. *Applied Microbiology and Biotechnology*. **90**, 59-68.

Nishiyama Y, Yun CS, Matsuda F, Sasaki T, Saito K, Tozawa Y (2010). Expression of bacterial tyrosine ammonia-lyase creates a novel p-coumaric acid pathway in the biosynthesis of phenylpropanoids in *Arabidopsis*. *Planta*. **232**, 209-218.

Ocampo A, Barrientos A (2011). Quick and reliable assessment of chronological life span in yeast cell populations by flow cytometry. *Mechanisms of Ageing and Development*. **132**, 315-323.

Olsen B, Murakami CJ, Kaeberlein M (2010). YODA: software to facilitate high-throughput analysis of chronological life span, growth rate, and survival in budding yeast. *BMC Bioinformatics*. **11**, 141.

Onken B, Driscoll M (2010). Metformin induces a dietary restriction-like state and the oxidative stress response to extend *C. elegans* healthspan via AMPK, LKB1, and SKN-1. *PLoS One*. **5**, e8758.

Orentreich N, Matias JR, DeFelice A, Zimmerman JA (1993). Low methionine ingestion by rats extends life span. *Journal of Nutrition*. **123**, 269-274.

Ou B, Hampsch-Woodill M, Flanagan J, Deemer E, Prior R, Huang D (2002). Novel fluorometric assay for hydroxyl radical prevention capacity using fluorescein as the probe. *Journal of agricultural and food chemistry*. **50**, 2772-2777.

Pan MH, Lai CS, Tsai ML, Wu JC, Ho CT (2012). Molecular mechanisms for anti-aging by natural dietary compounds. *Molecular Nutrition & Food Research*. **56**, 88-115.

Pan Y (2011). Mitochondria, reactive oxygen species, and chronological aging: a message from yeast. *Experimental Gerontology*. **46**, 847-852.

Pan Y, Schroeder EA, Ocampo A, Barrientos A, Shadel GS (2011). Regulation of yeast chronological life span by TORC1 via adaptive mitochondrial ROS signaling. *Cell Metabolism*. **13**, 668-678.

Park IJ, Kim MJ, Park OJ, Choe W, Kang I, Kim SS, Ha J (2012a). Cryptotanshinone induces ER stress-mediated apoptosis in HepG2 and MCF7 cells. *Apoptosis*. **17**, 248-257.

Park SJ, Ahmad F, Philp A, Baar K, Williams T, Luo H, Ke H, Rehmann H, Taussig R, Brown AL, Kim MK, Beaven MA, Burgin AB, Manganiello V, Chung JH (2012b). Resveratrol ameliorates aging-related metabolic phenotypes by inhibiting cAMP phosphodiesterases. *Cell*. **148**, 421-433.

Paucar-Menacho L, Berhow M, Mandarino J, de Mejia E, Chang Y (2010). Optimisation of germination time and temperature on the concentration of bioactive compounds in Brazilian soybean cultivar BRS 133 using response surface methodology. *Food Chemistry*. **119**, 636-642.

Payton-Stewart F, Khupse RS, Boue SM, Elliott S, Zimmermann MC, Skripnikova EV, Ashe H, Tilghman SL, Beckman BS, Cleveland TE, McLachlan JA, Bhatnagar D, Wiese TE, Erhardt P, Burow ME (2010). Glyceollin I enantiomers distinctly regulate ER-mediated gene expression. *Steroids*. **75**, 870-878.

Payton-Stewart F, Schoene NW, Kim YS, Burow ME, Cleveland TE, Boue SM, Wang TT (2009). Molecular effects of soy phytoalexin glyceollins in human prostate cancer cells LNCaP. *Molecular Carcinogenesis*. **48**, 862-871.

Pearson KJ, Baur JA, Lewis KN, Peshkin L, Price NL, Labinskyy N, Swindell WR, Kamara D, Minor RK, Perez E, Jamieson HA, Zhang Y, Dunn SR, Sharma K, Pleshko N, Woollett LA, Csiszar A, Ikeno Y, Le Couteur D, Elliott PJ, Becker KG, Navas P, Ingram DK, Wolf NS, Ungvari Z, Sinclair DA, de Cabo R (2008). Resveratrol delays age-related deterioration and mimics transcriptional aspects of dietary restriction without extending life span. *Cell Metabolism*. **8**, 157-168.

Pereira C, Saraiva L (2013). Interference of aging media on the assessment of yeast chronological life span by propidium iodide staining. *Folia Microbiol (Praha)*. **58**, 81-84.

Perrone CE, Malloy VL, Orentreich DS, Orentreich N (2013). Metabolic adaptations to methionine restriction that benefit health and lifespan in rodents. *Experimental Gerontology*. **48**, 654-660.

Pervaiz S, Holme A (2009). Resveratrol: its biologic targets and functional activity. *Antioxidants & Redox Signaling*. **11**, 2851-2897.

Pietsch K, Saul N, Menzel R, Sturzenbaum SR, Steinberg CE (2009). Quercetin mediated lifespan extension in *Caenorhabditis elegans* is modulated by age-1, daf-2, sek-1 and unc-43. *Biogerontology*. **10**, 565-578.

Piper MD, Partridge L, Raubenheimer D, Simpson SJ (2011). Dietary restriction and aging: a unifying perspective. *Cell Metabolism*. **14**, 154-160.

Porquet D, Casadesus G, Bayod S, Vicente A, Canudas AM, Vilaplana J, Pelegri C, Sanfeliu C, Camins A, Pallas M, Del Valle J (2012). Dietary resveratrol prevents Alzheimer's markers and increases life span in SAMP8. *Age (Dordr)*. 35, 1851-1865.

Powers RW, 3rd, Kaeberlein M, Caldwell SD, Kennedy BK, Fields S (2006). Extension of chronological life span in yeast by decreased TOR pathway signaling. *Genes Development*. **20**, 174-184.

Prior R, Wu X, Schaichs K (2005). Standardized methods for the determination of antioxidant capacity and phenolics in foods and dietary supplements. *Journal of agricultural and food chemistry*. **53**, 4290-4302.

Ramachandran V, Herman PK (2011). Antagonistic interactions between the cAMP-dependent protein kinase and Tor signaling pathways modulate cell growth in *Saccharomyces cerevisiae*. *Genetics*. **187**, 441-454.

Rascon B, Hubbard BP, Sinclair DA, Amdam GV (2012). The lifespan extension effects of resveratrol are conserved in the honey bee and may be driven by a mechanism related to caloric restriction. *Aging (Albany NY)*. **4**, 499-508.

Rice-Evans CA, Miller NJ, Paganga G (1996). Structure-antioxidant activity relationships of flavonoids and phenolic acids. *Free Radical Biology & Medicine*. **20**, 933-956.

Ristow M, Zarse K (2010). How increased oxidative stress promotes longevity and metabolic health: The concept of mitochondrial hormesis (mitohormesis). *Experimental Gerontology*. **45**, 410-418.

Robida-Stubbs S, Glover-Cutter K, Lamming DW, Mizunuma M, Narasimhan SD, Neumann-Haefelin E, Sabatini DM, Blackwell TK (2012). TOR signaling and rapamycin influence longevity by regulating SKN-1/Nrf and DAF-16/FoxO. *Cell Metabolism*. **15**, 713-724.

Rogina B, Helfand SL (2004). Sir2 mediates longevity in the fly through a pathway related to calorie restriction. *Proceedings of the National Academy of Sciences of the United States of America*. **101**, 15998-16003.

Rousakis A, Vlassis A, Vlanti A, Patera S, Thireos G, Syntichaki P (2013). The general control nonderepressible-2 kinase mediates stress response and longevity induced by target of rapamycin inactivation in *Caenorhabditis elegans*. *Aging Cell*. **12**, 742-751.

Rufer CE, Kulling SE (2006). Antioxidant activity of isoflavones and their major metabolites using different in vitro assays. *Journal of agricultural and food chemistry*. **54**, 2926-2931.

Sales J, Resurreccion A (2010). Phenolic profile, antioxidants, and sensory acceptance of bioactive-enhanced peanuts using ultrasound and UV. *Food Chemistry*. **122**, 795-803.

Salminen A, Kaarniranta K (2012). AMP-activated protein kinase (AMPK) controls the aging process via an integrated signaling network. *Ageing Research Reviews*. **11**, 230-241.

Santos J, Sousa MJ, Leao C (2012). Ammonium is toxic for aging yeast cells, inducing death and shortening of the chronological lifespan. *PLoS One*. **7**, e37090.

Schmidt A, Kunz J, Hall MN (1996). TOR2 is required for organization of the actin cytoskeleton in yeast. *Proceedings of the National Academy of Sciences of the United States of America*. **93**, 13780-13785.

Sehgal SN, Baker H, Vezina C (1975). Rapamycin (AY-22,989), a new antifungal antibiotic. II. Fermentation, isolation and characterization. *The Journal of Antibiotics (Tokyo)*. **28**, 727-732.

Shcheprova Z, Baldi S, Frei SB, Gonnet G, Barral Y (2008). A mechanism for asymmetric segregation of age during yeast budding. *Nature*. **454**, 728-734.

Shen T, Wang XN, Lou HX (2009). Natural stilbenes: an overview. *Natural Product Reports*. **26**, 916-935.

Sherman F (1991). Getting started with yeast. *Methods in Enzymology*. **194**, 3-21.

Shiffman ML, Stravitz RT, Contos MJ, Mills AS, Sterling RK, Luketic VA, Sanyal AJ, Cotterell A, Maluf D, Posner MP, Fisher RA (2004). Histologic recurrence of chronic hepatitis C virus in patients after living donor and deceased donor liver transplantation. *Liver Transplantation*. **10**, 1248-1255.

Shin DS, Kim HN, Shin KD, Yoon YJ, Kim SJ, Han DC, Kwon BM (2009). Cryptotanshinone inhibits constitutive signal transducer and activator of transcription 3 function through blocking the dimerization in DU145 prostate cancer cells. *Cancer Research*. **69**, 193-202.

Shin SY, Han NS, Park YC, Kim MD, Seo JH (2011). Production of resveratrol from p-coumaric acid in recombinant *Saccharomyces cerevisiae* expressing 4-coumarate:coenzyme A ligase and stilbene synthase genes. *Enzyme and Microbial Technology*. **48**, 48-53.

Simon JA, Bedalov A (2004). Opinion - Yeast as a model system for anticancer drug discovery. *Nature Reviews Cancer*. **4**, 481-488.

Simpson SJ, Raubenheimer D (2009). Macronutrient balance and lifespan. *Aging (Albany NY)*. **1**, 875-880.

Sinclair D (2002). Paradigms and pitfalls of yeast longevity research. *Mechanisms of ageing and development*. **123**, 857-867.

Sinclair D, Mills K, Guarente L (1998). Aging in *Saccharomyces cerevisiae*. *Annual Review of Microbiology*. **52**, 533-560.

Sinclair DA, Guarente L (1997). Extrachromosomal rDNA circles--a cause of aging in yeast. *Cell*. **91**, 1033-1042.

Singh R, Wu B, Tang L, Liu Z, Hu M (2010). Identification of the position of mono-o-glucuronide of flavones and flavonols by analyzing shift in online UV spectrum (lambdamax) generated from an online diode array detector. *Journal of agricultural and food chemistry*. **58**, 9384-9395.

Sivesind E, Seguin P (2005). Effects of the environment, cultivar, maturity, and preservation method on red clover isoflavone concentration. *Journal of agricultural and food chemistry*. **53**, 6397-6402.

Skorupa DA, Dervisefendic A, Zwiener J, Pletcher SD (2008). Dietary composition specifies consumption, obesity, and lifespan in *Drosophila melanogaster*. *Aging Cell*. **7**, 478-490.

Smith DL, Jr., Elam CF, Jr., Mattison JA, Lane MA, Roth GS, Ingram DK, Allison DB (2010). Metformin supplementation and life span in Fischer-344 rats. *Journals of Gerontology Series A: Biological Sciences and Medical Sciences*. **65**, 468-474.

Smith DL, Jr., McClure JM, Matecic M, Smith JS (2007). Calorie restriction extends the chronological lifespan of *Saccharomyces cerevisiae* independently of the Sirtuins. *Aging Cell*. **6**, 649-662.

Sobolev VS, Deyrup ST, Gloer JB (2006). New peanut (*Arachis hypogaea*) phytoalexin with prenylated benzenoid and but-2-enolide moieties. *Journal of agricultural and food chemistry*. **54**, 2111-2115.

Sobolev VS, Guo BZZ, Holbrook CC, Lynch RE (2007). Interrelationship of phytoalexin production and disease resistance in selected peanut genotypes. *Journal of agricultural and food chemistry*. **55**, 2195-2200.

Sobolev VS, Neff SA, Gloer JB (2009). New stilbenoids from peanut (*Arachis hypogaea*) seeds challenged by an *Aspergillus caelatus* strain. *Journal of agricultural and food chemistry*. **57**, 62-68.

Sobolev VS, Neff SA, Gloer JB (2010a). New dimeric stilbenoids from fungal-challenged peanut (*Arachis hypogaea*) seeds. *Journal of agricultural and food chemistry*. **58**, 875-881.

Sobolev VS, Neff SA, Gloer JB, Khan SI, Tabanca N, De Lucca AJ, Wedge DE (2010b). Pterocarpenes elicited by *Aspergillus caelatus* in peanut (*Arachis hypogaea*) seeds. *Phytochemistry*. **71**, 2099-2107.

Soh JW, Marowsky N, Nichols TJ, Rahman AM, Miah T, Sarao P, Khasawneh R, Unnikrishnan A, Heydari AR, Silver RB, Arking R (2013). Curcumin is an early-acting stage-specific inducer of extended functional longevity in Drosophila. *Experimental Gerontology*. **48**, 229-239.

Spindler SR (2012). Review of the literature and suggestions for the design of rodent survival studies for the identification of compounds that increase health and life span. *Age (Dordr)*. **34**, 111-120.

Stan R, McLaughlin MM, Cafferkey R, Johnson RK, Rosenberg M, Livi GP (1994). Interaction between FKBP12-rapamycin and TOR involves a conserved serine residue. *Journal of Biological Chemistry*. **269**, 32027-32030.

Staschke KA, Dey S, Zaborske JM, Palam LR, McClintick JN, Pan T, Edenberg HJ, Wek RC (2010). Integration of general amino acid control and target of rapamycin (TOR) regulatory pathways in nitrogen assimilation in yeast. *Journal of Biological Chemistry*. **285**, 16893-16911.

Steelman LS, Chappell WH, Abrams SL, Kempf CR, Long J, Laidler P, Mijatovic S, Maksimovic-Ivanic D, Stivala F, Mazzarino MC, Donia M, Fagone P, Malaponte G, Nicoletti F, Libra M, Milella M, Tafuri A, Bonati A, Basecke J, Cocco L, Evangelisti C, Martelli AM, Montalto G, Cervello M, McCubrey JA (2011). Roles of the Raf/MEK/ERK and PI3K/PTEN/Akt/mTOR pathways in controlling growth and sensitivity to therapy-implications for cancer and aging. *Aging-Us*. **3**, 192-222.

Steffen KK, MacKay VL, Kerr EO, Tsuchiya M, Hu D, Fox LA, Dang N, Johnston ED, Oakes JA, Tchao BN, Pak DN, Fields S, Kennedy BK, Kaeberlein M (2008). Yeast life span extension by depletion of 60S ribosomal subunits is mediated by Gcn4. *Cell*. **133**, 292-302.

Steinkraus KA, Kaeberlein M, Kennedy BK (2008). Replicative aging in yeast: the means to the end. *Annual Review of Cell and Developmental Biology*. **24**, 29-54.

Stevenson PC, Aslam SN (2006). The chemistry of the genus *Cicer* L. *Studies in Natural Products Chemistry*. **33**, 905-956.

Strong R, Miller RA, Astle CM, Baur JA, de Cabo R, Fernandez E, Guo W, Javors M, Kirkland JL, Nelson JF, Sinclair DA, Teter B, Williams D, Zaveri N, Nadon NL, Harrison DE (2013). Evaluation of resveratrol, green tea extract, curcumin, oxaloacetic acid, and medium-chain triglyceride oil on life span of genetically heterogeneous mice. *Journals of Gerontology Series A: Biological Sciences and Medical Sciences*. **68**, 6-16.

Suh SJ, Jin UH, Choi HJ, Chang HW, Son JK, Lee SH, Jeon SJ, Son KH, Chang YC, Lee YC, Kim CH (2006). Cryptotanshinone from Salvia miltiorrhiza BUNGE has an inhibitory effect on TNF-alpha-induced matrix metalloproteinase-9 production and HASMC migration via down-regulated NF-kappa B and AP-1. *Biochemical Pharmacology*. **72**, 1680-1689.

Sun J, Kale SP, Childress AM, Pinswasdi C, Jazwinski SM (1994). Divergent roles of RAS1 and RAS2 in yeast longevity. *Journal of Biological Chemistry*. **269**, 18638-18645.

Sun L, Sadighi Akha AA, Miller RA, Harper JM (2009). Life-span extension in mice by preweaning food restriction and by methionine restriction in middle age. *Journals of Gerontology Series A: Biological Sciences and Medical Sciences*. **64**, 711-722.

Sunagawa T, Shimizu T, Kanda T, Tagashira M, Sami M, Shirasawa T (2011). Procyanidins from apples (*Malus pumila* Mill.) extend the lifespan of *Caenorhabditis elegans*. *Planta Medica*. **77**, 122-127.

Talcott ST, Passeretti S, Duncan CE, Gorbet DW (2005). Polyphenolic content and sensory properties of normal and high oleic acid peanuts. *Food Chemistry*. **90**, 379-388.

Tang S, Shen XY, Huang HQ, Xu SW, Yu Y, Zhou CH, Chen SR, Le K, Wang YH, Liu PQ (2011). Cryptotanshinone suppressed inflammatory cytokines secretion in RAW264.7 macrophages through inhibition of the NF-kappa B and MAPK signaling pathways. *Inflammation*. **34**, 111-118.

ter Schure EG, van Riel NA, Verrips CT (2000). The role of ammonia metabolism in nitrogen catabolite repression in *Saccharomyces cerevisiae*. *FEMS Microbiology Reviews*. **24**, 67-83.

Tham DM, Gardner CD, Haskell WL (1998). Clinical review 97 - Potential health benefits of dietary phytoestrogens: A review of the clinical, epidemiological, and mechanistic evidence. *Journal of clinical endocrinology and metabolism*. **83**, 2223-2235.

Thevelein JM, de Winde JH (1999). Novel sensing mechanisms and targets for the cAMP-protein kinase A pathway in the yeast *Saccharomyces cerevisiae*. *Molecular Microbiology*. **33**, 904-918.

Thomas KC, Hynes SH, Ingledew WM (2002). Influence of medium buffering capacity on inhibition of *Saccharomyces cerevisiae* growth by acetic and lactic acids. *Applied and Environmental Microbiology*. **68**, 1616-1623.

Tissenbaum HA, Guarente L (2001). Increased dosage of a sir-2 gene extends lifespan in *Caenorhabditis elegans*. *Nature*. **410**, 227-230.

Toda T, Cameron S, Sass P, Zoller M, Scott JD, McMullen B, Hurwitz M, Krebs EG, Wigler M (1987a). Cloning and characterization of BCY1, a locus encoding a regulatory subunit of the cyclic AMP-dependent protein kinase in *Saccharomyces cerevisiae*. *Molecular and Cellular Biology*. **7**, 1371-1377.

Toda T, Cameron S, Sass P, Zoller M, Wigler M (1987b). Three different genes in *S. cerevisiae* encode the catalytic subunits of the cAMP-dependent protein kinase. *Cell*. **50**, 277-287.

Tolleson WH, Doerge DR, Churchwell MI, Marques MM, Roberts DW (2002). Metabolism of biochanin A and formononetin by human liver microsomes in vitro. *Journal of agricultural and food chemistry*. **50**, 4783-4790.

Toussaint M, Conconi A (2006). High-throughput and sensitive assay to measure yeast cell growth: a bench protocol for testing genotoxic agents. *Nature Protocols*. **1**, 1922-1928.

Troen AM, French EE, Roberts JF, Selhub J, Ordovas JM, Parnell LD, Lai CQ (2007). Lifespan modification by glucose and methionine in *Drosophila melanogaster* fed a chemically defined diet. *Age (Dordr)*. **29**, 29-39.

Tsao R, Papadopoulos Y, Yang R, Young JC, McRae K (2006). Isoflavone profiles of red clovers and their distribution in different parts harvested at different growing stages. *Journal of agricultural and food chemistry*. **54**, 5797-5805.

U.S. Department of Agriculture ARS (2010). Oxygen radical absorbance capacity (ORAC) of selected foods, release 2. *Nutrient Data Laboratory Home Page, http://www.ars.usda.gov/ba/bhnrc/ndl*.

Unger MW, Hartwell LH (1976). Control of cell division in *Saccharomyces cerevisiae* by methionyl-tRNA. *Proceedings of the National Academy of Sciences of the United States of America*. **73**, 1664-1668.

Unlu ES, Koc A (2007). Effects of deleting mitochondrial antioxidant genes on life span. *Annals of the New York Academy of Sciences*. **1100**, 505-509.

Urban J, Soulard A, Huber A, Lippman S, Mukhopadhyay D, Deloche O, Wanke V, Anrather D, Ammerer G, Riezman H, Broach JR, De Virgilio C, Hall MN, Loewith R (2007). Sch9 is a major target of TORC1 in *Saccharomyces cerevisiae*. *Molecular Cell*. **26**, 663-674.

Valenzano DR, Terzibasi E, Genade T, Cattaneo A, Domenici L, Cellerino A (2006). Resveratrol prolongs lifespan and retards the onset of age-related markers in a short-lived vertebrate. *Current Biology*. **16**, 296-300.

van Loon L, Rep M, Pieterse C (2006). Significance of inducible defense-related proteins in infected plants. *Annual Review of Phytopathology*. **44**, 135-162.

Veitch NC (2007). Isoflavonoids of the Leguminosae. *Natural Product Reports*. **24**, 417-464.

Veitch NC (2009). Isoflavonoids of the Leguminosae. *Natural Product Reports*. **26**, 776-802.

Vezina C, Kudelski A, Sehgal SN (1975). Rapamycin (AY-22,989), a new antifungal antibiotic. I. Taxonomy of the producing streptomycete and isolation of the active principle. *Journal of Antibiotics (Tokyo)*. **28**, 721-726.

Viswanathan M, Kim SK, Berdichevsky A, Guarente L (2005). A role for SIR-2.1 regulation of ER stress response genes in determining *C. elegans* life span. *Developmental Cell*. **9**, 605-615.

Wang C, Wheeler CT, Alberico T, Sun X, Seeberger J, Laslo M, Spangler E, Kern B, de Cabo R, Zou S (2013). The effect of resveratrol on lifespan depends on both gender and dietary nutrient composition in *Drosophila melanogaster*. *Age (Dordr)*. **35**, 69-81.

Wang KH, Lai YH, Chang JC, Ko TF, Shyu SL, Chiou RYY (2005). Germination of peanut kernels to enhance resveratrol biosynthesis and prepare sprouts as a functional vegetable. *Journal of agricultural and food chemistry*. **53**, 242-246.

Wang XQ (2011). Structure, function, and engineering of enzymes in isoflavonoid biosynthesis. *Functional & Integrative Genomics*. **11**, 13-22.

Wanke V, Cameroni E, Uotila A, Piccolis M, Urban J, Loewith R, De Virgilio C (2008). Caffeine extends yeast lifespan by targeting TORC1. *Molecular Microbiology*. **69**, 277-285.

Wei M, Fabrizio P, Hu J, Ge H, Cheng C, Li L, Longo VD (2008). Life span extension by calorie restriction depends on Rim15 and transcription factors downstream of Ras/PKA, Tor, and Sch9. *PLoS Genetics*. **4**, e13.

Wei M, Fabrizio P, Madia F, Hu J, Ge H, Li LM, Longo VD (2009). Tor1/Sch9-regulated carbon source substitution is as effective as calorie restriction in life span extension. *PLoS Genetics*. **5**, e1000467.

Weindruch R, Walford RL (1982). Dietary restriction in mice beginning at 1 year of age: effect on life-span and spontaneous cancer incidence. *Science*. **215**, 1415-1418.

Wilson WA, Roach PJ (2002). Nutrient-regulated protein kinases in budding yeast. *Cell*. **111**, 155-158.

Wood JG, Rogina B, Lavu S, Howitz K, Helfand SL, Tatar M, Sinclair D (2004). Sirtuin activators mimic caloric restriction and delay ageing in metazoans. *Nature*. **430**, 686-689.

Wu X, Beecher G, Holden J, Haytowitz D, Gebhardt S, Prior R (2004). Lipophilic and hydrophilic antioxidant capacities of common foods in the United States. *Journal of Agricultural and Food Chemistry*. **52**, 4026-4037.

Wullschleger S, Loewith R, Hall MN (2006). TOR signaling in growth and metabolism. *Cell*. **124**, 471-484.

Xin S, Wang Y, Zhang K, Zhao D, Wu Y, Yu L, Zheng Z (2009). Analysis of trace elements in black peanut and red peanut by ICP-AES with microwave digestion. *Chinese Journal of Spectroscopy Laboratory*. **26**, 1527-1530.

Xu ZG (2011). Modernization one step at a time. *Nature*. **480**, S90-S92.

Yan L, Vatner DE, O'Connor JP, Ivessa A, Ge H, Chen W, Hirotani S, Ishikawa Y, Sadoshima J, Vatner SF (2007). Type 5 adenylyl cyclase disruption increases longevity and protects against stress. *Cell*. **130**, 247-258.

Yang H, Baur JA, Chen A, Miller C, Adams JK, Kisielewski A, Howitz KT, Zipkin RE, Sinclair DA (2007). Design and synthesis of compounds that extend yeast replicative lifespan. *Aging Cell*. **6**, 35-43.

Yu BP, Masoro EJ, McMahan CA (1985). Nutritional influences on aging of Fischer 344 rats: I. Physical, metabolic, and longevity characteristics. *Journals of Gerontology*. **40**, 657-670.

Yu SL, An YJ, Yang HJ, Kang MS, Kim HY, Wen H, Jin X, Kwon HN, Min KJ, Lee SK, Park S (2013). Alanine-metabolizing enzyme Alt1 is critical in determining yeast life span, as revealed by combined metabolomic and genetic studies. *Journal of Proteome Research*. **12**, 1619–1627.

Yu X, Li G (2012). Effects of resveratrol on longevity, cognitive ability and aging-related histological markers in the annual fish *Nothobranchius guentheri*. *Experimental Gerontology*. **47**, 940-949.

Yu XY, Lin SG, Chen X, Zhou ZW, Liang J, Duan W, Chowbay B, Wen JY, Chan E, Cao J, Li CG, Zhou SF (2007). Transport of cryptotanshinone, a major active triterpenoid in *Salvia miltiorrhiza* Bunge widely used in the treatment of stroke and Alzheimer's disease, across the blood-brain barrier. *Current Drug Metabolism*. **8**, 365-377.

Zarse K, Schmeisser S, Birringer M, Falk E, Schmoll D, Ristow M (2010). Differential effects of resveratrol and SRT1720 on lifespan of adult *Caenorhabditis elegans*. *Hormone and Metabolic Research*. **42**, 837-839.

Zhang FY, Zheng WH, Pi RB, Mei ZR, Bao YX, Gao J, Tang WJ, Chen SR, Liu PQ (2009a). Cryptotanshinone protects primary rat cortical neurons from glutamate-induced neurotoxicity via the activation of the phosphatidylinositol 3-kinase/Akt signaling pathway. *Experimental Brain Research*. **193**, 109-118.

Zhang L, Huang D, Kondo M, Fan E, Ji H, Kou Y, Ou B (2009b). Novel high-throughput assay for antioxidant capacity against superoxide anion. *Journal of agricultural and food chemistry*. **57**, 2661-2667.

Zhao SH, Zhang LP, Gao P, Shao ZY (2009). Isolation and characterisation of the isoflavones from sprouted chickpea seeds. *Food Chemistry*. **114**, 869-873.

Zhou L, Zuo Z, Chow MS (2005). Danshen: an overview of its chemistry, pharmacology, pharmacokinetics, and clinical use. *Journal of Clinical Pharmacology*. **45**, 1345-1359.

Zimmerman JA, Malloy V, Krajcik R, Orentreich N (2003). Nutritional control of aging. *Experimental Gerontology*. **38**, 47-52.

Zimmermann MC, Tilghman SL, Boue SM, Salvo VA, Elliott S, Williams KY, Skripnikova EV, Ashe H, Payton-Stewart F, Vanhoy-Rhodes L, Fonseca JP, Corbitt C, Collins-Burow BM, Howell MH, Lacey M, Shih BY, Carter-Wientjes C, Cleveland TE, McLachlan JA, Wiese TE, Beckman BS, Burow ME (2010). Glyceollin I, a novel antiestrogenic phytoalexin isolated from activated soy. *Journal of Pharmacology and Experimental Therapeutics*. **332**, 35-45.

Zimmermann S, Martens UM (2008). Telomeres, senescence, and hematopoietic stem cells. *Cell and Tissue Research*. **331**, 79-90.

Zoncu R, Efeyan A, Sabatini DM (2011). mTOR: from growth signal integration to cancer, diabetes and ageing. *Nature Reviews Molecular Cell Biology*. **12**, 21-35.

Zou S, Carey JR, Liedo P, Ingram DK, Muller HG, Wang JL, Yao F, Yu B, Zhou A (2009). The prolongevity effect of resveratrol depends on dietary composition and calorie intake in a tephritid fruit fly. *Experimental Gerontology*. **44**, 472-476.